ProQuest LLC.
789 East Eisenhower Parkway
P.O. Box 1346
Ann Arbor, MI 48106 – 1346

Preparation, Characterisation and Catalytic Activity of Acid-Activated OrganoClays

Alexander J. Moronta

A thesis submitted in partial fulfilment of the requirement of
Sheffield Hallam University
For the degree of Doctor of Philosophy

September 1999

To my mother, Aide Moronta, to the memory of my forever-beloved father,

Audio Moronta and to my wife, María Elena.

ACKNOWLEDGEMENTS

I like to take this opportunity to extent my appreciation to several individuals who have contributed tremendously to this research.

First, I like to thank Cosejo Nacional de Investigaciones Científicas y Tecnológicas de Venezuela (CONICIT) and La Universidad del Zulia (Venezuela) for the financial support provided.

Secondly, I am very grateful to my Director of Studies, Dr. Christopher Breen for his scientific input, useful advises, good ideas and continuous enthusiasm throughout these three years of hard work.

I thank colleagues in the Slovak Republic for the preparation of the alkylammonium samples.

A salutation to all the technicians who helped me to make the experimental work a little easier, particularly Heather, Paul, David, Kevin and Bob. Thanks also to Scott Taylor for having helped me to obtain the TG-OTM-GC-MS data.

To all my colleagues and friends in the Research Office, I would like to express my appreciation for all their support directly and indirectly. The warm, friendly and amusing environment would certainly be missed.

To my family and my wife's family, which continued support and encouragement would not be forgotten.

Especial thanks are given to the personnel of Centro de Superficies y Catalísis (Universidad del Zulia) for their countless help. Particularly to Professor Eduardo Choren for having introduced me into the clays research field and to Dr. Jorge Sánchez for dealing with my personal matters whilst I was away.

My sincere gratitude to John Muirhead for taking the time to read this thesis and correct my English spelling. Thanks also to Ana Cáceres for her contribution with some of the figures presented in this thesis.

My wife and best friend, I thank for love, care, cooking, patience and her full sympathy.

ABSTRACT

Three montmorillonites SWy-2 (Wyoming, USA), STx-1 (Texas, USA) and SAz-1 (Cheto, Arizona, USA) and one saponite Sap-Ca (California, USA) were treated with different amounts of 12 M HCl and 1 M tetramethylammonium (TMA^+) solution. The catalysts were characterised by X-ray diffraction (XRD) and thermogravimetric analysis (TGA). The catalytic activity of these acid-activated organoclays (AAOCs) was measured using the isomerisation of α-pinene at 120 °C for 1 h to yield camphene and limonene and compared to clays acid-treated in the absence of TMA^+. The total conversion for the isomerisation was excellent for AAOCs formed from SWy-2 (88%) and STx-1 (73%), moderate for Sap-Ca (50%) and low for SAz-1 (20%). Samples treated alone with TMA^+ did not exhibit any marked catalytic activity, which reached an optimum at intermediate TMA^+-loadings. Acid-treated Sap-Ca and STx-1, which contained no TMA^+ cations were also effective catalysts for the isomerisation process. TMA^+ cations were unexpectedly resistant to exchange by protons. The same clays were activated with aluminium and TMA^+ to obtain materials with a combined Al^{3+} and TMA^+ content equal to their CECs. The number of acid sites was measured using the thermal desorption of cyclohexylamine and the catalytic activity was evaluated using the same test reaction and compared to clays in absence of TMA^+. A reduction in both acidity and catalytic activity was observed in samples activated with an Al:TMA ratio < 0.66. The activity of the catalysts remained almost constant for the overall conversion when the aluminium content was >70% in either the presence or absence of TMA^+. The total conversion followed the order Sap-Ca > STx-1 > SWy-2 > SAz-1 in both samples treated with Al^{3+} and Al^{3+}/TMA^+. Aluminium activated organoclays using divalent organocations (1,4-diazabicyclo[2.2.2]octane (DABCO) and 1,5-diaminopentane (DAP)) were also prepared from SWy-2 to compare the activity with those obtained using TMA^+. The order of activity was Al/TMA > Al/DABCO > Al/DAP. The increment in the Al content did not cause a significant effect on the activity. The acidity of these samples was given by protons arising from different equilibria. SWy-2, Sap-Ca and SAz-1 were ion-exchanged (IECs) with different cations (Al, Ca, Mg, Na and Ni) using various exchange treatments. It was found that the exchange treatment had a marked influence upon the total conversion of α-pinene. The order of activity for IECs was Al > Ni > Mg > Ca > Na, with Sap-Ca being more active than SWy-2 and SAz-1.

Aluminium activated clays and organoclays derived from STx-1 were saturated with hept-1-ene. The samples were heated and the gases evolved analysed by FTIR and GC-MS. Hept-1-ene reacted with the clays via proton transfer and resulted in the formation of a variety of reaction products (more than 60 hydrocarbons). TMA^+ cations reduced the population of protons to selectively produce isomerisation and hydration products.

The thermal stability of four clays [JP (montmorillonite, Jelšový Potok, Slovakia), SAz-1 (montmorillonite, Cheto, Arizona, USA), ST (beidellite, Stebno, Czech Republic) and SWa-1 (montmorillonite, Washington, USA)] in the Na- and autotransformed (An)-forms were exchanged with alkylammonium ions of variable chain lengths. The Na-organoclays were more resistant to thermal decomposition than for An-organoclays derived from SAz-1, JP and ST, but not for SWa-1 in which both series of samples had similar thermal behaviour. The weight loss registered for An-organoclays was higher than for Na-organoclays. TG-FTIR revealed the organoclays underwent thermal decomposition to produce ammonia, aliphatic hydrocarbons, CO_2 and water.

LIST OF ABBREVIATIONS

Å: Angstrom
AACs: Acid-Activated Clays
AAOCs: Acid-Activated OrganoClays
AlACs: Aluminium-Activated Clays
AlAOCs: Aluminium-Activated OrganoClays
°C: Degrees Celsius
ca: circa
CEC: Cation Exchange Capacity
cm: centimetre
CX: Cyclohexylamine
DABCO: 1,4-Diazabicyclo[2.2.2]octane
DAP: 1,5-Diaminopentane
DDTMA: Dodecyltrimethylammonium
e.g: for example
eV: electronvolts
FTIR: Fourier Transform Infrared Spectroscopy
g: grams
GC: Gas Chromatography
h: hours
HDPY: Hexadecylpyridinium
HDTMA: Hexadecyltrimethylammonium

ICP: Inductively Coupled Plasma
id: internal diameter
IECs: Ion-Exchanged Clays
kV: kilovolts
M: Molar
m: metres
mA: milliamperes
mequiv: milliequivalents
min: minutes
mg: milligrams
mm: millimetres
mmol: millimole
mol: Mole
MS: Mass Spectrometry
ODTMA: Octadecyltrimethylammonium
OTM: Organic Trap Module
PAACs: Pillared Acid-Activated Clays
PILCs: Pillared Clays
QACs: Quaternary Alkylammonium Cations
QUATs: Quaternary Ammonium Cations
RCM: Reduced Charge Montmorillonites
rpm: revolutions per minute
SMM: Synthetic Mica Montmorillonite
TGA: Thermogravimetric Analysis
TMA: Tetramethylammonium
TMPA: Trimethylphenylammonium
µl: microlitres
µm: micrometres
µmol: micromole
µS: microsiemens
vs: versus
VT-XRD: Variable temperature X-Ray Diffraction
XRD: X-Ray Diffraction
XRF: X-Ray Fluorescence

LIST OF FIGURES

LIST OF TABLES

TABLE OF CONTENTS

CHAPTER 1

Introduction to the Thesis

1.0 Overview

Clay minerals are among the world's most important and useful industrial materials. They play a key role in geology, agriculture and construction. Catalysts based on clays have been used in a wide variety of chemical reactions for many years. These minerals are highly versatile, affording both industrial (petroleum, etc.) and laboratory applications.[1-3] Currently, they are receiving considerable attention, because the environmental protection agencies want to move to less polluting industrial processes, which represent a convenient, cheap and alternative sources to the expensive manufactured catalysts. Catalysts derived from clay can provide such advantages.

Natural untreated clays possess a very low ability to catalyse reactions in either polar or non-polar media. However, the structural properties of these materials can be modified by various activation methods in order to produce catalysts with high acidity, surface area, porosity and thermal stability. In this investigation, acid treatment, intercalation of organic cations and ion-exchange have been employed alone and in combination. The resulting catalysts have been characterised by X-ray diffraction (XRD), thermogravimetric analysis (TGA), elemental analysis and inductively couple plasma (ICP) spectrometry.

Additionally, TGA has been used in combination with other analytical techniques to provide further information about the species evolved during the heating process, these are: (1) Fourier Transform Infrared Spectroscopy (TG-FTIR), (2) Mass Spectrometry (TG-MS), system in which the FTIR can be also assembled (TG-FTIR-MS) and (3) the coupling of an organic trap module with Gas Chromatography-Mass Spectrometry (TG-OTM-GC-MS).

1.1 Overall Objectives

To prepare, characterise and evaluate acid-activated organoclays as catalysts for a non-polar medium reaction.

To develop effective solid acid catalysts based on saponites and to compare them with montmorillonites.

To investigate how the type of the clay, the extent of acid treatment and the nature/loading of the organic and/or inorganic exchange cation affect the structural composition of the clays.

To enhance understanding of how surface acidity and catalytic activity are developed in clay-based catalyst.

To study the mechanism of olefin adsorption/desorption by combining different techniques and to attempt to identify the products desorbed from the surface of aluminium-activated clays and aluminium-activated organoclays at certain temperatures.

To examine the thermal desorption/decomposition of acid-treated clays exchanged with alkylammonium cations of increasing chain length and to compare the organoclays in terms of their thermal stability.

1.2 General Introduction to the Thesis

Acid-activated clays have been used as an effective source of protons for a considerable period, finding particular applications in industrial processes such as the alkylation of phenols,[4] polymerisation of unsaturated hydrocarbon,[5-6] clarification of edible oils[7] and carbonless copying paper.[8]

The surface properties of natural clays can be also modified by replacing natural inorganic exchange cations by larger alkylammonium ions.[9-12] These ions act as "pillars" which hold the aluminosilicate sheets permanently apart and increase the interlamellar spacing and expose new sorption sites on the clays.[13-15] As the inorganic cations are progressively replaced by organic cations, the surface properties of the clay change from highly hydrophilic to increasingly organophilic (hydrophobic). These materials, referred to as organoclays exhibit high adsorption capacity towards hydrophobic molecules.[16-18]

Useful modifications can be also produced by treating the clay with highly polarising species such as aluminium, chromium, iron or metal hydroxy polymeric cations.[19-23]

The research work presented in this thesis is a combination and expansion of all these ideas to produce novel materials based on clays (acid-activated organoclays) as catalysts.

A catalytic aggregate is a substance, which speeds up a chemical reaction and is recovered unchanged at the end of the reaction process. Many substances can act as catalysts including metals such as platinum, palladium, nickel, silver, molybdenum, tungsten, etc. and metal oxides such as alumina, silica gel, vanadium pentoxide, etc.

Catalysts based on natural clays were used more than 70 years ago to promote organic reactions, being later (in the mild-1960's) supplanted by zeolites and synthetic clays. Clays present two advantages that make them useful in catalysis: a large particle surface area due to the their small grain size; and a large internal, chemically active surface area due to their adsorptive properties.

Combining acid-activation with alkylammonium intercalation provides a potential enhancement of the clay properties. In the first instance, the clay is hydrogen-saturated by cation exchange in acid solution (acidifying process), resulting in a proton rich environment when presented to organic molecules. In the second instance, the catalytic abilities can be further improved by providing organic cations in the interlamellar space, which permit access to and interact effectively with organic molecules. The possibilities for catalysis in these systems are therefore much greater because both the internal and the external surfaces are available for reaction.[24-25] The first part of this study was to build a body of information concerning the effect of the acid treatment alone and in combination with tetramethylammonium (TMA^+) on the catalytic activity towards the isomerisation of α-pinene of three montmorillonites and one saponite. In addition, the ability of TMA^+- and trimethylphenylammonium ($TMPA^+$)-cations to compete with protons for clay exchange sites was assessed by consistently offering a fixed quantity of organocation in the presence of increasing quantities of acid. The properties and activities of the H^+/TMA^+- and $H^+/TMPA^+$-clays were compared with catalysts prepared without TMA^+ or $TMPA^+$.

Complementary studies involved the combination of Al^{3+} and TMA^+ to compare the clays directly without damaging the octahedral sheet and to further investigate if the Al^{3+}/TMA^+

exchange imparts a better acidity. The combination of aluminium with divalent organocations of different shapes (1,4-diazabicyclo[2.2.2]octane, DABCO and 1,5-diaminopentane, DAP) was also investigated. Supplementary techniques were used to correlate the number of acid sites, determined from the thermal desorption of cyclohexylamine, with the catalytic activity for the acid catalysed transformation of α-pinene to camphene and limonene. The test reaction was also applied to montmorillonites saturated with various inorganic cations to study the effect of the interlayer cation on the catalytic activity.

To complete the above-mentioned aims, clays from various sources were examined, since it is now widely accepted that clays with different structures are acid leached at variable rates. For example montmorillonites with high octahedral Mg or Fe content leach more readily than those which contain a high octahedral Al population.[26-29]

Numerous papers have been published describing the reaction of olefins on natural or exchanged clays in the range 80-150 °C. Nevertheless, very few of them have reported the adsorption of olefins on clays at room temperature. Thus a part of this thesis involves a series of studies addressed to evaluate and identify the desorption products formed during the heat treatment of hept-1-ene on aluminium-activated clays and aluminium-activated organoclays. Additionally, the adsorption/desorption of heptan-1-ol and heptan-2-ol on the same series of clays was carried out in order to verify dehydration of the respective alcohol and the corresponding formation of alkene products. A powerful analytical technique "Synergic chemical analysis" has been used, which is especially suited to catalyst research. The Synergy System involves the combination of versatile analytical techniques, the

thermogravimetric (TG) analyser being the principal component, in which the sample weight loss is recorded as it is heated up at a controlled temperature rate. Fourier Transform Infrared (FTIR) can identify the characteristic functional groups of the evolved gas during the heating process. This particular combination is named Real Time TG-FTIR. Useful information can be also achieved connecting the TG to a Mass Spectrometer, which breaks up the molecule (from the evolved gas) and identifies it from the diagnosis fragmentation pattern. This assembly is called Real Time TG-MS. If the evolved gas is a very complex mixture, then the individual compounds can be trapped using an organic trap module (OTM), being then transferred and separated using gas chromatography and finally analysed by MS. This arrangement of techniques is called TG-OTM-GC-MS.

The properties of organoclay complexes depend upon the nature of the intercalated organic molecule but also strongly upon the physicochemical nature of the host crystal. The final part of this work focused on the exchange of quaternary ammonium (n-alkylammonium chlorides), with a variable carbon chain length into, Na-exchanged and autotransformed clays with different crystallinity and homogeneity of charge distribution. In this part, special emphasis was placed on the thermal desorption/decomposition process of the organoclays and their spectral characteristics, followed by Real Time TG-FTIR.

In order to understand the chemistry of clay minerals as catalysts it is imperative to bear in mind their native crystalline structure, physicochemical properties and interactions. This is covered in Chapter 2, which is devoted to clay mineralogy.

CHAPTER 2

Properties of Clay Minerals

2.0 Introduction

Clay minerals are the most abundant sedimentary mineral group. They predominate in the colloidal fractions of soils, sediments, rocks and waters and are classified as phyllosilicates (usually hydrous aluminosilicates).

In Geology the word *clay* is used in two ways: firstly as a rock classification which generally implies an earthy, fine-grained material that develops plasticity on mixing with limited amount of water. Secondly, it is used as a particle term, which describes clays as minerals which have a particle size <4μm,[30] although the modern tendency is to define clays as having particles sizes <2μm as fractions of this size generally give a very pure mineral.[31]

Clays have been one of the most important minerals for man for centuries. The first recorded application of clay as a catalyst, was reported by Bondt, *et al.*,[32] who investigated the dehydration of alcohol in 1797. Nowadays, clay minerals science has found a diverse variety of industrial applications (Table 1).[33] In order to understand better the relationship between the clays and their uses, a brief discussion of the structure is given.

Drilling mud	Medical formulation	Crayons	Cement
Foundry bond clay	Polishing agents	Detergents	Desiccants
Pelletizing iron ores	Pharmaceutical	Aerosols	Cosmetics
Sealants Adhesives	Beer clarification	Paint	Paper
Animal feed bonds	De-inking paper	Fillers	Ceramics
Bleaching earth	Emulsion stabilisers	Catalysts	Pencil leads
Oil absorbents	Agricultural carriers	Food additives	

Table 1. Industrial uses of clays (smectites)[33]

2.1 Structure of Clays

2.1.1 Basic Units

Before describing a complete clay structure it is necessary to understand the fundamental molecular units involve in the clay structure and the arrangements of these units in the overall patterns common to all clays.

2.1.1.1 Octahedra

This unit consists of two sheets of closely packed oxygens or hydroxyls in which the Al^{3+}, $Fe^{2,3+}$, or Mg^{2+} atoms are embedded in an octahedral co-ordination, so that they are equidistant from six oxygens or hydroxyls (Figure 1). If only two of the three possible positions are occupied by trivalent aluminium the structure is called *dioctahedral*. If all three octahedral positions are occupied by divalent magnesium the structure is referred as *trioctahedral*.

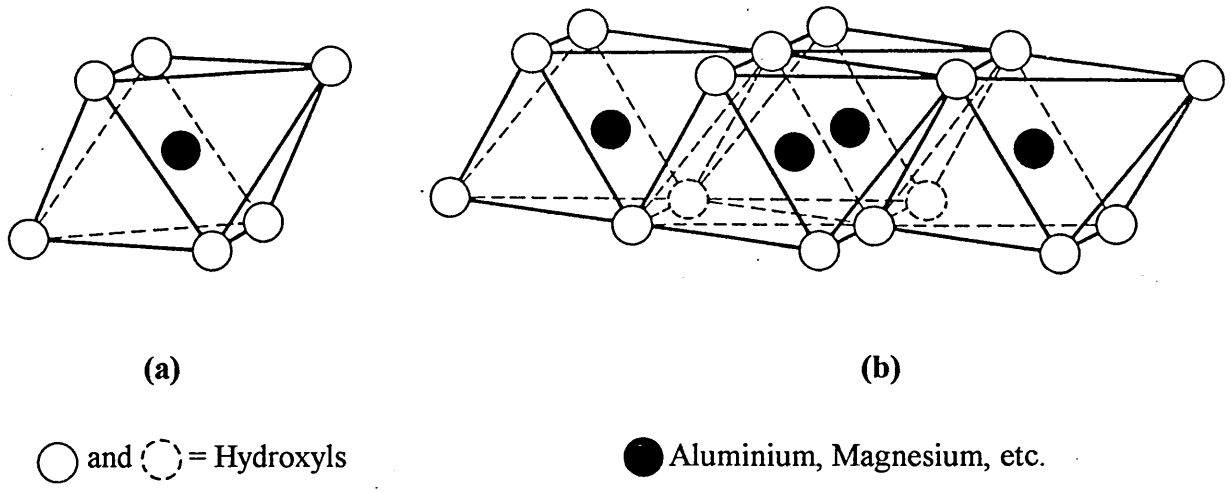

Figure 1. Diagrammatic representation of: (a) single octahedral unit and (b) the sheet of the octahedral units.

2.1.1.2 Tetrahedra

This unit is composed of silica tetrahedra (Figure 2a), in which each Si atom is bonded to four oxygens or hydroxyls. The silica tetrahedra are arranged to form a hexagonal network (Figure 2b), which is reproduced indefinitely to form a sheet of composition $Si_4O_6(OH)_4$ (Figure 2c).

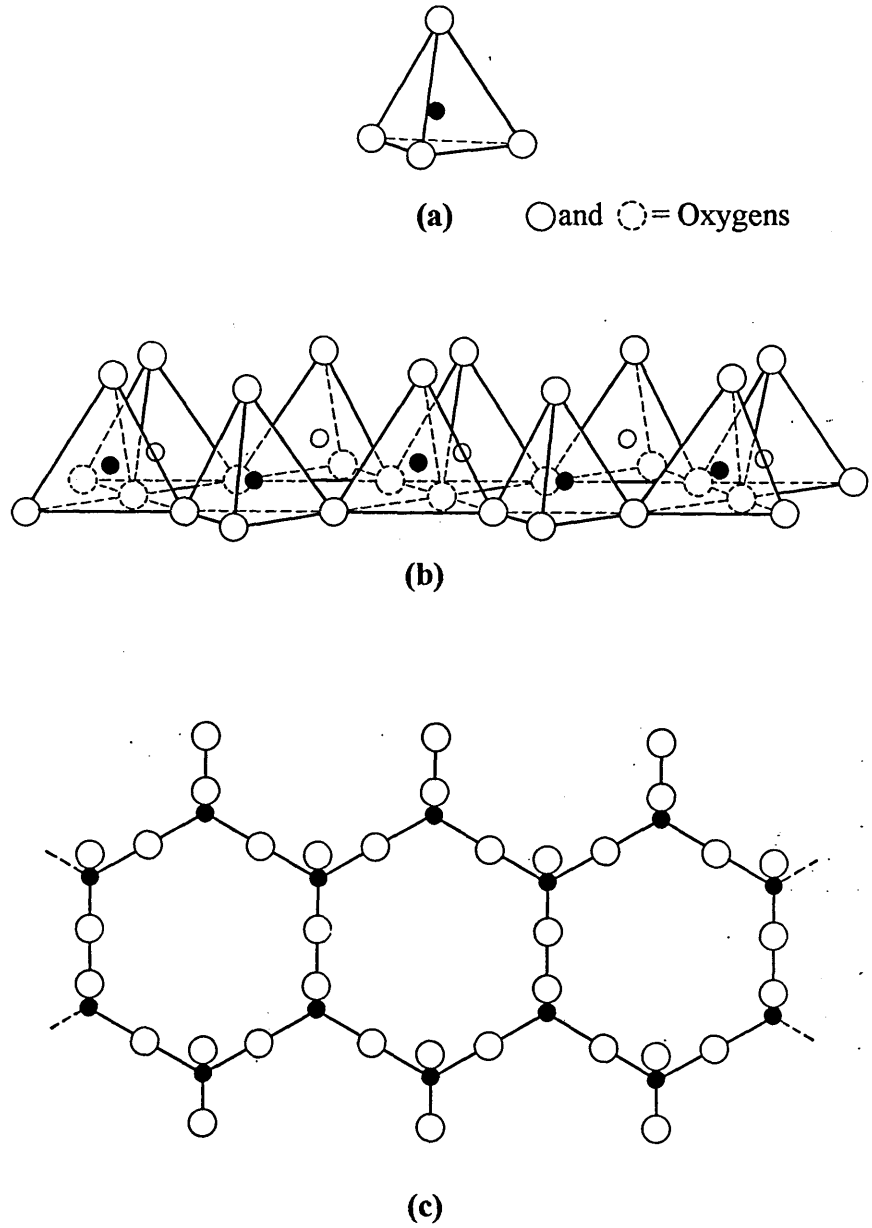

Figure 2. Diagrammatic representation of: (a) single tetrahedron unit, (b) the sheet of the tetrahedron units and (c) the double chain of silica tetrahedra projected on the *ab* plane.

2.1.1.3 The Formation of the Aluminosilicate Layer

Due to the symmetry and dimensional similarities of the octahedral and tetrahedral sheets, they can be combined in different structural arrangements resulting in a variety of clay mineral sub-groups. Condensation of one tetrahedral (T) sheet with one octahedral (O) sheet results in a structure referred to as 1:1 or T:O. It is also possible to combine a further tetrahedral sheet on the opposite side of the octahedral sheet resulting in a 2:1 or T:O:T structure. Depending on the combination ratio of these sheets, the clays can be classified in the following groups: Kaolin, Halloysite, Talc, Smectite, Chlorite, Micas and Vermiculite.

Smectite is one of the most useful of the swelling clays. It is composed of units consisting of two silica tetrahedral sheets with a central octahedral sheet T:O:T (Figure 3)[34-36] of both dioctahedral and trioctahedral types. Table 2 shows the principal members of the smectite group.

Origin of layer charge	Trioctahedral Smectites	Dioctahedral Smectites
Octahedral	Hectorites $(Mg_{6-x}Li_x)(Si_8)O_{20}(OH)_4.xM^+$	Montmorillonites $(Al_{4-x}Mg_x)(Si_8)O_{20}(OH)_4.xM^+$
Tetrahedral	Saponite $(Mg_6)(Si_{8-y}Al_y)O_{20}(OH)_4.yM^+$	Nontronite $(Fe_4^{3+})(Si_{8-y}Al_y)O_{20}(OH)_4.yM^+$ Beidelite $(Al_4)(Si_{8-y}Al_y)O_{20}(OH)_4.yM^+$

Table 2. The idealised structural formulae of the principal smectites.

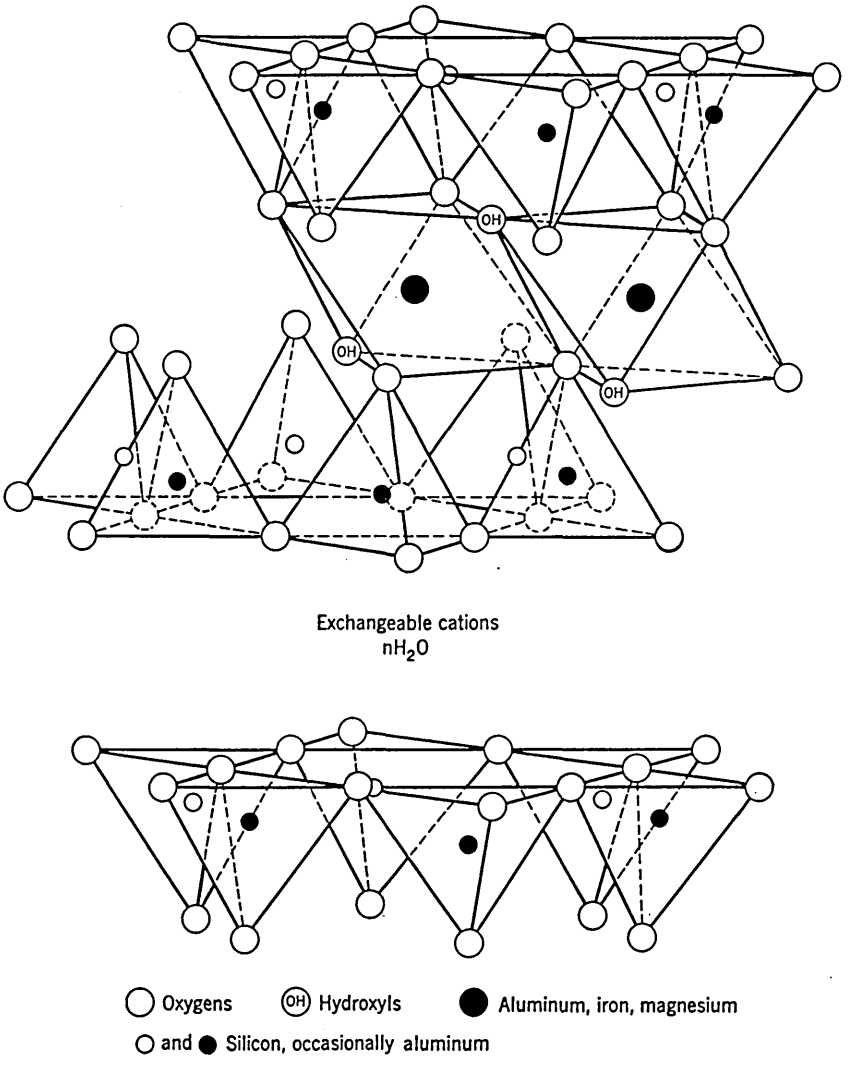

Figure 3. Diagrammatic representation of the structure of montmorillonite.[34-36]

2.2 Isomorphous Substitution

In smectites there can be considerable substitution in either the octahedral or tetrahedral sheet, giving rise to a varying degree of substitution in both sheets (Figure 4).[37] This phenomenon is responsible for some important properties of clays minerals. Substitution in the octahedral sheet usually by Fe^{3+} and Mg^{2+} for Al^{3+}, creates a de-localised charge

deficiency in the layer.[38] Also, there can be substitution in the tetrahedral sheets of Al for Si which again creates a more localised charge imbalance. In smectites this effect accounts for approximately 80% of the total cation exchange capacity (CEC). The generated charge deficiency is balanced by exchangeable cations between the unit layers and around the edges. In natural clays Ca, Mg, Na and K are the predominant exchangeable cations.[39]

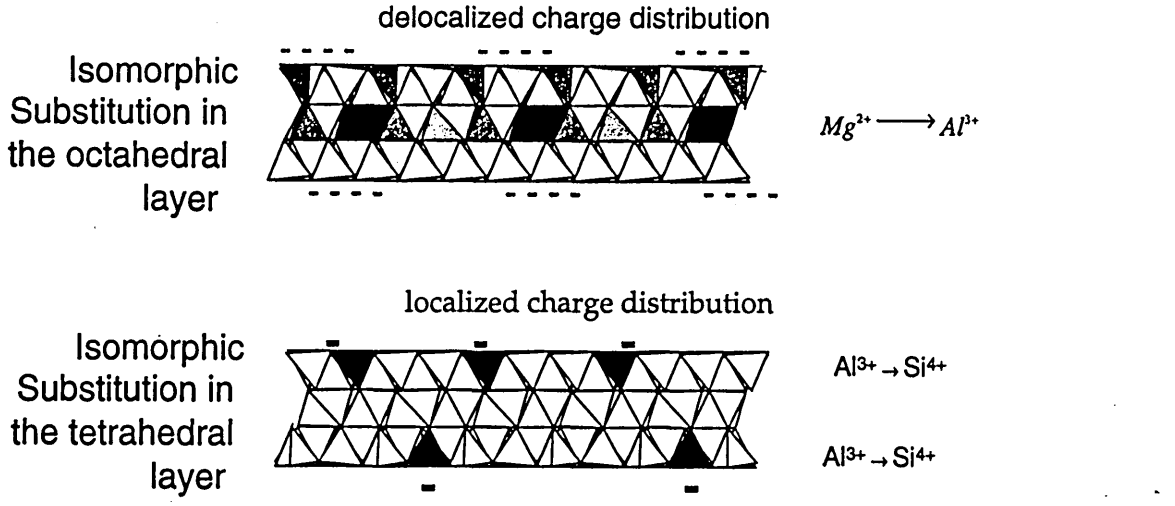

Figure 4. Showing the isomorphous substitution in the octahedral sheet (top) and tetrahedral (bottom) sheets.[37]

2.2.1 Broken Edges

Undercoordinated metal ions (Si^{4+}, Al^{3+}, Fe^{3+}) on the broken edges on the surface of the clay can react with water molecules to form surface hydroxyl groups (Figure 5)[37] in an attempt to complete their coordination sphere. The overall contribution of these edge sites to the CEC is approximately 20%, and depends strongly on the size and shape of the clay particle. As the particle size decreases, the contribution of broken sites to the reactivity of the clay particle becomes significant.

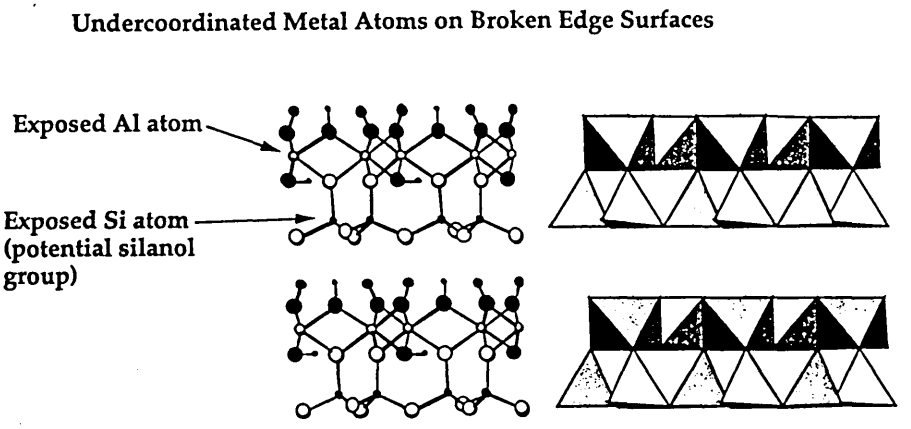

Figure 5. Showing the broken edges and undercoordinated metal ions (Si and Al) located on the edges of kaolinite.[37]

2.2.2 Layer Charge

Depending upon the degree of isomorphous substitution, clay minerals are classified into three major categories:

a. **Neutral lattice structures** (kaolinite and serpentine 1:1, talc and pyrophyllite 2:1, chlorite 2:1 + 1). In these structures the 2:1 or 1:1 units of interlinked tetrahedra and octahedra have a net charge of zero. The substitution within the sheets is cancelled electrostatically and the individual layers (2:1, 1:1 and 2:1 + 1) are bound into a crystal by low energy bonds (van der Waals type). The main bonding forces between the layers of kaolinite and halloysite are hydrogen bonds between –OH on one layer and a bridging -O- on the next.[40]

b. **High-charge mica structures** (0.9-1.0 charge) In these minerals there is a charge imbalance due to isomorphous substitution in the basic 2:1 structures, which is compensated by interlayer ions between the layers bonding them together. The charge on the 2:1 layer is near 1. The interlayer ion is firmly held between the adjacent layers and it is an integral part of the structure that is extremely difficult to exchange.

c. **Low-charge 2:1 structures** (0.2-0.9 charge) where there is a net charge imbalance on the tetrahedral-octahedral network of 0.2-0.9, compensated by loosely held ions in the interlayer position which can be easily exchanged in aqueous solution. These minerals swell (incorporate polar molecules between the layers) attracting various types of molecules between the 2:1 layers by the electrostatic charge. The low charge means that the cations are not fixed between the layers.

2.3 Cation Exchange Capacity (CEC)

To a greater or lesser degree, based on their layer charge, many clays have the ability to adsorb exchange cations from solution. It is this cation storage that makes clays such an important component of many soils. A typical montmorillonite can exchange over 100 millimoles of M^{n+} cations per 100g of clay.

The ideal structures of the clay minerals depicted above are often deviated from in a number of ways introducing charge imbalances into the structure, mainly isomorphous substitution. As mentioned above, the overall negative charge is balanced by adsorption of metal cations into the interlayer region of the clay mineral.[39]

More information is available regarding cation exchange than anion exchange. In clay minerals the common exchangeable cations are calcium, magnesium, hydrogen, potassium, ammonium and sodium, approximately in that order of general relative abundance. The common anions in clay minerals are sulphate, chloride, phosphate, and nitrate. A typical montmorillonite will have Na^+, Ca^{2+} or Mg^{2+} cations in the interlayer space. These cations are hydrated, usually hexa(aquo), and the remainder of the interlayer is filled by a variable amount of water which can swell the clay. The interlayer cations are much less strongly bound than the layer cations and will thus easily exchange with cations from an aqueous solution.[41] This sorption from solution is normally considered as a simple exchange process.

The exchangeability of cations related with the clay by cations of a particular aqueous solution is determined by:

- The nature of the clay mineral.
- The nature of the cation, *e.g.*, hydration energy, size, valency.
- The concentration of the electrolyte and pH of the exchange solution.
- The population of exchange sites on the clay.

Solutions of small size/high valency metal cations are very effective at displacing the interlayer exchangeable cations of a clay.[42,43] Similarly the ease of replacement of interlayer cations follows the reverse order. Thus, the following is given:[44]

$$M^+ << M^{2+} < H_3O^+ \approx K^+ \approx NH_4^+ < M^{3+} < M^{4+}$$

$$\xrightarrow[\text{(Decreasing Ease of Exchange)}]{\text{Increasing Exchanging Power}}$$

Figure 6. The exchange properties of cations with clays.[43]

2.3.1 Determination of the CEC

The cation exchange capacity of clays is determined experimentally by different analytical methods, most of which are based on the principle of replacement of the original resident exchange ions in an aqueous clay suspension. Among the most well known methods are the ammonium ion exchange and the methylene blue tests.[45,46] Other methods include the use of mechanical extraction[47] and the adsorption of the coloured $Co(H_2O)_6^{2+}$ ion.[48] More recently, a faster method for the determination of CEC has been reported, which involves the use of a Cu-ethylendiamine complex.[49]

The CEC represents the isomorphous substitutions in the clay layers if all compensating cations are accessible for exchange. If the CEC and in particular the chemical composition of the clay are known, then it is possible to attribute the substituting ions to the tetrahedral and octahedral sheets, taking the following assumptions into consideration:

1. The unit cell contains 20 oxygens and 4 hydroxyl groups.
2. All the Si atoms are assigned to the tetrahedral sheet.
3. Al atoms occupy the remainder of the tetrahedral positions. Any additional Al is assigned to the octahedral sheet, together with Mg, Fe and other non-exchangeable ions.

2.4 Cation Migration

The thermal treatment of a montmorillonite saturated by cations of small radii (<0.7 Å) results in a charge reduction and a concomitant fall in the cation exchange capacity. This was first shown for lithium[50] and then for magnesium and aluminium.[51]

It is widely considered that, on heating, Li^+ cations migrate from the interlayer space into the vacant octahedra,[50-54] into the hexagonal holes of the tetrahedral sheet[55-57] or into both.[58,59] This Li^+ fixation reduces the charge imbalance, due to isomorphous substitutions, and decreases the ability of the mineral to adsorb cations.

Many studies have used various temperatures (in the range 200-300 °C), different reaction times and clays for the preparation of reduced-charge montmorillonites (RCMs), thus rendering direct comparisons rather difficult. Calvet and Prost[59] were able to achieve 31-92% of total Li^+ in a Camp Berteaux montmorillonite heated at 108-220 °C. They stated, using IR, that Li^+ cations moved from the interlayer space towards the octahedral vacancy, assuming that Li^+ ions lie near the sites of isomorphous substitution.

More recently, Madejová, *et al.*,[60] and Komadel, *et al.*,[61] prepared a series of RCMs starting from a Li-montmorillonite by heating to various temperatures (105-210 °C) for 24 h, and studied the effect of acid treatment upon the dissolution of the clays. These authors demonstrated that the extent of acid dissolution decreased with increased amounts of Li fixed within the montmorillonite structure. Additionally, the Li^+ content increased with increasing heating temperature. Infrared spectroscopy revealed that Li^+ was trapped in the hexagonal cavities of the tetrahedral sheet at all temperatures.

The reduced charge montmorillonites perform little catalytic activity as Brønsted acid catalysts. However, the replacement of the residual interlamellar Li^+ by catalytically active cations, such as Al^{3+}, results in a more active material.[62]

In this thesis a series of Li^+ reduced-charge montmorillonites, derived from a high charge density clay, were prepared then the residual interlamellar Li^+ was exchanged by Al^{3+}. This study was addressed to compare the catalytic activity towards the isomerisation of α-pinene of these RCMs with those of aluminium-activated clays.

2.5 The Hydration and Swelling Capacity of Clays

The outstanding characteristic of the members of the smectite group is their capacity to absorb water and other polar molecules between the sheets, thus producing a marked expansion of the interlayer spacing. The presence of several layers of water molecules causes the basal spacing to increase from 10.5 Å to values in the order of 12.5-20.0 Å, depending on the type of clay and exchangeable cation (Figure 7).[63,64]

The swelling properties of smectites means that they are often called expanding clays. Only smectite clays have this particular property of increasing the interlamellar space; other 2:1 clay minerals such as mica and vermiculite do not expand as readily due to the excessively high layer charge.

The heating process, at a regular temperature rate, affects the weight loss of clays. These temperatures depend on the type of clay and the rate and time of heating. According to Bradley and Grim,[65] below 300 °C, water and other molecules are adsorbed reversibly between the clay laminae. Above 500 °C the water of hydration is removed and the laminae collapse irreversibly.[65,66] After calcination of the clay at 600 °C no water is adsorbed in the interlamellar space.

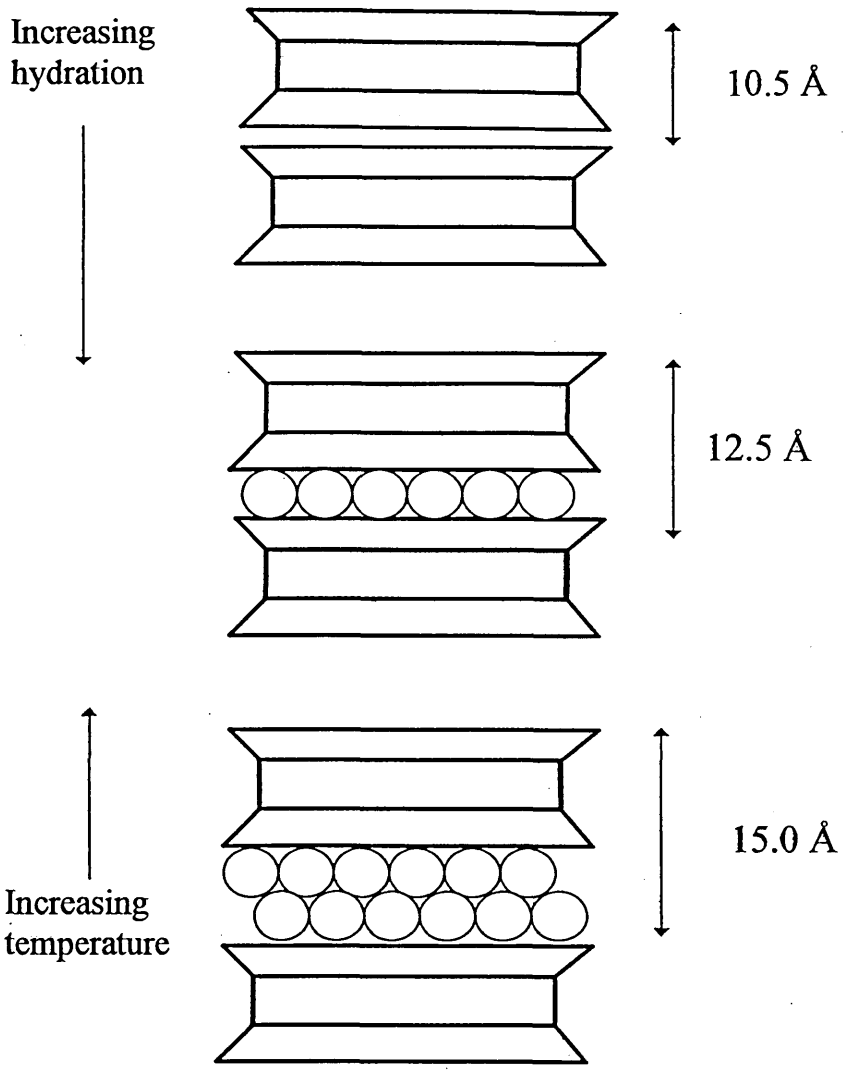

Figure 7. Swelling state of smectite in the presence of water vapour.

2.6 Acidity of Clays

Clays minerals show both Brønsted and Lewis acidity. Structural and environmental factors govern the degree to which each is present and normally one type predominates for a given set of conditions.[67]

Lewis acidity is normally associated with exposed Al^{3+} and Fe^{3+} at the broken crystallite edges and such acidity can be increased by heating the clay to >300 °C.[68] However, this heat treatment not only removes the interlayer water and dehydrates the aquated metal cations in the interlayer but also leads to the irreversible collapse of the clay layers.[69]

The most important source of Brønsted acidity derives from the dissociation of water molecules in the hydration sphere of the interlayer exchangeable cations (Equation 1).[67]

$$[M(OH_2)_n]^{m+} \rightleftharpoons [M(OH_2)_{n-1}OH]^{(m-1)+} + H^+ \qquad (1)$$

The acidity depends upon the water content of the clay and to a lesser extent upon whether the layer exchange arises mainly from substitution in the octahedral or tetrahedral sheet. Acidity is maximised when the water content of the clay is low and when highly polarising species such as M^{3+} cations are exchanged for natural Na^+ and Ca^{2+} cations.[67,70,71] Clays may be effectively dehydrated by heat or vacuum or by displacing the interlayer water with non-polar organic solvent.

2.6.1 Determination of the Surface Acidity

The first measurement of clay acidity was reported by Walling[72] who found that an acid treated clay imparted colour to p-nitrobenzene-azo diphenylamine. The acidity was thought to be due to the residual acid from the activation treatment. Since this study, a variety of methods and techniques have been used to measure the acidity of catalysts and catalyst supports, including the use of indicators,[71,73] measurement of the quantity of chemisorbed

ammonia at various temperatures,[74,75] the determination of the IR spectrum of chemisorbed ammonia,[76,77] carbocation formation of arylmethanol[78] and adsorption of pyridine by IR.[79-81]

The applications of these techniques have given conflicting and differing results on the same material. Nevertheless none of these methods, except the last one, distinguishes between protonic acidity (Brønsted) and aprotonic acidity (Lewis). This is because the IR spectrum of adsorbed pyridine on acid solids shows a band at 1548 cm^{-1} associated with the pyridinium ion formed when the molecule reacts with Brønsted acid sites and bands in the region 1440-1460 cm^{-1} attributed to pyridine co-ordinately bound to Lewis acid sites.[79]

The determination of the number of Brønsted and Lewis acid sites (in arbitrary units) results by dividing the integrated absorbances in the two regions by the weights of the wafer, and by the molar extinction coefficients, 1.67 (cm μmol^{-1}) for Brønsted and 2.22 for Lewis acid sites.[82]

Unfortunately, the use of all of these methods can be tedious, difficult and time consuming, particularly if the requirement is for a rapid evaluation of the acidity of the material produced.

It has been shown that the thermogravimetric analysis of the desorption/decomposition of bases such as cyclohexylamine, butylamine and pyridine can be used for the rapid semi-quantitative determination of the number of acid centres in clays.[83-85]

The desorption of pyridine from Brønsted acid sites appears in a prolonged and broad maximum at 340 °C, whilst that from Lewis acid sites is rapid and results in a sharp maximum in the derivative thermogram.[84,85] On the contrary, the desorption of cyclohexylamine from Brønsted acid sites results in a sharp and easily distinguished maximum near 290 °C in the derivative thermogram, but it does not distinguish Lewis sites very well.[83,85] This particular behaviour makes cyclohexylamine a suitable molecule to easily determine, semi-quantitatively, the total concentration of acid sites on acid catalysts based on the percentage weight loss at 290 °C. This region in the derivative curve gives a direct measure of the concentration of cyclohexylammonium ions in the clay sample, a value that is then interpreted as the concentration of protons in the clay available to interact with cyclohexylamine.[83,85]

2.7 Acid Activation of Clays

More than 50 year ago, Eugene Houndry[86] found that acid-modified smectites provide gasoline in high yield when used as petroleum-cracking catalysts. These modified clays were used extensively as commercial catalysts until the mid-1960's, when they were replaced by more thermally stable and selective zeolite catalysts. However, smectite clays are still used today as commercial catalysts.

Acid-treated clays are also commonly used commercially for decolourising oils. The effect of acid attack on properties such as surface area and the decolourising ability have been widely studied.[7,87] Another commercial usage of acid-treated clays is in colour formation with leuco dyes in pressure sensitive recording paper.[8,88]

The acid treatments increase the surface area (from *ca.* 40 m^2g^{-1} to *ca.* 500 m^2g^{-1})[89] of clay minerals by disaggregation of clay particles, elimination of several mineral impurities, removal of metal-exchange cations, and proton exchange, reasons for which they are usually known as "acid activation treatments".[90,91] The enhanced surface area depends significantly on the type of clay used; for example in non-swelling bentonites (Figure 8A-D)[92] it is dramatically improved, but the opposite trend is observed in swelling bentonites (Figure 8E).[92] In general, the surface area passes through a maximum beyond which further acid treatment reduces surface area.[9,92,93]

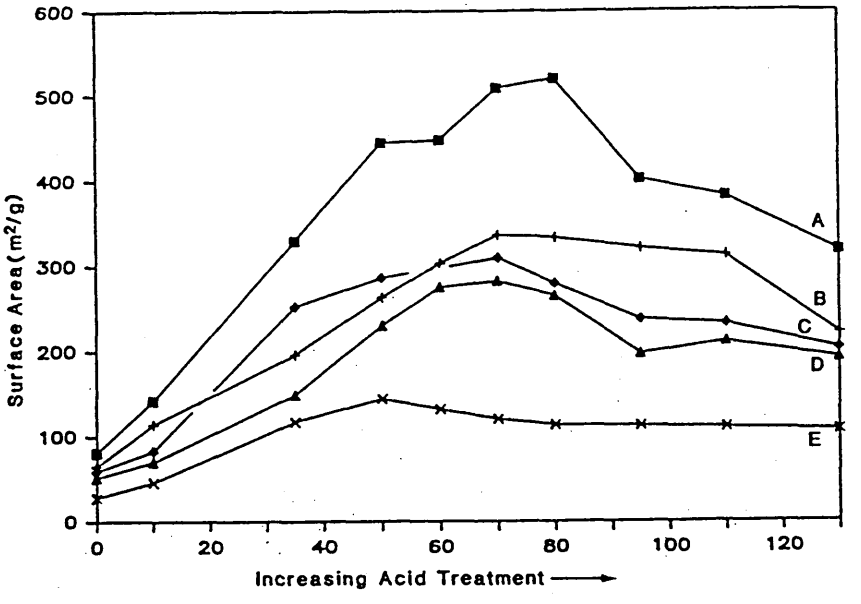

Figure 8. Effect of acid treatment on the surface area of various montmorillonites.[92]

The acid activation process is often quite severe and destroys much of the clay layer structure as it removes iron, aluminium and magnesium from the octahedral sheet (Figure 9).[94] The

exchangeable cations are replaced mainly by Al^{3+} and H^{+}-cations.[95,96] The CEC decreases with increasing acid treatment (Figure 10).[92]

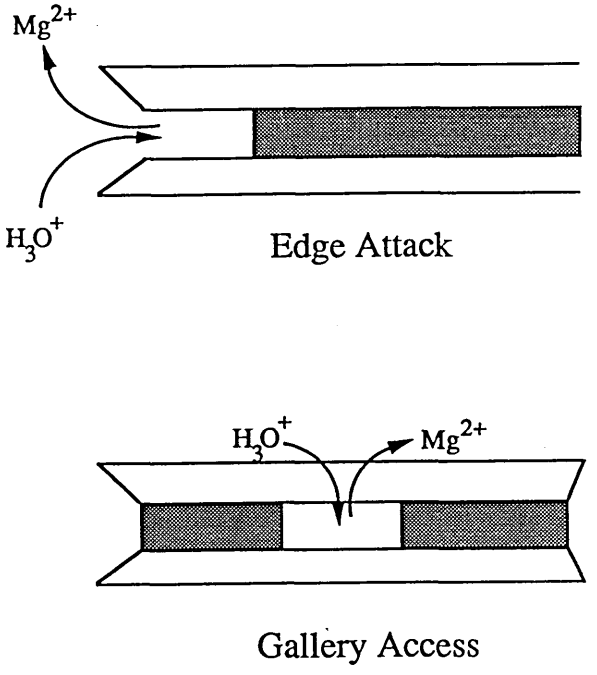

Figure 9. Diagrammatic representation of the effect of acid activation.[94]

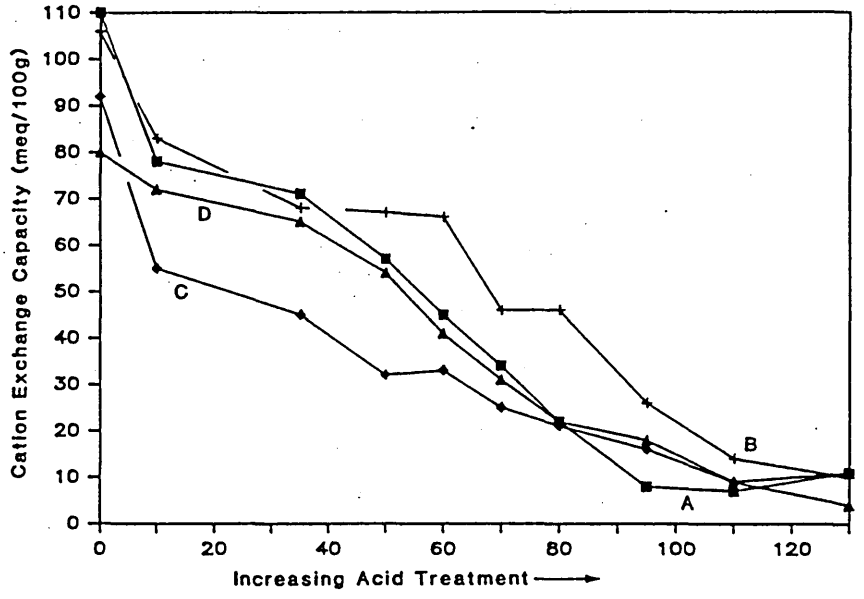

Figure 10. Effect of acid treatment of the CEC of various montmorillonites.[92]

Treatment of montmorillonite clays with cold, dilute acids has little effect on the elemental composition of the host layer and results in an essentially proton-exchanged clay, whereas activation with hot concentrated acids results in the removal of ions associated with the octahedral sheet and may not produce an exclusively proton-exchanged clay.[29,97,98] It is now generally accepted that clays with a high octahedral Mg or Fe content leach more readily than those which have a high octahedral Al population.[26-29,87,99-101] Acid activation causes little damage to the silicate layer and consequently the structure in the centre of the platelet, at the limit of acid attack, remains intact.[29,87,95] The rate of dissolution of the octahedral sheet is a first order process[26,102] which increases not only with increasing concentration of acid, temperature and contact time, but also with increasing Mg content in the octahedral sheet.[7,87]

Recent results obtained after acid-leaching five clays of differing elemental composition have shown that the type of clay used had little influence on the catalytic activity which was determined mainly by the extent of octahedral sheet depletion and proton content.[29] However, it is now imperative that the activation conditions are optimised for a given clay, although, it should be emphasised that the acid activation process really works well when selected bentonites are used. Other clays such as kaolin, attapulgite, etc., only improve slightly or not at all when they are treated with acids.[92]

2.8 Ion Exchange Activation

As mentioned before, the intercalated cation in naturally occurring clays is Na^+ or Ca^{2+} and occasionally K^+. Such clays are very weakly catalytic, if at all. When, however, these ions are exchanged by the simple process of immersion in an aqueous solution of the relevant cation

they become active. This process can be achieved using (i) active metal cations and (ii) hydroxy-metal polycations, "pillars".

2.8.1 Metal Cations

The resident exchangeable cations, which are strongly hydrated in the presence of water, are replaced by highly polarising species of small radius such as aluminium, chromium or iron.[19,21] Consequently, the high catalytic activity of Al^{3+}- compared to Fe^{3+}- and Cr^{3+}-exchanged montmorillonites has been attributed to the enhanced polarisation of water molecules in the primary co-ordination sphere of the Al^{3+} cation.[20,103,104]

There are of course numerous cations other than Al^{3+}, Fe^{3+} and Cr^{3+} that are also comparable in ionic radius, which also possess a polarising power. Examples of these are Mg^{2+}, Cu^{2+}, Ni^{2+}, Co^{2+} and Zn^{2+}.[105-107] The order of activity of ion-exchange clays with these cations was $Cu^{2+} > Zn^{2+} \geq Ni^{2+} \geq Co^{2+} \approx Mg^{2+}$, for both Brønsted and Lewis acid catalysed reactions.[108]

These ion activated clays have been shown to be efficient catalysts for a variety of organic reactions, which include formation of di-alkylethers from alcohols,[19] protonation of amines,[107] transformation of alkenes,[109,110] hydration of ethylene,[104] and esterification of organic acids,[111] among others.

It is worth mentioning that the choice of the reaction environment plays an important role in the catalysed process of ion-exchanged clays. For example, Al^{3+}-, Cu^{2+}-, Co^{2+}-, Ni^{2+}- and La^{3+}-exchanged Tonsil showed, in general, lower activity for the Diels-Alder reaction between cyclopentadiene and methyl vinyl ketone (24±4% conversion) than that of Cr^{3+}- and

Fe^{3+}-exchanged Tonsil (92±1% conversion).[112] Certainly, the acidity of Al^{3+}-exchanged clay is similar to that of Cr^{3+}-exchanged clay and higher than that of M^{2+}-exchanged clays.[113] This observation led Adams, *et al.*,[112] to postulate that *d* orbitals of the exchanged transition metal cations are responsible, in this particular reaction, for the catalytic activity of the ion-exchanged clay minerals where the role of Brønsted acid sites was discarded.

2.8.2 Pillared Clays

When clays are compared as catalysts to the more rigid cage-like zeolites, they are found to be comparable at lower temperatures but, due to a tendency to dehydrate and undergo layer collapse, clays are usually inferior at higher temperatures (*ca.* >150 °C). One way to overcome this disadvantage is to incorporate large inorganic cations. Such a process is known as pillaring and, in addition to the great improvements in available surface area and structural integrity, which is often obtained, these materials have the added advantage that the pillars themselves may be catalytically active.[114-116]

Pillared clays (PILCs) are prepared by exchanging polycations into the interlayer region of expandable clay minerals (usually montmorillonite and saponite) which, following calcination, are transformed to metal oxide pillars fixed to the layers of the clay to yield a rigid cross-linked material.[117-119] A variety of inorganic oxides, Al_2O_3,[120] ZrO_2,[121] TiO_2,[122] Cr_2O_3,[123] Ga_2O_3,[124] and mixed-metal oxides Al_2O_3-Ga_2O_3,[125] and Al_2O_3-SiO_2[126,127] have been successfully pillared in smectites to generate high surface area catalysts.

The catalytic properties of pillared clays are the result of the propping apart of the clay structure, which have an increased surface area (from *ca.* 50 to *ca.* 350 m^2g^{-1}) and pore

volume (from *ca.* 0.08 to 0.2-0.3 $cm^3 g^{-1}$). This exposes much of the interlayer region and any acid sites available to reactant molecules. The pillared structures are found to be stable up to 500-700 °C.[120, 127-129]

In contrast, the potential uses of PILCs demonstrate that the variation of the pillaring procedure can affect the properties of the resulting material.[130,131] One approach to varying the nature of the matrix is by acid activation, which further improves the surface area (up to 400 $m^2 g^{-1}$) and gives higher acidity values. Such acid-modified materials can be subsequently pillared and the resulting pillared acid-activated clays (PAACs) possess enhanced chemical and physical properties compared to those of conventional PILCs.[22,132,133] The truth of this assertion has been confirmed by an enhanced catalytic activity of PAACs, which showed to be better catalysts that those derived from acid-treated clays or PILCs, towards the dehydration of butan-1-ol and pentan-1-ol, alkylation of benzene by dodec-1-ene and conversion of cumene,[22,133,134] as well as improved adsorption of chlorophyll from edible oils.[135]

2.9 Clay-Organic Cation Interactions

The exchange cations can also be replaced with different organic cations by a simple ion exchange. A variety of organic cations may be used in this regard to form organoclays that, unlike natural clay, are effective adsorbents for removing organic contaminants from water.[13,15,136-141] One class of organic cations that have been widely used to synthesise organoclays are quaternary ammonium cations (QUATs) of the general form:[142]

$$[(CH_3)_3NR]^+ \text{ or } [(CH_3)_2NRR']^+$$

where R and R' are aromatic or alkyl hydrocarbon species. Substituting such organic cations for native metal cations drastically alters the surface properties of the clay, which change from hydrophilic to organophilic. This occurs because the heat of hydration of the organic cations is very low so that they do not attract water, and because of the substantial amount of organic carbon associated with the clay surface and interlayers. Additionally, the intercalated organic cations act as pillars to prop open the aluminosilicate sheets resulting in greater interlayer spacing that do not change substantially in the presence of water.

2.9.1 Nature of the Organocation

The interaction of quaternary alkylammonium cations (QACs) with clays is affected by the size and structure of the R group, the clay type, solution conditions and the nature of the exchange cation. In general, the interactions between clays and QACs are strong.

The synthesis or organoclays using short-chain QACs is relatively straightforward. This is because short-chain length organocations have high solubilities in water and are sorbed on the clay exclusively by cation exchange. For QACs with large hydrophobic moieties [*e.g.*, hexadecyltrimethylammonium, ($HDTMA^+$)], there are two complicating factors (i) they have a very low solubility in water so that solvents such as methanol may be needed to dissolve the organic modifiers and (ii) both a cation exchange and non-exchange mechanism may contribute to the overall adsorption of such organocations by clays. The non-exchange adsorption of QACs is due to non-electrostatic interactions between the alkyl moieties (tails) of QACs that have bound to the clay surface by cation exchange and the alkyl tails of QACs that have not undergone ion exchange.

Depending on the size of the organic cations and the layer charge of the mineral, the alkyl chain of organic cations may form flat lying monolayer, bilayer, pseudotrimolecular layer, or paraffin complexes.[138,143,144] These types of interlayer alkylammonium complexes are illustrated in Figure 11. From the figure it is clear that both sides of the organocation in a monolayer arrangement contact the basal surface, only one side of the QACs in the bilayers contacts the surface directly and no direct contact between basal surface and the alkyl chain occurs in a paraffin configuration.[143,144]

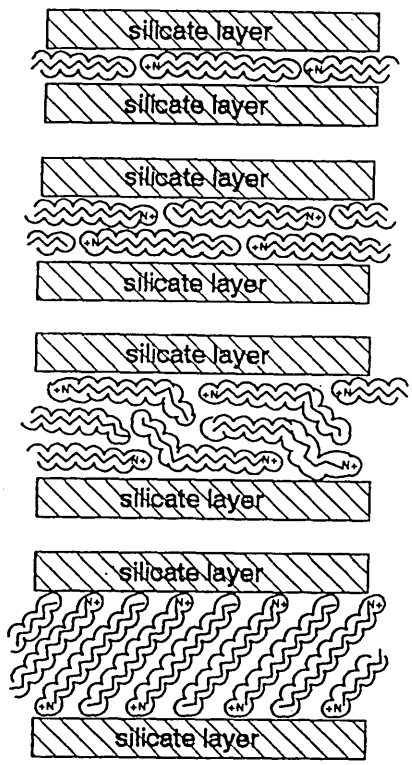

Figure 11. Alkylammonium expansion of expansible clay minerals.[138]

Cowan and White[145] studied the adsorption of straight-chain monoalkylammonium salts by Na-Bentonites. A linear relationship between the change in the free energy and the number of

carbon atoms in the aliphatic chain was found. The increment in the free energy was ascribed to van der Waals interactions. Consequently, a mechanism of the exchange process was proposed, in which the length of the hydrocarbon chain was considered to play the most important role.

Similarly, Theng, *et al.*,[146] reported the replacement of the resident cations (Na^+, Ca^{2+}) on montmorillonite by different alkylammonium cations. They found that the affinity of the mineral for the organic molecules was linearly correlated to molecular weight with the exception of the smaller methylammonium and the larger quaternary ammonium ions such as tetra-n-propylammonium and tetra-n-butylammonium. Therefore, the greater the length of the alkylammonium chain, the greater is the contribution of physical, non-coulombic forces to adsorption. Within a group of primary, secondary and tertiary amines, the affinity of the alkylammonium ions for the clay decreases in the series $R_3NH^+ > R_2NH_2^+ > RNH_3^+$. Similar conclusions were reached by Vansant and Peeters.[147] The differences were explained in terms of the size and shape of the ions. In a study by Theng, *et al.*,[146] Na^+ was more easily exchanged by the organic cations than was the Ca^{2+}.

TMA^+ and $TMPA^+$ are small organic cations that form monolayers in the interlayer of both high- and low-charge smectites (Figure 12).[138] The interionic distance between nearest neighbour pairs of exchanged $TMPA^+$ should be greater in the low-charge TMPA-smectite, leaving more of the interlayer clay surface available for adsorption. Perhaps, more important than the absolute amount of mineral surface area available is the size of the adsorptive regions between the exchanged $TMPA^+$ ions, which would be greater in the low-charge clay allowing it to more effectively accommodate aromatic hydrocarbon adsorbates.[142] The charge

density of the clay mineral also affects the orientation or the adsorbed organic cation through steric effects.[148,149]

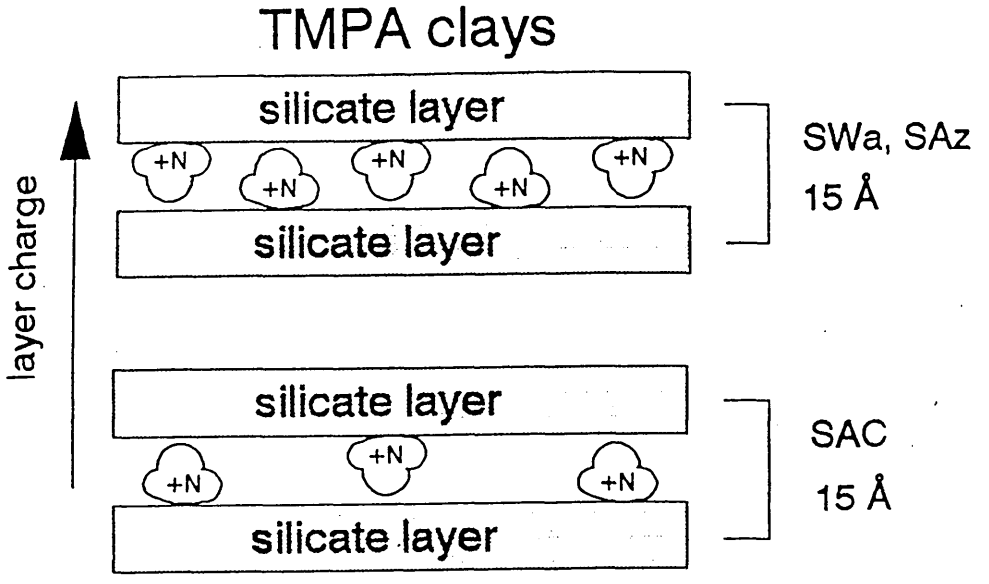

Figure 12. Trimethylphenylammonium cations in smectite layer. SWa (nontronite, Washington-USA) and SAz (montmorillonite, Arizona-USA) are high charge smectites whilst SAC (montmorillonite, American Colloid Co.) is a low charge smectite.[143,144]

Quaternary alkylammonium ions are preferentially adsorbed on to the cation-exchanges sites of montmorillonites. Thus solvents do not significantly displace the organocation from the clay, and the structure is stable in the presence of high concentrations of metal cations.[150] In this regard, Mortland and Barake[151] reported that the order or effectiveness in replacing ethylammonium ion was $Al^{3+} > Ca^{2+} > Li^{+}$.

2.9.2 Organo-Clay Complexes

Organic chemicals in surface and ground-water supplies have become a major environmental problem. Adsorption by activated carbon is widely used to remove these pollutants from drinking water. Although clays have been recognised as sorbents of such organic compounds, few studies have been conducted to determine whether certain clays could serve as practical sorbents in the treatment of water and waste-water.

The literature dealing with interactions between alkylammonium montmorillonites and organic compounds suggests that modified montmorillonites may be potentially effective adsorbents to improve water quality. Interaction mechanisms of clay-organic complexes include ion exchange, protonation co-ordination/ion dipole, hydrogen bonding and van der Waals forces.

2.9.2.1 Ion Exchange

Organic complexes will be intercalated in the clay mineral structure by ion exchange with cations neutralising the negative electrical charge responsible for the CEC of the mineral. The organic molecules are positively charged because of the protonation of an amine group as in the case of alkyl amines.

In addition to the adsorption of organic compounds by ion exchange, many amines can be protonated at the clay surface.[84-86] The source of protons for this reaction are (i) exchangeable H^+ occupying exchange sites, (ii) water associated with the metal cations at exchange sites or (iii) proton transfer from another cationic species already at the clay surface.

2.9.2.2 Ion-Dipole and Co-ordination

Many polar molecules can be adsorbed on clay minerals. Depending on the nature of the saturating cation, it serves as an adsorption site by ion-dipole or as a co-ordination type of interaction.[152,153] The greater the affinity that the exchangeable cations have for electrons, the greater will be the energy of interaction with polar groups of organic molecules capable of donating electrons. Hence, transition metal cations on the exchange complex having unfilled *d* orbitals will interact strongly with electron supplying groups.[154] In the case of molecules such as water and ammonia, the solvation of the exchangeable cation on the clay surface is the most energetic and therefore the primary mechanism of adsorption.[155,156]

2.9.2.3 Hydrogen Bonding

This is an extremely important bonding process in many clay-organic complexes. Whilst it is less energetic than coulombic interactions, it becomes very significant particularly in large molecules where additive bonds of this type coupled with a large molecular weight may produce a relatively stable complex. Three classes of hydrogen bonds are distinguished:

Water Bridge: It involves the linking of a polar organic molecule (*e.g.*, ketone, benzoic acid, etc.) to an exchangeable metal cation through a water molecule in the primary hydration shell.[157]

Organic-Organic Hydrogen Bonding: This phenomenon appears when the exchangeable cation on the clay is an organic cation, where the possibility of interaction with another species of organic compound through hydrogen bonding exists.[158]

Clay Mineral Oxygens and Hydroxyls: It requires the interaction of molecules capable of hydrogen bonding with oxygens or hydroxyls of the clay mineral surface.

2.9.2.4 Van der Waals Forces

Van der Waals or physical forces are interactions operating between all atoms, ions or molecules, but are relatively weak. They result from attractions between oscillating dipoles in adjacent molecules. They decrease very rapidly with an increasing distance between the interacting species. They are quite significant in clay-organic complexes, particularly for organic compounds of high molecular weight.[146,147]

2.9.3 Adsorption Behaviour

If a clay mineral has metal cations occupying exchange sites, its surface is hydrophilic because of the water molecules in the hydration shell solvating the cations. Such surfaces are not good adsorbents for removing hydrophobic, poorly water-soluble organic molecules from water.

If certain organic cations are placed on the exchange complex by ion exchange, however, the surface becomes hydrophobic and, in turn, organophilic. Organic cations possessing long-chain alkyl groups are particularly able to impart the hydrophobic quality to the mineral surface.[159] Such organoclay complexes are able to sorb molecules which themselves are hydrophobic by what has been called hydrophobic bonding.[13,160] This process is essentially a non-polar interaction between the organic phase of the clay organic complex and the hydrophobic organic molecule.[149,160]

Numerous reports have been devoted to the study of organoclay complexes since the 1940's. However, only a small amount of data has been assembled regarding the quantitative aspects of the adsorption of organic molecules from aqueous solution by clay minerals. A number of scientists have shown that amines in the ionic form can penetrate between the layers of clay resulting in the production of interlamellar complexes.

Cowan and White[161] showed dodecylammonium bentonite, in a series of ethyl- to octadecyl-ammonium bentonite, to be the most active adsorbent for mono- and dihydric phenols. Slabaugh and Carter[162] reported adsorption of 31 milligrams of methanol per gram of dodecylammonium montmorillonite. Stul, *et al.*,[141] were able to adsorb 9 to 330 milligrams of hexanol and 40 to 530 milligrams of octanol per gram of dodecylammonium montmorillonite in studies conducted over a wide range of alcohol concentrations.

Mortland, *et al.*,[163] showed that phenol and its chlorinated congeners were sorbed by hexadecyltrimethylammonium ($HDTMA^+$)-smectite and hexadecylpyridinium ($HDPY^+$)-smectite in proportion to the number of chlorine atoms on the phenol structure. Thus phenol itself was not adsorbed significantly by these complexes, but trichlorophenol was strongly sorbed. In other words, as the hydrophobicity of the molecule is increased, the sorption is also increased.

Mortland, *et al.*,[163] and Boyd, *et al.*,[14] used quaternary alkylammonium cations exchanged on smectites to enhance the uptake of phenol and chlorophenols from water. They showed that in general the adsorptive capacity of modified clays exchanged with large quaternary alkylammonium ions was greatly increased, compared with that of the unmodified clays.

Charge density effects were first noted by Lee, *et al.*,[11] and Jaynes and Boyd,[164] who found that low charge TMA- and TMPA-montmorillonite generally adsorbed larger quantities of arenes, from aqueous solution, than did high-charge TMA- or TMPA-montmorillonites. A similar increase in aqueous-phase arene adsorption with decreasing surface-charge density, (and hence with an increasing area of uncharged siloxane surface) for a range of TMPA-montmorillonites led Jaynes and Boyd[138] to conclude that arenes adsorb preferentially onto the free uncharged siloxane surface. They further concluded that adsorbed $TMPA^+$ ions are not involved directly in aqueous-phase arene adsorption, but prop open the clay layers so that arenes can penetrate the interlamellar region and adsorb on the uncharged siloxane surface.

The adsorption capacity of arenes by high charge smectite was substantially improved when the clay was subjected to Li^+ charge reduction prior to exchanging with $TMPA^+$ ions.[142] Indeed, using this procedure, the surface area was enhanced and the organic carbon content in the reduced charge organoclay decreased steadily as the charge reduction process decreased. The increase in the adsorptive behaviour was because the reduced charge clays contained less $TMPA^+$, which appeared to have little direct interaction with the adsorbates, and only function to prop open the clay interlayer.

2.10 Acid-Activated Organoclays (AAOCs)

As stated in section 2.7, the catalytic properties of natural clays can be greatly modified using acid treatment, which removes the desired fraction of exchangeable cations and produces materials with enhanced surface area, acidity and porosity making them powerful catalysts for a wide range of polar reactions. Useful modifications are also obtained by exchanging the resident cations by an active metal cation (*e.g.*, Al^{3+}), see section 2.8.

In this regard, Rhodes and Brown[165] have studied the activity of acid-treated and aluminium-exchanged acid-treated clays using the formation of tetrahydropyranyl ether from 3,4-dihydropyran and methanol and the isomerisation of α-pinene to camphene and limonene as test reactions. Comparing the catalytic activities of Al^{3+}-exchanged acid-treated clays with the unexchanged acid-treated clays, they found that, there was little difference in the activity between the two clays at a treatment time > 2 h for both reactions. However, at short mid treatments times (<15 min for the polar and <1 h for the non-polar reaction), the Al^{3+}-exchange forms were significantly more active. The catalytic activity in the non-polar medium of α-pinene was optimised when the external surface area reached a maximum (Figure 13), which occurs with extensive acid leaching (4 h acid treatment, Figure 14). The catalyst at this stage has an essentially hydrophobic surface that served to attract the non-polar molecules. The maximum activity in the polar media (shown by Al^{3+}-exchanged montmorillonite) was optimised when the acidity and swelling ability of the catalyst was at a maximum because the hydrophilic clay attracts the polar reactants to the surface, where the acid centres reside. The main disadvantage of using extensively acid-leached clays is that depletion of the octahedral sheet causes a significant reduction in the number of cation-exchange sites, which is where the protons reside,[99,166] with the concomitant loss in catalytic activity.

As discussed previously in this chapter (section 2.9), the hydrophilic aluminosilicate surface of swelling clays can be rendered hydrophobic by displacing the natural occurring inorganic cations with organocations, resulting in expanded layers that creates favourable conditions for non-polar molecules to access the interlamellar spacing.

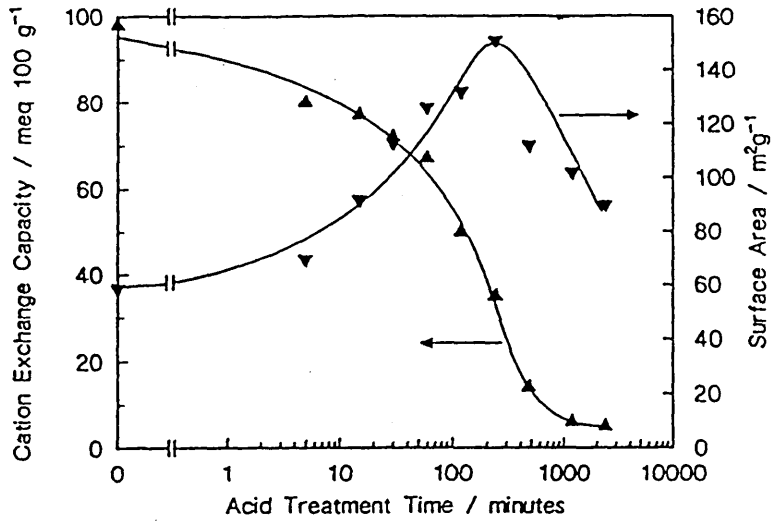

Figure 13. Showing the effect of acid treatment time on the surface area by N_2 adsorption (▼) and the CEC (▲) of Texas montmorillonite.[165]

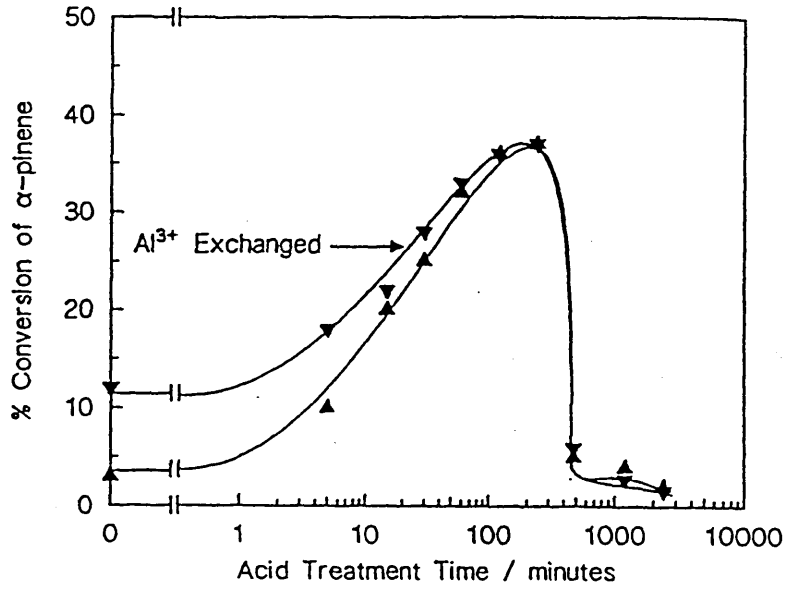

Figure 14. Showing the effect of acid treatment time on the isomerisation of α-pinene to camphene for acid treated clay (▲) and Al^{3+}-exchanged acid-activated clay (▼).[165]

Certainly, acid activation and organocation exchange can be combined to provide protons and expanded layers, which also produce a balance between the hydrophilic and organophilic character on the clay surface and produce effective catalysts that promote reactions in non-polar media.

Recently, Breen, *et al.*,[25] studied the effect of different acid treatments on the organoclays formed from clays of different initial composition and evaluated the resistance of organocation to acid leaching. The clays utilised were an aluminium-rich montmorillonite (JP), a ferruginous smectite (SWa-1) and an iron-rich beidelite (ST). The organocations used were tetramethylammonium (TMA^+), dodecyltrimethylammonium ($DDTMA^+$) and octadecyltrimethylammonium ($ODTMA^+$). These authors tested the ability of the prepared catalysts using the isomerisation of α-pinene to camphene and limonene. In general, the catalytic activity of the non-acid-treated organoclays was very low, and followed the order $TMA^+ > DDTMA^+ > ODTMA^+$. Similarly, mild acid treatment alone (0.1 M HCl for 1 h at 25 °C) did not to produce a large amount of camphene and limonene, but severe acid treatment (1 M HCl for 1 h at 95 °C) did enhance it. Moreover, mild acid treatment on the organoclays resulted in a fourfold increase in the product yield. Additionally, the conversion was further increased as the severity of acid treatment increased. Similarly, a relative increased yield was only observed in organoclays containing the smallest amounts of $DDTMA^+$ and $ODTMA^+$ (0.25 CEC) and treated with mild acid conditions, the former being more active that the latter. The activity of organoclays prepared with small amounts $DDMTA^+$ and $ODTMA^+$ was particularly more appreciable when acid treatment became more severe. In general trend, $DDMTA^+$ and $ODTMA^+$ cations were more resistant than TMA^+ to displacement by H^+.

In particular TMA^+-exchanged clays, treated at room temperature with only 0.1 M HCl, proved to be effective catalysts for the conversion of α-pinene to camphene and limonene. Total conversions of 60 to 90% were obtained making them effective competitors for zeolites and pillared clays for this isomerisation.[167] The enhanced activity was attributed to the spatial separation of the TMA^+ ions in the interlamellar spacing, which probably controlled the effective size of the catalytic site.[11] The order of activity for the clays studied was ST = SWa-1 > JP.

This study indicated that (i) acid-activated organoclays (AAOCs) were more effective when the galleries were not congested with large organocations, hence AAOCs derived from TMA^+-exchanged clays were found to be the most effective, (ii) the activity was influenced by the nature of the starting clay and (iii) that preadsorbed-TMA^+ cations appeared unexpectedly less resistant to subsequent displacement by protons.

In a similar work, Breen and Watson[24] study the influence of acid treatment on organoclays prepared using a polycation (Magnafol 206) in samples derived from a Na-montmorillonite (SWy-2) and a Ca-montmorillonite (SAz-1). The clays were first exchanged with the polycation to satisfy 0.25, 1 and 1.5 times the CEC of both clays and then acid activated using 6 M HCl at 95 °C for 30, 90 and 180 min. Acid-activated samples, absent of the polycation, were also prepared either at 25 °C or at 95 °C. They found that hot acid treatment increased the total conversion of α-pinene for both SWy-2 (77%) and SAz-1 (65%) more than cold mild acid treatment (43% for SWy-2 and 15% for SAz-1). The highest yields were achieved using a mild acid activation treatment (90 min) in clays with the lowest polycation content (0.25 CEC), total conversions of 90% and 83% for SWy-2 and SAz-1, respectively

(Figure 15). At more prolonged treatment time (180 min) the total conversion was catastrophically decreased (especially for SAz-1) because the samples presented a much-reduced polycation loading. Catalysts prepared with intermediate and high polycation loadings were, in general, less effective for the reaction process.

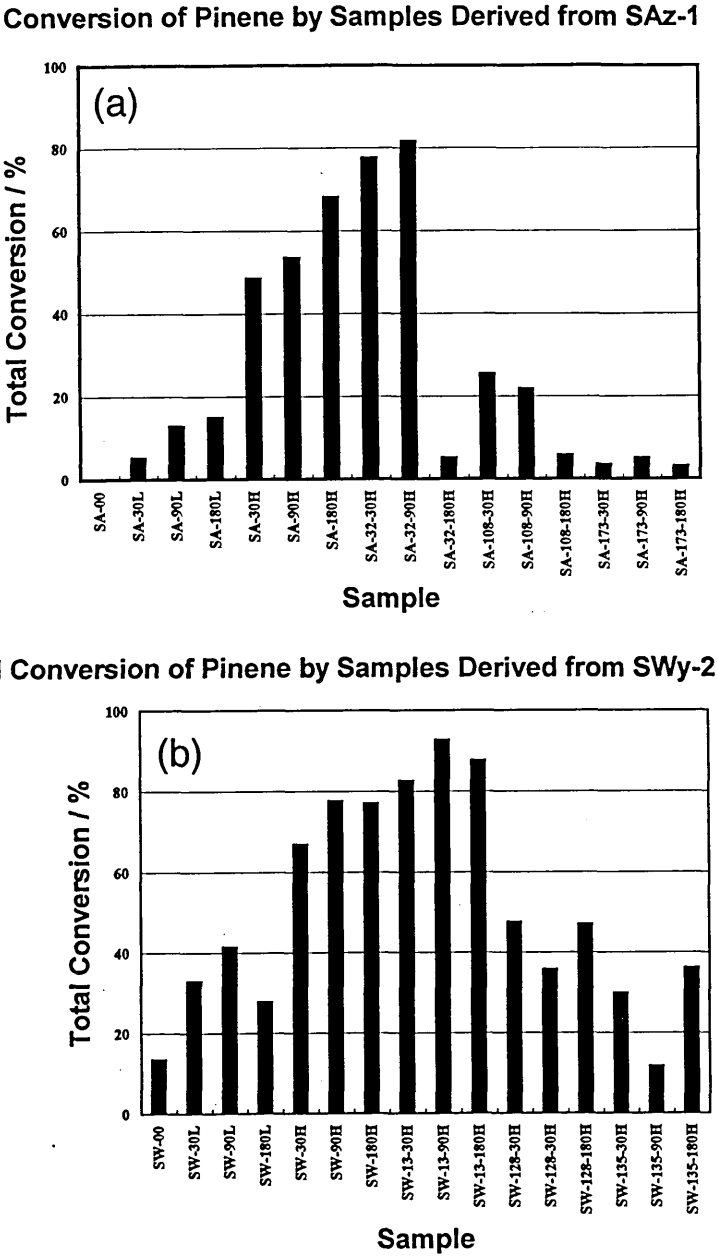

Figure 15. Total conversion of α-pinene over acid-activated clays and acid-activated polycationclays derived from (a) SAz-1 and (b) SWy-2. Samples were treated at 25 °C (low temperature, L) or at 95 °C (high temperature, H) for 30, 90 and 180 min.[24]

The presence of polycation had a more marked influence on the activity of samples derived from SAz-1 increasing the yield from 25% for acid-activated SAz-1, in the absence of polycation, to 50% camphene for acid-activated polycation exchanged SAz-1, whilst the increase in percentage of camphene formed for SWy-2 was only from 42 to 52%. Breen and Watson[24] concluded that the enhancement in yield for SAz-1 was due to the increased hydrophobicity of the polycation loaded clay, whereas the comparable yield for SWy-2 in the absence and presence of polycation may suggest that this clay disperses well in the non-polar α-pinene. Again, the conversions were comparable to those of zeolites and pillared clays for this isomerisation.[167]

Breen's studies[24,25] have demonstrated that the amount of either organocation or polycation plays a key role as well as the severity of acid treatment and the type of clay utilised. Indeed, there is a competitive mechanism between protons and organocations for the clay surface (external and internal) that governs the hydrophobic/hydrophilic character and consequently the catalytic activity. However, in both studies Breen's group has firstly fixed the amount of organocations or polycation and then displaced (partially or completely) it from the clay surface using acid treatment, without taking into consideration the preference of the clays for organocations and protons when both are present in aqueous solution.

Therefore, the central aim of this thesis has been designed to further elucidate the factors that influence the activity (based on the isomerisation of α-pinene) of AAOCs. These factors include the effect of the acid concentration on the organocations' [tetramethylammonium (TMA^+) or trimethylphenylammonium ($TMPA^+$)] loading when both protons and organocation are in aqueous solution, the charge density and locus of isomorphous

substitution of different source clays. Additionally, the competition behaviour between aluminium and organocations is investigated. Under these circumstances the resulting aluminium-activated organoclays (AlAOCs) will not have a depleting octahedral sheet and a more direct comparison will be possible.

Another route considered in this thesis is the preparation of AlAOCs using divalent organocations such as 1,4-diazabicyclo[2.2.2]octane (DABCO) and 1,5-diaminopentane (DAP). The catalytic activity of these two series of AlAOC samples will be compared with those of Al^{3+}/TMA^{+}-clays to corroborate the findings of Shabtai, *et al.*,[118] who reported that montmorillonites exchanged with DABCO possessed a higher catalytic activity for the esterification of carboxylic acids compared to ordinary alkylammonium- or α,ω-alkylenediammonium-exchanged montmorillonites. The internal surface of the modified clays were found to be available for the adsorption of nitrogen, ethane and 2,4-dimethylpentane.[168]

2.11 Isomerisation of α-Pinene

α-Pinene is known to react readily in the presence of acids, the reaction involving either ring expansion to derivatives of bornane or fenchane or ring opening to derivatives of *p*-menthane. The main products under acid conditions are camphene and limonene with a very low percentage of other isomers (Figure 16).[169-171]

De Stefanis, *et al.*,[167] have studied the reaction of terpenes over severely dehydrated zeolites and pillared clays at 100 °C for 5 h. They found that the main reaction products were: α-pinene > limonene > α-terpinene, in all the catalysts tested.

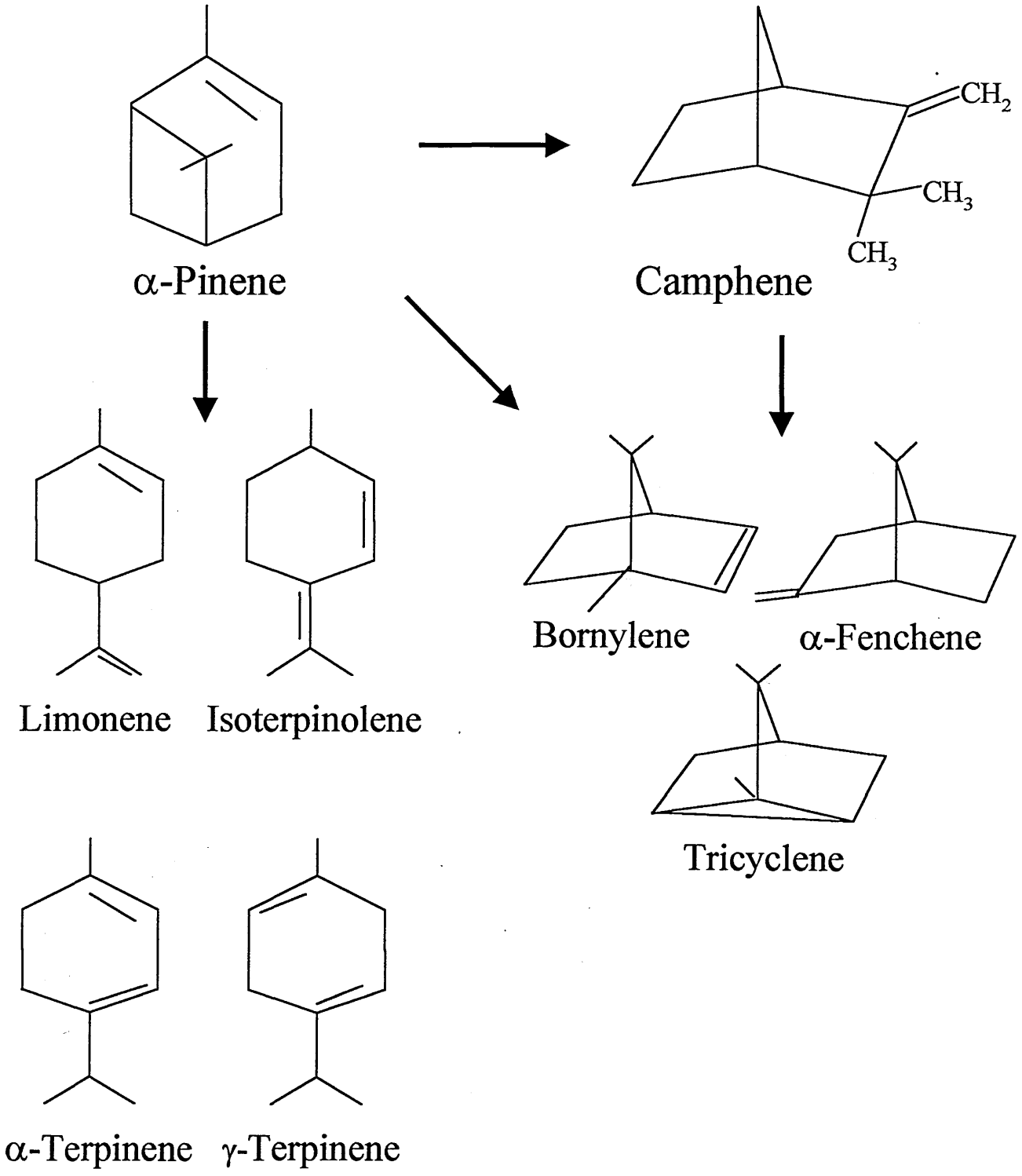

Figure 16. Isomerisation products of α-pinene.[176]

In this thesis, the α-pinene reaction has been carried out on acid-activated clays (AACs), acid-activated organoclays (AAOCs), aluminium-activated clays (AlACs), aluminium-activated organoclays (AlAOCs) and ion-exchanged clays (IECs) to evaluate and compare the catalytic activity of these novel materials. The selective conversion of α-pinene to camphene indicates a hydrophobic reaction environment, which is why it was selected for this work. The conversion of α-pinene to camphene has industrial significance because camphene is an intermediate in the synthesis of camphor, which has value due to its aroma and pharmaceutical properties.[172,173]

Acid titanium oxide is usually employed in the transformation of α-pinene to camphene,[171,173] although recent studies have considered the use of zeolites,[167,174] pillared interlayer clays (PILCs),[167] Pt-Al_2O_3 catalysts[175] and AAOCs.[25]

In this thesis, the conversion of α-pinene to camphene, via ring expansion, and limonene, via ring opening[176] is reported. Particularly interest was taken to produce cost-effective, hydrophobic catalysts of relatively high acidity using simple exchange procedures. Moreover, the ability of organoclays to swell in non-polar solvents should provide the opportunity to access a considerable portion of the interlamellar region.

2.12 Reaction of Alkenes Catalysed by Clays

M^{3+}-exchanged montmorillonites can catalyse the addition of alkenes to give products of isomerisation, oligomerisation, condensation, etherification and hydration. These reactions work best if the acidity of the clay is increased by equilibrium at low relative humidity. M^{2+}-exchange montmorillonites show some reactivity whilst M^{+}-exchange clays are essentially

unreactive,[177,178] therefore confirming that the Brønsted acidity of the clay is mainly due to dissociation of water molecules in the hydration sphere of exchangeable interlayer cations.[67]

Adams, *et al.*,[177-178] found that when refluxing hex-1-ene, hept-1-ene or oct-1-ene in a range of cation-exchanged montmorillonites, the alkenes are converted to the corresponding bis-sec-alkylether in the temperature range 44 to 72 °C. However, with an increase in temperature (100-120 °C) the reaction gave a much more complex mixture, consisting of over 40 products. Similar observations were also reported by Thomas.[179]

The reaction mechanism is represented in Figure 17, in which the role of $M^{2,3+}$-montmorillonite is to supply the proton and the water molecule. The mechanism of this reaction involves the Markovnikoff addition of water to the most stable secondary carbocation intermediate to give a molecule of the alkan-2-ol, which then reacts with another molecule of the secondary carbocation to produce the di-(alk-2-yl) ether.[3] Hydration of the olefin to the corresponding formation of alcohol is also possible.[20]

Reactions between methanol and some alkenes using M^{3+}-exchanged montmorillonites produce the petroleum anti-knock additive, methyl t-butyl ether in high yield with minor amounts of t-butanol.[180,181]

The nature of the adsorbed species derived from unsaturated hydrocarbons, adsorbed from the gas phase on clays or zeolites at room temperature is unclear so far and still remains a subject for discussion. It is natural to suggest that the reaction of a small olefin in the

presence of acidic catalyst should give rise to the olefin also, but with a long hydrocarbon skeleton.

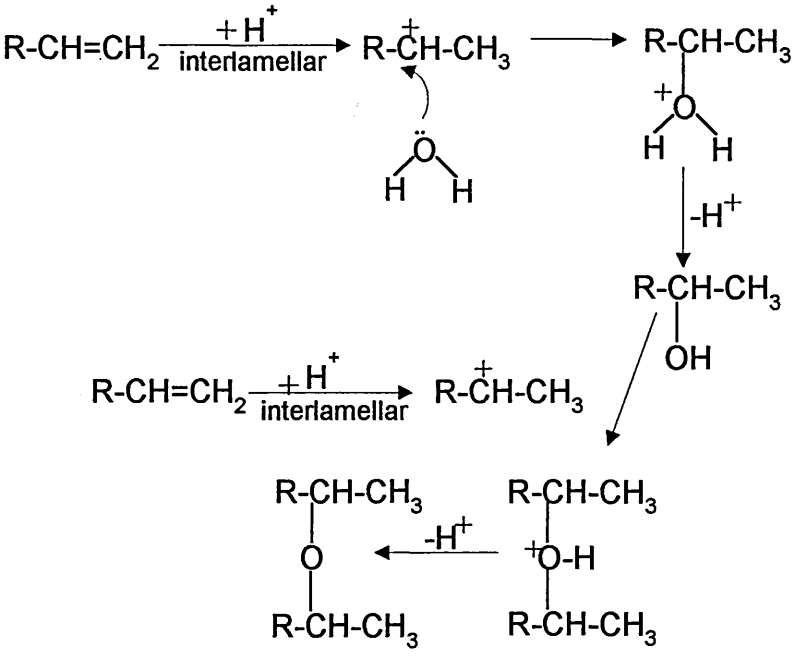

Figure 17. Reaction mechanism for the etherification of alkenes.[3]

Vogel, *et al.*,[182] studied the adsorption/reaction of iso-butene on pure and metal-substituted synthetic mica-montmorillonite (SMM) using TG analysis. The adsorption reaction was carried out isothermally at 30 °C for 1 h and then the sample heated at 3 °C min^{-1} to 500 °C. They noted that the conversion of the olefin over Ni-SMM was too low to analyse the gases evolved during the heating process. However, experiments in a micro reactor showed that at 60-70 °C the primary liquid product of iso-butene oligomerisations was a C_{12} oligomer (66%) as well as ethane, propene, propane, isomers of butene and butane, hexene and hexane in the gas phase. They concluded that the incorporation of Ni^{2+}, Co^{2+} and Zn^{2+} into the SMM increased the catalytic activity whilst the presence of water in the olefinic feed reduced it.

Choren, *et al.*,[183,184] have reported the adsorption of propylene, but-1-ene and cis-but-2-ene over clays, alumina and a porous and nonporous silica at room temperature. They stated that the alumina and silica adsorb olefins and paraffins reversibly and are unable to condense olefins. Similar observations were found for paraffins adsorbed on clays, yet olefins were strongly bonded to the clay surface and were not desorbed under vacuum conditions. Infrared spectroscopy showed that the condensation products had a paraffinic oligomeric spectrum, because of the absence of the characteristic signal from olefinic >C=C< moiety in IR spectra. However, the disappearance of the double bond could give rise to the formation of an alcohol. The lack of the signals from olefinic double bonds in adsorbed oligomers was explained in terms of the presence of carbenium ions being formed on the clay surface as a consequence of the polarised water. Nevertheless, this group was not able to identify the products formed over the catalysts utilised.

Another interesting example of this problem appears during the adsorption of ethylene on zeolites at room temperature. Stepanov, *et al.*,[185] have recently shown that ethylene oligomers strongly retained by the zeolite framework give a mixture of more than 50 hydrocarbons, with a carbon chain length range from C_5 to C_{14} and even higher carbon atoms in a molecule. They concluded that the oligomeric species existed in three interconverting states (i) long chain alkoxide, (ii) carbenium ion and (iii) olefin, with the alkoxy species being the main adsorbed form. Again, their attempts to analyse the composition of the mixture by GC-MS of the extracted hydrocarbon were not successful.

In this thesis, thermogravimetric analysis is combined with Fourier Transform Infrared Spectroscopy (Real Time TG-FTIR) and with a gas trap module connected to a gas

chromatography-mass spectrometer (TG-OTM-GC-MS) to obtain additional information of the products desorbed during the adsorption/desorption of hept-1-ene over AlACs and AlAOCs at room temperature. Supplementary, studies involve the adsorption of heptan-1-ol and heptan-2-ol to further evaluate the alkene or ether produced from the intramolecular/intermolecular dehydration of these alcohols (Figure 18).[19,186-188]

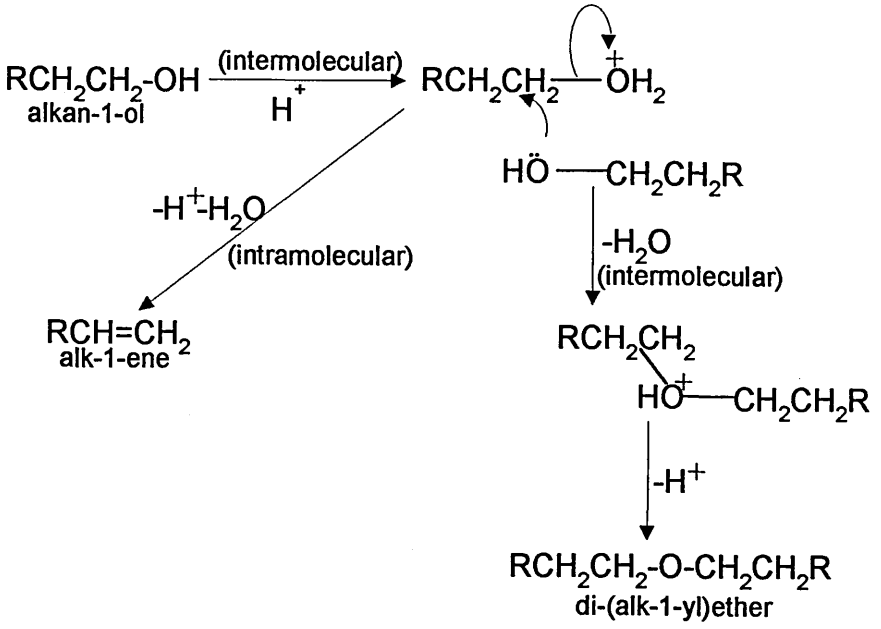

Figure 18. Reaction mechanism for the dehydration of alcohols.[19]

CHAPTER 3

Sample Preparation and Analytical Techniques

3.0 Introduction

This chapter is divided into two parts. The first part provides the details of sample preparation, *e.g.*, acid-activated clays (AACs) and acid-activated organoclays (AAOCs), aluminium-activated clays (AlACs) and aluminium-activated organoclays (AlAOCs), ion-exchanged clays (IEC) together with charge reduction and thermal activation. The second part gives the description of the analytical techniques utilised to characterise the catalysts prepared, *e.g.*, Inductively Coupled Plasma (ICP) Spectrometry, X-ray Diffraction (XRD), Thermogravimetric (TG) Analysis, Elemental Analysis and TG combined with Fourier Transform Infrared Spectroscopy (Real Time TG-FTIR), Mass Spectrometry (Real Time TG-MS) and Organic Trap Module-Gas Chromatography-Mass Spectrometry (TG-OTM-GC-MS).

Part 1 – Catalyst Preparation

3.1 Clay Minerals Investigated

Three montmorillonites and one saponite were used in this study. All clays were obtained from The Clay Mineral Repository of the Clay Mineral Society and used without further purification. The general descriptions are given in Table 3 and the elemental composition is listed in Table 4.

Sample	Mineralogy	Source
STx-1	Ca-montmorillonite	Texas-USA
SWy-2	Na-montmorillonite	Wyoming-USA
SAz-1	Ca-montmorillonite	Arizona-USA
Sap-Ca	Saponite	Ballarat, California-USA

Table 3. General descriptions of the clay mineral used in this study.

	SiO_2	Al_2O_3	MgO	Fe_2O_3	TiO_2	CaO	Na_2O	K_2O	Total
STx-1	76.65	16.80	3.56	0.78	0.05	1.76	0.38	0.020	100
SWy-2	68.04	20.60	2.77	4.63	0.09	1.76	1.70	0.41	100
SAz-1	67.72	19.74	7.24	1.59	0.27	3.16	0.07	0.21	100
Sap-Ca	61.40	5.29	28.21	1.36	0.66	1.50	1.37	0.22	100

Table 4. Clays' chemical composition

As can be seen from Table 4, the four source clays present different elemental chemical composition, charge density, and locus of isomorphous substitution. Hence, these clays are classified as: Ca-Montmorillonite (STx-1 dioctahedral, bentonite of low iron content); Na-Montmorillonite (SWy-2, dioctahedral, aluminium rich bentonite); Ca-Montmorillonite (SAz-1, dioctahedral, magnesium rich bentonite); and Ca-Saponite (Sap-Ca, trioctahedral, magnesium rich saponite). The cation-exchange capacity (CEC) of STx-1, SWy-2, SAz-1 and Sap-Ca are: 0.80, 0.87, 1.20 and 0.92 mequiv $(gclay)^{-1}$. SAz-1 has a higher charge density than STx-1 and SWy-2 even though isomorphous substitution occurs mainly in the octahedral sheet of all three. On the contrary, isomorphous substitution in Sap-Ca occurs in the tetrahedral sheet. Moreover, because of its high octahedral magnesium content, Sap-Ca will be extensively leached under the mild acid-activation conditions to be used in this work and will thus provide an interesting comparison with the activity of mildly acid-activated clays, which will lose little of their octahedral population.

3.2 Sample Preparation

3.2.1 Acid-Activated OrganoClays (AAOCs)

1 g of STx-1, SWy-2, SAz-1 or Sap-Ca H^+/TMA^+-clays were prepared by adding the raw clay to a solution containing sufficient 1 M tetramethylammonium chloride, TMACl (Aldrich, 97%) to satisfy 1 CEC and selected volumes of 12 M hydrochloric acid (Fisons, 38%) to prepare solutions with an aqueous H^+ content from 1.2 to 120 mmol (from 1.2 to 120 times the CEC). This approach was used to evaluate the effect of different acid concentrations on the organoclays formed using a fixed initial concentration of TMA^+ and to indirectly survey the competitive sorption behaviour between TMA^+ and H^+. H^+-clays were made in exactly the same way except that the TMACl was excluded. Other pre-treatments are indicated herein.

The mixture was maintained at 25 °C for 18 h, centrifuged at 17,000 rpm for 20 min and the centrifugate washed with 30 cm^3 of de-ionised water. Additionally, a set of samples was subjected to successive centrifuge-washing treatment with water, and the carbon content determined. Clay samples were dried at 120 °C overnight, and ground <0.2 mm prior to storage. The supernatant from each treatment was analysed by ICP to quantitatively determine the amount of metal cations released from the clay structures. The nomenclature used to identify the AACs or AAOCs is given in Table 5. For example, the highlighted SCa-TMA/96H sample in Table 5 indicates that Sap-Ca was treated with 1 CEC TMA^+ and 96 mmol HCl $(gclay)^{-1}$.

HCl mmol	TMA CEC	SWy-2	STx-1	SAz-1	Sap-Ca
0	0	SW-Nat	ST-Nat	SA-Nat	SCa-Nat
0	1	SW-TMA	ST-TMA	SA-TMA	SCa-TMA
12	1	SW-TMA/12H	ST-TMA/12H	SA-TMA/12H	SCa-TMA/12H
24	1	SW-TMA/24H	ST-TMA/24H	SA-TMA/24H	SCa-TMA/24H
48	1	SW-TMA/48H	ST-TMA/48H	SA-TMA/48H	SCa-TMA/48H
72	1	SW-TMA/72H	ST-TMA/72H	SA-TMA/72H	SCa-TMA/72H
96	1	SW-TMA/96H	ST-TMA/96H	SA-TMA/96H	SCa-TMA/96H
120	1	SW-TMA/120H	ST-TMA/120H	SA-TMA/120H	SCa-TMA/120H
12	0	SW-12H	ST-12H	SA-12H	SCa-12H
24	0	SW-24H	ST-24H	SA-24H	SCa-24H
48	0	SW-48H	ST-48H	SA-48H	SCa-48H
72	0	SW-72H	ST-72H	SA-72H	SCa-72H
96	0	SW-96H	ST-96H	SA-96H	SCa-96H
120	0	SW-120H	ST-120H	SA-120H	SCa-120H

Table 5. Sample identification for clays derived from the H^+ and H^+/TMA.

Additionally, samples derived from SWy-2 were acid-activated using trimethylphenylammonium ($TMPA^+$), in exactly the same way as SW-TMA/H to compare the competition behaviour of both TMA^+ and $TMPA^+$ cations against protons. In this series of samples, the same nomenclature was utilised.

3.2.2 Aluminium-Activated OrganoClays (AlAOCs)

AlAOCs were prepared by adding 1g of the same clays (as mentioned in section 3.2.1) to a solution containing 29 cm^3 of de-ionised water and selected volumes of 1 M TMACl solution and 0.1 M Al^{3+} ($AlCl_3.6H_2O$, Aldrich, 99%) in different ratios to prepare samples in which the Al^{3+}/TMA^+ ratio was systematically varied without exceeding the CEC of the chosen clays. Al^{3+}-activated clays (AlACs) were made in exactly the same way except that the TMACl was excluded. The mixtures were vigorously stirred overnight at room temperature and then centrifuged. The centrifugates were washed and centrifuged repeatedly with de-ionised water to remove excess exchanging salt. Clay samples were dried at 120 °C overnight, and ground <0.2 mm prior to storage. The designation for Al^{3+} or Al^{3+}/TMA^+ samples is given in Table 6.

Complementary AlAOC samples (from SWy-2) were prepared in the same manner as SW-Al/TMA, using 1,4-diazabicyclo[2.2.2]octane (DABCO, Aldrich, 98%) or 1,5-diaminopentane dihydrochloride (DAP, Aldrich, 99%). The diprotonated forms of DABCO and DAP were obtained by mixing each organocation with concentrated HCl to give a final solution of 1M DABCO in 2M HCl or 1M DAP in 2M HCl. In this case, the amount of aluminium offered was: 25, 50 and 75%, satisfying the remaining percentage of the CEC with $DABCOH_2^{2+}$, $DAPH_2^{2+}$ or TMA^+. The sample identification for this treatment is similar to that given in Table 6. Thus, SW-Al25/DABCO75 means that SWy-2 was treated with 25% of its CEC with Al^{3+} and 75% DABCO. This procedure was used to determine the effect of the shape and charge of the organocation on the isomerisation of α-pinene, comparing the catalytic activity data of SW-Al/DABCO and SW-Al/DAP catalysts with their SW-Al/TMA counterparts.

Al %	TMA %	SWy-2	STx-1	SAz-1	Sap-Ca
10	0	SW-Al10	ST-Al10	SA-Al10	SCa-Al10
20	0	SW-Al20	ST-Al20	SA-Al20	SCa-Al20
30	0	SW-Al30	ST-Al30	SA-Al30	SCa-Al30
40	0	SW-Al40	ST-Al40	SA-Al40	SCa-Al40
50	0	SW-Al50	ST-Al50	SA-Al50	SCa-Al50
60	0	SW-Al60	ST-Al60	SA-Al60	SCa-Al60
70	0	SW-Al70	ST-Al70	SA-Al70	SCa-Al70
80	0	SW-Al80	ST-Al80	SA-Al80	SCa-Al80
90	0	SW-Al90	ST-Al90	SA-Al90	SCa-Al90
100	0	SW-Al100	ST-Al100	SA-Al100	SCa-Al100
10	90	SW-Al10/TMA90	ST-Al10/TMA90	SA-Al10/TMA90	SCa-Al10/TMA90
20	80	SW-Al20/TMA80	ST-Al20/TMA80	SA-Al20/TMA80	SCa-Al20/TMA80
30	70	SW-Al30/TMA70	**ST-Al30/TMA70**	SA-Al30/TMA70	SCa-Al30/TMA70
40	60	SW-Al40/TMA60	ST-Al40/TMA60	SA-Al40/TMA60	SCa-Al40/TMA60
50	50	SW-Al50/TMA50	ST-Al50/TMA50	SA-Al50/TMA50	SCa-Al50/TMA50
60	40	SW-Al60/TMA40	ST-Al60/TMA40	SA-Al60/TMA40	SCa-Al60/TMA40
70	30	SW-Al70/TMA30	ST-Al70/TMA30	SA-Al70/TMA30	SCa-Al70/TMA30
80	20	SW-Al80/TMA20	ST-Al80/TMA20	SA-Al80/TMA20	SCa-Al80/TMA20
90	10	SW-Al90/TMA10	ST-Al90/TMA10	SA-Al90/TMA10	SCa-Al90/TMA10

Table 6. Sample identification for clays derived from Al^{3+} and Al^{3+}/TMA^{+} treatment. The highlighted sample means that STx-1 was exchanged with 30% CEC of Al^{3+} and 70% of TMA^{+}.

3.2.3 Reduced Charge Montmorillonite (RCM)

SAz-1 clay has a significantly higher CEC (120 mequiv/100g) than the other two montmorillonites (STx-1, 80 mequiv/100g and SWy-2, 87 mequiv/100g). Hence, in order to compare SAz-1 clay with the other two it was Li^+-saturated as follows:

The Na-form of SAz-1 was first prepared and then reduced by 30%, 50% and 70% of its original charge density (-1.14),[189] using appropriate volumes of 0.1 M LiCl solution, compensating the remaining percentage of the CEC with a 0.1 M NaCl solution. Samples were stirred overnight at room temperature and then, subsequently separated and the excess salt was removed by washing with de-ionised water until a low conductivity was detected. The Li/Na-exchanged samples were allowed to dry slowly at room temperature and then heated at 250 °C for 15 h. After cooling, the resulting clays were ground and stored in sealed sample vials. The series of reduced-charge specimens were later exchanged with aluminium (20, 50, 70 and 100% of CEC, assuming no charge reduction) as described in section 3.2.2.

Materials prepared in this manner are thereafter referred to as RCM30-20, which means that natural SAz-1 was 30% Li^+ reduced, heated at 250 °C for 15 h and finally treated with Al^{3+} = 20% of original CEC; and RCM70-100 denotes Na^+-SAz-1 was 70% Li^+ reduced, heated at 250 °C for 15 h and then treated with Al^{3+} = 100% of original CEC.

3.2.4 Ion-Exchanged Clays (IECs)

Three experimental procedures were utilised to prepare IECs:

1. 1g of SWy-2, SAz-1 and Sap-Ca, in the natural form, was ion-exchanged with Al^{3+}, Ni^{2+}, Mg^{2+}, Ca^{2+} and Na^{+}, using 29 cm^3 of de-ionised water and the exact volume from 0.1 M solutions of the metal chlorides or nitrates to satisfy the CEC. These samples were stirred overnight at room temperature, centrifuged and the resulting catalysts washed once with de-ionised water, dried, ground and stored in closed sample vials. A sample from this procedure is designated, for examples, as Nat-SW-Ni which denotes that natural SWy-2 was exchanged with Ni^{2+} = 100% of original CEC.

2. The three clays were repeatedly leached with a solution of 0.5 M NaCl, washed free of excess ions using de-ionised water until the conductivity was low (<30 μS), dried and ground. From these samples the ion-exchanged forms were obtained using procedure 1. The treatment is identified in the sample name. Thus, Na-SCa-Mg indicates that Sap-Ca was first fully Na-exchanged and then treated with Mg^{2+} = 100% of original CEC.

3. Samples, in the natural form, (1g) were fully exchanged washing them three times with 0.5 M solution of the desired metal cation (as described in 2) to convert them into 100% M^{n+}-clays.[108] A sample name for this treatment is, for example, Fully-SW-Al, which means that SWy-2 was three times treated with 0.5 M Al^{3+} solution.

3.2.5 Alkylammonium Exchange

For simplicity, the preparation details for these samples are given separately in Chapter 7.

Part 2 - Catalyst Characterisation

3.3 Inductively Coupled Plasma-Atomic Emission Spectroscopy

A Spectro (Analytical Instrument) model P, direct emission spectrometer was used to perform the analyses of the supernatants from the various preparation procedures. The five elements determined were: aluminium, calcium, iron, magnesium, and sodium.

Stock solutions were prepared by dissolution of each standard element in a minimum amount of diluted hydrochloric acid. Reference solutions were then prepared via a de-ionised water dilution of stock solutions. All were stored in polyethylene bottles.

3.4 X-Ray Diffraction Analysis XRD

X-ray diffraction (XRD) has proven to be an indispensable method for investigating clay minerals. XRD established the crystalline nature of clays in the 1920's and the basic structures of the main groups were elucidated over the following ten years. Subsequent pre-treatment methods were developed which allowed the precise characterisation of samples which contained more than one type of clay mineral.

X-ray diffraction analysis was used to monitor the structural changes occurring in the clays due to acid treatment and also to determine whether the TMA^+ cations are adsorbed onto the interlamellar surface of the clay. This information was found from monitoring changes in the d-spacing of the first order basal reflection (d_{001} spacing) using the Bragg equation:

$$n\lambda = 2d\sin\theta$$

where θ is the angle of diffraction, d is the distance between each set of atomic planes of the crystal lattice, n represents the order of diffraction (n = 1 for $d_{(001)}$) and λ is the wavelength of the X-ray beam.

XRD and VT-XRD profiles were recorded using Cu-K_α radiation (λ = 1.5418 Å) on a Philips PW1130 diffractometer operating at 30 kV and 30 mA at a 2θ scan rate of 2° min^{-1} utilising a simple heating stage for VT-XRD.[190] Samples were run as pressed powders in a depression mount or as oriented films on glass slides. The latter were heated at 100, 150, 200 and 300 °C. The samples were held at those temperatures for 20 min prior to recording the XRD trace.

3.5 Thermogravimetric Analysis

Thermogravimetry (TG) analysis provides a quantitative measurement of any weight changes associated with only thermally induced transitions. For example, TG can record the loss of weight as a function of temperature for transitions that involve dehydration or decomposition. In TG the weight of the sample is continuously recorded as the sample is subjected to a precise temperature program.[191]

Thermogravimetic analysis (TGA) was utilised to measure the thermal stability of the AAOC, AlAOC complexes and the desorption of cyclohexylamine, hept-1-ene and heptan-1-ol and heptan-2-ol. TGA was carried out in a Mettler TG 50 thermobalance equipped with a TC10A processor. 8-15 mg of samples were weighed into a ceramic crucible and subjected to a heating program from 35-800 °C at 20 °C min^{-1} under a 20 cm^3 min^{-1} nitrogen carrier gas. In general samples were conditioned in the nitrogen flow for 15 min until a stable weight was

registered. Mass losses and the negative first derivative thermograms were plotted directly after each run.

3.6 X-Ray Fluorescence Analysis XRF

XRF was utilised to estimate the chemical composition of the clays used in this study. Each sample was ground into a powder and dried at 120 °C. The dried material (500 mg) was mixed with powdered lithium-tetraborate (5 g), put into a platinum crucible and heated at 125 °C for 6 min. The mixture was then swirled to improve the mixing process, heated for a further 6 min, poured into a mould and allowed to solidify before analysis. A Philips PW 2400 XRF spectrometer was used for all the analysis. The samples were prepared and analysed by staff in the XRF unit.

3.7 Elemental Analysis

The percentages of carbon, hydrogen and nitrogen were obtained from MEDAC Ltd laboratories.

3.8 TG-FTIR

The ability to couple the thermobalance (via a heated transfer line) to an infrared spectrometer is a valuable technique for an informed complete characterisation of the gases evolved during thermal processes.

The thermal degradation of selected samples were carried out using a thermobalance (TG131, Cahn) connected through a heated transfer line to an infrared gas cell (10 cm path length) contained in an infrared (FTIR) spectrometer (Infinity Series, Mattson). Usually, 20-40 mg of

samples were place in the TG sample crucible and then heated from 25 °C to 900 °C at 20 °C min^{-1} in a dry nitrogen purge gas at atmospheric pressure (60 cm^3 min^{-1}).

3.9 Synergic Chemical Analysis

This system connects the TG-FTIR assembly through another transfer line to an adsorbent trap (VOCARB 4000, Supelco) contained in an organic trap module (OTM, Cahn). The outlet from the OTM was also coupled to a gas chromatograph-mass spectrometer (GC-MS) (Automass System 2, Unicam). The general arrangement of the synergic chemical analysis is illustrated in Figure 19.

Upon completion of the TG run, the species contained in the trap were thermally desorbed (at 250 °C for 4 min) onto the GC capillary column (DB-1, 30 m x 0.25 mm id) where the compound mixture was separated before identification by MS. The transfer lines were maintained at 250 °C throughout the analysis. In an ordinary experiment the capillary column was held at 35 °C for 4 min before ramping the temperature at 5 °C min^{-1} to 250 °C. The final temperature was held for 5 min. To ensure cleanliness of the trap, it was baked for 3 h at 300 °C before starting the subsequent analysis.[192]

3.10 Acidity Determination

In order to estimate the acid site population on AACs, AAOCs, AlACs, AlAOCs and IECs, samples were exposed to a cyclohexylamine vapour (Aldrich, 99%) at room temperature for periods in excess of 48 h using a gas jar saturator. The weight loss (from TG) observed between 240 and 350 °C was used to monitor the acidity. The number of acid sites was calculated on the assumption that one molecule of base reacts with one acid site.[85]

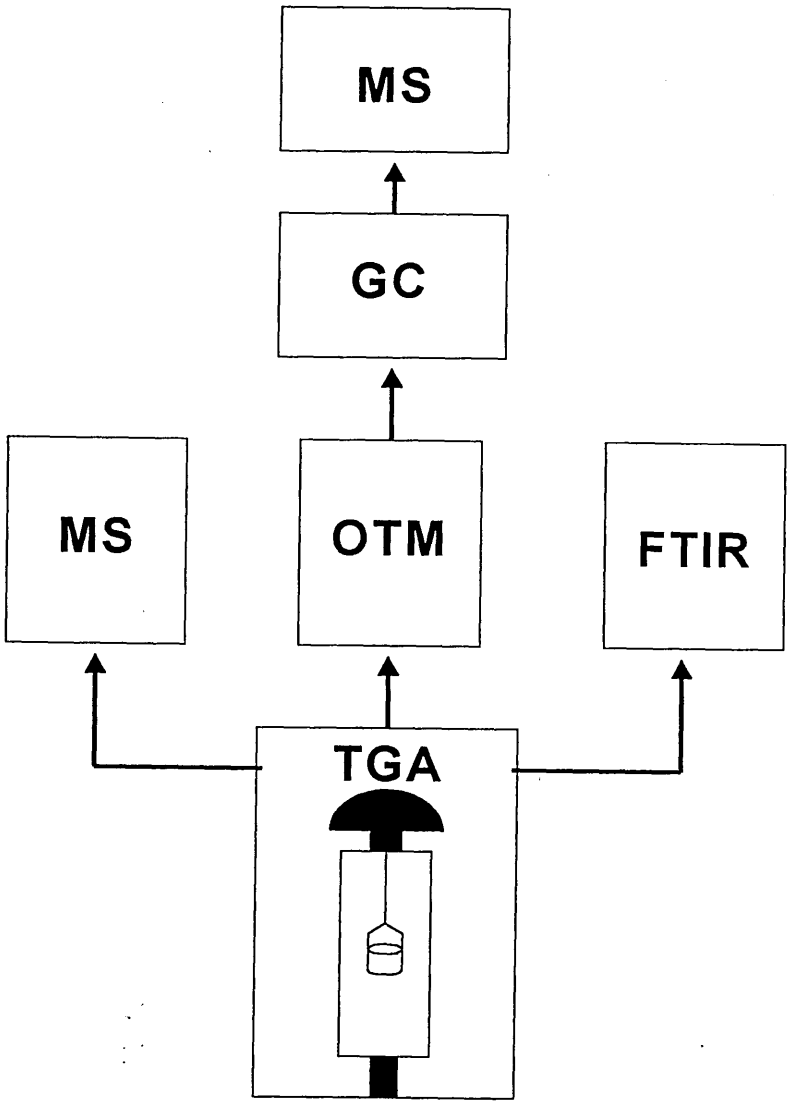

Figure 19. Schematic representation of the Synergic Chemical Analysis.

However, this treatment does not provide information on the distribution of acid sites and only gives an average of acid strength. Additionally, selected samples were analysed by Synergic chemical analysis to study the desorption profile of cyclohexylamine.

3.11 Adsorption of Hept-1-ene, Heptan-1-ol and Heptan-2-ol

AlACs and AlAOCs derived from STx-1 clay were exposed to hept-1-ene (Aldrich, 99+%) in the manner used for cyclohexylamine. The desorption profiles were monitored using TG and the identification of the products formed at room temperature was carried out using Synergic chemical analysis. Additionally, these series of samples were saturated with heptan-1-ol (Aldrich, 98%) and/or heptan-2-ol (Aldrich, 98%) to further investigate the formation of heptene from the dehydration of these alcohols.

3.12 Catalytic Activity Measurement

The catalytic activity was determined by reacting α-pinene to yield camphene and limonene as the main products. The reaction involves changes in the carbon skeleton of the molecules. Protonation of the less substituted end of the double bond of α-pinene leads to an inductively stabilised carbocation in which the cyclobutane ring strain is relieved by the migration of one of the ring bonds to the positive carbon atom. This 1,2-migration is known as a Wagner-Meerwein rearrangement.[193] The formation of camphene with its less strained structure provides the primary driving force for the rearrangement, rather than carbocation stability (Figure 20).

In order to establish the best operational conditions, the α-pinene reaction was carried out at 80, 100, 120 and 140 °C for 2 h using SW-TMA/48H. The system was not under reflux but a condenser was attached. A 1 cm^3 aliquot of the reaction mixture was taken every 15 min and analysed by GC. It was evident that increasing the reaction temperature caused a substantial increase in reactivity (Figure 21).

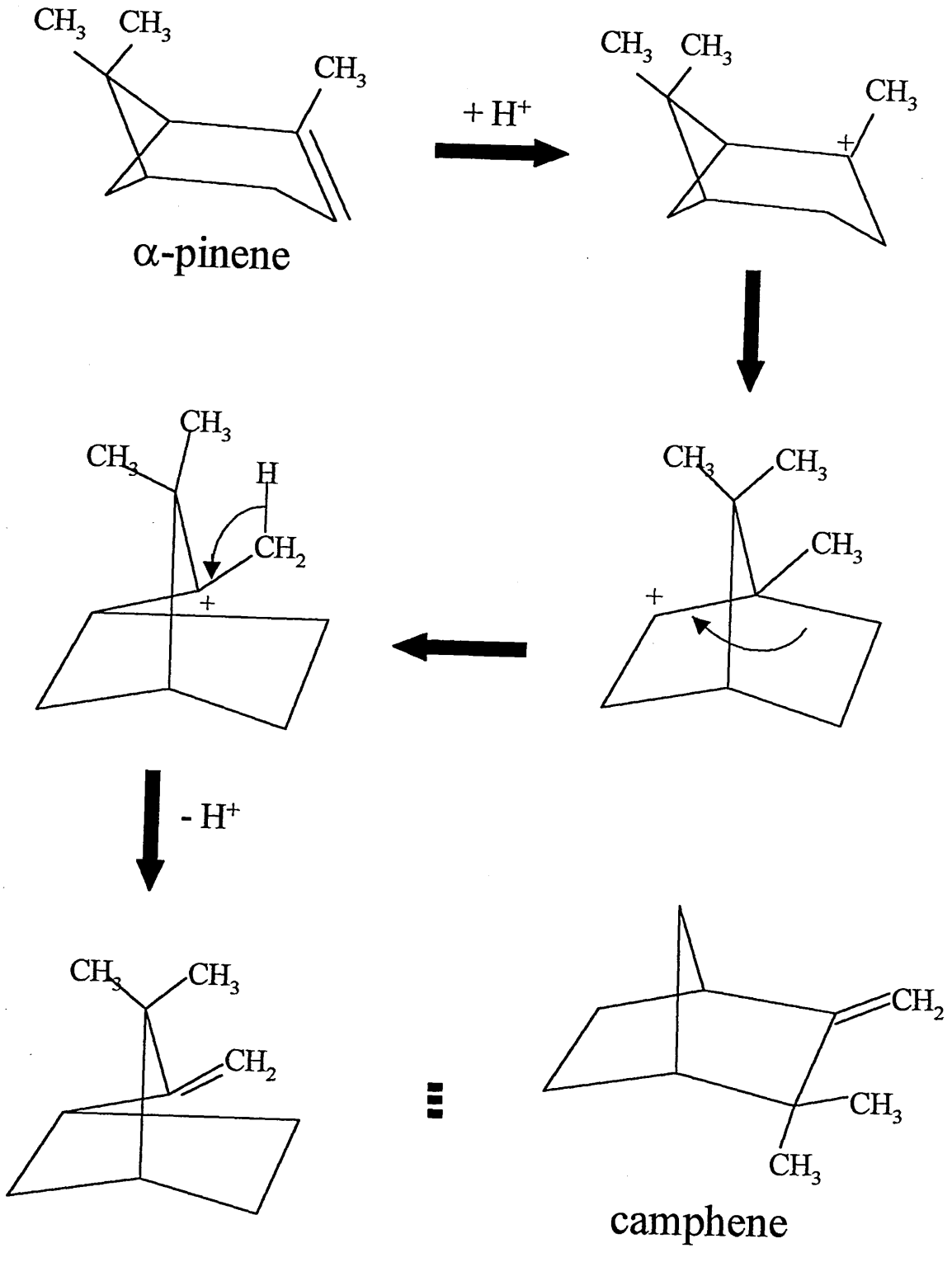

Figure 20. Mechanism for the formation of camphene.

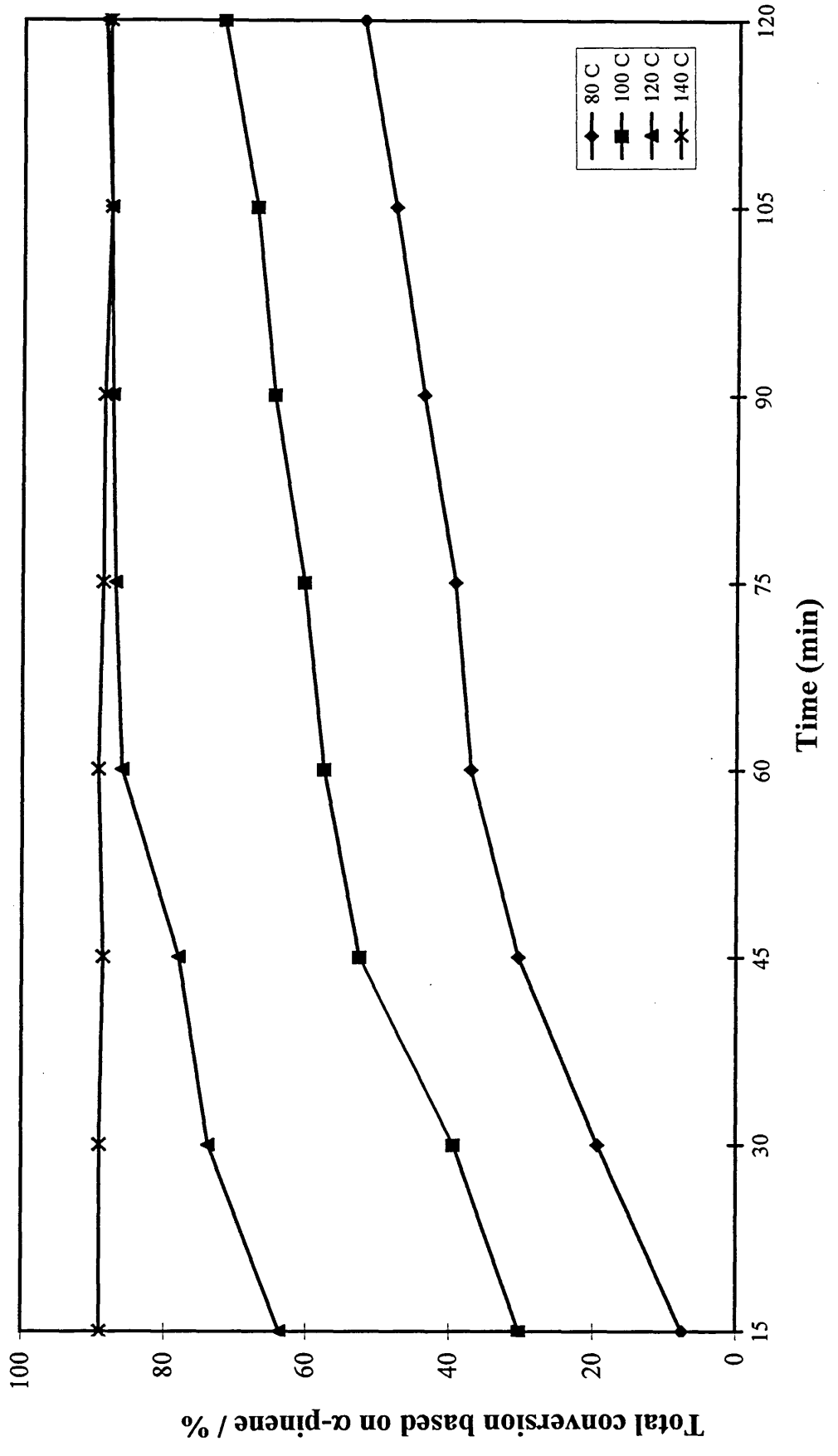

Figure 21. Total conversion of α-pinene as a function of time and reaction temperature over SW-TMA/48H.

At 80 °C and 100 °C the conversion after the first 15 min was quite low and then gradually increased to a maximum of 52% and 72% at 2 h, respectively. At 120 °C the activity changed drastically compared with that at 80 and 100 °C. A high percentage yield was initially noticed, and reached a maximum of 82% after 60 min and then remained almost constant.

At 140 °C the maximum yield was achieved in less than 15 min (90% conversion) and was invariant through the total reaction time. GC analysis confirmed that no isomerisation products occurred as a result of pre-heating the α-pinene before addition of the catalyst. Based on these preliminary results, 120 °C and 1 h, were taken as optimal conditions to carry out the α-pinene reaction for AACs, AAOCs, AlACs and AlAOCs. For IECs samples the reaction was performed at 80 °C for 2 h.[24,25]

3.12.1 Experimental Procedure

100 mg of organoclay was dried at 120 °C overnight. This was placed in stoppered containers and placed in a dessicator to cool and prevent rehydration. The catalyst was then added rapidly to the pre-heated (120 °C) 10 cm^3 (0.06 mol) of α-pinene (Aldrich 98%, used as received) and maintained at 120 °C for 1 h, using a hotplate and a sand bath to ensure an even temperature distribution. A condenser was fitted. The final solution was drawn up into a syringe and passed through a syringe filter into a dry sample vial whilst still warm.

3.12.2 Gas Chromatography

The product mixtures from the α-pinene reaction were quantified in a Perkin-Elmer 8310B gas chromatograph using a flame ionisation detector. A packed column 6'x1/8" SS,

containing 3% OV 225 chromosorb WHP mesh sized 80/100, with a nitrogen carrier gas, was used for all separations. The experimental conditions employed were: 0.2μl of the sample; isothermal for 10 min at 70 °C; injector temperature 150 °C; detector temperature 150 °C; air and hydrogen pressure of 20 psi; and nitrogen flow rate of 12 cm^3 min^{-1}.[24,25,194]

3.12.3 Gas Chromatography – Mass Spectrometry

The reaction products were identified by gas chromatography coupled with mass spectrometry (GC-MS), as described in section 3.9. The experimental conditions used are given in Table 7.[194]

Splitless injection	10 seconds
Isothermal at 50°C	10 minutes
Gradient up to 225°C	35 °C/minute
Isothermal at 225°C	10 minutes
Interface temperature	250 °C
Source temperature	130 °C
Ionisation energy	70 eV
Detector gain	750 volts
Mass range scan	4-200

Table 7. Experimental conditions of the GC-MS for the identification of the isomers' mixture.

CHAPTER 4

Characterisation and Catalytic Activity of Acid-Activated Clays and Acid-Activated OrganoClays

4.0 Introduction

As mentioned in Chapter 2 (section 2.3), the intercalated cation in naturally occurring clays is Na^+ or Ca^{2+}. Such clays are very weak catalytically, if at all. However, the catalytic properties of clays can be improved by acid activation, which increases the nitrogen surface area, the number (and type) of acid sites and the adsorptive capacity of the resulting material.[9,90-94] Additionally, the hydrophilic nature of swelling clays can be rendered hydrophobic by displacing the exchangeable inorganic cations with different organocations by simple ion exchange, giving rise to the so called organoclays. The aim of the organocations is to hold the aluminosilicate sheets of clays permanently apart and increase the interlamellar spacing.[13,15, 136-142]

Combining acid activation treatment with organocation intercalation provides a potential enhancement of the clay properties because it presents a proton rich environment when presented to organic molecules and expanded layers due to the presence of the organocation.

Breen's group has recently prepared organoclays, initially with fixed amounts of a polycation[24] or different organocations,[25] and then evaluated the resistance of polycation/organocations to acid leaching. They tested the prepared catalysts using the isomerisation of α-pinene and found that the highest yields were achieved using mild acid activation treatment in clays with the lowest polycation loading. Similarly, a relative increased yield was only observed in organoclays containing the smallest amounts of organocation treated with mild acid conditions. In general, they observed that the ability of protons to compete or displace effectively the organic aggregates from active sites was decreased at high polycation or organocations loadings. However, in both studies Breen's

group did not take into consideration the preference of the clays for organocations and protons when both are present in aqueous solution.

Therefore, in this chapter the attention has been focused to further elucidate the factors that influence the activity (based on the isomerisation of α-pinene) of acid-activated organoclays (AAOCs). These factors include the effect of the acid treatment on the organocations [tetramethylammonium (TMA^+) or trimethylphenylammonium ($TMPA^+$)] loadings when both protons and organocation (at a fixed concentration) are in aqueous solution, and the charge density and locus of isomorphous substitution of different source clays. The catalytic activity of AAOCs is compared with that prepared in the absence of organocation, in this chapter called acid-activated clays (AACs).

The clay minerals used in this section were: STx-1, SWy-2, SAz-1 and Sap-Ca. Sap-Ca differs from the other three montmorillonites in having the isomorphous substitution located in the outer tetrahedral sheet, adjacent to the surface, rather than in the octahedral sheet in the centre of the layer. The potential advantage of this is that the strength of the associated sites should be higher than in montmorillonites. A series of progressive acid-activated organoclay samples were prepared, from each clay, according to the procedure described in section 3.2.1.

Sap-Ca also possesses a higher octahedral Mg^{2+} content than the other clays and will be extensively leached under the mild acid-activation conditions used herein and will therefore provide an interesting comparison with the activity of STx-1, SWy-2, SAz-1 which have an aluminium rich octahedral sheet and will therefore only be mildly leached under the conditions used.

4.1 Catalyst Characterisation

4.1.1 Chemical Analysis

ICP analysis provided information about the metal cations displaced during acid treatment and/or TMA^+ exchanged into the clays. Figures 22 and 23 show the percentage of metal oxide released as a function of the amount of acid in the initial solution for clays derived from SAz-1 and Sap-Ca. It is well known that protons displace the resident exchange cations during mild acid treatment whilst increasing the severity of acid treatment progressively leaches the basic clay constituents -magnesium, iron, and aluminium- at similar rates.[95] Severe acid treatment is also known to increase the surface area and change the pore-size distribution whilst mild acid activation causes little damage to the silicate layer.[7,88,92,93,195]

Complete displacement of the exchangeable Na^+ and Ca^{2+} ions by H^+ (or TMA^+) was observed for all the clays, provided at least 1.2 CEC was used. ICP data also confirmed that a small portion of the total Mg^{2+} content was easily removed from SWy-2, STx-1 and SAz-1 samples suggesting the presence of Mg^{2+} on exchange sites. However, for Sap-Ca, which contains much more octahedral Mg^{2+}, significant amounts of Mg^{2+} were released at $[H^+] > 10$ mmol g^{-1}. A gradual increment in Al^{3+} was observed in the leachate from SWy-2 and STx-1 (not illustrated), although the total amount removed as a percentage of Al available was small. The addition of TMA^+ to the initial mixture had no effect on the removal of cations from SWy-2, STx-1 and SAz-1 because this was simply an ion-exchange process. However, it did increase the amount of Mg^{2+} released from Sap-Ca (Figure 23), perhaps because the TMA^+ cations propped the layers apart and facilitated the ingress of protons into the interlayer space where they could enter the layer through the ditrigonal cavity and displace

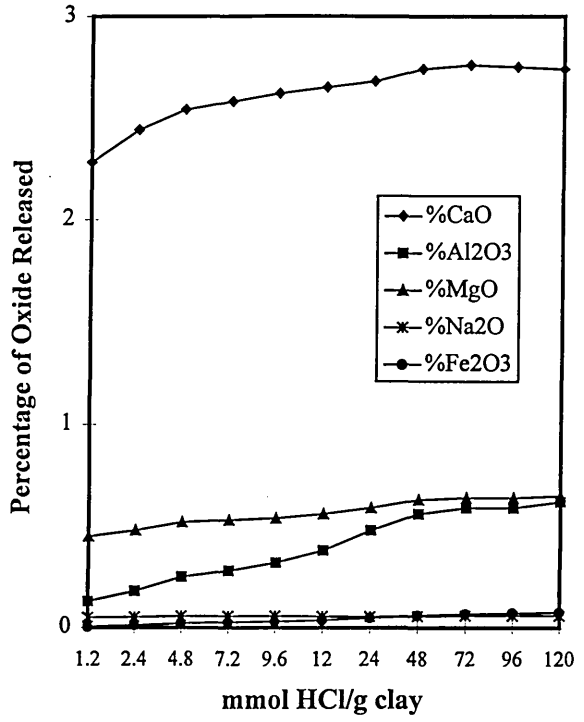

Figure 22. Percentage of oxide released during acid treatment of AAOCs derived from SAz-1 (✳) Na_2O, (◆) CaO, (■) Al_2O_3, (●) Fe_2O_3 and (▲) MgO.

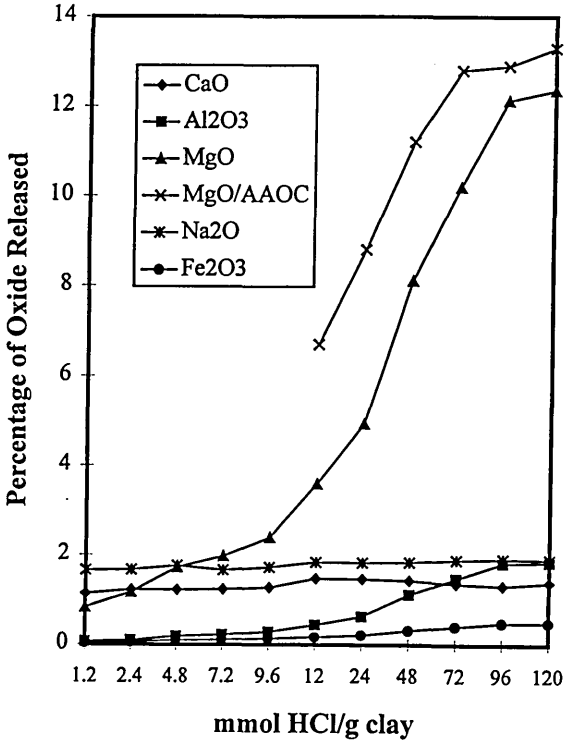

Figure 23. Percentage of oxide released during acid treatment of AACs derived from Sap-Ca (✳) Na_2O, (◆) CaO, (■) Al_2O_3, (●) Fe_2O_3, (▲) MgO and (x) MgO/AAOC.

Mg^{2+}. Breen, *et al.*,[25] found that octahedral depopulation was retarded when the gallery is fully occupied by alkyltrimethylammonium cations. Thus, the nature of the organocation has an influential role to play in the preparation of AAOCs.

4.1.2 XRF Determinations

The relationship between the amount of cation released (reported as percentage of metal oxide) using 120 mmol of H^+ and the total available metal oxide content, determined by XRF[194] is listed in Table 8. For example 54.8% of the available MgO content (28.2 wt %MgO) of saponite was released which means that there is still 12.8 wt %MgO remaining in the leached clay. It can clearly be seen that Sap-Ca was substantially affected by the acid treatment. The relatively high percentage of Mg^{2+} and Fe^{3+} released from SWy-2 is due to Mg^{2+} cations on exchange sites and dissolution of Fe-containing impurities.

	SWy-2	STx-1	SAz-1	Sap-Ca
$\%Na_2O$	66.4 (1.70)	84.2 (0.38)	66.6 (0.07)	96.5 (1.37)
%CaO	91.0 (1.76)	83.5 (1.76)	94.6 (3.16)	98.4 (1.50)
%MgO	18.0 (2.77)	10.3 (3.56)	9.6 (7.24)	54.8 (28.2)
$\%Al_2O_3$	1.5 (20.6)	2.2 (16.8)	3.4 (19.7)	43.9 (5.29)
$\%Fe_2O_3$	8.5 (4.63)	5.1 (0.78)	2.5 (1.59)	42.9 (1.36)

Table 8. Percent of available oxide released from the clay at 120 mmol H^+. Figures in parentheses represent the actual weight percentage of the oxide in the clay structure.

4.1.3 X-Ray Diffraction

The X-ray powder diffractograms of SWy-2 (SW-TMA/12H, SW-TMA/72H and SW-TMA/120H) and similar series of samples derived from Sap-Ca are shown in Figures 24 and 25, respectively. The d-spacings were 13.5, 13.8 and 13.7 Å for SWy-2 and 13.7, 13.5 and

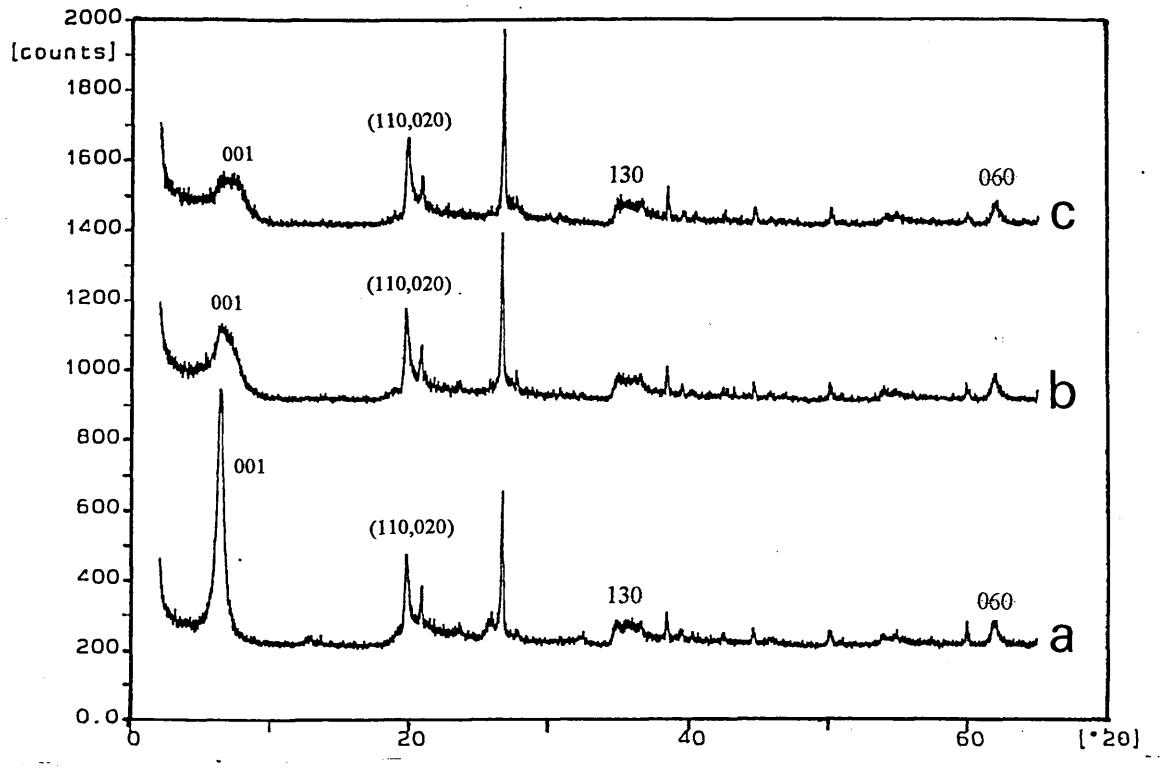

Figure 24. XRD traces for (a) SW-TMA/12H, (b) SW-TMA/72H and (c) SW-TMA/120H.

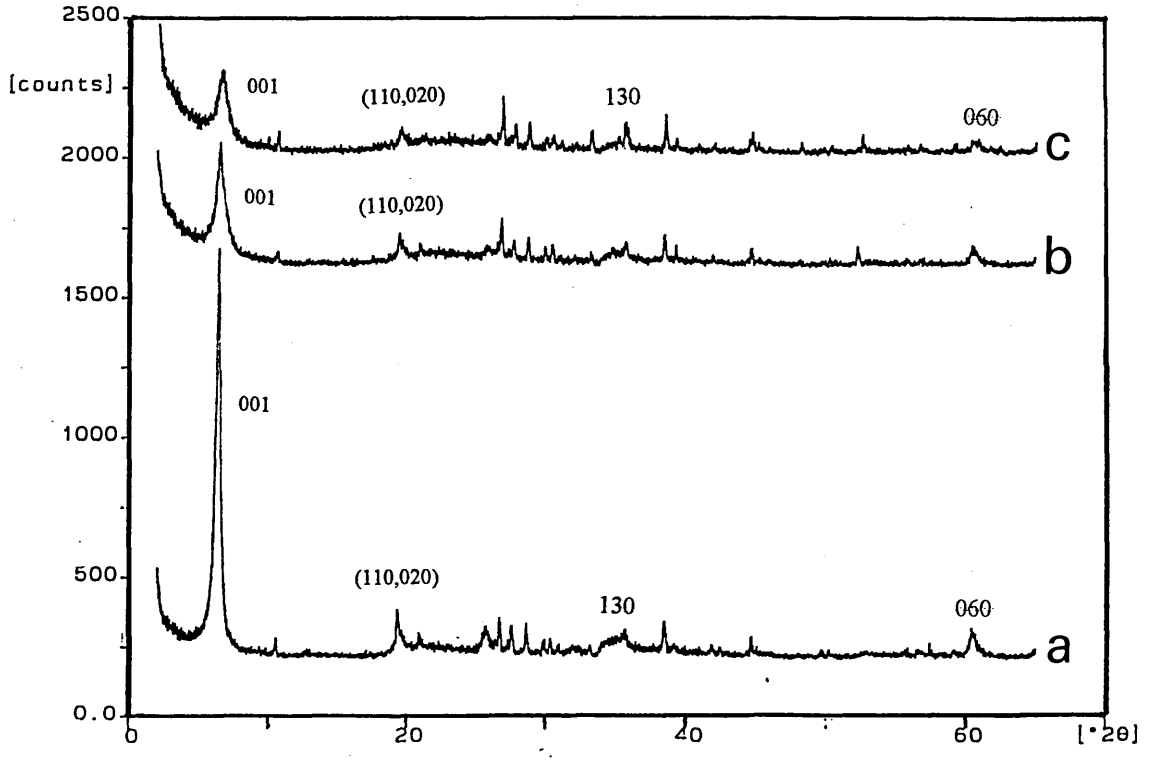

Figure 25. XRD traces for (a) SCa-TMA/12H, (b) SCa-TMA/72H and (c) SCa-TMA/120H.

13.3 Å for Sap-Ca samples. The d-spacings were essentially the same although a small reduction was observed at higher acid concentrations.

The diffraction traces for these samples exhibited narrow and intense 001 peaks, together with several higher order reflections. After acid treatment with 72 and 120 mmol H^+, the 001 reflections together with higher 00*l* reflections were weaker and much broader as the acid treatment used became more severe, suggesting that the acid-activated organoclay samples became more substantially disordered than the parent clay materials. The transformation to pure silica was not complete for SWy-2 samples because the 001 peak was still present together with *hk*0 reflections near 20° and 35° (2θ) and the 060 peak near 62° (θ). Nonetheless, these peaks become less pronounced as the severity of acid treatment increased (120 mmol H^+), particularly for Sap-Ca samples, indicating that its structure has been considerably affected. Evidence of crystalline impurities such quartz was found in these samples, mainly because no extensive purification procedure was carried out.

4.1.4 Thermogravimetric Analysis of the Organoclay Complexes

Organoclay complexes were characterised by thermogravimetric analysis to establish their thermal stability.

In Figure 26 a typical thermogram of an organoclay is plotted, which includes the weight loss and the negative first derivative curve. The derivative curve shows three maxima. The first region, at lower temperature corresponds to the loss of interlayer water, and reaches a maximum at 90 °C. The second region of the curve is attributed to the desorption/breakdown of the organocation (TMA^+) from 300 °C to 440 °C.

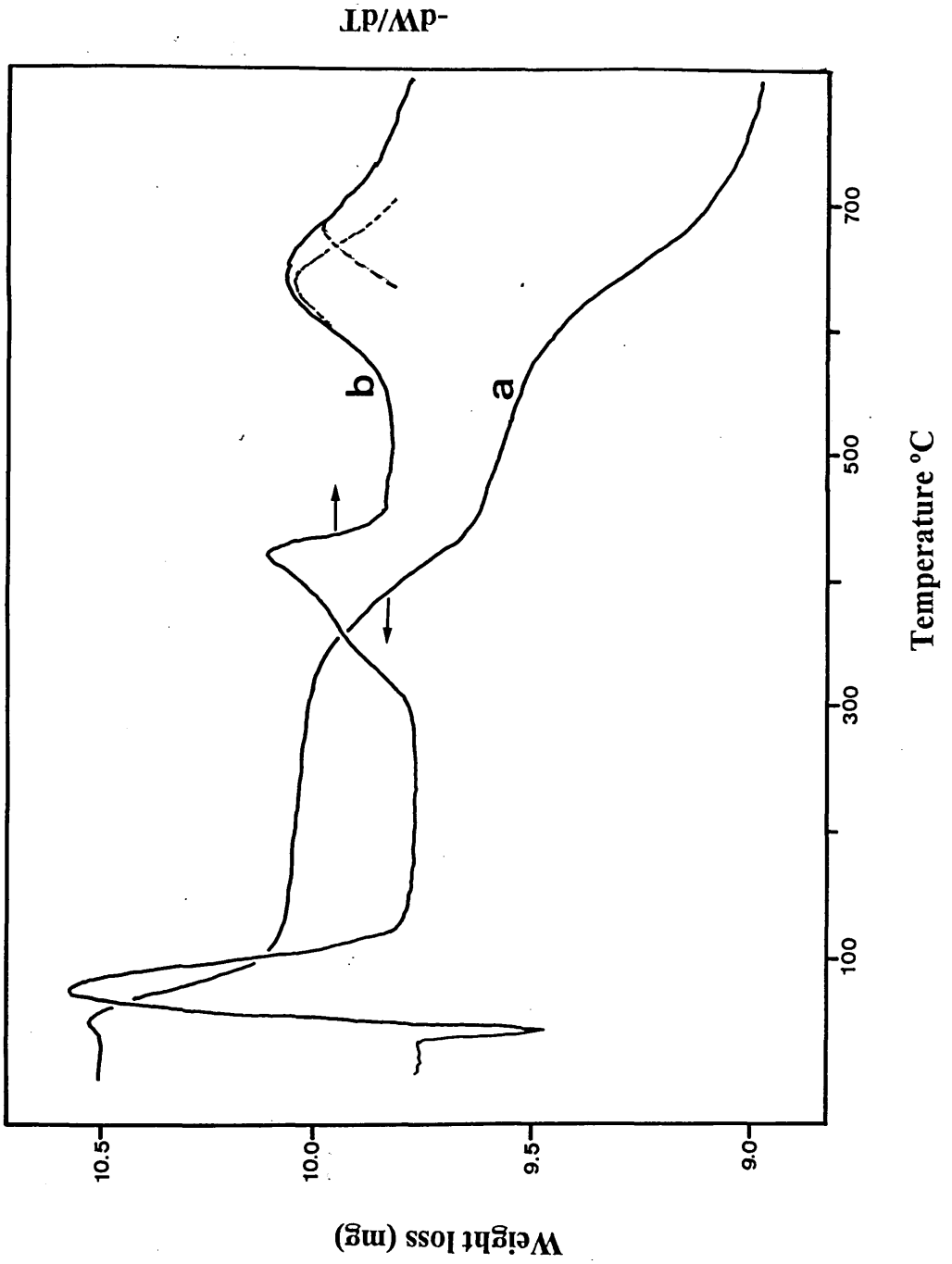

Figure 26. Typical thermogram of an organoclay (SW-TMA/12H). (a) weight loss curve and (b) negative first derivative curve.

The third region is associated with both the losses of strongly adsorbed water and structural hydroxyl groups[84] along with the evolution of CO_2 from residual carbonaceous deposits of the organocation. The latter, seen as a broad peak, is observed between 560 and 800 °C. In this region, the CO_2 evolution and dehydroxylation maxima at 640 °C appear in a unique band in which both species are overlapped, as shown by the dotted lines drawn for schematic purposes.

Figure 27a shows the thermogram of untreated SWy-2 clay, where only the maxima at 90 °C and at 700 °C are observed. Acid-activated organoclays show these two peaks alone with that of TMA^+ between 300-420 °C (Figures 27b-e). The assumption pointed out in the paragraph above that the evolution of CO_2 and the dehydroxylation are overlapped is clearer in Figure 27. If the thermogram of the untreated SWy-2 sample is compared with one of the acid-activated organoclays, it is evident that the maximum at 700 °C for the former is shifted to the lower temperature of 640 °C in the latter, commencing at 530 °C and extended up to 730 °C.

These results indicate that TMA^+ is present in the clay structure and that the complexes are thermally stable up to 300 °C. The reduction in the TMA^+ maximum with increasing $[H^+]$ confirms that H^+ was able to compete with TMA^+ when the $[H^+]$ level was high. The amount of TMA^+ present in the H^+/TMA^+-samples was, semi-quantitatively, determined using TGA and followed the order: SAz-1 > SWy-2 = STx-1 > Sap-Ca in all cases. The calculations were done subtracting the weight losses at 320 °C and at 480 °C, then the amount (in mg) was divided by the molecular weight of the organocation and the weight of sample (in mg) and

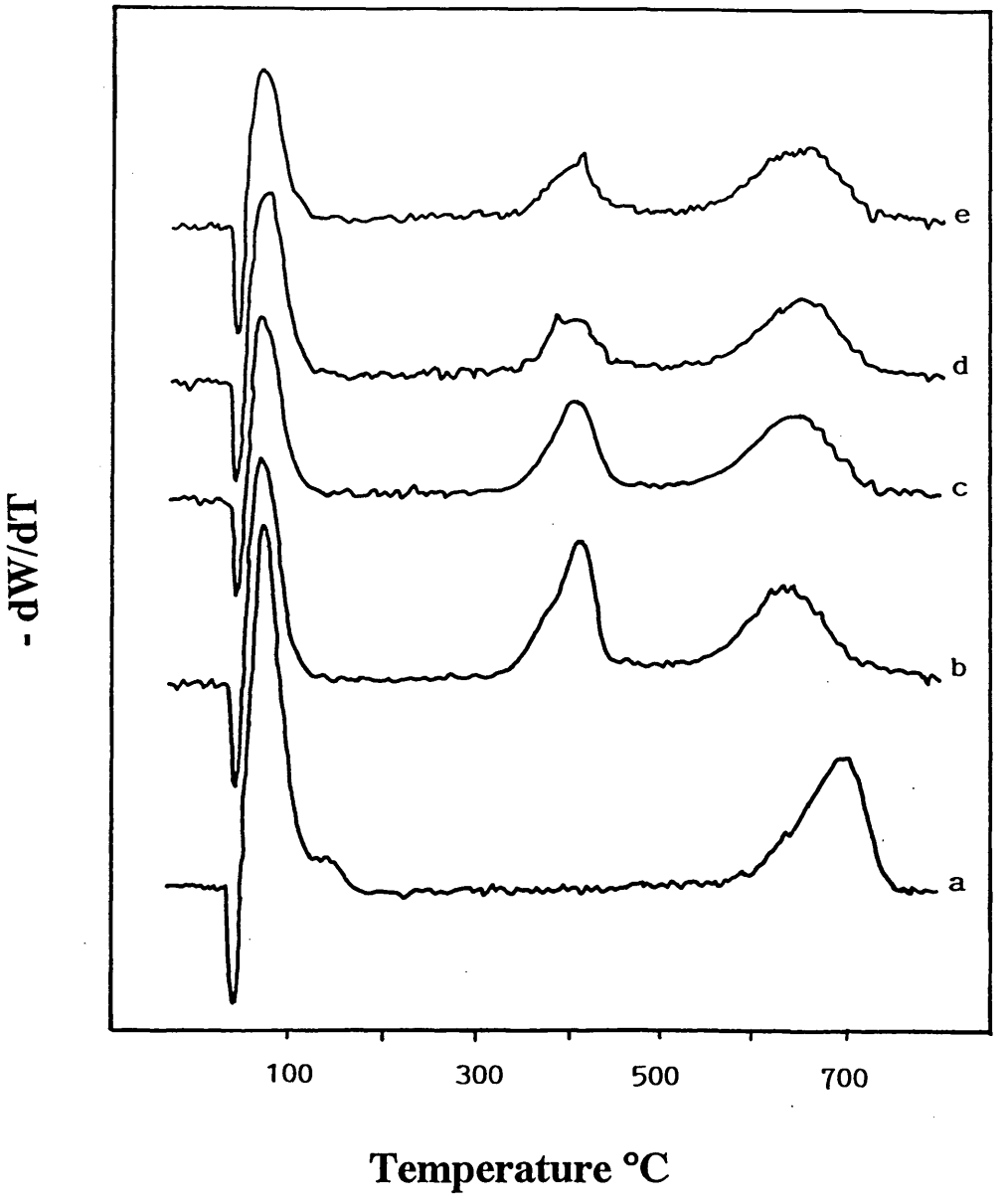

Figure 27. Derivative thermograms for (a) untreated SWy-2, (b) SW-TMA/12H, (c) SW-TMA/24H, (d) SW-TMA/96H, and (e) SW-TMA/120H.

finally divided by the CEC of the clay and multiplied by 100. This gives an approximate idea of the percentage contribution of the organocation to the CEC of the clay.

Moreover, the amount of TMA^+ in SAz-1, SWy-2 and STx-1 was high even when in competition with substantially higher amounts of acid. The TMA^+ content (as %CEC) remaining in the clays after activation (Table 9) reinforces the TMA^+ cations' remarkable resistance to displacement by protons. A considerable amount of TMA^+ was present in SWy-2, STx-1 and SAz-1 when only 1 mmol TMA^+ was competing with 120 mmol H^+.

	SW-TMA	ST-TMA	SA-TMA	SCa-TMA
0 mmol H^+	44	37	37	25
1.2 mmol H^+	50	42	52	34
12 mmol H^+	42	37	45	26
24 mmol H^+	32	37	45	22
48 mmol H^+	30	26	40	22
72 mmol H^+	26	24	38	21
96 mmol H^+	24	24	36	17
120 mmol H^+	24	24	35	16

Table 9. Percentage of TMA^+ to initial CEC present in the samples after activation.

Indeed, the amount of TMA^+ on the exchange sites was increased by small quantities of acid (Table 9). This increment was more marked in SAz-1, which in all cases showed the highest affinity for TMA^+ cations, even at severe acid activation treatment. This observation, perhaps, can be explained in terms of differences in charge density and in magnitude of van der Waals contribution. Certainly, Maes and Cremers[196] studied the influence of charge

density on the ion exchange equilibria and stated that the free energy of the exchange decreases linearly with the logarithm of the charge density. Therefore, the significant higher TMA^+ content detected in SAz-1 clay can be attributed to the high charge density compared to the other clays.

ICP-AES analysis of the supernatants confirmed that TMA^+ was effective at displacing Na^+-cations but less able to displace Ca^{2+} and Mg^{2+}. These results are in line with those reported by Theng, *et al.*,[146] who found that Na^+ was more easily exchanged by the organic cations than was the Ca^{2+}. This conclusion is further supported if one compares the significantly higher value of TMA^+ in SWy-2, where no acid was added, with those of the other clays. SWy-2 is a Na/Ca-montmorillonite whilst the others are Ca-clays. As a result, TMA^+ easily displaces the exchangeable Na^+ ions in SWy-2 than Ca^{2+} in the other clays. Additionally, it appears that TMA^+ was able to displace some of the protons, which had already replaced Ca^{2+} and Mg^{2+} ions. Much less TMA^+ was retained in the Sap-Ca samples because the number of cations on exchange sites decreased as the layer was leached.

In order to determine the effect of the washing process on the retention of TMA^+ in AAOCs, SA-TMA/24H sample was subjected to six-successive centrifuge-washing treatments with water, as described in section 3.2.1. A portion of the washed clay was removed at each stage and analysed for carbon, nitrogen and hydrogen as well as TG analysis, for selected samples. The results are summarised in Table 10. The figures indicated that 0.66 mequiv of TMA^+ per gram of clay was initially present on the prepared sample prior to washing treatment; that after the single washing the TMA^+ decreased to 0.60 mequiv g^{-1} and no significant removal of the cation was observed with further centrifuge-washing treatment.

Washes	%C	%H	%N	TMA(CEC)
None	3.27	2.14	0.94	
1	3.12	2.08	0.96	47
2	3.09	2.05	0.93	
3	3.12	2.06	0.92	47
4	3.06	2.05	0.90	
5	3.13	2.09	0.91	
6	3.14	2.08	0.94	48

Table 10. Effect of the washing treatment on the TMA^+ retention.

Similar findings were reported by Vansant and Uytterhoeven[197] and by Kinter and Diamond.[198] The latter authors pointed out that intercalated organocations are occupying the exchangeable sites and a small fraction may be partially embedded in the oxygen-ring cavities of the clay surface, where it is thought that such embedding may, perhaps, account for the ability of the clay to retain the organocation against the subsequent washing treatment.[198]

Additional proof of the high retention power of alkylammonium cations were given by Mortland and Barake[151] who investigated the exchangeability of ethylammonium ions on montmorillonite by Li^+, Ca^{2+} and Al^{3+} ions. They stated that the ability of the metal ions to displace the organocation decreased in the order $Al^{3+} > Ca^{2+} > Li^+$.

The derivative thermograms of acid-activated organoclays derived from SWy-2 using trimethylphenylammonium ($TMPA^+$) are shown in Figure 28. Three maxima at approximately 300, 580 and 700 °C are clearly observed. They can be attributed to (i) desorption and breakdown[83] of $TMPA^+$ and (ii) formation of CO_2 from carbonaceous deposits combined with the dehydroxylation maximum. In this case both maxima appear well-separated, perhaps because the $TMPA^+$ produces CO_2 in two stages, the first from the phenyl-ring and the second from the methyl groups. In SW-TMA/H samples the desorption/breakdown of TMA^+ gradually decreased as the acid concentration increased (Figure 27).

Elemental chemical analysis of SW-TMPA/H samples are given in Table 11. The C, H and N contents were essentially the same, which correspond to 66-71% of $TMPA^+$ in terms of the CEC for SWy-2.

Sample/Element	Carbon	Hydrogen	Nitrogen
SW-TMPA/12H	6.80	1.45	0.88
SW-TMPA/24H	6.59	1.45	0.84
SW-TMPA/48H	6.66	1.43	0.85
SW-TMPA/72H	6.55	1.42	0.84
SW-TMPA/96H	6.52	1.42	0.82
SW-TMPA/120H	6.32	1.40	0.81

Table 11. Elemental analysis for SW-TMPA/H samples.

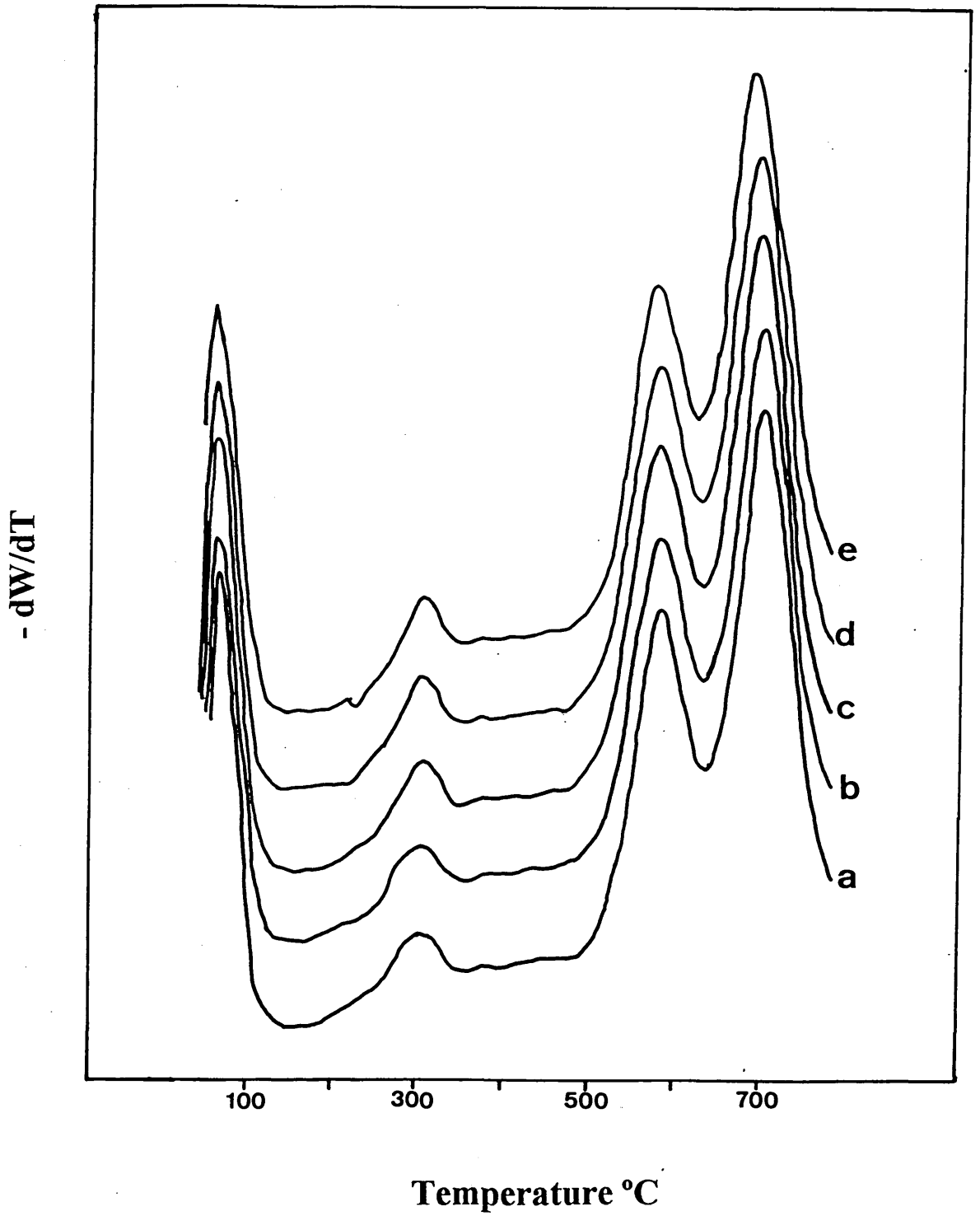

Figure 28. Derivative thermograms for (a) SW-TMPA/12H, (b) SW-TMPA/24H, (c) SW-TMPA/48H, (d) SW-TMPA/72H and (e) SW-TMPA/120H.

Additionally, VT-XRD patterns of SW-TMPA/12H and SW-TMPA/120H were taken using thin, oriented layers on glass slides under the following conditions: (a) room temperature, (b) 100 °C, (c) 150 °C, (d) 200 °C and (e) 300 °C. The results, summarised in Table 12, give values of $d_{(001)}$ in Å. The measurements were made mainly on the first order diffraction peak, higher orders being generally weak and broad (Figure 29).

	RT	100 °C	150 °C	200 °C	300 °C
SW-TMPA/12H	14.5	14.3	14.2	14.2	13.5
SW-TMPA/120H	14.4	14.2	14.2	14.1	13.1

Table 12. Values of $d_{(001)}$, in Å, of SW-TMPA/H at various temperatures.

The spacings in all cases are significantly higher than would be obtained with the usual forms of Na- or Ca-saturated smectites.[103,120] The values are maintained from 100 to 200 °C, which means that the expanded nature of TMPA-exchanged montmorillonite is stable over a wide range of temperature conditions and the d-spacing is controlled by the $TMPA^+$ content. However, at 300 °C, the d-spacing is slightly reduced by 1 Å. This indicates that the TMPA-clay complex has partially broken down.

It is obvious, from Table 12, that the increment in acid concentration has little effect on the expansion of AAOCs prepared using $TMPA^+$. One would expect a complete collapse of the clay structure (given by a considerable reduction in the d-spacing) as the severity of acid treatment was increased.

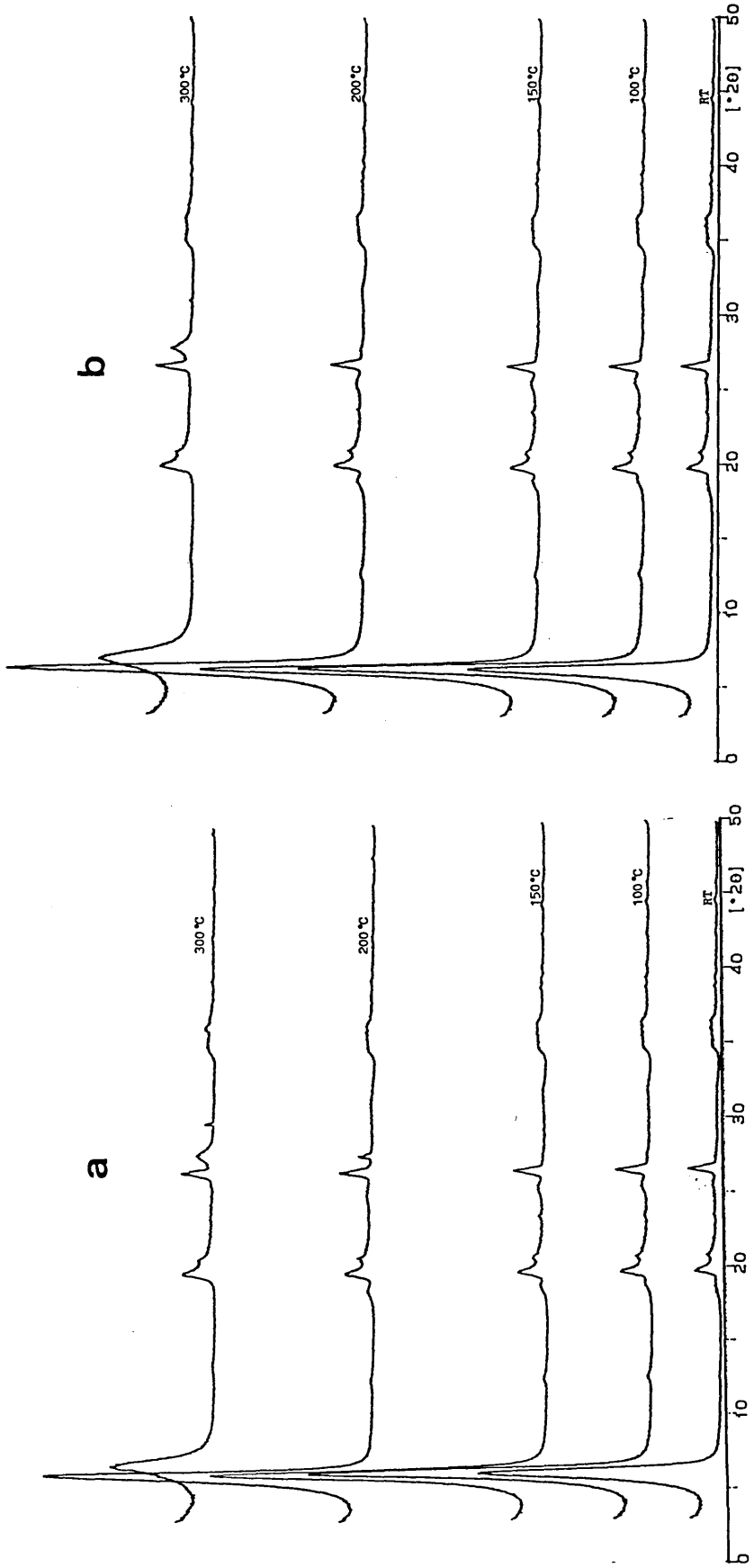

Figure 29. VT-XRD traces for (a) SW-TMPA/12H and (b) SW-TMPA/120H.

These figures, together with TGA and elemental analysis results, further support the contention that $TMPA^+$ had a higher affinity for the clay surface than TMA^+ when in competition with protons. An explanation for this apparent discrepancy is that the affinity of SWy-2 clay for alkylammonium ions is related to the molecular weight.[146,147] Therefore, $TMPA^+$ cations (FW = 136 g mol^{-1}) would compete more effectively with protons for exchangeable sites than TMA^+ cations (FW = 74 g mol^{-1}). These affinity sequences have been attributed to important van der Waals contributions and changes in the hydration state.[147] Another possibility is that the bulky phenyl group may occupy more of the siloxane surface than the methyl group[199] making more difficult the displacement by protons. More recently, Watson[194] studying the effect of acid treatment on clays treated with different organocations [tetramethylammonium (TMA^+), dodecyltrimethylammonium ($DDTMA^+$) and octadecyltrimethylammonium ($ODTMA^+$)] found similar results. The order of affinity of the organocation for the clays was $ODTMA^+ > DDTMA^+ > TMA^+$, confirming that the retention of the alkylammonium ions on clays is directly related to the molecular weight. Protons were able to displace $ODTMA^+$ and $DDTMA^+$ when the loadings of these organocations were low (0.25 CEC).

4.1.5 Desorption of Cyclohexylamine

In order to confirm the presence of protons in the H^+/TMA^+ samples, a selection of samples was exposed to cyclohexylamine vapour. Figure 30a shows that the derivative thermogram for the desorption of cyclohexylamine, from SW-TMA, exhibited three desorption maxima (prior to the dehydroxylation region), at 90, 140 and 410 °C, which correspond to the loss of physisorbed water and the desorption of cyclohexylamine and TMA^+, respectively.

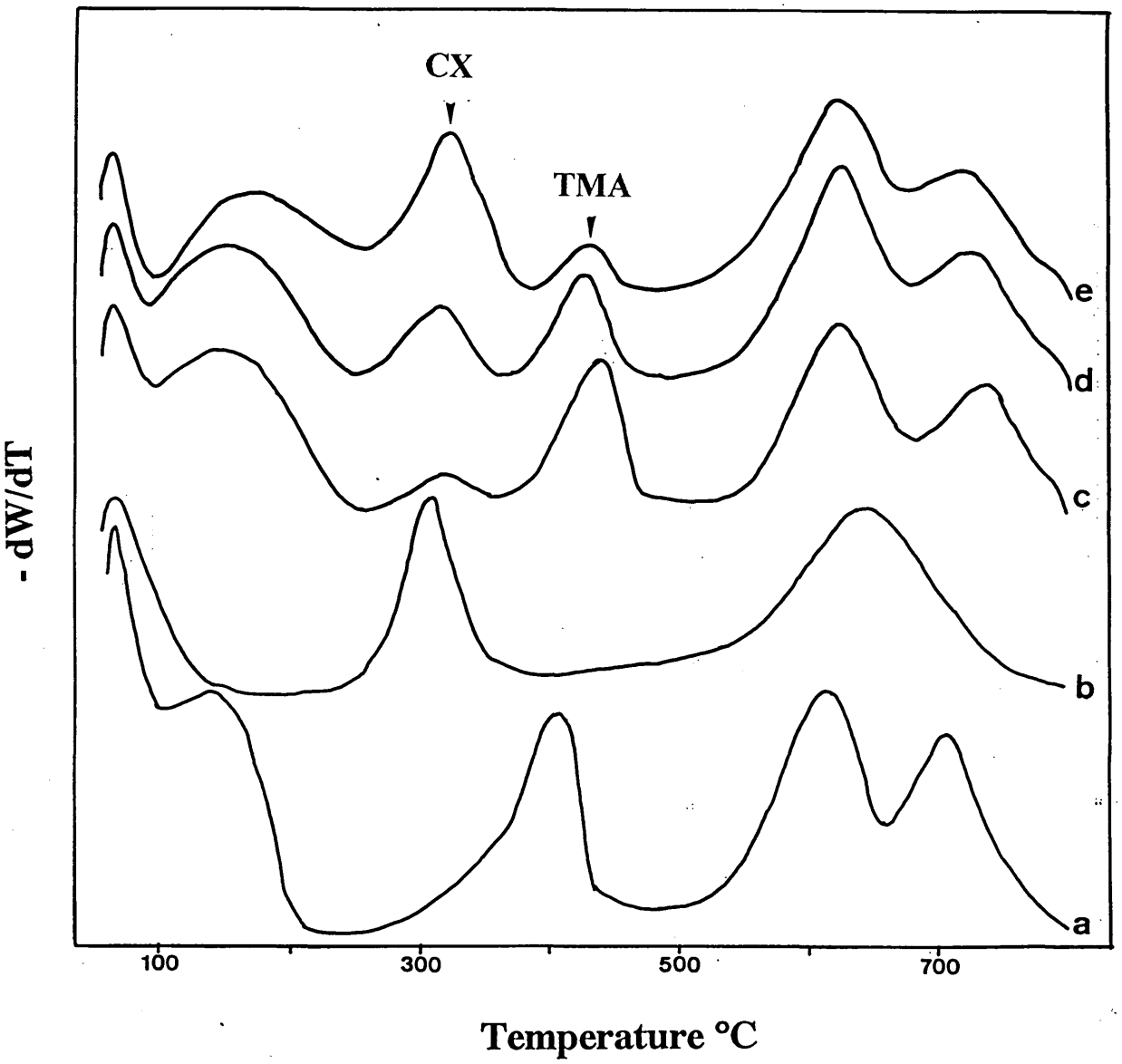

Figure 30. Desorption thermograms of cyclohexylamine on (a) SW-TMA, (b) SW-12H, (c) SW-TMA/12H, (d) SW-TMA/48H and (e) SW-TMA/120H.

Ballantine, *et al.*,[83] and Breen[85] have shown in their studies on Al^{3+}-montmorillonites and acid-activated montmorillonites that the desorption of cyclohexylamine from strong acid sites occurs near 300 °C, but there is little evidence for such a peak in this sample. This particular sample contains no protons able to interact with cyclohexylamine, and only a weak association of the base with exchange sites of TMA^+ could be established, giving rise to the desorption peak at 140 °C. Additionally, at the dehydroxylation region, two maxima are observed at 600 °C and 700 °C.

The assumptions already given for the $TMPA^+$/H system can be also utilised to explain the cyclohexylamine system in the region 560-750 °C. The peak at 600 °C could be attributed to the evolution of CO_2 from residual carbonaceous deposits derived from cyclohexylamine (present in the interlamellar space) combined with water, and that at 700 °C could be ascribed to carbon dioxide from deposits derived from TMA^+ with water evolved during the dehydroxylation process. This conclusion was reached by comparing Figure 30a with Figure 27b.

In contrast, the desorption thermogram of cyclohexylamine from an acid-treated SWy-2 (Figure 30b) did exhibit a sharp, intense peak at 320 °C corresponding to the desorption of cyclohexylamine from strong acid sites.[83] It is worth noticing that in this thermogram the broad peak between 110-220 °C was absent, which may indicate that the interaction of cyclohexylamine was, exclusively, with strong protonic sites. Additionally, in the region 550-750 °C only one broad peak is observed. This is due to CO_2 from carbonaceous deposits of cyclohexylamine combined with water evolved during the dehydroxylation. This observation supports the inferences established in the previous paragraph.

The derivative thermogram for the desorption of cyclohexylamine from SW-TMA/H samples (Figures 30c-30e) contained evidence for both protonated cyclohexylamine and TMA^+ cations, indicated as CX and TMA in Figure 30. The broad peak in the 110-220 °C region is again clearly observed, which becomes less intense and slightly shifts as more acid was used. The TMA^+ desorption maximum shifted to 440 °C for SW-TMA/12H (Figure 30c) is much more intense than that for cyclohexylamine desorption at 320 °C, which reflects the low proton content. However, as the amount of acid used in the sample preparation increased the maximum at 320 °C grew whilst that at 440 °C decreased. This confirms that both protons and TMA^+ cations reside on the exchange sites and that the relative occupancy of protons increased as the acid concentration increased. This figure further reinforces the fact that TMA^+ ions can compete very effectively with protons for exchange sites on the clay.

The desorption in the dehydroxylation region shows again two peaks with maxima at 620 and 715 °C. The intensity of the former remained constant in all samples, but the maximum at 715 °C, which was resolved from its neighbour, decreased in intensity. This behaviour undoubtedly supports the assumptions that two CO_2 species are produced from cyclohexylamine and TMA^+ cations. As the severity of acid treatment increased the population of TMA^+ gradually decreased. Therefore, a reduction in the intensity of the peak at 715 °C was expected.

4.1.6 Real Time TG-FTIR for the Desorption of Cyclohexylamine

The gases evolved during the thermal decomposition of cyclohexylamine from SAz-1 clay treated with 48 mmol H^+ were analysed by real time TG-FTIR. The results are presented in Figure 31.

At temperatures below 100 °C, four spectral regions are distinguished (Figure 31a): (i) 3950-3500 cm^{-1} and (ii) 1900-1300 cm^{-1}, which correspond to the stretching and deformation bands of physisorbed water from the clay structure, combined with the bending modes of the molecule, (iii) 2937 and 2862 cm^{-1} associated with the stretching bands of CH and (iv) a sharp doublet centred at 2366 and 2332 cm^{-1} attributed to the formation of CO_2.[200]

At temperatures >100 °C (Figure 31b), significant changes occurred in the IR spectrum. The intensity of the bands associated to ν(CH) and CO_2 increased. Additionally, two more bands are noticed at 1458 cm^{-1} common to the ionic and molecular form of cyclohexylamine[201] and the other, a doublet at 966 and 931 cm^{-1}, assigned to the symmetric deformation mode of ammonia.[195]

The infrared spectrum, at which the desorption maximum of cyclohexylamine occurs (near 300 °C) was also recorded (Figure 31c). The intensity of the CH band was even higher, whilst those of CO_2 and H_2O were invariant. However, a sharp band at 3030 cm^{-1} (not as prevalent as before) was evident and is certainly associated with unsaturated =CH stretching.[202] This band is corroborated by the appearance of another band centred at 1630 cm^{-1} due to superposition of the stretching >C=C< bond on the bending of water. It is important to notice that this spectrum is characterised by the presence of a weak band at 3350 cm^{-1} attributed to NH stretching.[203] The dynamic decomposition of cyclohexylamine at temperatures over 450 °C indicated that residual carbonaceous deposits are left on the clay structure and undergo transformation to carbon dioxide. This conclusion is verified by the clear presence of hydrocarbons (2800-3000 cm^{-1}) that have remained strongly bonded even up to 740 °C (Figure 31d).

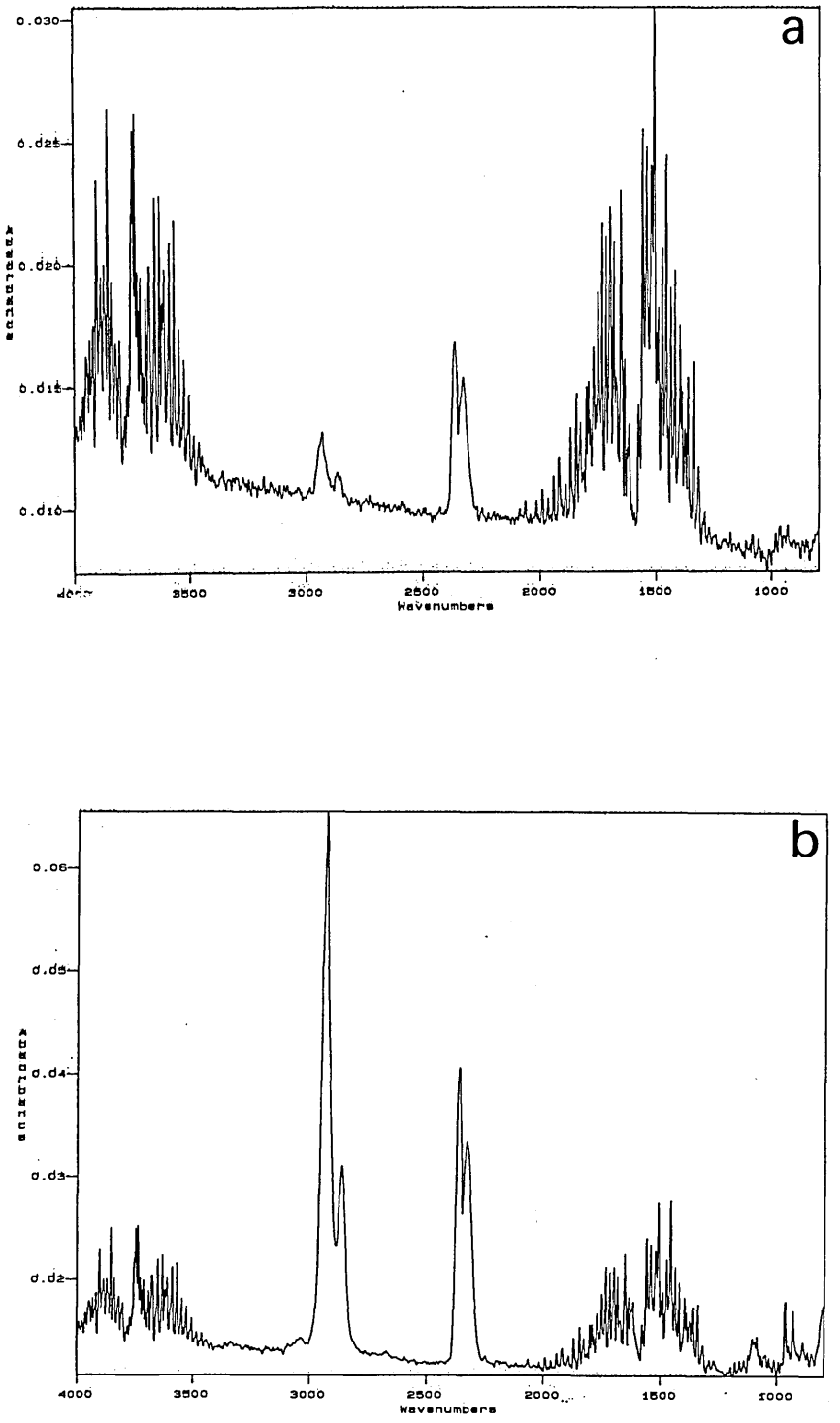

Figure 31. FTIR spectra for the desorption of cyclohexylamine on SA-48H at (a) 90 °C and (b) 190 °C.

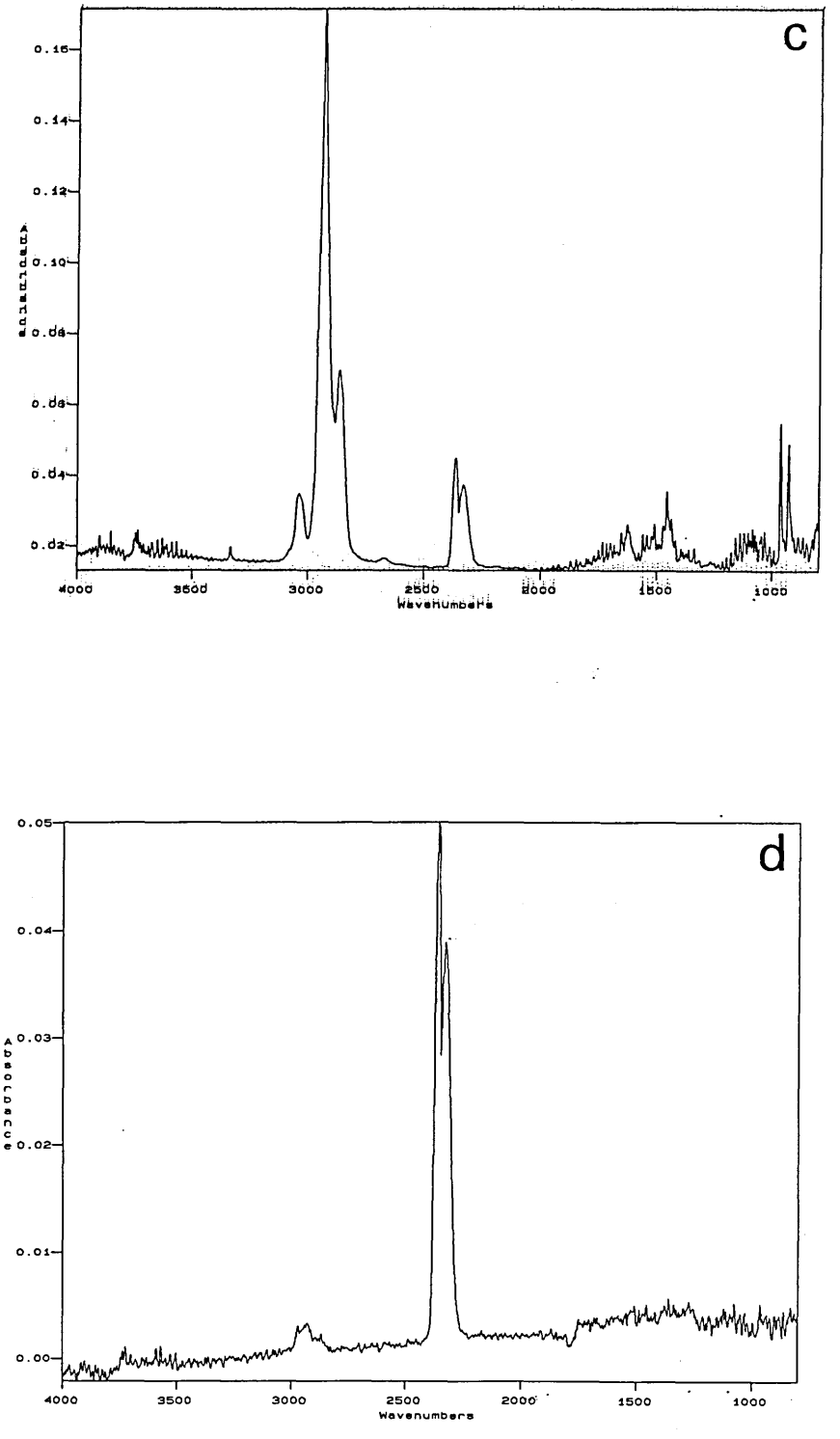

Figure 31. Continued. FTIR spectra for the desorption of cyclohexylamine on SA-48H at (c) 300 °C and (d) 740 °C.

Figure 32 shows, in a 3D plot, the evolution and changes in the infrared spectra from the cyclohexylamine desorption as a function of time when the temperature rate increased. The maximum absorbance for the desorption of cyclohexylamine appears at approximately. 30 min (near 300 °C). Measurable quantities of carbon dioxide are evolved at temperatures as low as 200 °C,[204] and at higher temperatures only the band associated with CO_2, water and hydrocarbon residues (at low intensity) are noticed.

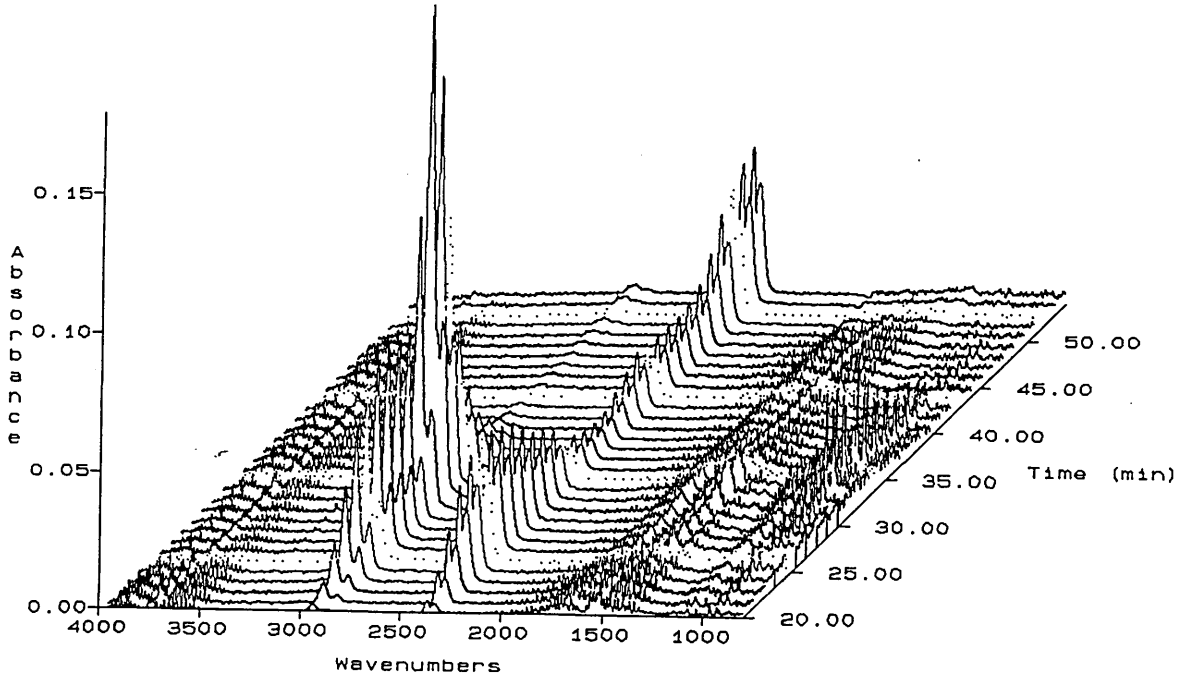

Figure 32. 3D FTIR spectra of the species evolved during the desorption of cyclohexylamine from SA-48H sample.

Figure 33 illustrates the contribution of gases evolved during the desorption of cyclohexylamine to the total FTIR chromatogram *vs.* time. Undoubtedly, the desorption/breakdown of the base gives rise to different species, consisting of aliphatic and unsaturated hydrocarbons, ammonia and CO_2 as well as water from the clay. Most of these species appear at the same temperature (310 °C) indicating transformation of the base on the

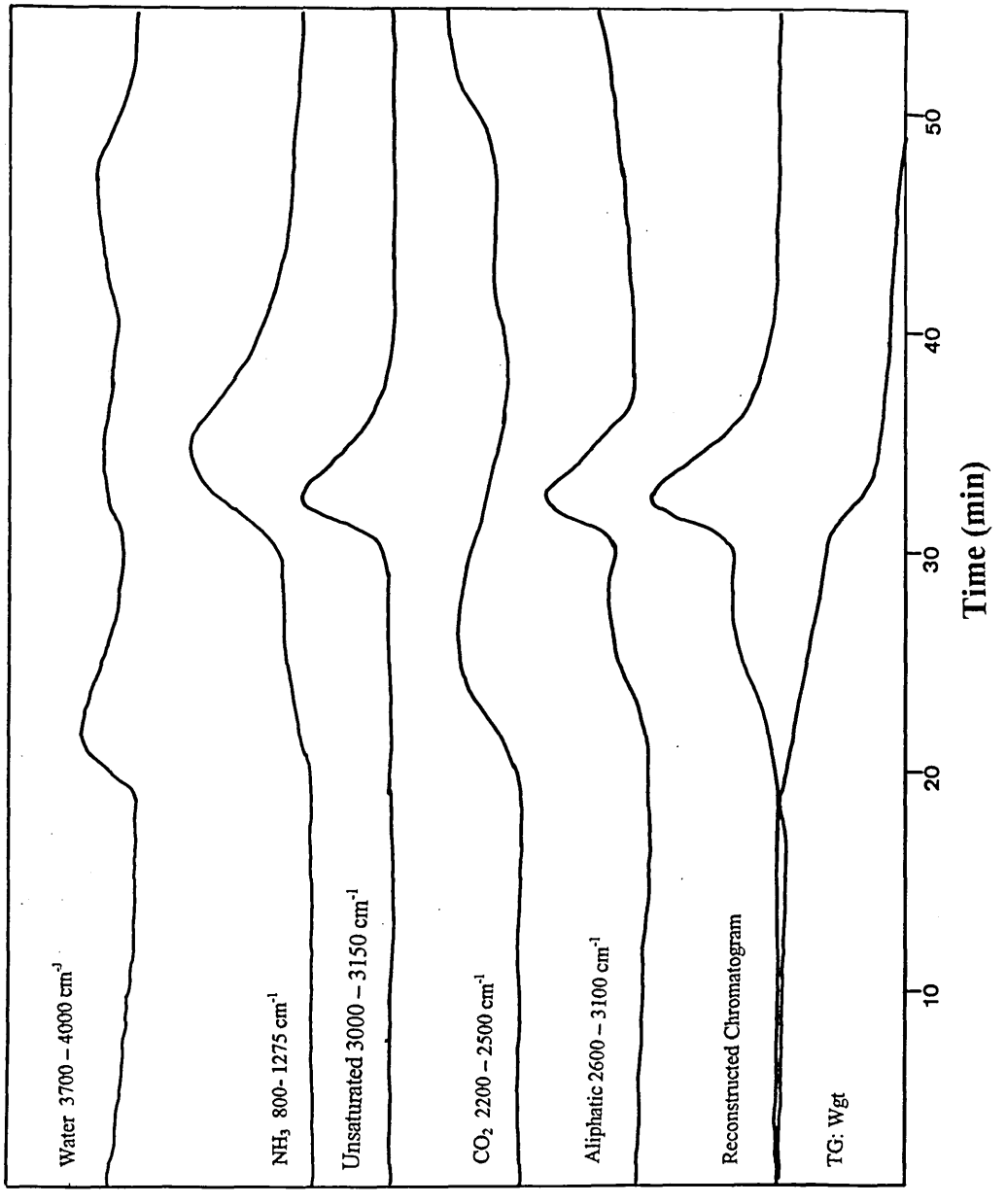

Figure 33. FTIR chromatogram of the species evolved during the desorption of cyclohexylamine from SA-48H sample.

clays' acid sites, although the NH_3 bands maximise at a slightly higher temperature and NH_3 continues to evolve until 45 min (600 °C).

These results clearly demonstrate that the effect of heating on protonated cyclohexylamine causes a breakdown of the molecule to give new rearrangements. GC-MS analysis of the fragmentation pattern of each ion (from ion-exchanged clays) indicated that the products formed were ammonia, cyclohexene, 1,3-cyclohexadiene, benzene, cyclopentene and 1,3-cyclopentadiene. Further details and discussion of these observations along with a proposed mechanism will be given in the next chapter, where considerable attention was given to the interaction of cyclohexylamine with aluminium-activated clays, aluminium-activated organoclays and ion-exchanged clays.

4.2 The Catalytic Conversion of α-Pinene

As described in sections 2.11 and 3.12, α-pinene reacts readily in the presence of acid.[176] Under non-aqueous conditions isomerisation via ring expansion takes place to yield camphene. In highly polar protic solvents (*e.g.*, H_2SO_4) monocyclic terpenes are formed via a ring-opening process to give a mixture of p-menthadienes, including limonene.

Camphene is formed readily[205] by elimination of a proton from the ion I (Figure 34). Williams and Whittaker[176] suggested that camphene results from II by elimination and a simultaneous bond shift.

Elimination from II probably is initiated by a proton loss from either C-3 or C-10. In the former case, this must result in displacement of the partial bond, C-2 to C-7, which gives α-

pinene. If however, a proton is lost from C-10, two possible rearrangements are possible. Displacement of the partial bond from C-2 to C-7 yields β-pinene, whilst the alternative, shift of the electrons of the C(2)-C(3) bond to give a bond between C-3 and C-1, displaces the partial bond between C-1 and C-7. This leaves a bond between C-2 and C-7, yielding structure III, which is that of camphene. Formation of α-fenchene probably involves an analogous process in the ion (Figure 16) in which the shift of the C(2)-C(3) bond gives α-fenchene (competes with displacement of the partial bond from C-2 to C-6 to give β-pinene). The latter bond would be expected to be weaker than the C(2)-C(7) bond in II since the rate of formation of II from cis-2-pinyl p-nitrobenzoate exceeds the rate of formation of α-fenchene from the trans-isomer.

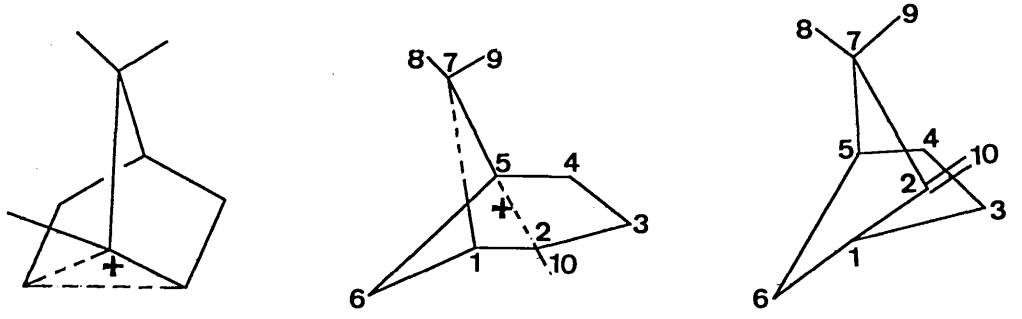

(I) (II) (III)

Figure 34. Rearrangement of α-pinene to camphene.

This isomerisation was chosen by Rhodes and Brown[165] to support their contention that extensively acid-leached clays, which are essentially hydrophobic silica, were particularly suited for conversions involving non-polar substrates. Their results, based upon work with a clay similar to STx-1, showed that the nature of that particular clay surface was more significant than the number of available acid sites.

4.2.1 Effect of the Type of Clay on the Catalytic Activity

The type of clay has a profound effect upon the catalytic activity for α-pinene isomerisation (Figure 35). In the absence of TMA^+ both Sap-Ca and STx-1 were more effective catalysts for the process than SWy-2 and SAz-1. Clays from different deposits are attacked to different levels by the same acid treatment. In this case, for example, the high activity of Sap-Ca could realistically be attributed to the extensive leaching of the clay as acid treatment progressed because it possesses a magnesium rich octahedral sheet, presenting a similar behaviour to the catalyst used by Rhodes and Brown.[165] As magnesium, from the octahedral sheet, is leached out a considerable portion of the internal surface area (in the octahedral sheet, Figure 36a) is created. This surface becomes available to α-pinene molecules to interact with protons from either the acid treatment or with those resulting from the polarisation of water by aluminium in the tetrahedral position due to isomorphous substitution with the corresponding enhancement in the catalytic activity. However, this cannot explain the comparable activity of STx-1 since this was not significantly leached under the conditions utilised herein. STx-1 clay has an aluminium rich octahedral sheet that gives it a high resistance to acid leaching and, therefore, the montmorillonitic structure is partially preserved.

Preliminary studies associated with acid-activated polycation exchanged clays have shown that mildly acid-activated SWy-2 is a more effective catalyst for this process than SAz-1.[24] The catalytic activity of SWy-2 and SAz-1 samples treated with 6 M HCl for 90 min at 25 °C was 42% and 12%, respectively. Hot acid treatment, at 95 °C for 180 min, increased the yield in both samples up to 78% (SWy-2) and 66% (SAz-1). Clearly, these results suggested that acid treatment at 95 °C for180 min was sufficient to achieve significant dissolution of the octahedral sheet of SWy-2 and SAz-1, resulting in catalysts similar to that of Sap-Ca clay.

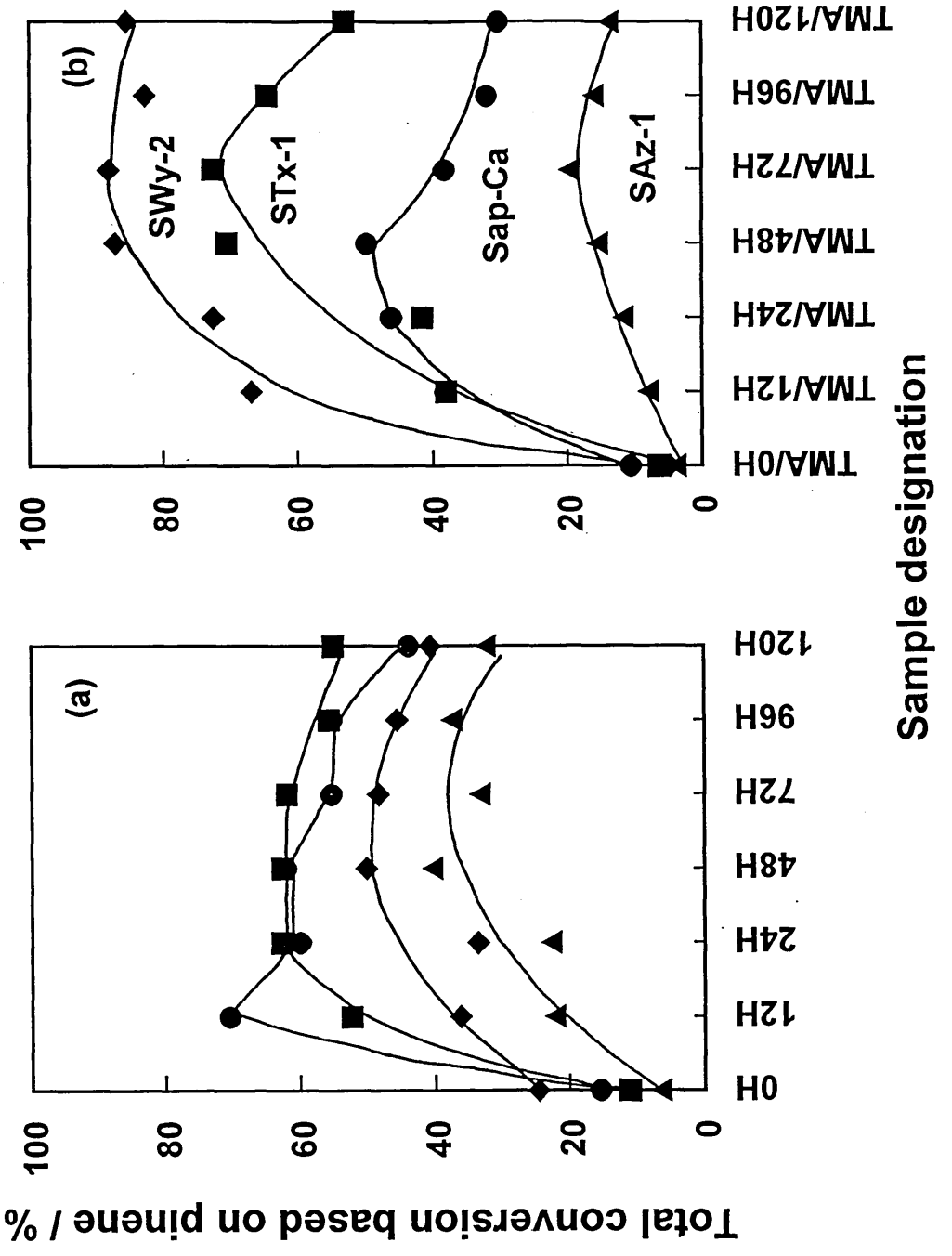

Figure 35. Total conversion of α-pinene for (a) natural and acid-treated clays and (b) TMA^+-exchanged and TMA/H-clays: (◆) SWy-2; (■) STx-1; (▲) SAz-1; (●) Sap-Ca.

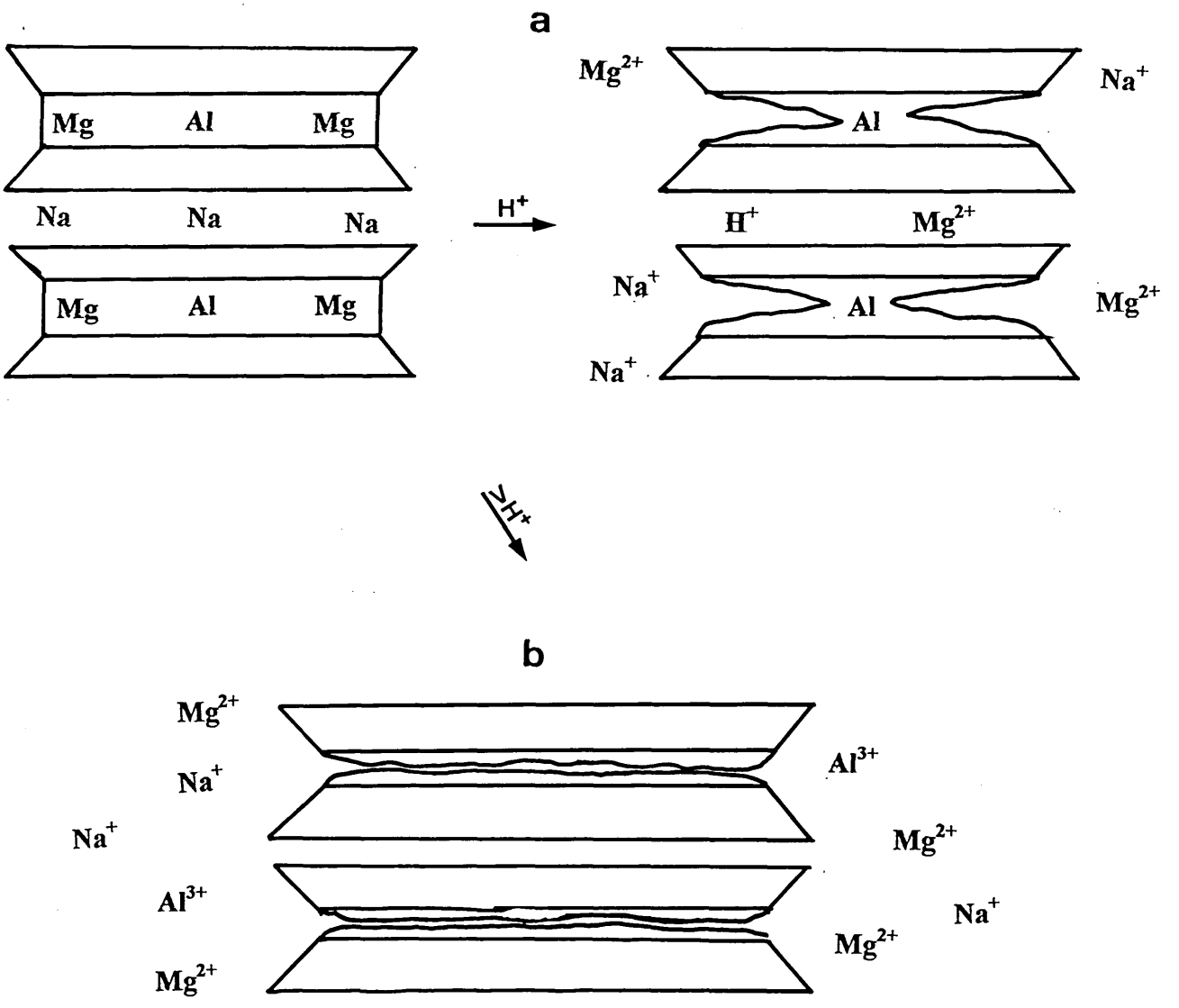

Figure 36. Showing the effect of acid treatment on an octahedral Mg-rich clay. (a) octahedral sheet partially leached at mild acid treatment and (b) octahedral sheet totally collapsed at severe acid treatment.

The effect of acid treatment is more markedly noticed in Sap-Ca samples (Figures 23 and 25), in which the maximum conversion is observed between 48 and 72 mmol H^+. Under these conditions the surface area available in the octahedral sheet is maximised and then with a more intense acid treatment it is reduced as a consequence of the collapse of the clay structure[7,92,93] (Figure 36b) with the concomitant drop in the catalytic activity.

The type of clay utilised also influenced the activity of the TMA/H samples. In all cases the lowest activities were recorded using the TMA^+-saturated clays, confirming, as anticipated, that exchange with TMA^+ alone did not enhance the catalytic activity. Samples treated with 1 CEC of TMA^+ (no acid added), displaces 20%, 28%, 40% and 56% of total Ca^{2+} in STx-1, SWy-2, SAz-1 and Sap-Ca. Figure 35 clearly shows that the major activity in samples treated with TMA^+, is achieved in Sap-Ca (10%) where the displacement of calcium is relatively higher than in the other three clays (6.6 %, 3.5% and 5.0% yield for STx-1, SWy-2 and SAz-1, respectively). Sodium and calcium are strongly hydrated in the presence of water, resulting in a hydrophilic environment at the clay surface. As a result, natural clays are ineffective catalysts for the isomerisation of α-pinene.

The total conversion for SW-TMA/H samples exhibited the largest increase in yield (from 50% for SW-H) to 88%, which incidentally represents an eightfold increase over SW-TMA. The conversion over ST-TMA/H samples increased slightly from 62% to 73% whereas the yields for SCa-TMA/H and SA-TMA/H samples decreased from 60% to 50% and from 35% to 20%, respectively.

The high activity of SW-TMA/H could be perhaps because this clay swells and interacts very well with α-pinene. A similar explanation could be given to the behaviour of STx-1. The most probable explanation for reduction in activity of SCa-TMA/H could be that TMA^+ cations occupy the available surface already created by the protonic attack of the octahedral sheet and then those active sites are not accessible to α-pinene molecules (Figure 37). In this case, α-pinene molecules only can access the acid sites in the interlamellar space. Finally, SA-TMA/H presented a very low H^+ content and a high TMA^+ content (Table 9) which represents a reduction in space availability toward the isomerisation of α-pinene.

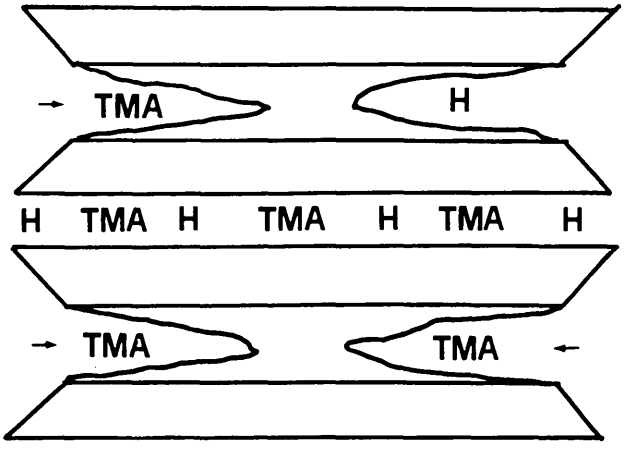

Figure 37. Showing the occupancy of TMA^+ cation in the octahedral sites created during the acid attack.

In general, the activity for all TMA/H samples increased with the extent of acid treatment reaching a plateau between 48 and 72 mmol H^+ before declining after preparation in more concentrated acid.

The following considerations should be pointed out in order to compare the results obtained herein with those achieved by De Stefanis, *et al.*,[167] Watson,[194] and Rhodes and Brown:[165]

De Stefanis, *et al.*,[167] investigated the isomerisation of α-pinene in several alumina-pillared clays (denoted Al-PILC and FAZA) under Lewis acid conditions and compared the produced yield with those obtained with two mid-pore zeolites (denoted USY and NH_4^+-ZSM-5, with SiO_2/Al_2O_3 = 35 and 235). They carried out the reaction at 100 °C for 5 h in a sealed glass reactor, and found that the bicyclic α-pinene gave the highest conversion in all catalysts, giving >50% camphene. The yield showed that USY was the strongest acid, after which the acidity order was: BP-PILC = ZSM-5 (35) > FAZA > H-mordenite.

Watson[194] carried out the isomerisation of α-pinene at 80 °C for 2 h over moderated loading of TMA^+ (5 times the CEC) acid-activated Ca-montmorillonite, Na-montmorillonite, beidellite, nontronite and Al-montmorillonite (denoted SAz-1, SWy-2, ST, SWa-1 and JP). It was found that the total conversions were between 60 and 80% in order of activity, JP = SAz-1 < SWa-1 < ST = SWy-2. The results obtained by Watson[194] were used to evaluate the isomerisation of α-pinene in similar clays with a significantly smaller amount of TMA^+ (1 CEC) and in simultaneous competition with protons in aqueous solution.

Rhodes and Brown[165] tested the catalytic ability of α-pinene at 80 °C over extensively leached clays, which were essentially hydrophobic silica. The catalysts were activated under N_2 at 150 °C for 1 h prior to reaction. They observed that acid-treated clays (subsequently exchanged with Al^{3+} ions) showed only slightly higher activities than the unexchanged acid-

activated clays and that the conversion of α-pinene reached a maximum of 40% yield on clays acid treated for four hours. The activity was reduced with more severe acid treatments.

The results found in this work have shown that the total conversions were between 50 and 90% for catalysts derived from STx-1, SWy-2 and Sap-Ca (excluding SAz-1 samples). These conversions are considerably higher than those reported for extensively acid leached Texas bentonite,[165] however the same conclusion pointed out by Rhodes and Brown[165] that the catalytic activity was at a maximum after extensive acid treatment, was observed herein, especially for acid-activated Sap-Ca samples.

The catalytic activities are similar to the values reported by De Stefanis, *et al.*,[167] and Watson,[194] even when a higher reaction temperature was used (120 °C for 1 h). However, a maximum conversion of 52% was observed herein when the isomerisation of α-pinene was carried out at 80 °C for 2 h (Figure 21). This result was lower if compared with that obtained by Watson[194] under the same experimental conditions. A possible explanation of this discrepancy would be that the materials prepared herein have a higher TMA^+ content than those prepared by Watson,[194] therefore a reduction in the catalytic activity is presumed at a lower temperature reaction due to less available space.

4.2.2 Product Distribution

As anticipated, the product distribution of terpenes (Figure 38) followed the order camphene > limonene > others, with the exception of the SW-TMA/H clays, where the yield of other products is higher than that of limonene. The selectivity towards camphene, limonene, and the minor products was essentially the same for all the clays and can be broadly described as

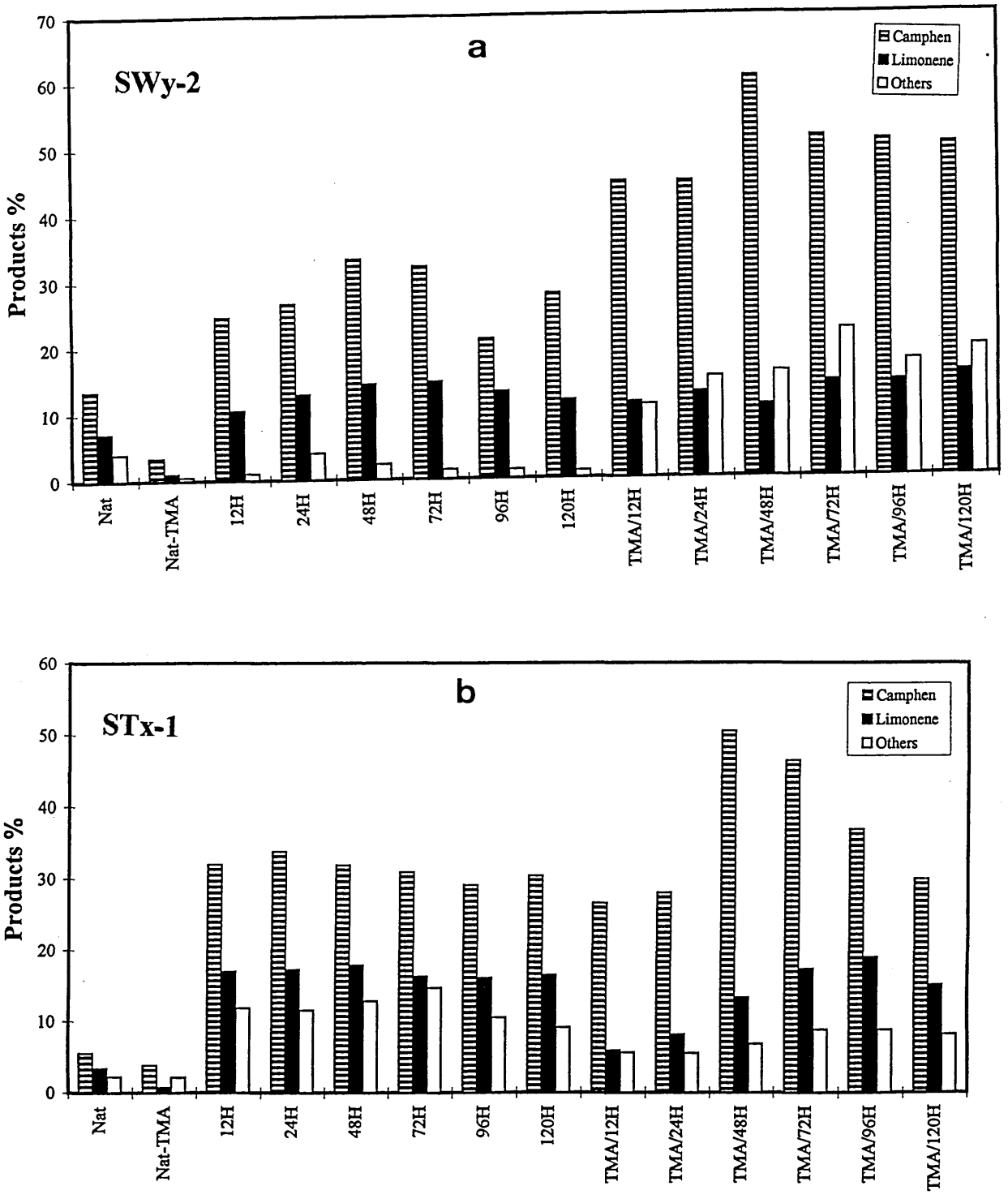

Figure 38. Product distribution for the catalysts derived from (a) SWy-2 and (b) STx-1.

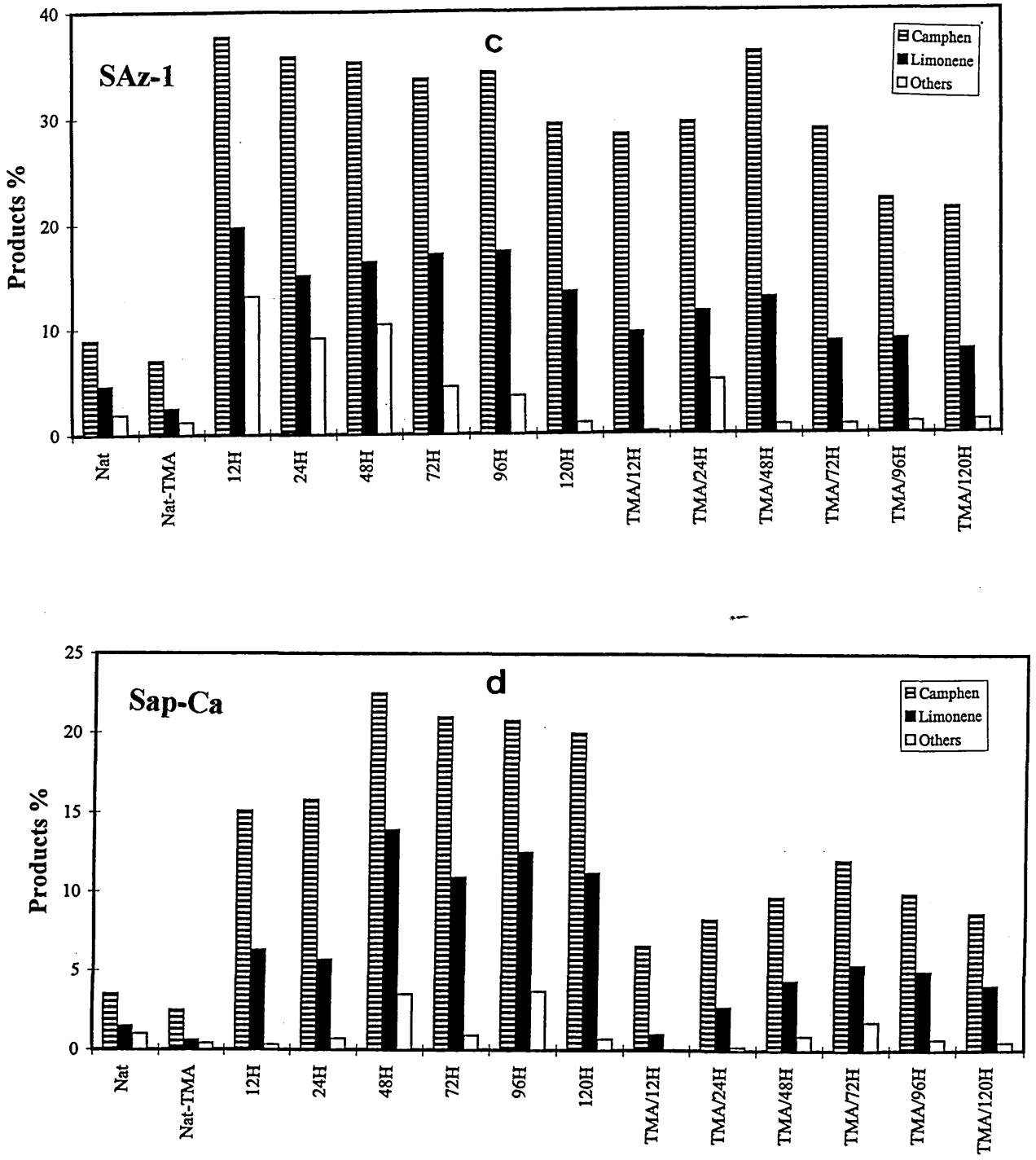

Figure 38. Continued. Product distribution for the catalysts derived from (c) SAz-1 and (d) Sap-Ca.

65±10%, 25±8% and 12±8%, respectively, to encompass all the catalysts. The ratio of camphene to limonene is near 2.6:1.0 compared with a value of 2.2:1.0 obtained at 80 °C for 2 h[194] and less than the ratio 3.0:1.0 obtained over USY, Al-PILC and Al,Fe-PILC.[167] Thus, the clay based samples are not as selective towards camphene as the permanently porous catalysts. Nevertheless, the yields are competitive and the catalysts are more economic to produce.

Comparing the results obtained from SW-TMPA/H samples (Figure 39) with those from SW-TMA/H for the isomerisation of α-pinene, it is evident that the total conversions for the former are relatively lower that the latter, within 40-50% less at lower acid-activation treatment (12-48 mmol H^+). However, as the severity of the acid activation increased, the activity for SW-TMPA rises, but the conversions are still lower in comparison with SW-TMA/H samples (10-20%). This reduction in activity, in samples treated at low acid concentration, could be attributed to the significantly higher $TMPA^+$ content, which, as mentioned before, showed more resistant to displacement by protons than did TMA^+. Additionally, the phenyl ring may cause steric hindrance to the reactant molecule and limit access to the interlamellar space.

In SW-TMPA samples treated at more severe acid conditions (96 and 120 mmol H), a fraction of the organocation is removed (see Table 11). Additionally, these samples present an expanded layer even at high temperature (13.1 Å at 300 °C, see Table 12). At the reaction temperature (120 °C) the d-spacing was 14.2 Å for SW-TMPA/120H. This may suggest that SW-TMPAH samples treated at higher acid conditions have propped some galleries apart and the α-pinene thus can access the interlamellar space where a substantial amount of acid sites

are found. This behaviour can also explain the enhancement in catalytic activity of SW-TMA/H samples. In the latter case the TMA^+ content was not so high because it showed less resistance than $TMPA^+$ to displacement by protons, therefore all samples present an expanded interlayer space where α-pinene isomerisation is tailored.

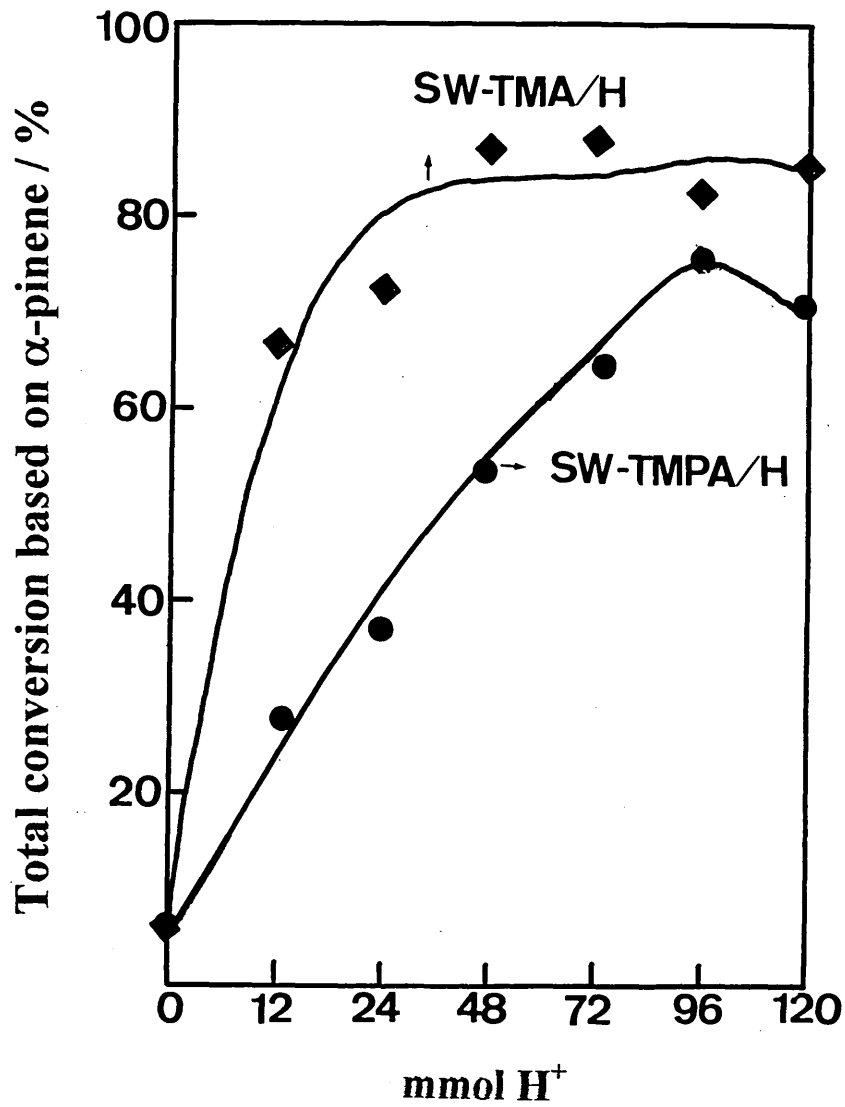

Figure 39. Showing the total conversion of α-pinene over catalysts derived from SW-TMPA/H and SW-TMA/H.

The studies carried out by Breen, *et al.*,[24,25] were addressed to evaluate how the nature of the selected organocations influenced the catalytic activity of a particular series of AAOCs and this unequivocally demonstrated that clays containing TMA^+ cations were much more effective than those containing alkyltrimethylammonium cations or polycations. This difference in catalytic activity was attributed to congestion of the galleries in clays containing significant quantities of large organocations and, in the case of polycations, an inability of the organoclay complex to expand in the presence of the organic reagent. The work of Watson[194] suggested that there was a correlation between the amount of TMA^+ on the AAOCs and the resulting catalytic activity but there was no comparative data with catalysts prepared using the same amount of acid in the absence of TMA^+ cations. Figure 40 suggests that the total conversion (based on α-pinene) was optimised when 25-30% of the exchange sites of SWy-2 and STx-1 were occupied by TMA^+ cations.

The higher loading of TMA^+-cations on the surface may influence the yield over SAz-1. The TMA^+ cations on SAz-1 were much more resistant to displacement by protons than TMA^+ on the other clays under investigation. Moreover, it has been suggested that the high charge density on the surface of SAz-1 means that the distance between neighbouring TMA^+ cations is insufficient to accommodate benzene, toluene and xylene molecules, thus reducing the ability of TMA^+-SAz-1 to function as an effective sorbent for the removal of these pollutant molecules from water.[11,17,142] Therefore, the low activity of the SA-TMA/H samples may be attributed, in part, to insufficient space to accommodate the α-pinene molecules at the active site because TMA^+ cations are in close proximity (Figure 41a).

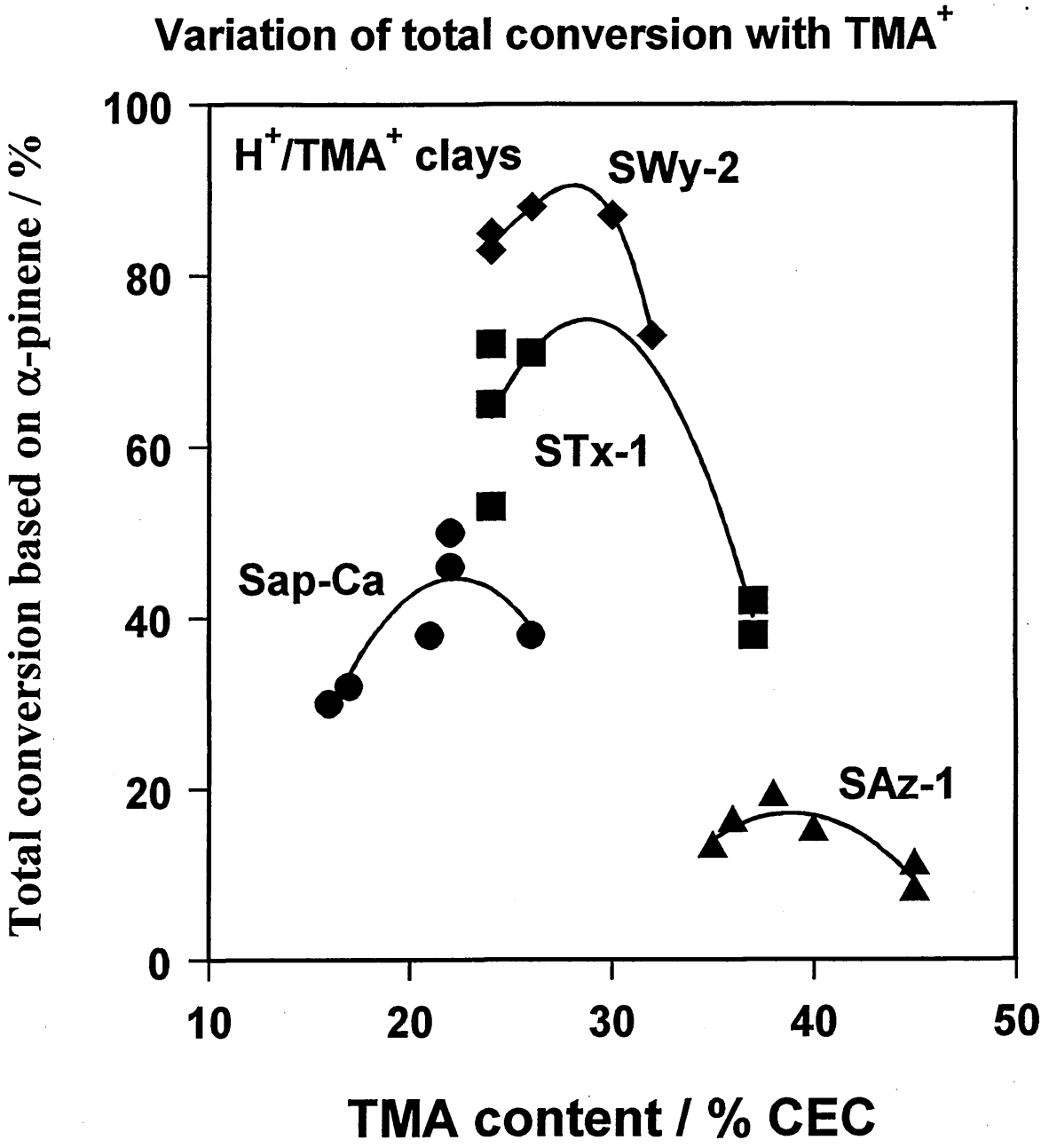

Figure 40. Correlation of the percentage of TMA^+ vs percentage of total conversion of α-pinene for acid-treated organoclays (◆) SWy-2, (■) STx-1, (▲) SAz-1 and (●) Sap-Ca.

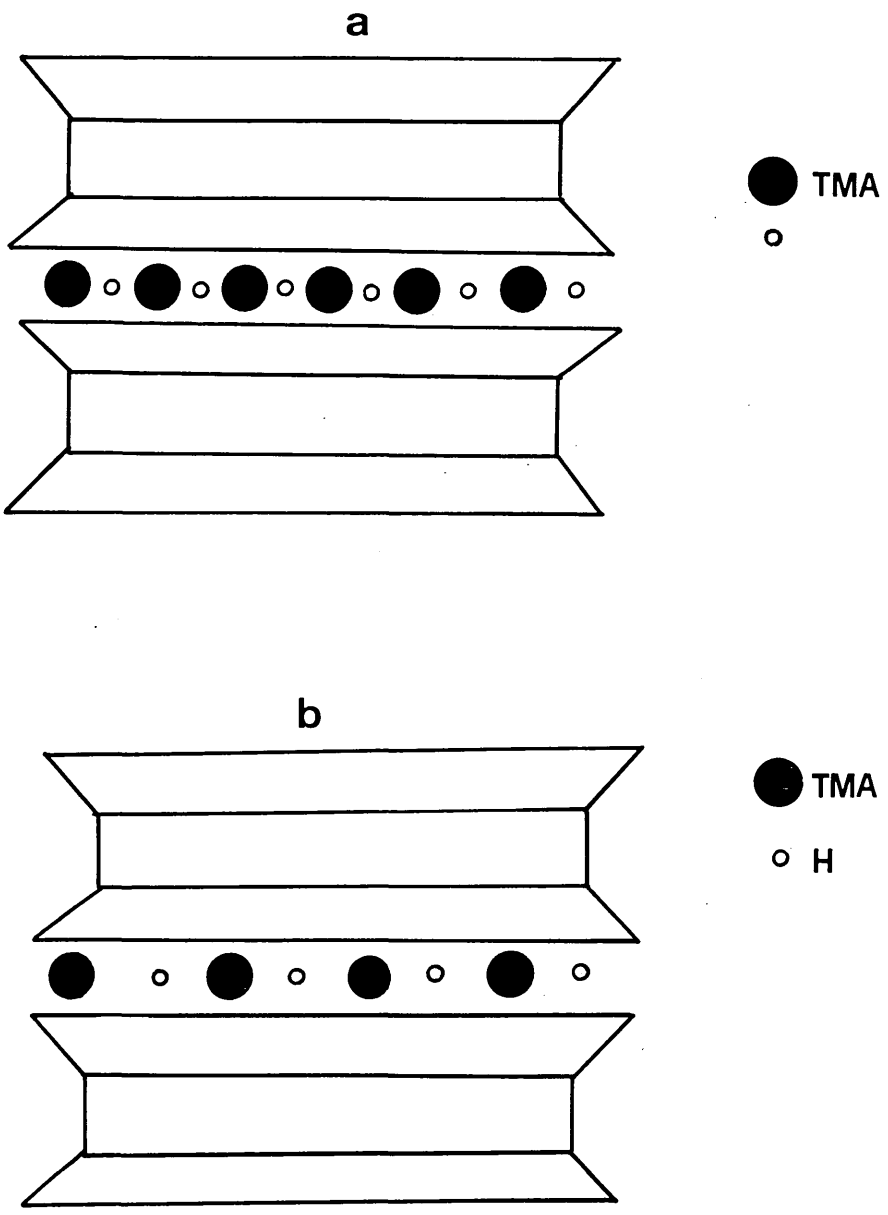

Figure 41. Schematic representations of the possible distribution of TMA^+ cations and H^+ in (a) high charge montmorillonite (SAz-1) and in (b) low charge (SWy-2) montmorillonite.

Both SWy-2 and STx-1 have the same CECs, but the former has a homogeneous charge distribution whilst in STx-1 it is heterogeneously distributed[206] and one would expect STx-1 to behave more like SAz-1. However, they worked in a discordant manner in this study. In these two low charge clays, TMA^+ cations are further apart (Figure 41b) so that the access for the reactant molecules to the interlamellar space and the interaction with protons is more favoured than that in a high charge clay, in addition to the expanded layers, mentioned above.

Feldkamp and Stauffer[207,208] reported an equation which corroborated that adsorption of polar compounds would be enhanced as the charge density of the layer increased. This assumption can be used to forecast that the isomerisation of α-pinene (non-polar medium reaction) over SAz-1 samples may not work as well as that of SWy-2 and STx-1, which have a lower charge density and therefore the non-polar reaction is developed. Currently, there is no complete explanation for the marked activity of STx-1, although a dispersion of STx-1 has a pH of 7 compared with SWy-2, which has a pH of 9. This may imply that the edge sites on STx-1 are inherently more acidic than those on SWy-2.

SCa-H samples were much more catalytically active than their TMA^+-containing counterparts. Hence, the reduction in overall yield over the SCa-TMA/H samples probably reflects an extensively leached saponite surface, which has TMA^+ cations occupying exchange sites that would be more effective in the isomerisation process if they were occupied by protons.

4.3 Summary of Catalysis Investigation

This investigation has demonstrated that the catalytic ability of acid-activated organoclays provided reasonable levels of activity, hydrophobicity and swelling ability for use with non-polar reagents.

The nature of the raw clay plays an important role in the resulting catalytic properties of the AAOCs. The behaviour of SWy-2 closely mimics that previously observed in an investigation using a Slovak montmorillonite, a Czech beidellite and a ferruginous smectite[25] insofar as an apparent synergy between an organophilic surface and protons significantly enhanced the activity of the AAOC for a reaction involving a non-polar substrate.

The results, obtained in this work, demonstrated that the metal ions released from the octahedral sheet indicated that Sap-Ca was extensively leached when high hydrochloric acid concentrations were used, resulting in a destruction of the lamellar structure. Therefore, samples based on Sap-Ca must remain outside the present discussion because the depopulation of the octahedral sheet is more like clays rich in octahedral aluminium, that have been activated in hot acid.[165] Nonetheless, it serves as an appropriate marker and emphasises that similar activity can be imparted to SW-TMA/H samples without the production of large quantities of acidic Al^{3+} or Mg^{2+} containing solutions. The behaviour of SAz-1 and STx-1 are more difficult to explain since these samples behave incongruously. Mildly acid-activated STx-1 is an excellent catalyst for the isomerisation of α-pinene and its activity is only marginally enhanced via the incorporation of TMA^+ cations, although the dependence of total conversion on TMA^+ content closely follows that for SWy-2 (Figure 40).

The major products of the isomerisation of α-pinene were camphene and limonene, indicating that the reaction proceeded via a ring expansion to derivatives of bornane and ring opening to derivatives of p-menthane. The selectivity was: camphene > limonene > other.

The catalytic activity for the isomerisation of α-pinene was excellent for organoclays formed from STx-1, SWy-2 and Sap-Ca and low for SAz-1. The activity of SAz-1 is significantly reduced by the incorporation of TMA^+ cations, as it was by the incorporation of polycations.[24] One possible explanation for this behaviour is that the gallery surface accessible to α-pinene in the presence of TMA^+ cations is insufficient to allow access to the catalytic sites. The activity of the more active AAOCs organoclay was optimised when 25-30% of the exchange sites were occupied by TMA^+ ions. The AAOCs prepared demonstrated to be very efficient catalysts with total conversions comparable to those achieved by PILCs, zeolites and AACs as reported in the literature.

In this study it was demonstrated that the activity (based on α-pinene isomerisation) strongly depends on layer charge. The poorest catalytic activity was observed in SAz-1 samples, which display the highest layer charge. In clays with low layer charge (SWy-2 and STx-1) the maximum conversions were obtained.

Finally, the catalytic activity of acid-activated organoclays can be carefully optimised for specific reactions. Changes in the surface area, the cation exchange capacity, the nature of the exchangeable cation, the organocation loading and the charge density influence activity in different ways.

CHAPTER 5

Characterisation and Catalytic Activity of Aluminium-Activated Clays, Aluminium-Activated OrganoClays and Ion-Exchanged Clays

5.0 Introduction

As demonstrated in the previous chapter, one of the selected source clays (Sap-Ca), in which the octahedral sheet is composed almost entirely of magnesium, was extensively leached even when using mild acid activation conditions. Therefore, it was not possible to compare its catalytic activity directly with that of the other three acid-activated organoclays (AAOCs) nor to distinguish between the influence of substantial depletion of the octahedral sheet (which leads to a hydrophilic surface in clays with high tetrahedral Al content) and the contribution of the TMA^+ cations. Moreover, it is well known that even mildly acid-activated clays can undergo autotransformation, in which the interlamellar protons enter the layer and replace Mg^{2+}, Fe^{3+} and Al^{3+} cations from the octahedral sheet.[28,94,209] Once released these multivalent ions take up exchange positions within the gallery and may contribute to the observed catalytic activity. Autotransformation is known to be accelerated at elevated temperatures or in wet and warm environments and could thus have occurred during thermal activation of the catalysts prepared using H^+/TMA^+.

It is well established that the properties of clays can be altered by displacing the exchangeable cations (*e.g.*, Na^+, K^+, Ca^{2+}), which are strongly hydrated in the presence of water, with high polarising species such as aluminium, chromium, iron or polymeric oxyhydroxy cations.[19-23] Indeed, the enhanced catalytic activity of Al^{3+}- compared to Fe^{3+}- and Cr^{3+}-exchanged montmorillonites has been attributed to the greater polarisation of water molecules in the primary coordination sphere of the Al^{3+} cations[67,103,104] which results in the generation of acidic protons in the interlayer gallery. Under these conditions, the ion exchange does not affect considerably the octahedral sheet of a magnesium rich clay such as Sap-Ca.

The ion exchange treatment can be combined with alkylammonium ion exchange to produce effective ion-activated organoclays which possess both acidity and expanded layers when presented to organic molecules.

Therefore, in this chapter attention was initially focused on the combination of Al^{3+} and TMA^{+} cations on the exchange sites in order to compare all four clays directly without depleting the octahedral sheet and to evaluate whether the Al^{3+}/TMA^{+} exchange mimics autotransformation in the H^{+}/TMA^{+} clays and contributes to an enhanced activity. The catalytic activity of aluminium-activated organoclays (AlAOCs) is compared with samples prepared in the absence of TMA^{+}, denoted as aluminium-activated clays (AlACs). Secondly, to compare the catalytic activity (based on the isomerisation of α-pinene) of one of the source aluminium-activated organoclays (SW-Al/TMA) with AlAOCs prepared using divalent organocations of different shapes [1,4-diazabiclyclo[2.2.2]octane, (DABCO) and 1,5-diaminopentane, (DAP)].

Finally, the test reaction was applied to montmorillonites saturated with various cations (ion-exchanged clays, IECs), using different exchanging procedures, to study the effect of a range of interlayer cations on the catalytic activity.

The catalytic activity of the AlACs, AlAOCs and IECs is correlated with the acidity values determined using the desorption of cyclohexylamine.

5.1 Aluminium-Activated Clays (AlACs) and Aluminium-Activated OrganoClays (AlAOCs)

5.1.1 Samples' Identification

AlACs and AlAOCs were prepare by combining selected volumes of 1 M TMA^+ solution and 0.1 M Al^{3+} in different ratios to satisfy 1 CEC of the studied clays (STx-1, SWy-2, SAz-1 and Sap-Ca). AlACs were made in exactly the same way except that the TMA^+ was excluded (section 3.2.2). The preparation procedure is identified in the sample name, for example: SW-Al90 means that SWy-2 was treated with 90% Al^{3+} of original CEC and SCa-Al20/TMA80 indicates that Sap-Ca clay was prepared using 20% CEC of Al^{3+} and 80% CEC of TMA^+.

5.1.2 Chemical Analysis

The amount of resident exchange cation (expressed as a percentage of metal oxide released) as a function of the amount of Al^{3+} and/or TMA^+ in the initial exchange solution is shown in Figures 42 and 43 for SAz-1 and STx-1 samples. Catalysts derived from Sap-Ca and SWy-2 showed a similar trend (not illustrated). A complete displacement of the exchangeable Na^+ and Mg^{2+} by Al^{3+} or protons (from the acidic aluminium solution, pH = 2.8) was observed for all four clays when Al^{3+} > 70% CEC. However, samples containing Ca^{2+} showed more resistance and Ca^{2+} was only completely removed when samples were treated with Al^{3+} = 100% (Figures 42a and 43a). In contrast, the removal of the resident exchange cations was essentially constant for all four clays regardless of the Al^{3+}/TMA^+ ratio, because the Al^{3+}/TMA^+ content always equalled at least 100% CEC (Figures 42b and 43b) which was sufficient to displace the resident ions. Nonetheless, even though all the resident exchange cations were released it was not possible to achieve 100% CEC of Al^{3+} on the exchange sites

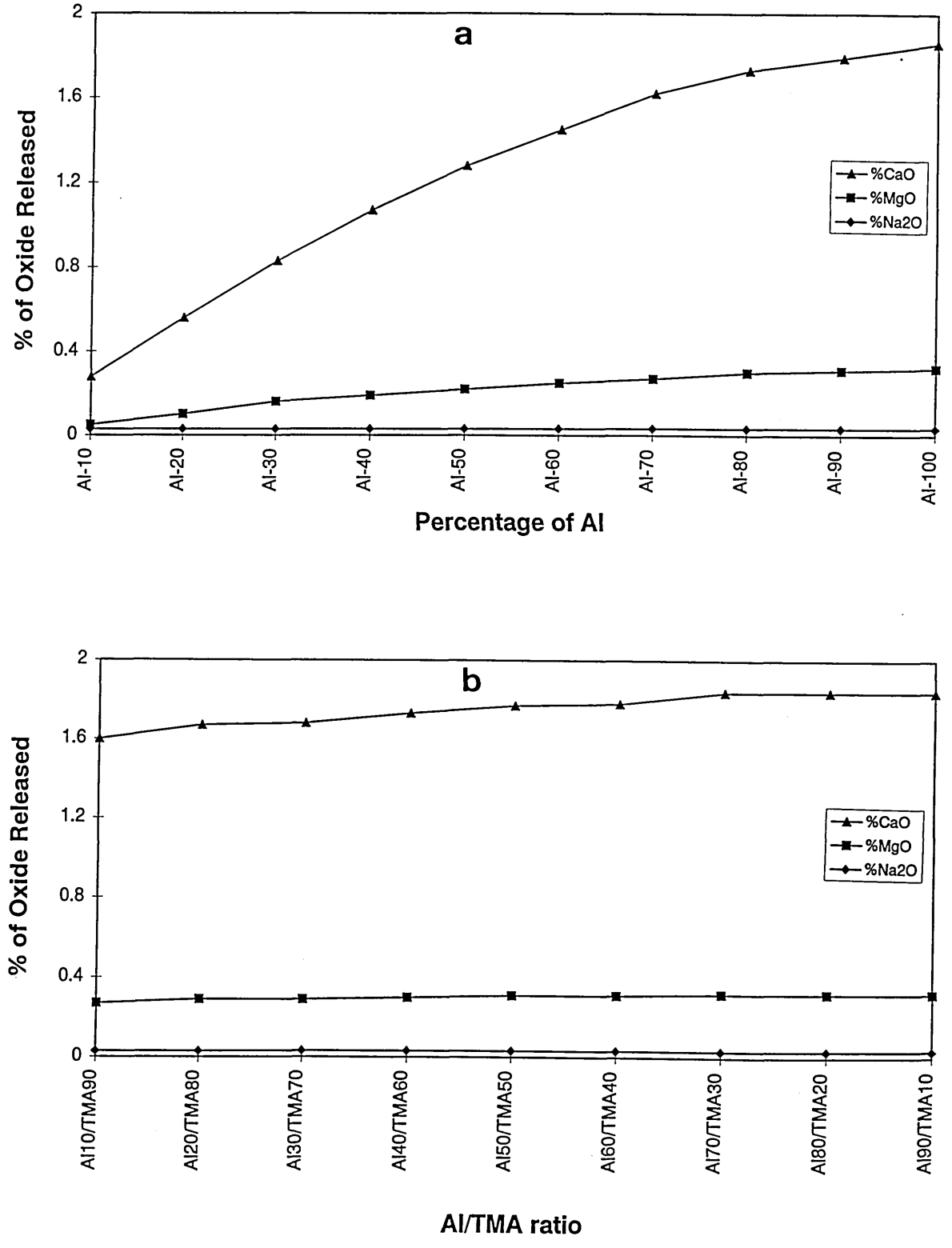

Figure 42. Percentage of metal oxide released during treatment of SAz-1 clay (a) AlACs and (b) AlAOCs. (▲) CaO, (■) MgO and (◆) Na_2O.

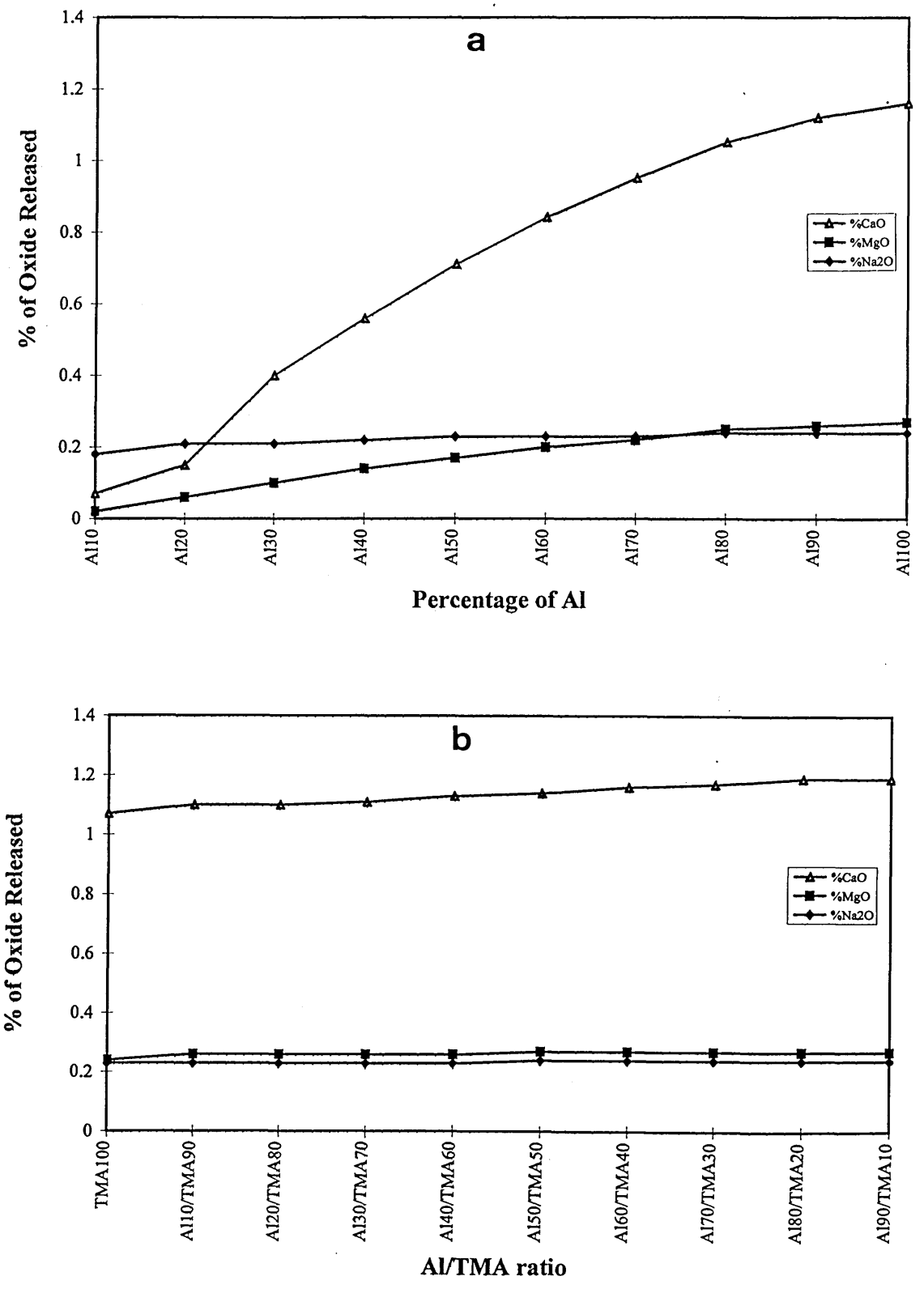

Figure 43. Percentage of metal oxide released during treatment of STx-1 clay (a) AlACs and (b) AlAOCs. (▲) CaO, (■) MgO and (◆) Na_2O.

which suggests that some exchange sites were satisfied by the protons available in the exchange solution.

In all four AlAC series, the amount of Al^{3+} occupying the exchange sites correlated well with the amount offered in the 10-50% CEC region, but not so well in the >60% region. This was expected due to the anticipated incorporation of protons from the increasingly acidic Al^{3+}-exchange solution. In general, the aluminium content in AlACs clays followed the order: SWy-2 > Sap-Ca > SAz-1 > STx-1.

The presence of TMA^+ cations did not significantly influence the uptake of aluminium, but it did appear to reduce the number of protons on exchange sites which agrees with the observations shown in Chapter 4, regarding the ability of TMA^+ cations to compete effectively with H^+ ions for exchange sites.

5.1.3 Catalytic Activity as a Function of the Aluminium Content

Figure 44 shows how the total conversion (based on α-pinene) varied with the aluminium content (expressed as % CEC) in AlACs and AlAOCs. The maximum yields obtained are very similar to those observed using H^+- and H^+/TMA^+-exchanged clays (see previous chapter, section 4.2.1) and are directly comparable with the conversion of α-pinene values of 80% and 90% reported for zeolite Y (USY), Al- and Al,Fe-pillared clays and Pt/Al_2O_3 catalysts.[167,175,210,211] Clearly, the type of clay used exerted a considerable effect on the total conversion obtained using this test reaction. In either the absence or presence of TMA^+ both Sap-Ca and STx-1 were more efficient catalysts for the process than SWy-2 and SAz-1. In all cases the presence of Al^{3+} resulted in improved catalytic activity.

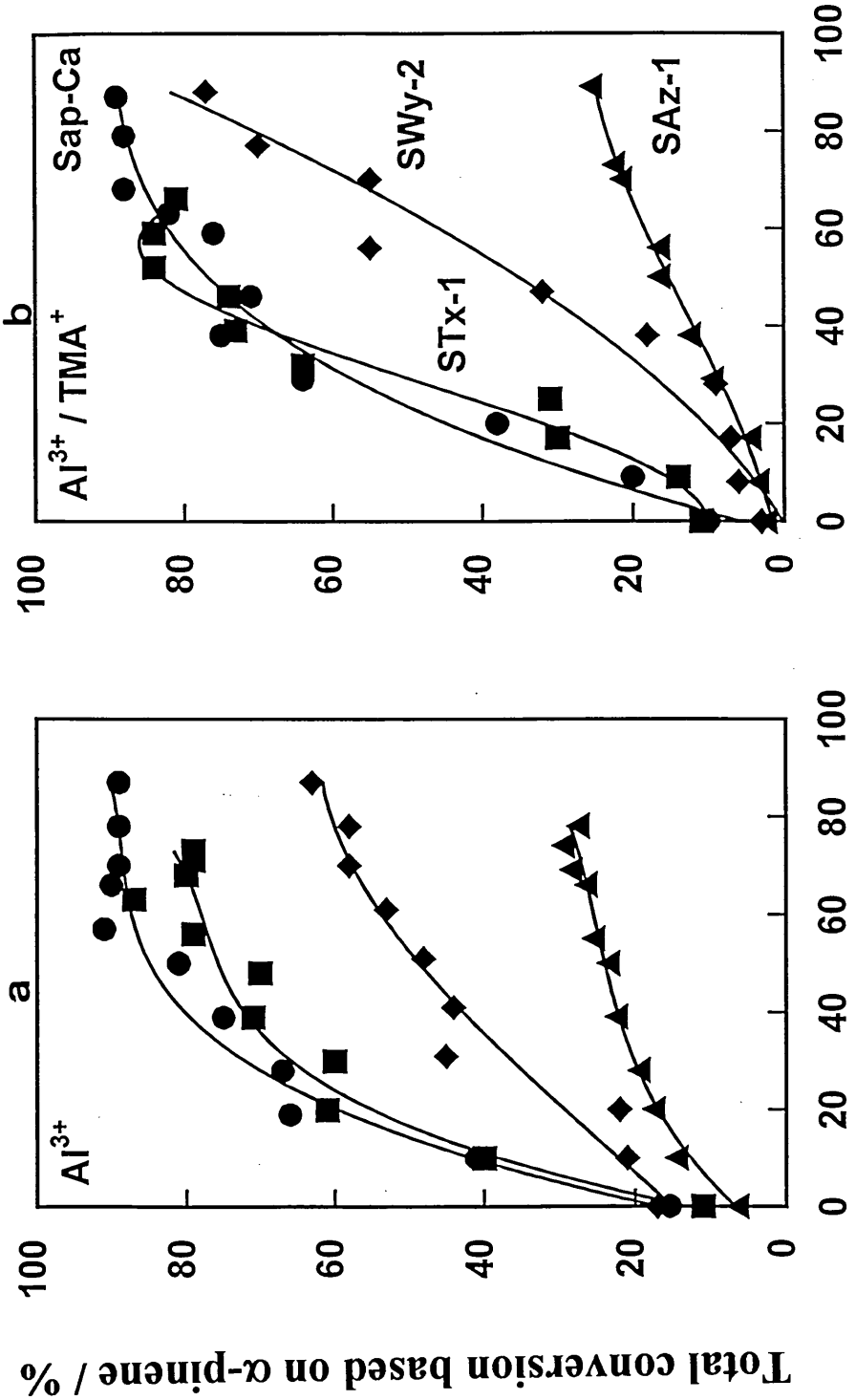

Figure 44. Total conversion of α-pinene vs percentage of aluminium incorporated in (a) AlACs and (b) AlAOCs (●) Sap-Ca, (■) STx-1, (◆) SWy-2 and (▲) SAz-1.

As little as 20% CEC of Al^{3+} resulted in a threefold increase in the activity compared to unmodified Sap-Ca and STx-1, where the activity then increased steadily to 70% CEC.

The increase in activity of SW-Al samples was less marked and SAz-1 achieved little more than 20% conversion at the highest Al^{3+} content. These observations concur with those of Purnell, *et al.*,[62] who observed a similar diminution in catalytic activity towards the esterification of ethanoic acid by hexene and the dehydration of pentanol as the loading of Al^{3+} increased above 70% CEC. Thus, it is clear that small amounts of interlayer Al^{3+} derived from autotransformation during thermal activation at 120 °C would make a significant contribution to the total conversion of α-pinene.

5.1.4 Product Distribution

In general the distribution of products which make up the total conversion (Figure 45) followed the order camphene > limonene > others, except for catalysts derived from STx-1 with high Al^{3+} contents (ST-Al60 to ST-Al100 and ST-Al70/TMA30 to ST-Al80/TMA20) where the yield of other products exceeded that of limonene. The selectivity towards camphene, limonene and the minor products was very similar for all the clays and can be broadly represented as 57±7%, 26±5% and 16±7% to encompass all the catalysts. These values are very similar to those of 65±10%, 25±8% and 12±8% obtained over H^+- and H^+/TMA^+ clays (see section 4.2.2). The ratio of camphene to limonene is near 2.2:1.0 which is identical to the value obtained at 80 °C for 2 h,[25] but marginally lower than the values of 2.6:1.0 obtained using H^+/TMA^+-clays and 3.0:1.0 obtained over USY, Al-PILC and Al,Fe-PILC.[167]

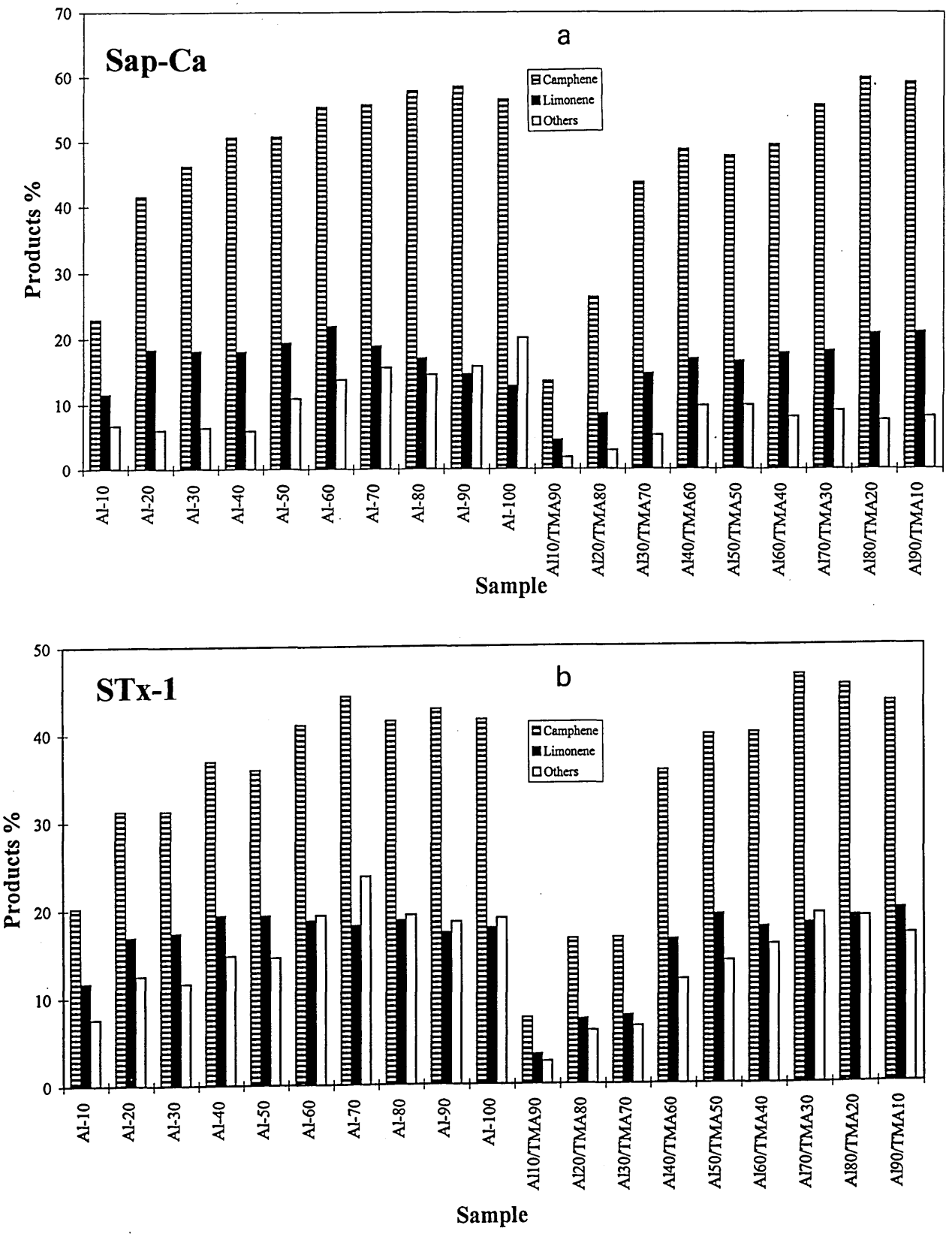

Figure 45. Product distribution for the catalysts derived from (a) Sap-Ca and (b) STx-1.

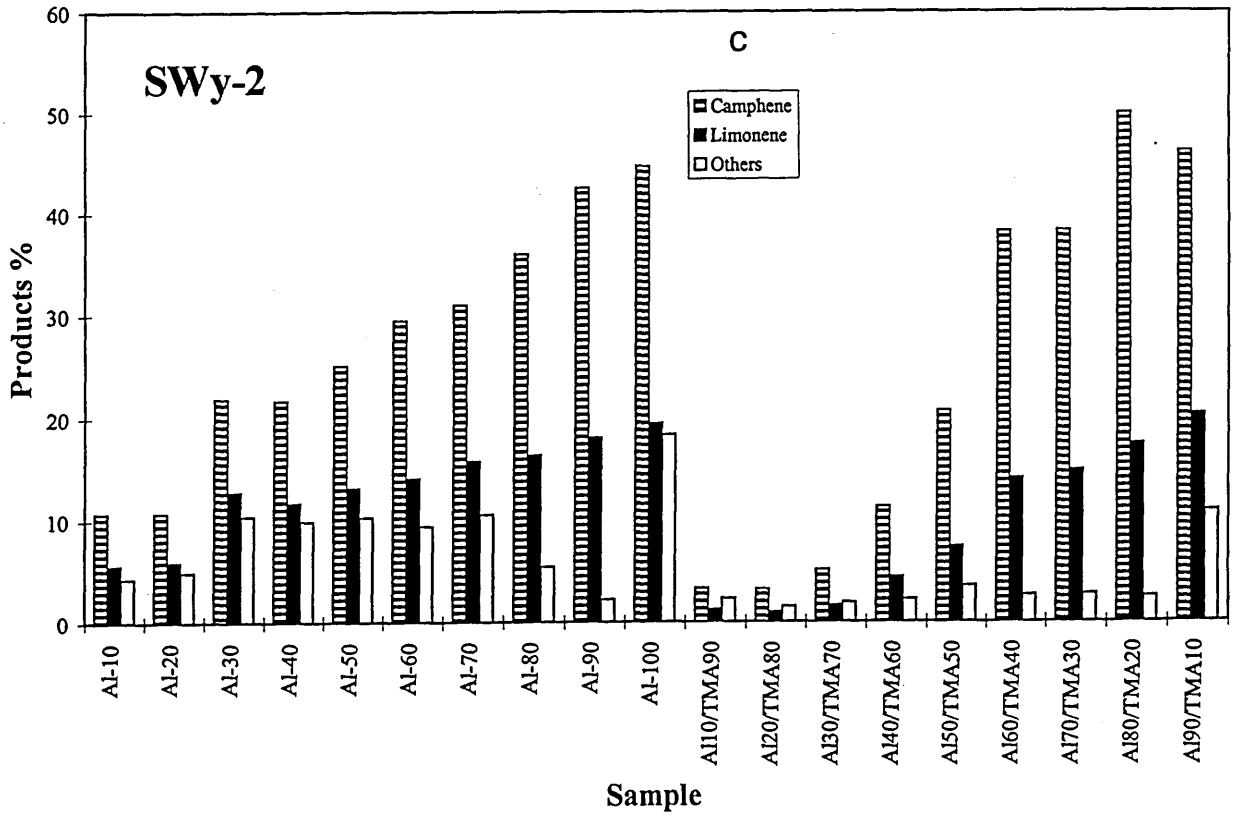

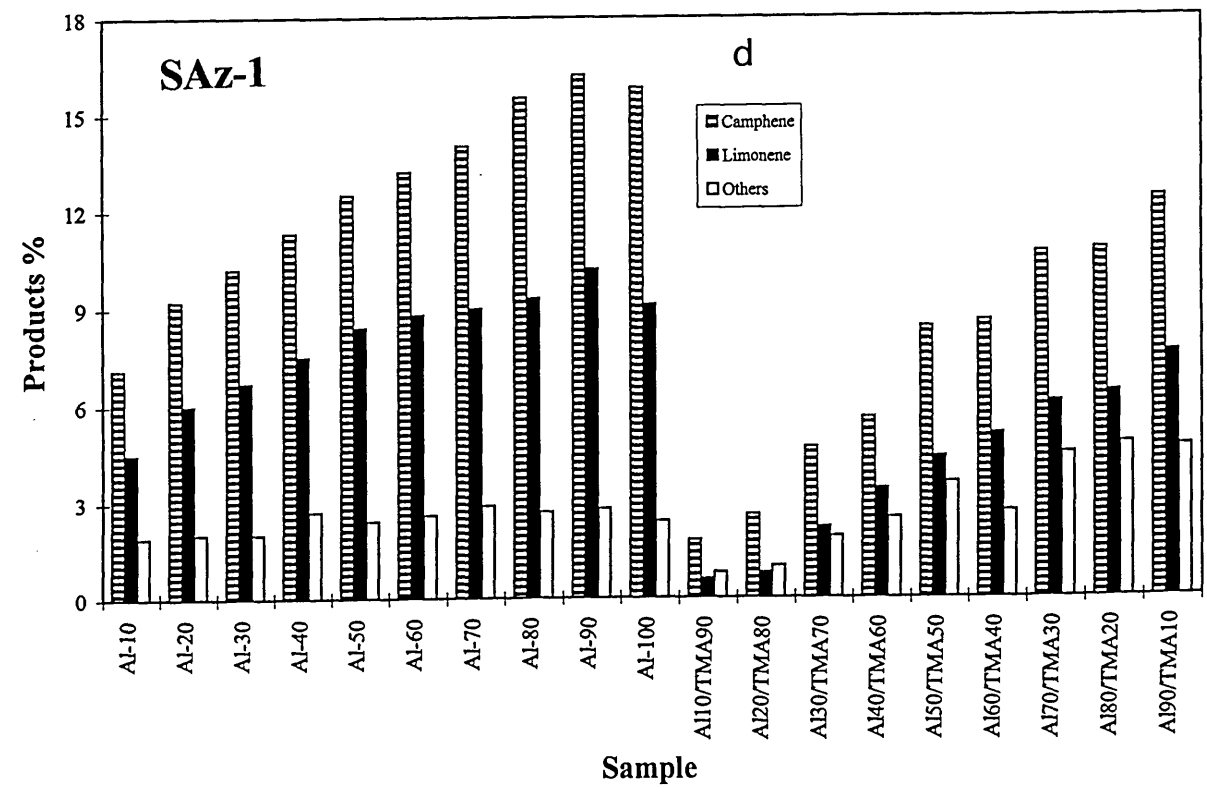

Figure 45. Continued. Product distribution for the catalysts derived from (c) SWy-2 and (d) SAz-1.

These clay catalysts are not as selective towards camphene as the permanently porous catalysts. However, the yields are extremely competitive and the catalysts are less expensive to prepare.

In contrast to the behaviour of H^+/TMA^+ clays[25] where the presence of TMA^+ at intermediate loading enhanced the activity, even when conversions were low (SAz-1), the AlAOCs gave lower conversions than their AlAC counterparts with low Al^{3+} content (10-40% CEC). However, the values were similar at Al^{3+} contents > 50% CEC when the amount of TMA^+ present began to decrease significantly. Clearly, all samples gave poor correlation with TMA^+ loading.

The reduced conversion of α-pinene to its isomers in AlAOCs suggested a significant reduction in the number of acid centres available, perhaps because of displacement of protons by TMA^+ cations which are known to compete effectively with protons for exchange sites. When the Al:TMA ratio increased from 0.42 to 9.0, the percentage conversion of α-pinene increased and reached a maximum when this ratio was 2.3 and then remained constant at higher Al:TMA ratios.

5.1.5 Desorption of Cyclohexylamine

It is well known that ion exchange with polyvalent cations increases the acidity of the interlayer water in montmorillonites due to the hydrolysis of the cation solvating water molecules.[67] The release of these protons within the interlamellar region is generally accepted as the major source of the Brønsted acidity in these minerals.

In order to understand how the acidity of AlACs and AlAOCs correlated with the catalytic activity, samples were exposed to cyclohexylamine vapour at room temperature (as described in section 3.10). The acid sites measured by this method are those that are accessible and strong enough to interact with the base. In computing the values, it is assumed that each molecule of base interacts with one protonic (Brønsted) acid site.[85] Figure 46a presents the characteristic derivative thermogram for a Ca^{2+}/Na^{+}-SWy-2 before treatment with cyclohexylamine vapour. As mentioned in the previous chapter, the maxima, at 90 °C and 690 °C, corresponds to the removal of physisorbed water and the dehydroxylation of the clay layer.[83,85,212] The desorption of cyclohexylamine from samples with different aluminium contents (Figures 46b-f) showed that, in addition to the peaks mentioned above, three maxima at 140, 310 and 620 °C were also clearly distinguished. These peaks, as described in Chapter 4, have been attributed to (1) the desorption of physisorbed cyclohexylamine combined with water, (2) the desorption of cyclohexylamine from acid sites (chemisorbed cyclohexylamine) and (3) the desorption of water and CO_2 arising from a combination of layer dehydroxylation and oxidation of carbonaceous deposits derived from cyclohexylamine.[83,85]

Figures 46b-f, show that the maximum at 310 °C increased with aluminium content, whilst that at 140 °C decreased slightly. These data confirmed that sites with sufficient acid strength interact with cyclohexylamine were present in the AlACs.

The derivative thermograms for the desorption of cyclohexylamine from SW-Al/TMA samples (Figures 47a-e), contained the maxima described above together with those arising from the desorption of TMA^{+} at 410 °C, which diminished as the Al:TMA ratio increased.

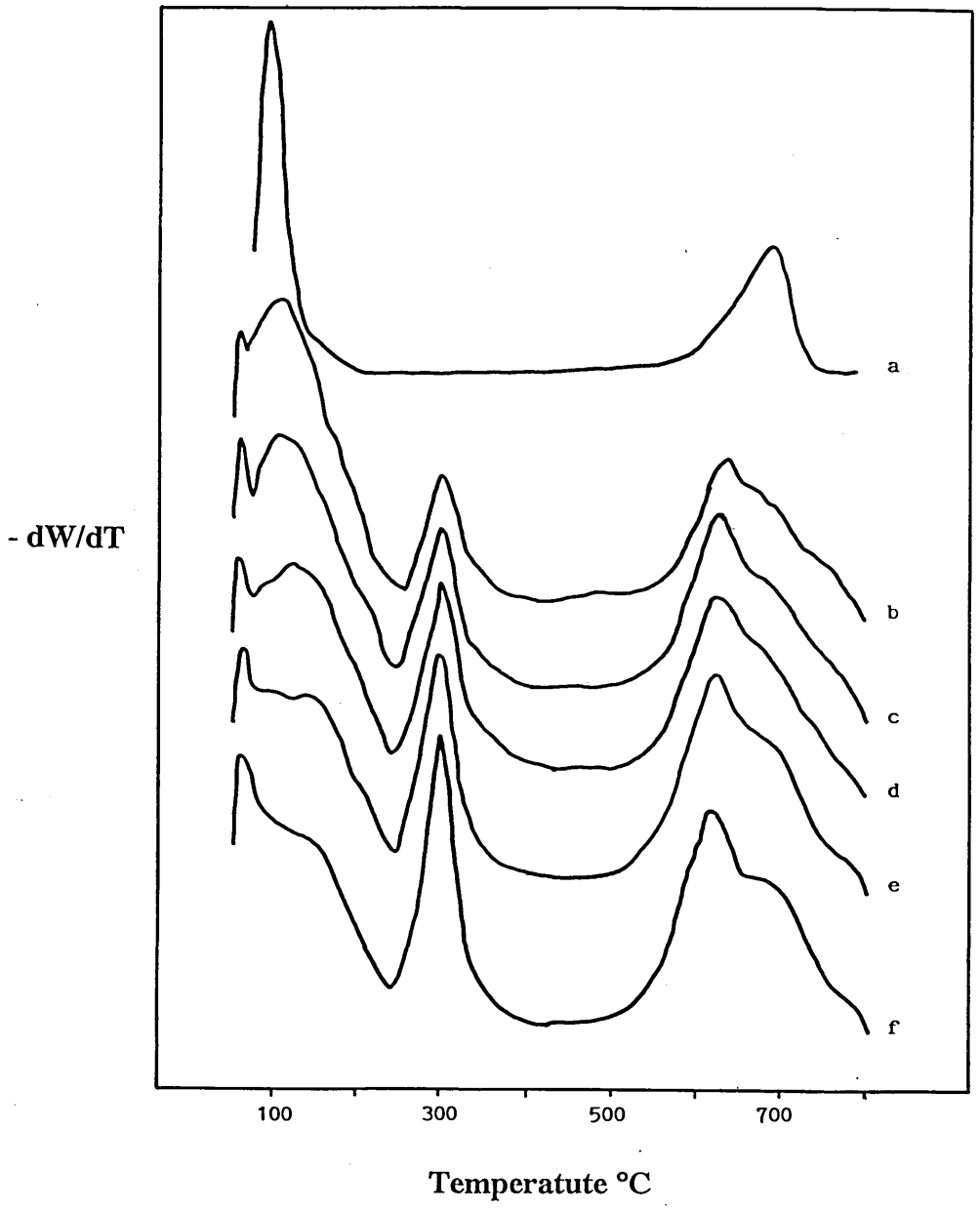

Figure 46. Derivative thermograms for (a) untreated SWy-2 and the desorption of cyclohexylamine from (b) SW-Al10, (c) SW-Al30, (d) SW-Al50, (e) SW-Al70 and (f) SW-Al90.

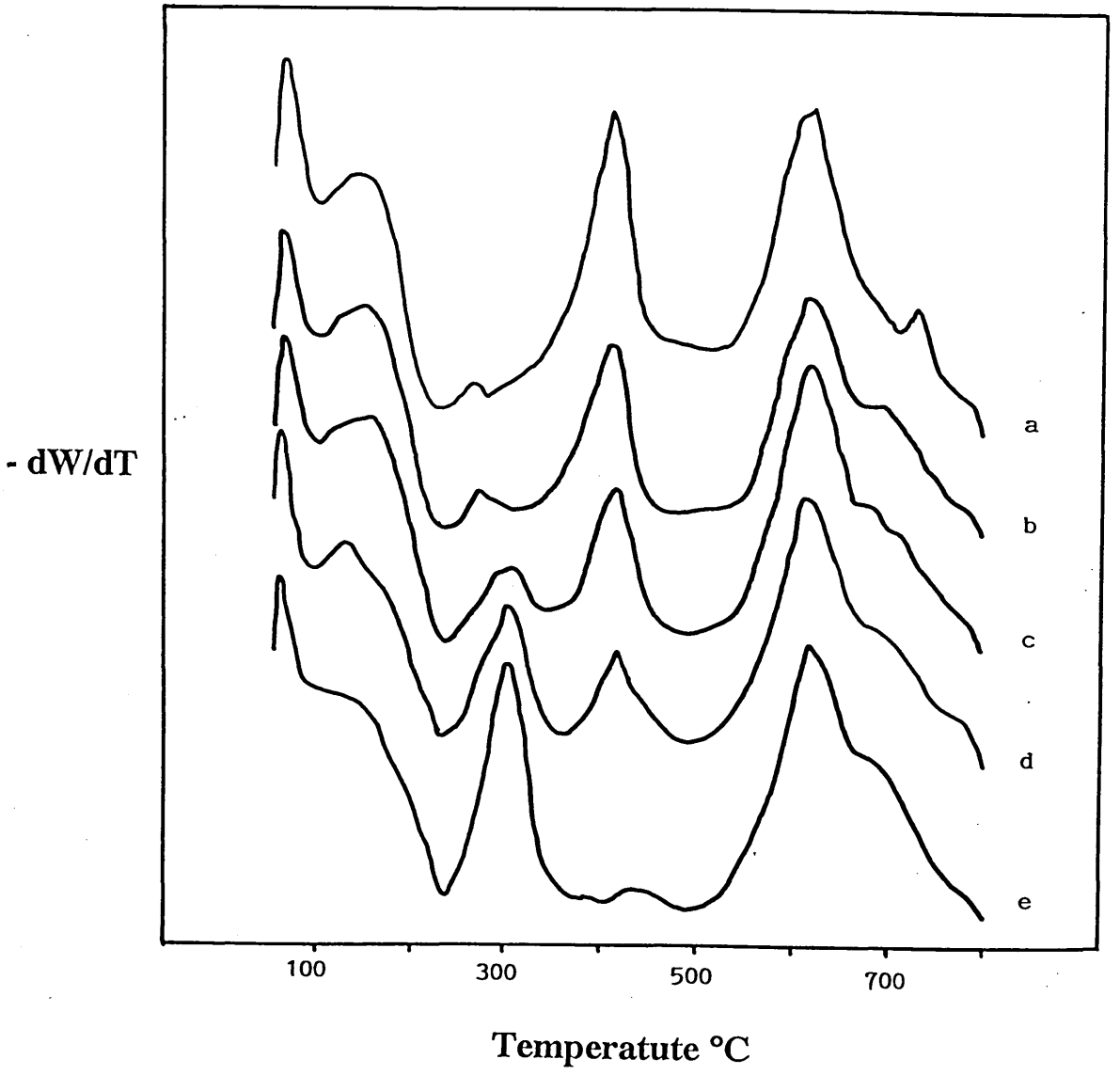

Figure 47. Derivative thermograms of cyclohexylamine from (a) SW-Al10/TMA90, (b) SW-Al30/TMA70, (c) SW-Al50/TMA50, (d) SW-Al70/TMA30 and (e) SW-Al90/TMA10.

ICP-AES results demonstrated that the amount of aluminium incorporated into both the AlACs and AlAOCs was very similar. However, the 310 °C maxima increased significantly at aluminium contents above 70% CEC, but were still at a lower intensity than the corresponding maxima in samples prepared without TMA^+ (Figure 46). These results may suggest that TMA^+ cations, even at low loadings (<30% CEC), are able to displace protons with the concomitant drop of the acidity, reflected in the lower intensity peak at 310 °C in AlAOCs compared with that of AlACs. The weight loss associated with the 310 °C maximum increased as the TMA^+ loading decreased and the Al^{3+} loading increased.

For all four clays, this weight loss was much less for the samples prepared using an Al:TMA ratio < 1 than for the corresponding AlACs. Thereafter, as the Al:TMA ratio increased, this weight loss increased to a maximum. The weight loss decreased as SAz-1 > STx-1 > SWy-2 = Sap-Ca.

For Sap-Ca AlACs and AlAOCs there was a reasonable correlation between this weight loss and the conversion of α-pinene. This was also true for STx-1 and SWy-2 and agrees with reports that the catalytic activity for the pentanol dehydration was proportional to the acidity (measured using the desorption of cyclohexylamine) of pillared acid-activated clays[133] and aluminium pillared clays.[213] However, this correlation was not reflected in the percentage of the α-pinene converted, especially for the SAz-1 series. Undoubtedly, SAz-1 is a poor catalyst for the isomerisation of α-pinene, whether in acid-activated clays (AACs) or acid-activated organoclays (AAOCs) and AlACs or AlAOCs, although the latter are marginally more active than the former.

A similar discrepancy between acidity values (determined using the desorption of cyclohexylamine) and the production of tetrahydropyranyl ether from 2,3-dihydropyran and methanol was observed for acid activated samples of SAz-1 and a Slovak montmorillonite (JP).[99] Both SAz-1 and JP were acid-activated with 400 cm^3 of 6 M HCl at 95 °C for periods of 30, 300 and 900 min. A fraction of the prepared samples was exchanged with 1 M $CaCl_2$ to displace protons in the interlamellar space. The acidities found in the acid-treated clays were identical to the acidities determined for the corresponding Ca-exchanged samples. Nonetheless, the Ca-exchanged samples were ineffective catalysts for the formation of tetrahydropyranyl ether, which requires Brønsted acid sites. This behaviour was attributed to the strong basicity of cyclohexylamine (pKb = 3.3) which enables it to interact with both weak acid sites, as in the Ca-form, and strong Brønsted acid sites, as in acid-treated clays. Therefore, the high apparent acidity noted herein for SAz-1, in comparison with the other three clays (Table 13), is attributed to the combined interaction of cyclohexylamine with the catalytically active Al^{3+}-ions and the catalytically inactive Ca^{2+} ions which are progressively displaced by Al^{3+}-ions. Both Al- and Ca-montmorillonites are able to interact with strong and weak bases immediately upon exposure in either liquid or vapour phase.[85,201,214]

As can be seen in Table 13, it is evident that the presence of TMA^+ causes a dramatic reduction in the number of acid centres (50% in samples in the range of 10-50% Al^{3+}) available for reaction with cyclohexylamine. Therefore, this observation supports the assumption that TMA^+ displaces protons with the subsequent reduction in the catalytic activity or that the weight loss in AlAOCs is not a good marker of the acidity.

	Sap-Ca	STx-1	SWy-2	SAz-1
Al-10	0.21	0.35	0.23	0.48
Al-20	0.23	0.36	0.23	0.49
Al-30	0.26	0.38	0.23	0.54
Al-40	0.27	0.38	0.28	0.55
Al-50	0.28	0.40	0.28	0.57
Al-60	0.32	0.41	0.29	0.58
Al-70	0.32	0.41	0.30	0.60
Al-80	0.32	0.42	0.32	0.61
Al-90	0.33	0.44	0.34	0.64
Al-100	0.34	0.47	0.36	0.67
Al10/TMA90	0.11	0.13	0.12	0.22
Al20/TMA80	0.12	0.15	0.13	0.24
Al30/TMA70	0.13	0.18	0.14	0.27
Al40/TMA60	0.16	0.22	0.14	0.29
Al50/TMA50	0.17	0.25	0.15	0.31
Al60/TMA40	0.25	0.28	0.21	0.37
Al70/TMA30	0.27	0.31	0.21	0.43
Al80/TMA20	0.28	0.36	0.25	0.51
Al90/TMA10	0.31	0.42	0.31	0.63

Table 13. Acidity values (mmol H^+/g clay) for AlACs and AlAOCs.

In the previous chapter, the principal objective was to determine how the presence of TMA^+ influenced the catalytic activity of a series of acid activated organoclays. It was demonstrated

that SWy-2 and STx-1 were more effective for α-pinene isomerisation when they contained 25-30% TMA^+ cations on the exchange sites than those prepared without TMA^+ whereas acid treated samples derived from Sap-Ca and SAz-1 were more active than their TMA^+-containing counterparts. This increased activity for Sap-Ca was attributed to the extensive depopulation of the magnesium rich octahedral sheet of saponite using these relatively mild acid treatments. The poor yield over SA-TMA/H was ascribed to reduced access to the active surface because of the inability of SA-TMA to disperse in α-pinene or because α-pinene can not get into the interlayer. However, AAOCs containing TMA^+ cations were more effective than AAOCs containing polycations[24] or alkyltrimethylammonium ions.[25] This behaviour was attributed to the congestion of the clay galleries at high loading of large organocations or polycations so that the activity decreased.[24,25]

In this section, it has been demonstrated that the AlACs were more active for α-pinene conversion than the corresponding AlAOCs at low aluminium contents, although they were similar when Al^{3+} was the predominant exchange ion. Figure 48 shows clearly that increasing the TMA^+ content above 20-30% catastrophically affected the isomerisation process. Indeed, SAz-1 was even more sensitive to the TMA^+ content which is in accord with the results for both SA-TMA/H and SA-polycation/H.[24] Al^{3+} exchange of Sap-Ca and STx-1 produced very effective catalysts equal in activity to SW-TMA/H which was the most effective H^+/TMA^+-based catalyst, as was demonstrated in Chapter 4.

5.1.6 Gas Chromatography - Mass Spectrometry

The main products from isomerisation of α-pinene are camphene and tricyclene when the

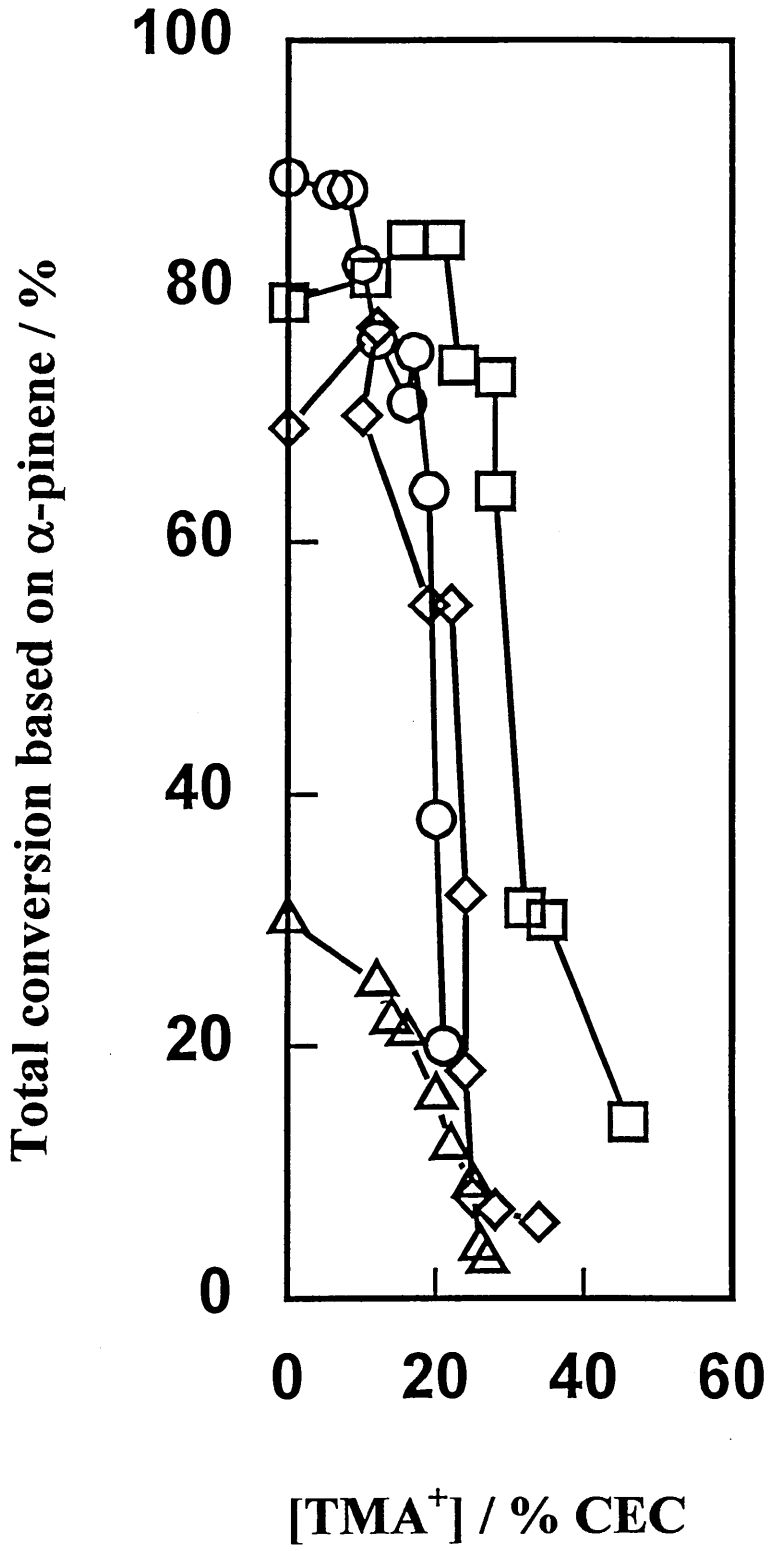

Figure 48. Total conversion of α-pinene vs TMA^+ content in AlAOCs. (○) Sap-Ca, (□) STx-1, (◇) SWy-2 and (△) SAz-1.

reaction is carried out over bentonite treated with 10% HCl.[215] These results guided De Stefanis, *et al.*,[167] to propose that the absence of tricyclene in the products derived from USY and PILCs indicated that the reactions were taking place within the pore network. Tricyclene was not found in the mixture of products derived from the AlACs or AlAOCs (Figure 49) which implies that the reaction takes place in the clay gallery. Certainly, the catalytic activity is significantly reduced when the interlayer is made inaccessible due to the presence of large quantities of organocations or polycation.[24,25]

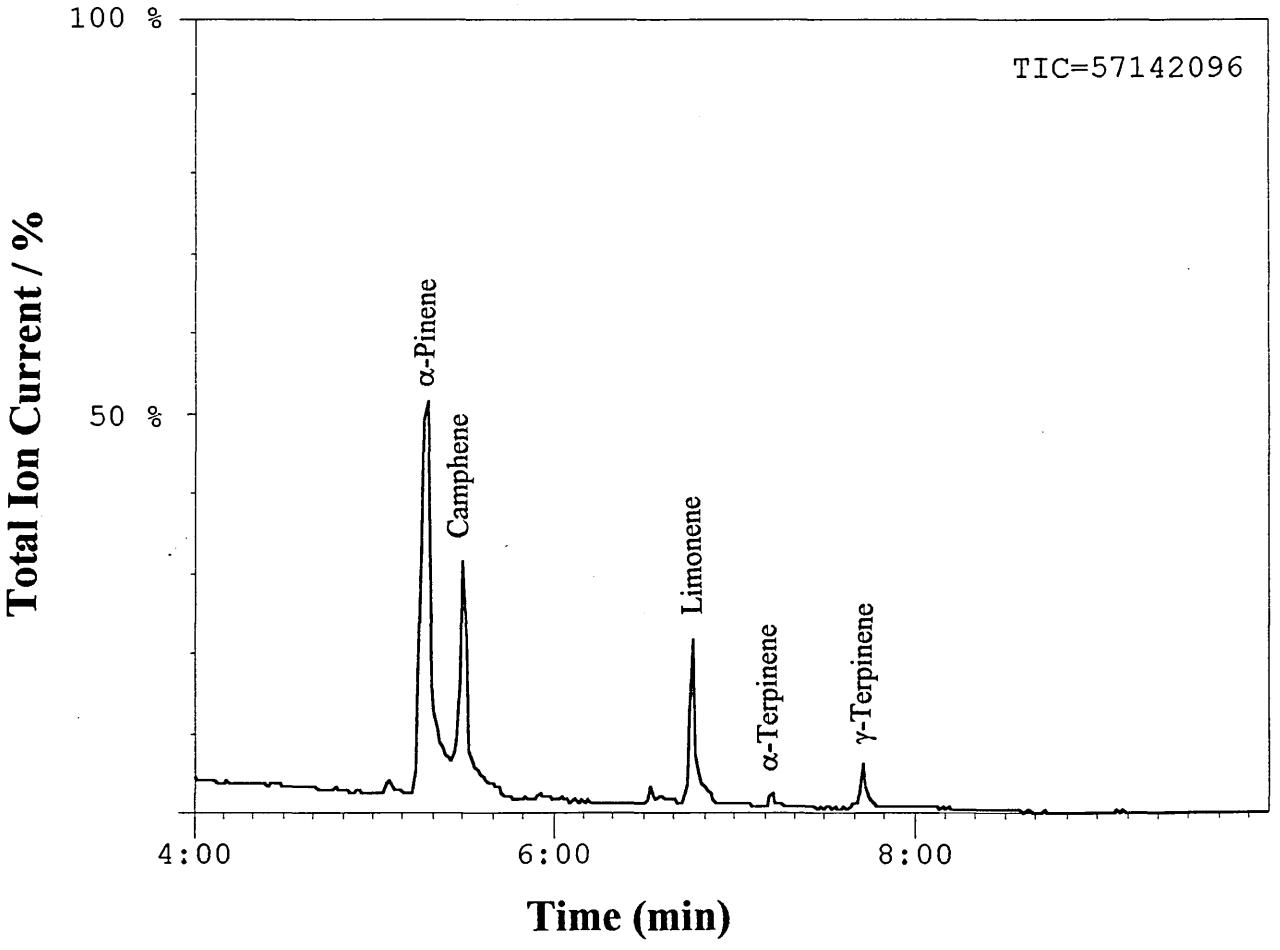

Figure 49. GC-MS chromatogram of the reaction products of α-pinene over SCa-Al20.

5.1.7 VT-XRD

VT-XRD of selected AlACs and AlAOCs were exposed to α-pinene vapour. The results, showing the d-spacing (in Å), are illustrated in Table 14.

	RT	100 °C	150 °C	200 °C	300 °C
ST-Al100	14.0	13.5	13.5	13.0	12.8
ST-Al10/TMA90	14.3	13.8	13.4	12.7	12.5

Table 14. Showing the basal spacing for selected AlAC and AlAOC exposed to α-pinene.

As can be seen from Table 14, the d-spacing in the AlAOC is dominated by the presence of the organocation and is essentially maintained at temperatures up to 300 °C. Surprisingly, the AlAC also keeps the layers expanded in the same temperature range. It is worth noticing that the thermal stability of the basal spacing is much higher than the temperature at which the reaction is carried out (120 °C). This observation clearly indicates that the AlACs have expanded layers allowing the reactant molecules to get into the interlamellar region and reach the acid centres, as for AAOCs with low TMA^+ loadings (20-30% CEC). This conclusion explains the similarity in catalytic activity showed by AlAOCs and AlACs at higher aluminium contents >70%. Additionally, in contrast, the AACs are likely to be largely collapsed after activation at 120 °C. Thus, it seems to appear that the 20-30% CEC of TMA^+ on the exchange sites in the most active AAOCs (SWy-2, previous chapter) serves to prop some galleries apart and promote the accessibility of α-pinene to react with available protons.

Both AAOCs and AlAOCs with high TMA^+ loadings possess a high population of the organocation in the interlamellar spacing and limit the ingress of α-pinene. Additionally, in AlAOCs, TMA^+ cations displace protons and decrease the possibilities for reaction, as has been demonstrated herein.

5.1.8 Reduced Charge Montmorillonite (RCM)

As demonstrated in Chapter 4 and herein, the poorest catalysts for the isomerisation of α-pinene have been those derived from the SAz-1 source clay. The reasons for this abnormal behaviour have been explained in terms of (i) its highest TMA^+ content in either AAOCs or AlAOCs, (ii) the significant amount of Ca^+ that is not easily displaced by Al^{3+} in AlACs and (iii) the highest layer charge and suspected inability to expand the layers in AACs.

In an attempt to reduce the charge density and to diminish the incorporation of TMA^+ cations, Na-SAz-1 samples were exchanged first with lithium in different percentages, heated at 250 °C for 15 h and finally Al^{3+}-exchanged (see section 3.2.3). Figure 50 illustrates the total conversion of α-pinene as a function of the amount of Al^{3+} offered (assuming no charge reduction).

As can be seen from Figure 50, the charge reduction in Na-SAz-1 caused a significant improvement in the catalytic activity in all cases, if compared with SAz-1 samples prepared by simple aluminium exchange. The highest conversion is observed when SAz-1 is charge reduced by 50% of original CEC (sample denoted as RCM50). The catalysts become progressively much more active as the aluminium offered increased. RCM50 reached a level of catalytic activity similar to that shown by its SW-Al100 analogue (67% conversion).

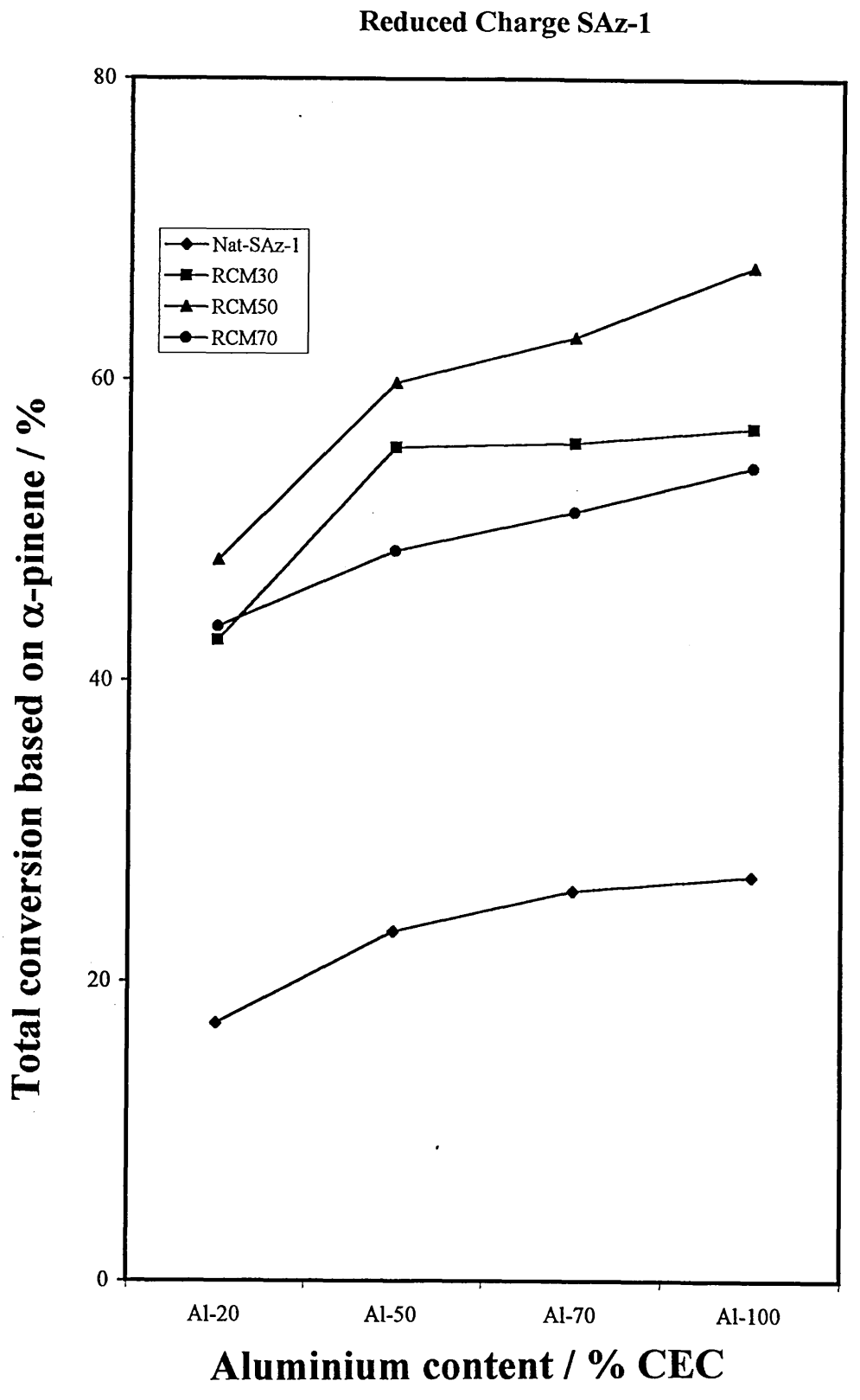

Figure 50. Total conversion of α-pinene vs Al^{3+} content in reduced charge SAz-1.

Both RCM30 and RCM70 presented a lower catalytic activity than for RCM50. These differences can be explained in terms of the extent of the charge reduction process. As the charge reduction proceeds, all the layers retain some exchangeable cations until about half the original charge is reached at which point collapsed layers begin to appear.[216] This is the case with the RCM70 samples.

Boyd and Jaynes[142] demonstrated that Li^+ charge reduction in SAz-1 followed by exchange with trimethylphenylammonium ($TMPA^+$) ions improved the adsorption of benzene, alkylbenzene and naphthalene. They prepared charge reduced SAz-1 samples in different percentages: RCM30, RCM60, RCM80 and RCM100, and noticed that the nitrogen surface areas increased and the $TMPA^+$ content decreased steadily as the layer charge decreased. The order in the surface area found was: RCM60 > RCM80 ≥ RCM30 > RCM100. These findings can be used to further support the data shown in Figure 50. Consequently, in the RCM50 samples the nitrogen surface area might be at a maximum, in this case the ability of aluminium to prop the layer apart is the maximum. In RCM30 there could be an enhancement in the surface area, but not enough acid sites to achieve the maximum conversion, and finally RCM70 could present less aluminium in the interlamellar space that does not optimise the expandability of the layers and therefore a fall in the catalytic activity was anticipated (Figure 51).

Williams, *et al.*,[217] found that Li^+-exchanged montmorillonite was able to catalyse the production of dicyclohexylamine from cyclohexylamine in the temperature range 185-250 °C at various times (0-25 h). They interpreted their results on the basis of a sequence of events, the first being the thermally induced migration of Li^+ into the octahedral layer,[51,59] the second

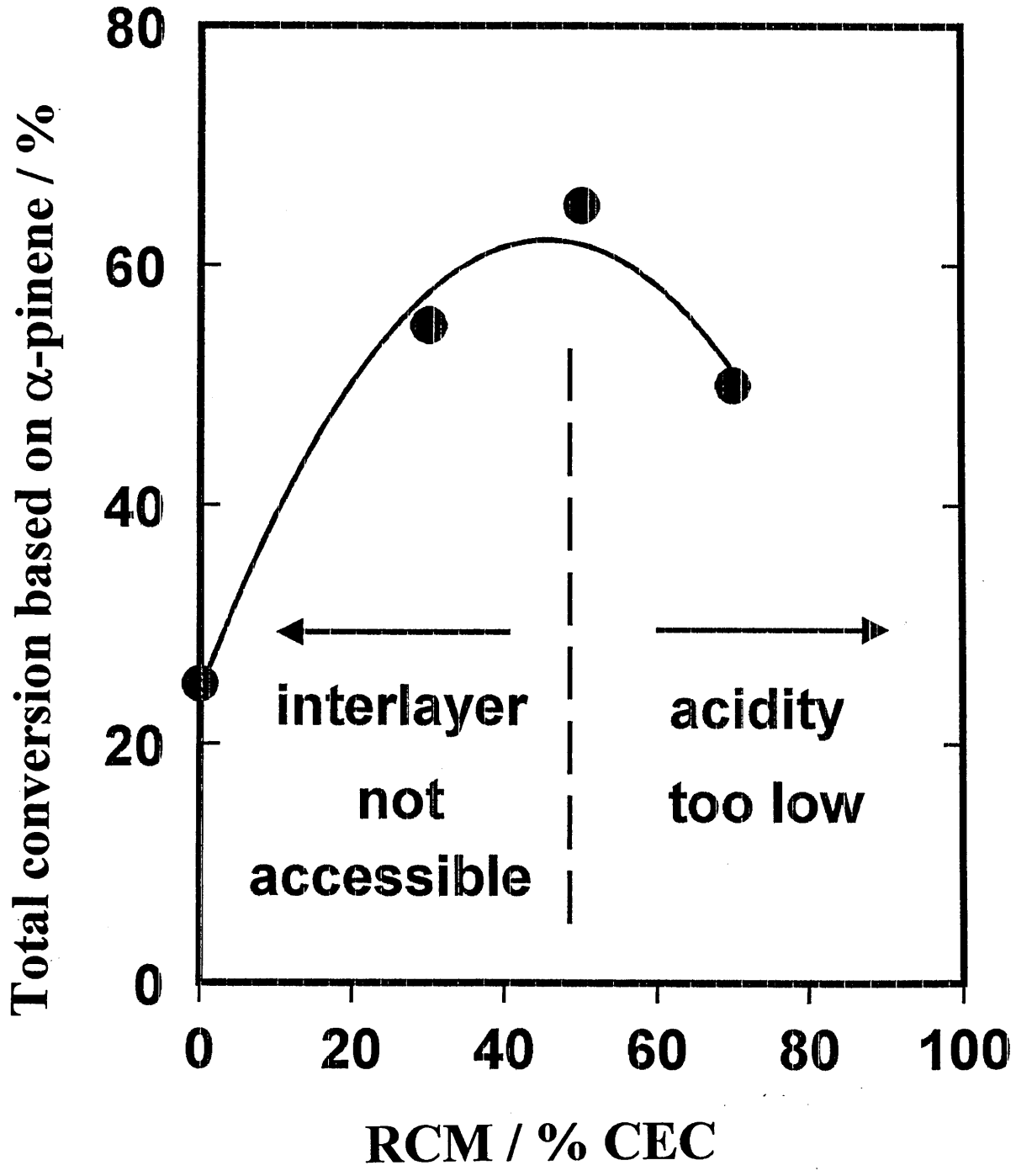

Figure 51. Showing the total conversion of α-pinene vs the extent of charge reduction for the most active RCMs (100% Al^{3+}).

the interaction of Li^+ with the available –OH group and finally the extraction of H^+ by cyclohexylamine into the interlamellar space. However, thermal activated Li^+-reduced samples (without Al^{3+}) prepared in this study were, in general, inactive towards the isomerisation of α-pinene, under the experimental conditions utilised. The explanation for this is that the cyclohexylamine is strong enough to subtract protons, whereas α-pinene is very weak in that regard.

In conclusion, a correlation of catalytic activity with layer charge does exist, especially when samples are exchanged with an active ion. The charge reduction treatment turns a high charge montmorillonite (SAz-1) into a low charge clay making it similar to SWy-2 or STx-1 clays where the hydrated aluminium incorporated in the interlayer region is able to expand the layers and facilitate the ingress of α-pinene, favouring the catalytic process.

5.2 Effect of the Shape and Valence of the Organocations.

In this study the dependence of the catalytic activities of AlAOCs on the shape and valence of the organocation [*e.g.*, 1,4-diazabicyclo[2.2.2]octane (DABCO) and 1,5-diamimopentane (DAP)] is investigated. $DABCOH_2^{2+}$ is thought to be a suitable organocation because it is a bulky molecule, which orientates parallel to the interlamellar space, whilst $DAPH_2^{2+}$ cation (linear organocation) will be accommodated in the horizontal position. Both divalent organocations should occupy less of the interlamellar space than their equivalent monovalent ones (*e.g.*, TMA^+). Additionally, $DABCOH_2^{2+}$ and $DAPH_2^{2+}$, with two positive ends, could exercise a tie effect between each pair of negatively charged tetrahedral sheets. This has proven to reduce the activity of polycation-treated clays.[24]

In this section the thermal stability, acidity and catalytic activity of SWy-2 clay prepared by mixing $DABCOH_2^{2+}$ or $DAPH_2^{2+}$ with aluminium in different ratios is studied. The results obtained with these series of AlAOCs are compared with those of AlAOCs derived from Al^{3+}/TMA^+. The sample designation is identical to that given for Al^{3+}/TMA^+ samples.

5.2.1 XRD

The spacings obtained for SWy-2 treated with Al^{3+} and TMA^+, $DAPH_2^{2+}$ or $DABCOH_2^{2+}$ in different ratios, (as described in section 3.2.2) were uniform (Figure 52).

When SWy-2 was saturated with TMA^+, a 13.6 Å spacing was obtained, whilst those obtained for SW-Al/DAP and SW-Al/DABCO samples the spacings were 12.8 Å and 14.6 Å, respectively. The increment of aluminium content caused a slight reduction in the d-spacings, but in general the values were essentially the same. This indicates that the spacing between the adjacent silica layers of these alumino-organoclay complexes are apparently governed by the presence of the organocation. Differences in the XRD interlayer spacings among the AlAOCs is due to the different sizes of TMA^+, $DABCOH_2^{2+}$ and $DAPH_2^{2+}$ cations.

These results indicate that (i) tetrahedral TMA^+ cations are present in the interlamellar space from the mid point between the layers,[142,218,219] (ii) $DAPH_2^{2+}$ cations are oriented in the horizontal position on the basal surface of the silica lamellae[220,221] and (iii) $DABCOH_2^{2+}$ cations have the N-H groups imbedded in vertical orientation directly in contact with adjacent silicate layers.[118,168] However, Slade, *et al.*,[222] reported a d-spacing of 12.5 Å for DABCO-Vermiculite, which is considerably less than that observed with montmorillonites by Shabtai, *et al.*,[118] Mortland and Berheiser[168] and herein. Slade, *et al.*,[222] attributed this

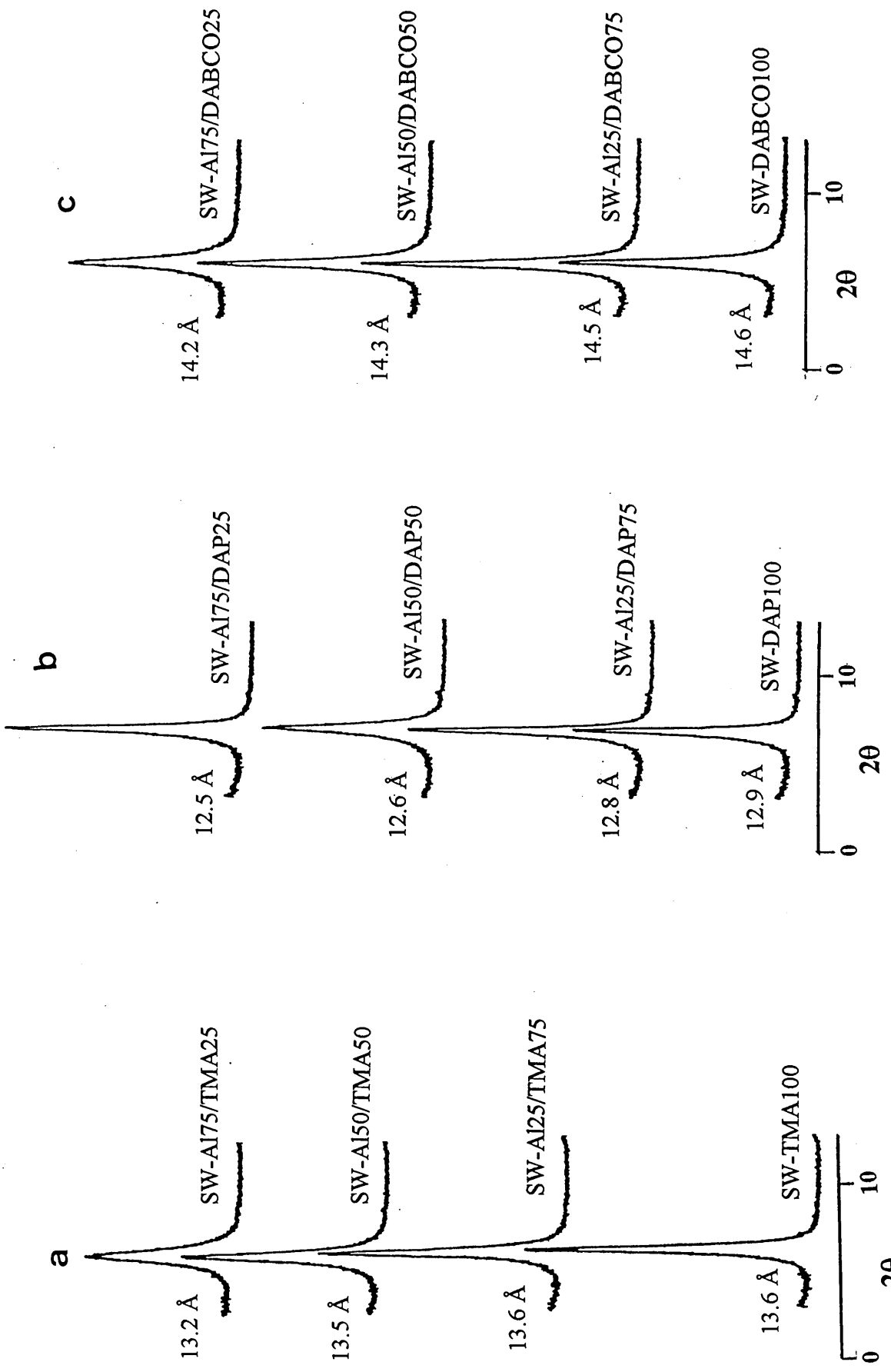

Figure 52. XRD patterns of (a) SW-Al/TMA, (b) SW-Al/DAP and (c) SW-Al/DABCO.

difference to the collapse of the interlayer structure due to the high vacuum conditions utilised, which decreases the water content and therefore a reduction in the d-spacing was expected. Additionally, they concluded that under those circumstances only organic fragments separated the silica layers.

5.2.2 Elemental Analysis

Table 15 lists the nitrogen content in SWy-2 clays 100% exchanged with TMA^+, $DAPH_2^{2+}$ and $DABCOH_2^{2+}$. The results are compared with the calculated values for these organocations.

	%N calc.	%N found	% Incorporated
SW-TMA	1.21	0.91	75
SW-DAP	1.21	0.99	81
SW-DABCO	1.21	1.19	98

Table 15. Showing % nitrogen and organocation incorporation in 100%-exchanged SWy-2.

As can be seen from a comparison of the results represented in Table 15, it is clear that the amount of the organocations incorporated follows the sequence: $DABCOH_2^{2+} > DAPH_2^{2+} > TMA^+$. The reason for this dichotomy could be attributed to the presence of protons in $DABCOH_2^{2+}$ and $DAPH_2^{2+}$ solutions, which favour the displacement of the exchangeable cations and allow the access of these alkyldiammonium ions to the interlamellar space. This observation will be considered later to explain the apparent acidity and the catalytic activity shown by these catalysts.

5.2.3 Thermal Stability

Figures 53a and 53b present the derivative thermograms for the desorption/decomposition of $DAPH_2^{2+}$ and $DABCOH_2^{2+}$ from samples prepared in different ratios of these organocations with Al^{3+}. The regions corresponding to the loss of sorbed water and the dehydroxylation are clearly observed together with the desorption maxima for $DAPH_2^{2+}$ and $DABCOH_2^{2+}$ centred at 340 °C and 300 °C, respectively. It was shown that the maximum desorption/breakdown of TMA^+ occurred at 410 °C, which means that TMA^+ is thermally more stable than the alkyldiammonium cations. The thermogravimetric analysis in nitrogen flow indicated negligible decomposition at < 150 °C.

It is worth mentioning that the maximum desorption of $DABCOH_2^{2+}$ is higher than that of $DAPH_2^{2+}$, supporting the results found by elemental analysis (Table 15).

Similarly, regarding the behaviour observed in Al^{3+}/TMA^+ samples, a reduction in the desorption maximum for $DABCOH_2^{2+}$ occurred upon increasing the Al^{3+} content. Conversely, this effect was not reflected in SW-Al/DAP samples, in which the maximum remained essentially unchanged. An explanation in accord with these experimental data is that the $DAPH_2^{2+}$ cations are more resistance to displacement by Al^{3+} than that for TMA^+ and $DABCOH_2^{2+}$.

Additionally, clays saturated with different shape cations of moderate size, those organocations taking the more closely spaced sites ($DAPH_2^{2+}$), might therefore effectively fill the space between the tetrahedral sheets (Figure 54a), whilst those on the more widely spaced sites ($DABCOH_2^{2+}$ and TMA^+) might leave empty channels of greater width, large enough to

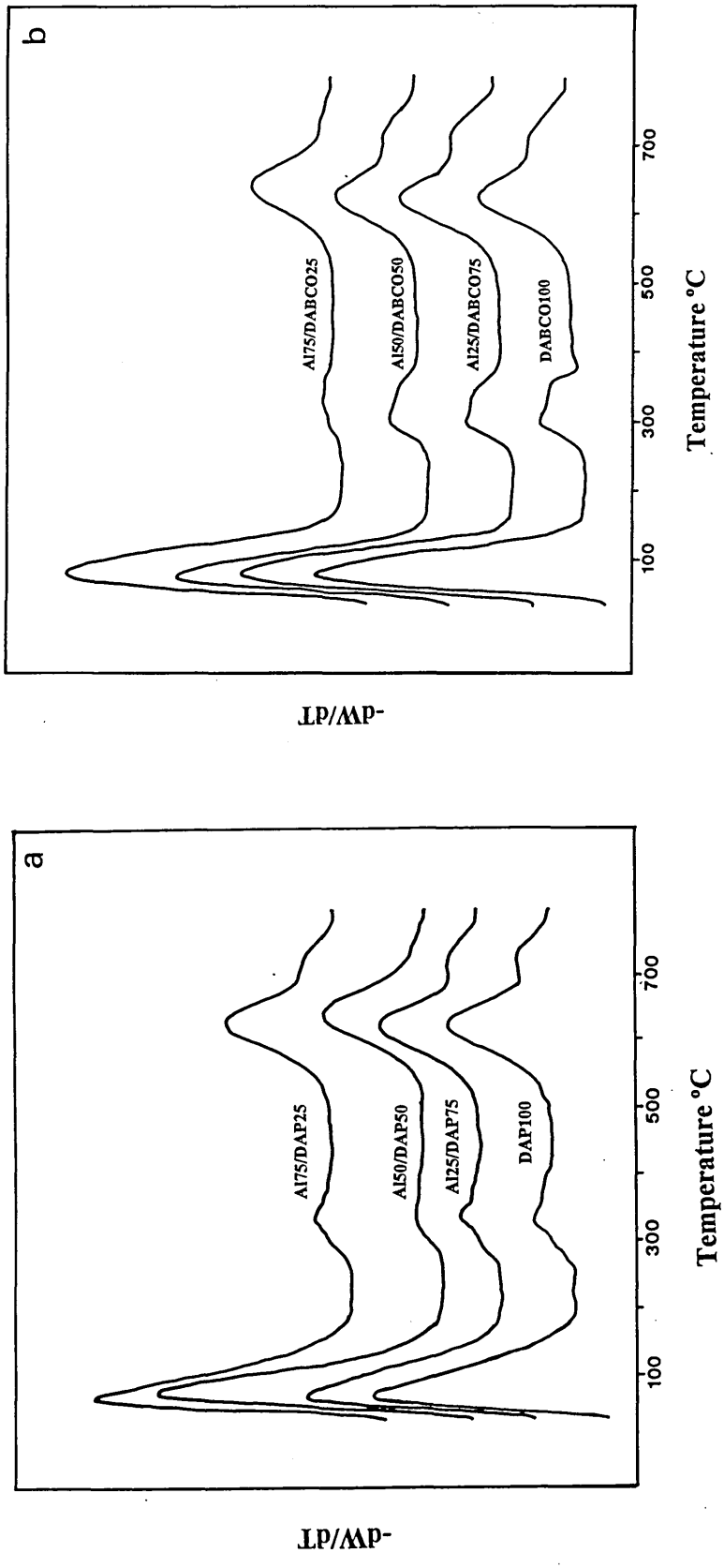

Figure 53. Derivative thermograms for (a) SW-Al/DAP and (b) SW-Al/DABCO.

accommodate organic molecules (Figure 54b).[221] As a result, a low α-pinene conversion is anticipated in SWy-2 samples derived from Al^{3+}/$DAPH_2^{2+}$.

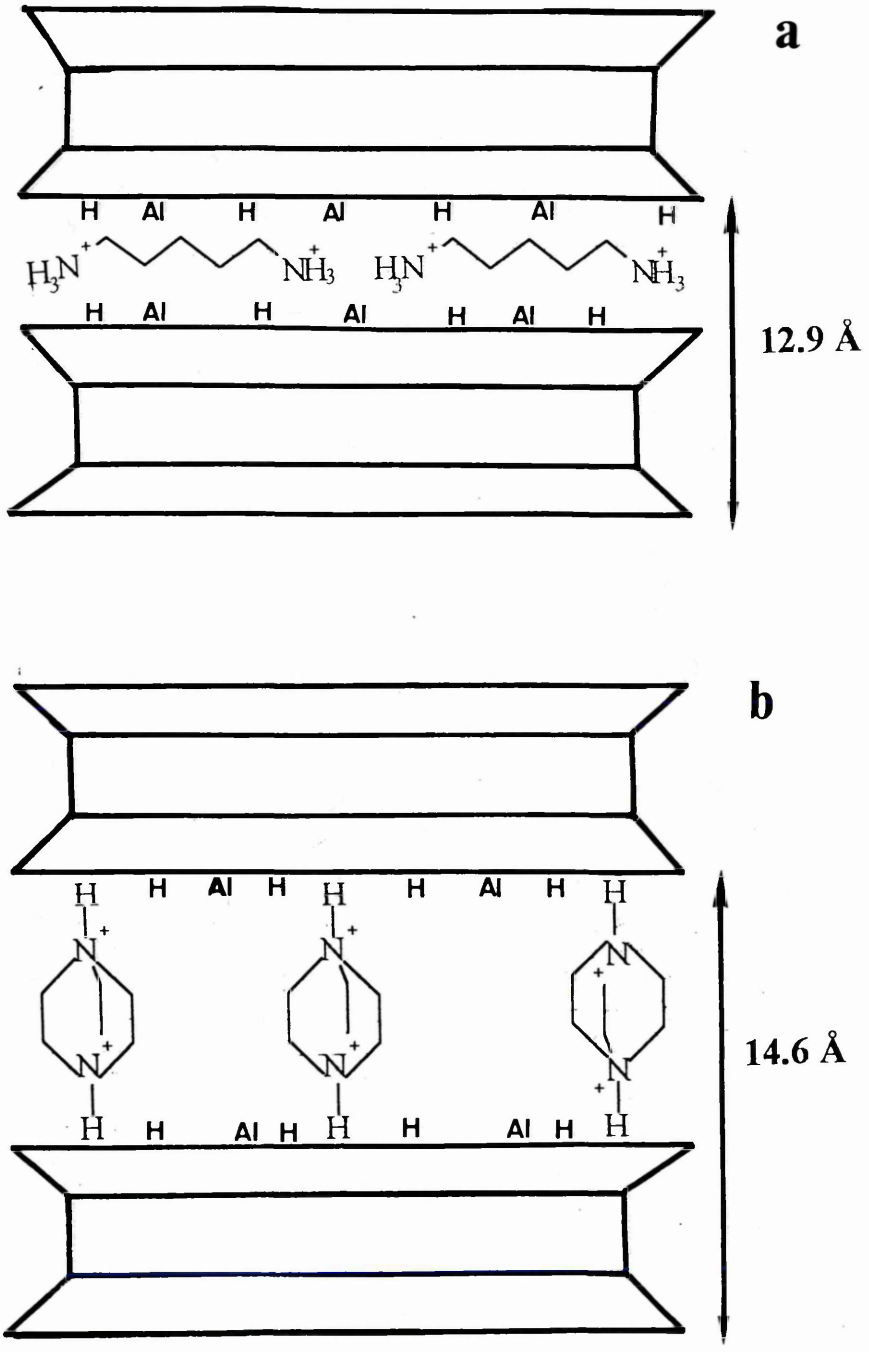

Figure 54. Schematic models showing (a) the arrangement of $DAPH_2^{2+}$ and (b) $DABCOH_2^{2+}$ in SWy-2.

It is important to recall that the diprotonated forms of DAP and DABCO were obtained by mixing each organocation with concentrated HCl to produce a final concentration solution of 1 M DABCO in 2 M HCl or 1 M DAP in 2 M HCl ($DAPH_2^{2+}$ $DABCOH_2^{2+}$). Both divalent organocations are then able to neutralise two exchange sites. Given that a lateral (interpillar) distance is 22 Å for M^{2+} ions whilst for monovalent cations (*e.g.*, TMA^+) the interpillar distance is 11 Å (Figure 55), these distances represent the average of calculated values.[223]

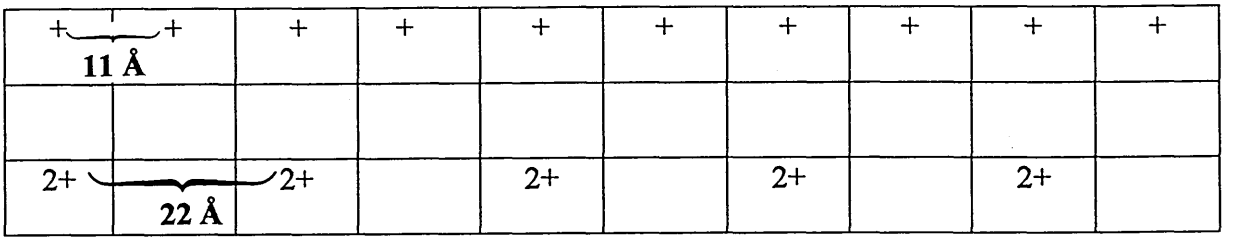

Figure 55. Showing the interpillar distance between monovalent and divalent organocations.

5.2.4 Cyclohexylamine Interaction

The result of adsorption of cyclohexylamine vapour on SW-Al/DABCO and SW-Al/DAP samples is illustrated in Figure 56. The desorption thermograms for cyclohexylamine from SW-Al/DABCO (Fig. 56a) exhibited the same desorption maxima as those of SW-Al/TMA at 140, near 300, 600 and 720 °C, which were attributed to (i) the desorption of physisorbed cyclohexylamine with water, (ii) desorption of the base from acid sites, which overlapped the desorption maximum for $DAPH_2^{2+}$ and/or $DABCOH_2^{2+}$ and (iii) desorption of water and CO_2. The SW-Al/DAP samples give thermograms differing markedly from those of SW-Al/DABCO (Fig. 56b) in having an 'extra' maximum centred at 220 °C.

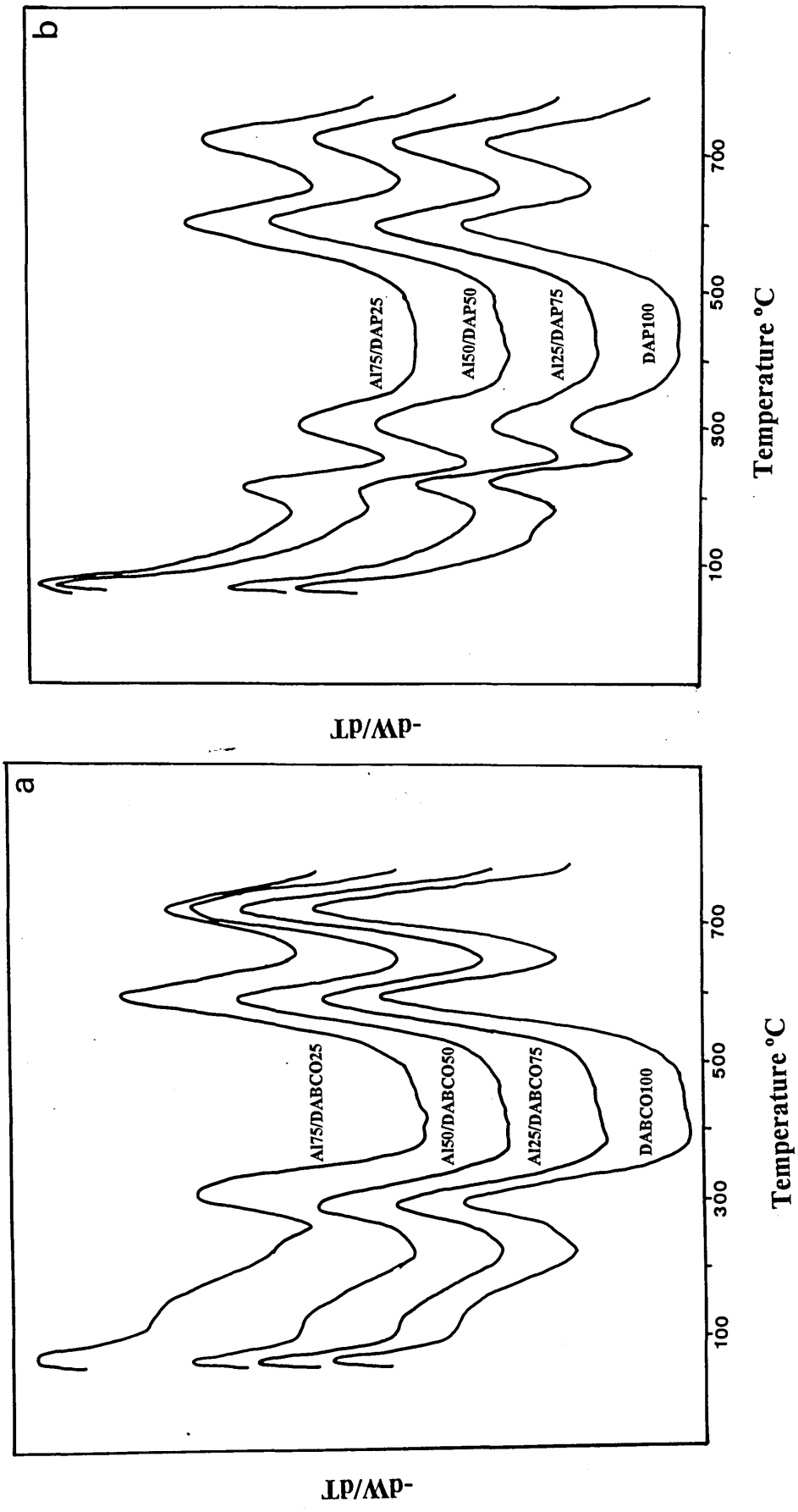

Figure 56. Differential thermogravimetric plot of (a) SW-Al/DABCO and (b) SW-Al/DAP saturated with cyclohexylamine vapour.

The 220 °C maximum presents a higher intensity than that at 310 °C. Ballantine, *et al.*,[83] observed a similar peak in the region of 150-180 °C over Al^{3+}-exchanged montmorillonites saturated with cyclohexylamine for 4 and 6 h. Additionally, they noticed that the intensity of this maximum decreased as the exposure time increased from 7-130 h. They supported their observations with the findings of Farmer and Mortland who attributed this peak to another chemisorbed species of cyclohexylamine coordinated either to an interlamellar cation[224] or to the proton of a cyclohexylammonium species via a hydrogen bond.[225]

One interesting feature is that the desorption region, observed herein, differs from that noticed by Ballantine, *et al.*,[83] because it appears between 180-260 °C. It could be possible to propose that the SW-Al/DAP system resembles that of samples partially saturated with cyclohexylamine vapour (4-6 h). However, a plausible explanation for the appearance of this peak at 220 °C is still unclear, therefore the assumption given is merely speculative.

It should be pointed out that a direct determination of the acidity was unsuccessful because the intensity of the maximum at 310 °C remained invariant as the Al^{3+} content offered increased. The intensity of the maximum at 310 °C was higher for SW-Al/DABCO samples than that of SW-Al/DAP counterparts. The "apparent" acidity observed in both series of samples is probably governed by the presence of protons arising from different competition equilibria. These equilibria come from (1) water molecules polarised by aluminium, (2) dissociation of the diprotonated forms of $DAPH_2^{2+}$ or $DABCOH_2^{2+}$ and (3) free protons from the acidic solution that did not protonate the organocations and participated in the clay exchanging process (Figure 57).

(1) $Al(OH)_6^{3+} \rightleftharpoons [Al(OH)(H_2O)_5]^{2+} + H^+$

(2) $DAPH_2^{2+} \rightleftharpoons DAPH^+ + H^+ \rightleftharpoons DAP + 2H^+$

(2) $DABCOH_2^{2+} \rightleftharpoons DABCOH^+ + H^+ \rightleftharpoons DABCO + 2H^+$

(3) DAP or DABCO + $nH^+ \rightleftharpoons DAPH_2^{2+}$ or $DABCOH_2^{2+} + H^+$ (free)

Figure 57. Equilibria involved in the protonation of cyclohexylamine over SW-Al/DAP and/or SW-Al/DABCO samples.

5.2.5 α-Pinene Conversion

Figure 58 shows the total conversion over samples derived from SW-Al/DAP and SW-Al/DABCO, the conversion over SW-Al/TMA samples is also included to provide a comparison. Evidently, the type of organocation utilised showed a significant effect on the total conversion obtained using the isomerisation of α-pinene. The lowest catalytic activity is registered in SW-Al/DAP, suggesting, as anticipated, that the exchange with $DAPH_2^{2+}$ cations results in a sterically restricted diffusion of pinene in the interlayer space of the catalyst and or no useful acidity.

The activity in SW-Al/DABCO samples is considerably higher than for SW-Al/DAP. This enhancement in activity can be ascribed to the greater openness in the interlamellar space for α-pinene to react, except for the internal surface fraction occupied by the immobilised DABCO ions. On the other hand, the vertical orientation of $DABCOH_2^{2+}$ produces channels between the alkyldiammonium cations in the interlayer space, allowing access to reactant

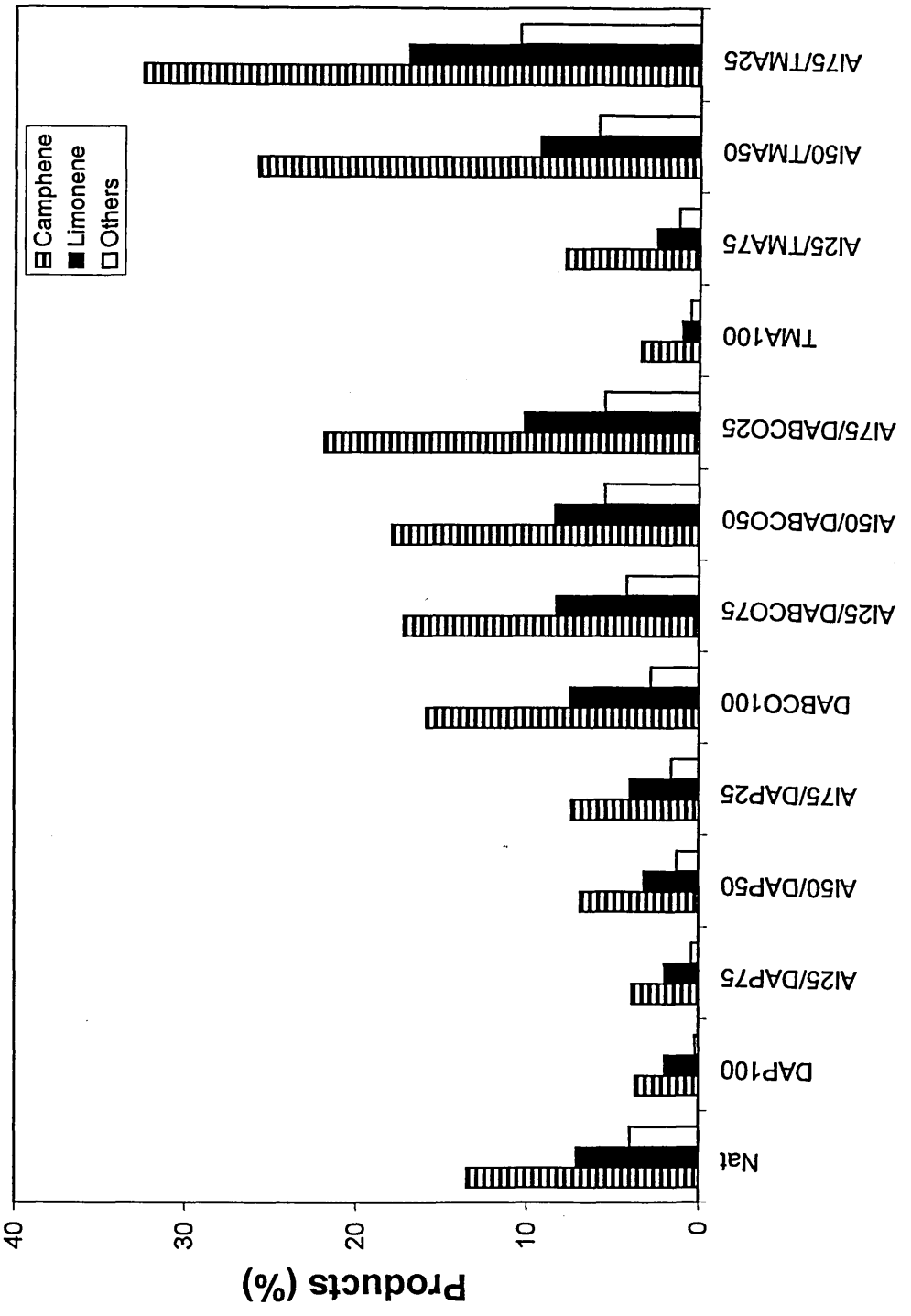

Figure 58. Product distribution for the catalysts derived from SWy-2.

molecules, whereas in $DAPH_2^{2+}$ there is a lack of height that may prevent the access of α-pinene to the interlamellar space.

In all cases the increment of the aluminium content did not cause a significant improvement in the catalytic activity as in the Al^{3+}/TMA^+ samples. The total conversion of the SW-DABCO100 sample is very similar to those observed for SW-Al25/DABCO75 and SW-Al50/DABCO50. However, a slightly higher conversion was noted in SW-Al75/DABCO25. One could suppose that $DAPH_2^{2+}$ cations are more effective in blocking the access to both Al^{3+} and protons than $DABCOH_2^{2+}$ cations. This supposition is confirmed by the fact that in both systems the Al^{3+} and H^+ contents offered were the same for similar samples, even though the lowest activity was observed in the former.

As stated before the "apparent" activity of SW-Al/DAP and SW-Al/DABCO samples is given by the presence of protons coming from different equilibria. Thus, a direct comparison with Al^{3+}/TMA^+ samples was not possible because in these samples the fraction of protons available arises only from the polarisation power of aluminium cation and, in all cases, the increment of Al^{3+} content produced a substantial enhancement of the activity.

In summary, the understanding of both $Al^{3+}/DAPH_2^{2+}$ and $Al^{3+}/DABCOH_2^{2+}$ systems is very complex and requires an extensive investigation to elucidate the source of protons, from the different equilibria that contributes to the catalytic activity, especially for $Al^{3+}/DABCOH_2^{2+}$ samples, which behaved catalytically better than those of $Al^{3+}/DAPH_2^{2+}$.

In this section, it has been demonstrated that the shape of the organocation played an important role in controlling the ability to catalyse the isomerisation of α-pinene. The best catalysts were those derived from Al^{3+}/TMA^{+} exchanged clay and, in addition, the interpillar distance between each cation is lower (11 Å) than that of divalent organocations (22 Å).[223] One would have expected an enhanced activity in the latter system due to the larger separation distance. However, this was not the factor that controlled the catalytic process and it is believed that, more than the interpillar distance, the most determinant condition is given by the size of the organocation.

5.3 Ion Exchanged Clays (IECs)

In this section, SWy-2, SAz-1 and Sap-Ca clays were exchanged with different cations (Al^{3+}, Ca^{2+}, Mg^{2+}, Na^{+} and Ni^{2+}) utilising various exchanging procedures: (i) using volumes of 0.1 M solution of each cation to satisfy the CEC of the clays; (ii) preparing first the Na-form of each clay and then the ion-exchanged as (i); and (iii) the Na-clays were fully ion-exchanged, washing the clays three times with 0.5 M solution of each cation. Samples prepared in these forms are identified as, for example Ni^{2+}-exchanged SWy-2: (i) Nat-SW-Ni, (ii) Na-SW-Ni and (iii) Fully-SW-Ni (see section 3.2.4 for details). The α-pinene isomerisation (at 80 °C for 2 h) was applied to all the IECs. The aim of this study was to evaluate both the different exchanging procedures and the effect of interlayer cation on the catalytic activity. In particular the plan was to relate gallery expansion and cation acidity to α-pinene isomerisation activity.

The catalytic activity of the IECs is correlated with the acidity values determined using the desorption of cyclohexylamine. Additionally, the desorption of cyclohexylamine was

followed by Real-Time TG-FTIR and Real-Time TG-MS to elucidate the mechanism process and to identify the desorption/decomposition products.

5.3.1 Effect of the Ion-Exchange Procedure on the Catalytic Activity

The product distribution for SWy-2, Sap-Ca and SAz-1 exchanged with Al^{3+}, Ca^{2+}, Mg^{2+}, Na^{+} and Ni^{2+} towards the Brønsted acid catalysed reaction of α-pinene as a function of the exchange procedure is shown in Figure 59. The distribution for IECs derived from the natural form (Figure 59a) shows that the highest conversion was obtained over Sap-Ca clays, followed by SWy-2 and SAz-1, which presented the lowest activity.

The order of activity of the IECs was $Al^{3+} > Ni^{2+} > Mg^{2+} > Ca^{2+} > Na^{+}$. This order of activity is in complete agreement with the charge-to-radius ratios of the metal ions (Al = 0.021, Ni = 0.016, Mg = 0.012, Ca = 0.010 and Na = 0.005), which consequently displays the polarisation power of coordinated water molecules.

Additionally, ICP data showed that the metal uptake from natural samples was not 100%. Therefore, the same series of samples were prepared from Na-SWy-2 and Na-Sap-Ca forms and their results are illustrated in Figure 59b. Indeed, an enhancement was obtained in the total conversion for Al^{3+}, Mg^{2+} and Ni^{2+} whilst that of Ca^{2+} and Na^{+} was almost invariant and the selectivity favoured towards other products. A further improvement in the catalytic activity was obtained in samples fully exchanged with Mg^{2+} and Ni^{2+}, but a reduction was noticed for Ca^{2+} (Figure 59c).

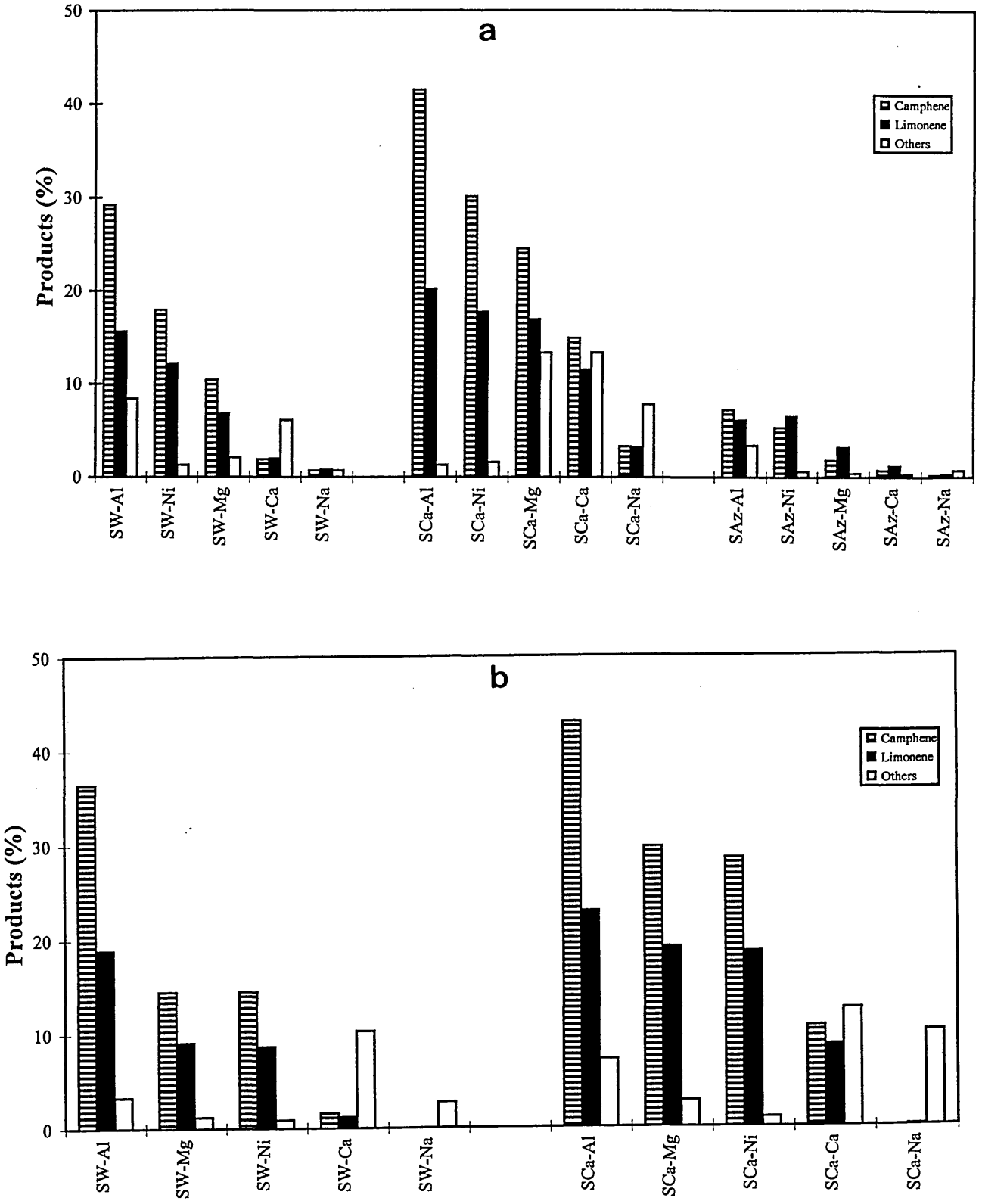

Figure 59. Product distribution for IECs from (a) Natural and (b) Na^{+}-forms.

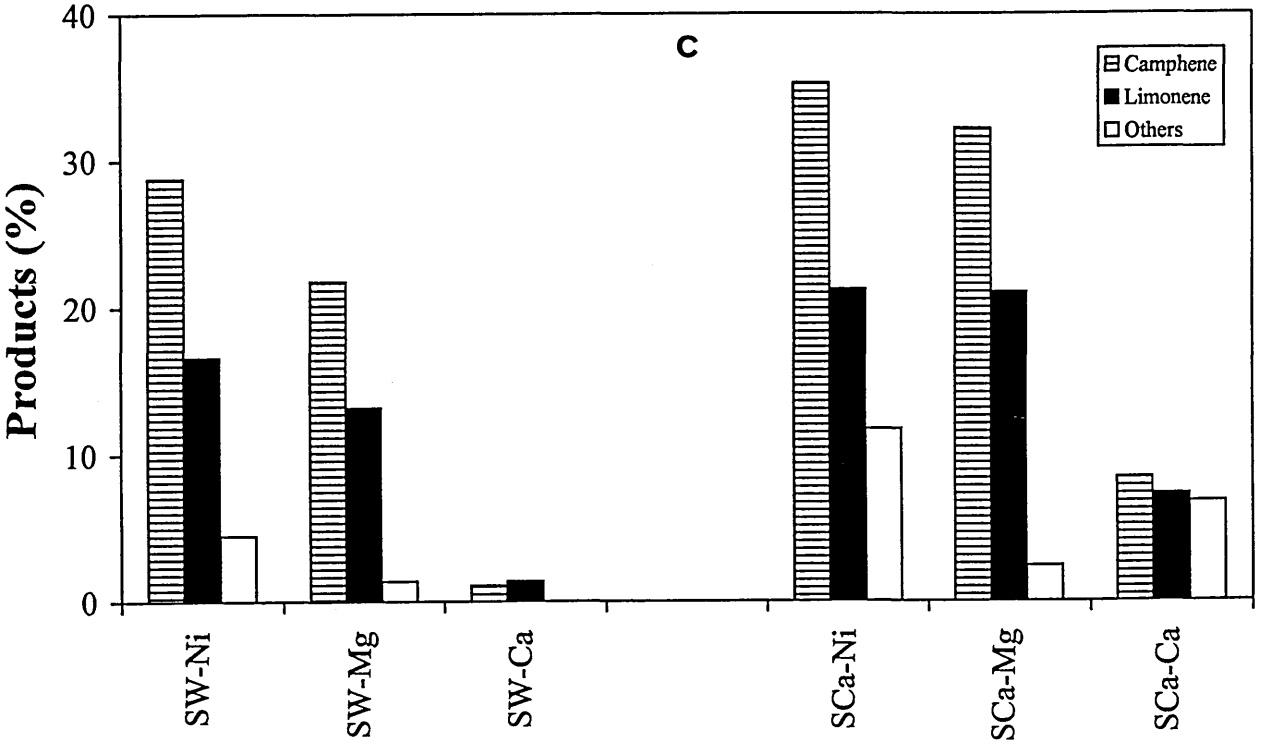

Figure 59c. Continued. Product distribution for fully-IECs.

These observations indicated that Mg^{2+} and Ni^{2+} are not so effective in displacing the exchangeable cations from the clays when IECs are prepared using procedures (i) and (ii). The activities of the Na^{+}-exchanged clays were too low in all cases.

It is worth examining the trend found in SCa-Ca in which the order of catalytic activity was Natural > Na^{+}-form > fully-exchange. A reason for this is that the Ca^{2+} ions, using procedure (i), did not fully displace the exchangeable Mg^{2+} (0.34% CaO), which is moderately active for the reaction process. Nonetheless, as the severity of the exchange treatment proceeds, either in Na^{+}- (ii) or in Ca^{2+}-form (iii), Mg^{2+} is more susceptible to displacement by the catalytically inactive Na^{+} or Ca^{2+} cations. As a result a reduction in activity was suspected.

The data obtained herein is in line with the findings of Brown and Rhodes.[108] They prepared fully-exchanged samples with Al^{3+}, Fe^{3+}, Cu^{2+}, Zn^{2+}, Ni^{2+}, Co^{2+} and Na^{+} from an acid-treated montmorillonite. The order of activity towards the isomerisation of α-pinene was Al^{3+} (8.8) > Fe^{3+} (7.0) > Cu^{2+} (3.0) > Zn^{2+} (2.1) > Ni^{2+} (1.8) = Co^{2+} (1.7) > Na^{+} (0), values given in rate constant/x10^{-5} s^{-1}. They found that, for this particular reaction, the maximum in activity was reached after thermal activation at 150 °C, in which the Brønsted acidity was at a maximum. Additionally, using the rearrangement of camphene hydrochloride to isobornyl chloride, to test the effectiveness as a Lewis acid catalyst, over the same series of samples, activated at 250-300 °C, the activity recorded in Al^{3+}-exchanged clay was dramatically reduced. A slight diminution in activity for Fe^{3+}-exchange clay was also noticed. However, the activity was increased in Ni^{2+}-exchanged samples, which means that Ni^{2+}-exchanged samples exhibited Lewis acid sites.

Overall therefore, the nature of the catalytic activity depends considerably on the extent of the exchange process. In this regard, certainly Al^{3+} was the most effective ion in displacing the resident cations in all the exchanging treatments. However, with the other ions the exchange is essentially complete when samples are treated several times with a concentrated aqueous solution of each cation.[108,226,227]

5.3.2 Characterisation of Acidities

The derivative thermograms for the desorption of cyclohexylamine for SWy-2 and Sap-Ca IECs prepared from the Na-forms are shown in Figure 60. Clearly, the desorption maxima of cyclohexylamine, at 310 °C, depends on the cation incorporated into the clay.

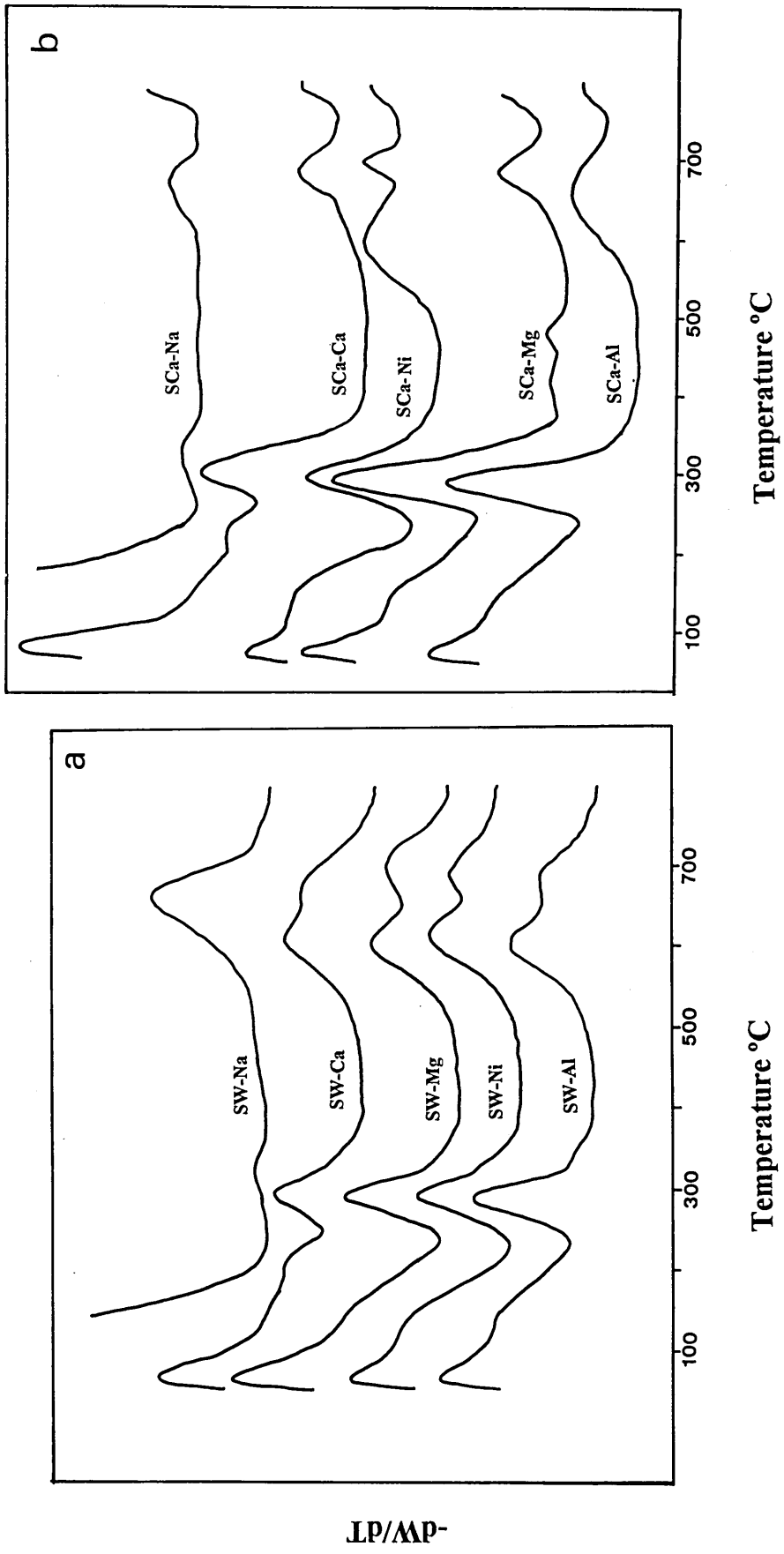

Figure 60. Differential thermogravimetric plot for the desorption of cyclohexylamine over IECs (a) SWy-2 and (b) Sap-Ca.

From the TG curves, the weight loss between 240 and 360 °C was used to compute the acidity in terms of millimoles cyclohexylamine desorbed. A relatively high lower temperature 240 °C was chosen so that differences in the amount of physisorbed base or non-exchanged water do not affect the determined values. The acidity values for all the IECs prepared using different exchanging procedures are given in Table 16. No significant differences in acidity were observed for Al^{3+}-exchanged samples, a slight increment was noticed for Ni^{2+} and Mg^{2+}, whereas those for Ca^{2+} were invariant and for Na^{+}-exchanged samples there was a reduction of 50%. Indeed, these data are marginally in accord with the results observed for the catalytic activity, in which the increase of ion incorporation (Ni^{2+} and Mg^{2+}) induced an enhancement in the total conversion of α-pinene, whilst a reduction was anticipated as the uptake Ca^{2+} and Na^{2+} increased. Ca^{2+} ions adsorb cyclohexylamine effectively,[99,201] but they are inactive for the isomerisation reaction.[108]

	Al^{3+}	Ni^{2+}	Mg^{2+}	Ca^{2+}	Na^{+}
Nat-SW	0.32	0.29	0.29	0.26	0.13
Na-SW	0.33	0.30	0.30	0.28	0.06
Fully-SW	0.33	0.31	0.32	0.29	0.06
Nat-SCa	0.30	0.24	0.32	0.29	0.12
Na-SCa	0.31	0.26	0.33	0.28	0.06
Fully-SCa	0.31	0.27	0.35	0.30	0.06

Table 16. Effect of the exchange treatment on the surface acidity (mmol H^{+}/g clay).

The concentration of surface acid sites for IECs derived from SWy-2 follows the order: $Al^{3+} > Ni^{2+} = Mg^{2+} > Ca^{2+} > Na^{+}$ whilst that for Sap-Ca is: $Mg^{2+} > Al^{3+} > Ca^{2+} > Ni^{2+} > Na^{+}$.

In contrast, the trend in catalytic activity of ion-exchanged clays is not very well reflected in the surface acidity of the clays. This is because the acidity determinations carried out in IECs were in the same range for Al^{3+}, Ca^{2+}, Mg^{2+} and Ni^{2+}, whilst the total conversions were different, in all cases. In summary, the desorption of cyclohexylamine is not a useful test for predicting the catalytic activity of IECs, for this reaction involves a non-polar substrate.

5.3.3 Real-Time TG-FTIR of the Evolved Gases during the Desorption of Cyclohexylamine.

It is worth returning to the thermogravimetric traces of the desorption of cyclohexylamine shown in Figure 60, in which there is a noticeable difference between Na-SCa-Ni and the other IECs. In the presence of cyclohexylamine, the CO_2 evolution in Na-SCa-Ni is shifted to a lower temperature, showing a broad and prolonged desorption band in the region 480-650 °C whilst this band appears at a slightly higher temperature range for the other four IECs.

A Real-Time TG-FTIR profile showed that the breakdown of cyclohexylamine over Na-SCa-Ni is much faster than that of the other samples. Certainly, this fact is supported by comparing the FTIR chromatograms of Na-SCa-Ni and Na-SCa-Mg (Figure 61), where the evolution of the different species that come out (aliphatic, unsaturated hydrocarbons, CO_2 and NH_3) as a function of time is shown during the thermal desorption of cyclohexylamine. Na-SCa-Ni shows three maxima for the evolution of NH_3, with the most intense peak centred at 29 min (280 °C) whilst Na-SCa-Mg only presents two maxima and the most intense occurs at a much higher time of 34 min (370 °C). At higher temperatures, Na-SCa-Ni presents two

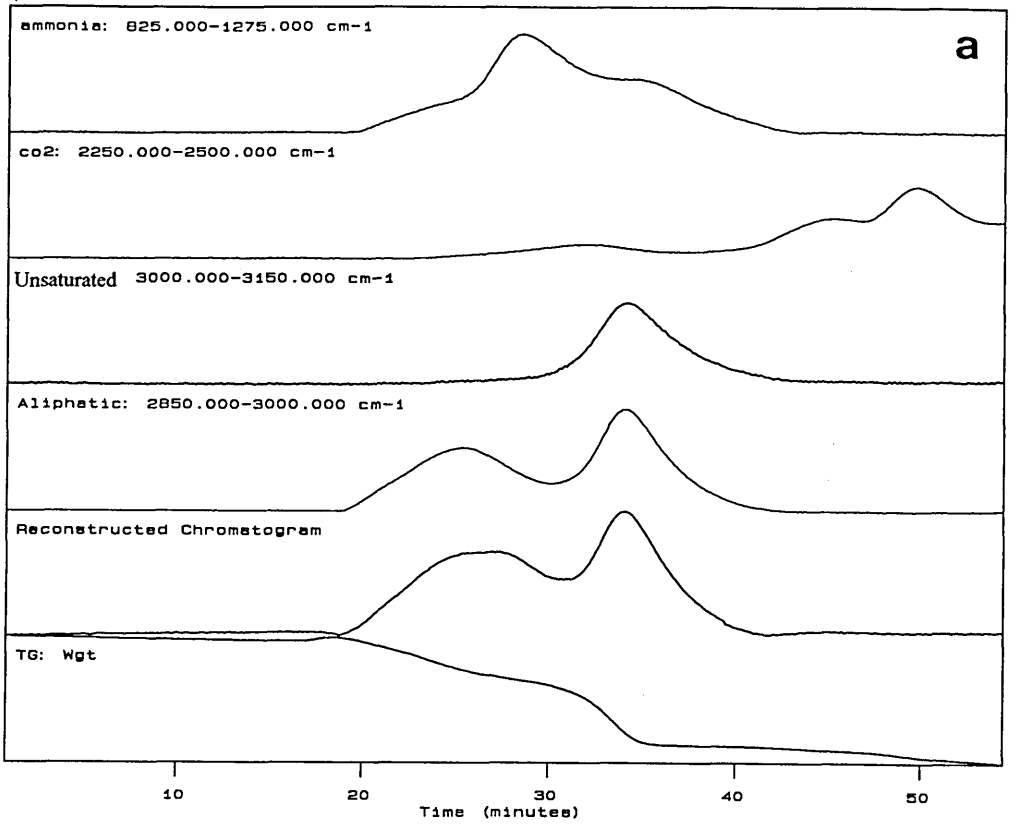

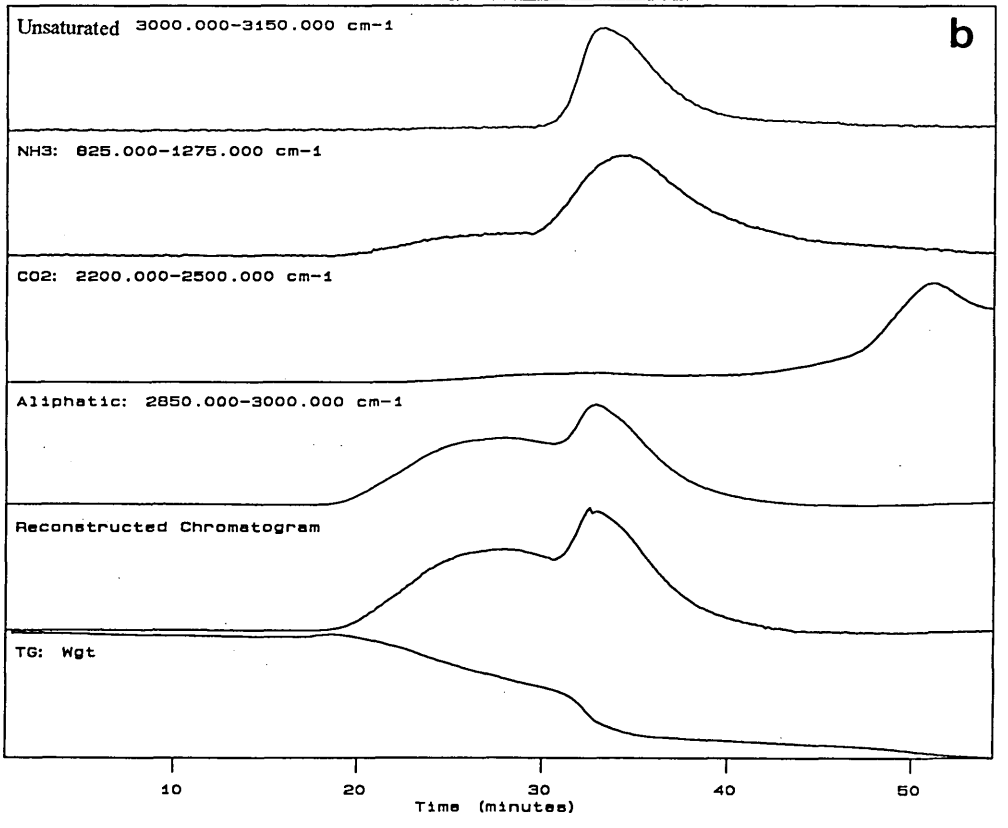

Figure 61. FTIR chromatograms for the desorption of cyclohexylamine from (a) Na-SCa-Ni and (b) Na-SCa-Mg.

broad and prolonged bands for the evolution of CO_2 at 44 and 49 min (570 and 650 °C), Na-SCa-Mg only has one maximum for CO_2 at 51 min (690 °C), reinforcing the data presented in Figure 60.

According to these observations, it is expected that cyclohexylamine will undergo faster hydrolytic degradation giving an earlier CO_2 desorption peak. Such a shift may be the consequence of either the incomplete penetration of the organic molecule into the pores or the result of a different desorption mechanism in Na-SCa-Ni.

The contribution of aliphatic and unsaturated species in both samples are very significant. However, in Na-SCa-Ni the aliphatic bands are more resolved than for Na-SCa-Mg, where the two bands observed are quite prolonged and less separated. Only one aromatic/alkene maximum is clearly observed in both samples.

Real-Time TG-FTIR gives a helpful idea of what is happening during the desoprtion of cyclohexylamine in IECs, but it does not identify the different hydrocarbon species generated during the heating process.

5.3.3.1 Identification of Evolved Gases

Thermal analysis combined with mass spectrometry has been used to study the desorption of butylamine from clays,[200] zeolites,[228-230] and from silica-alumina.[231,232] It was shown that when these catalysts were heated in the presence of sorbed butylamine, the adsorbed molecule decomposed into ammonia, butanes and butenes as well as forming methane and aromatic compounds.

A mass-spectrometric analysis in a temperature-programmed desorption mode (Real-Time TG-MS) showed that the product obtained at temperatures less than 240 °C was cyclohexylamine and those between 250 and 400 °C were a mixture of ammonia, cyclohexene, 1,3-cyclohexadiene, benzene, cyclopentene and 1,3-cyclopentadiene. Above 400 °C the desorption products are mainly water, CO and CO_2.

Figure 62 shows the 3D-FTIR spectra of the gases evolved during the desorption of cyclohexylamine from Na-SCa-Mg. From 15 to 27 min (equivalent to a temperature of 35 and 240 °C) the observed spectra are mainly due to the desorption of the base. The intensity of bands at 2937 and 2862 cm^{-1}, the CH stretching bands, increased as the temperature program proceeded. Very small bands at 2366 and 2332 cm^{-1} started to appear at 25 min (180 °C), associated with the CO_2 evolution.

The aliphatic CH stretching band (largely attributed to cyclohexylamine) slightly decreases its intensity at 28 min (~250 °C) and then increased with the rise in the heating rate at 33 min (340 °C), in which the product mixture, mentioned above, was found. In this temperature range the doublet at 966 and 931 cm^{-1} reaches a maximum as well as those at 1900-1300 cm^{-1} that correspond to the stretching and deformation bands of physisorbed water from the clay structure, combined with the bending modes of the organic molecules.

With a further temperature increment at >38 min (>400 °C) the bands associated with stretching and bending of the organic products, water and ammonia, decrease in intensity dramatically, but are still present at a very low intensity. At this stage only the appearance of water, CO_2 and CO (characteristic bands centred at 2180 and 2100 cm^{-1}) contribute to the

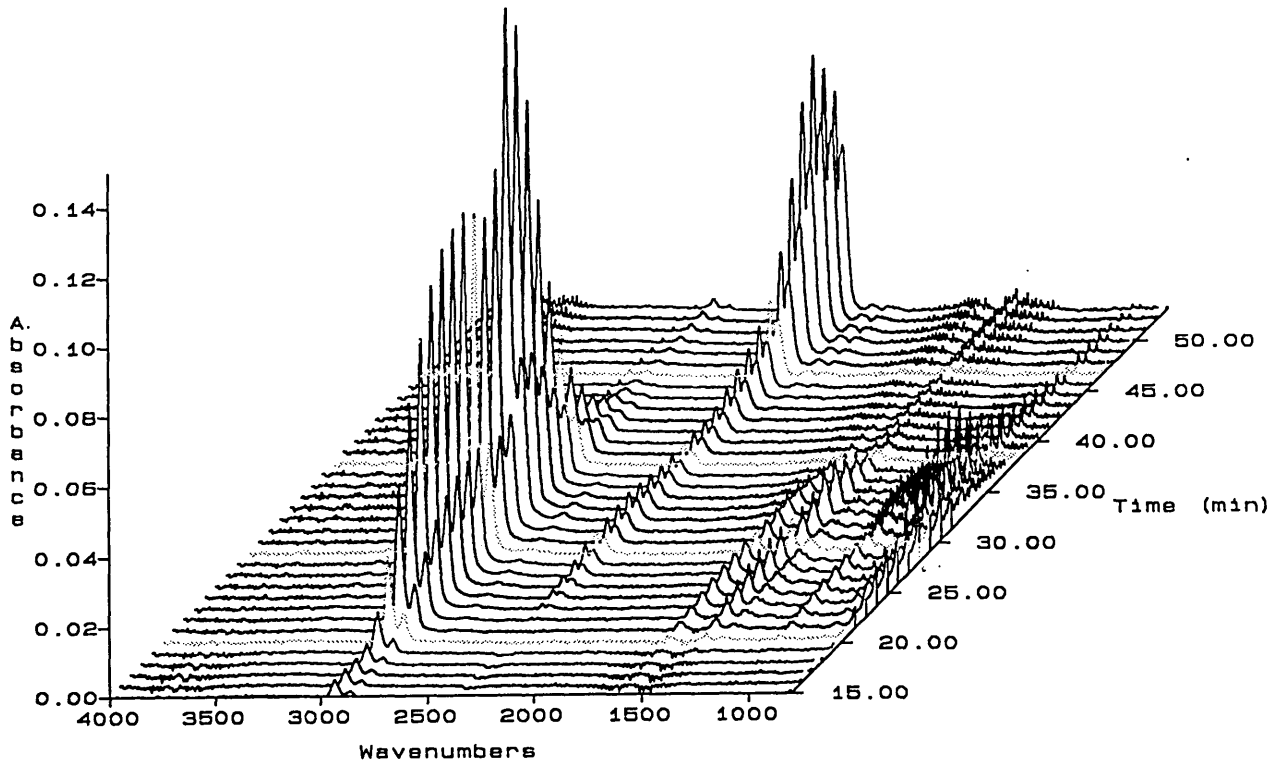

Figure 62. Showing the 3D-FTIR spectra of the desorption of cyclohexylamine from the Na-SCa-Mg sample.

total IR spectra. The evolution bands of CO_2 appear as a plateau at 51 min (690 °C) and then slowly decrease in intensity at higher temperatures. These observations provide further evidence that the evolution of CO_2 is due to the combination of carbonaceous deposits with water.

The Hofmann degradation, used to explain the decomposition mechanism of butylamine, could be applied to cyclohexylamine:

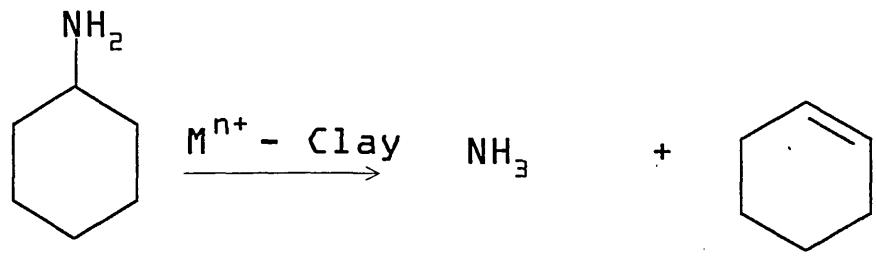

The degradation is followed by dehydrogenation of cyclohexene to produce 1,3-cyclohexadiene, which further dehydrogenates to form benzene:

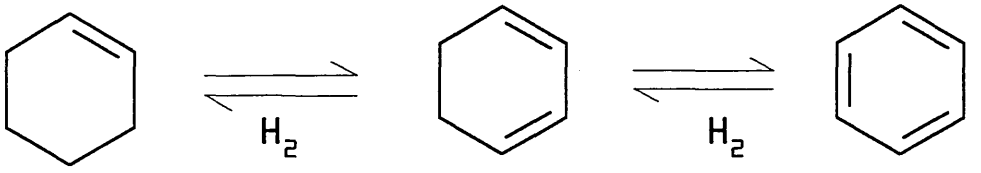

Another parallel decomposition reaction appears to occur together with hydrolysis leading to the evolution of CO, CO_2 and cyclopentene. The latter again dehydrogenates to give 1,3-cyclopentadiene:

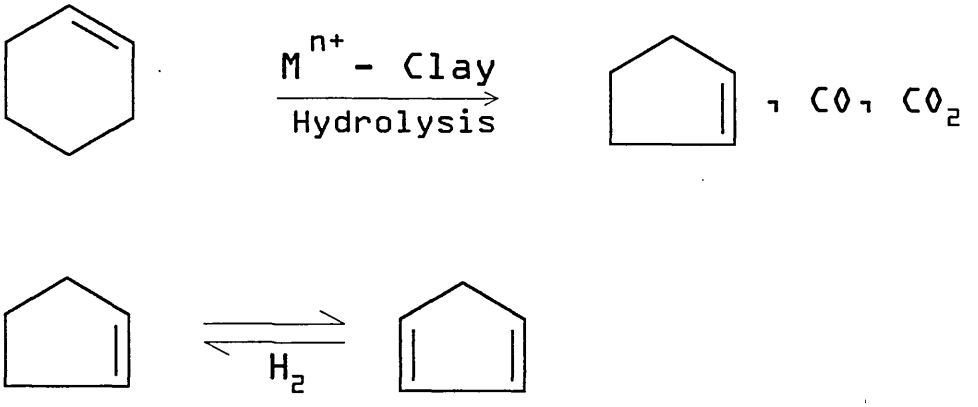

5.4 Summary of the Results Obtained for AlACs, AlAOCs and IECs

It has been demonstrated that mild activation with Al^{3+} and Al^{3+}/TMA^{+} over Sap-Ca, STx-1, SWy-2 and SAz-1 produced materials in which the layer structure was unaffected and a comparison of their catalytic abilities was possible. The type of clay had considerable effect on the total conversion. Sap-Ca and STx-1 were more effective for the process than SWy-2 and SAz-1. In general, the catalytic activity obtained over AlACs and AlAOCs was very similar to those observed using H^{+} and H^{+}/TMA^{+}. Al^{3+}/TMA^{+}-exchanged clays gave lower conversions than their Al^{3+}-exchanged counterparts when the Al^{3+} offered was low (10-40%), but the values were similar at an Al^{3+} content of >50% CEC. Certainly, at high TMA^{+} content there was a reduction in acidity and therefore a decrease in activity was expected. The high catalytic activity found for AlAOCs, especially for those derived from STx-1, Sap-Ca and SWy-2, was attributed to their ability to keep the layers permanently apart thus facilitating the ingress of α-pinene.

There was a good correlation between the acidity and the catalytic activity for both AlACs and AlAOCs derived from Sap-Ca, STx-1 and SWy-2. However, this was not true for SAz-1, which has a high Ca^{2+} content that considerably contributes to the adsorption of cyclohexylamine, but it is inactive for the isomerisation of α-pinene.

The low catalytic activity in samples derived from SAz-1 has been attributed to its inability to accommodate the reagent because of its high charge density. Nonetheless, reducing the layer charge using the well established Hofmann-Klemen[50] effect followed by Al^{3+} activation resulted in a considerably improved activity for SAz-1. The fact that no tricyclene was

adsorbed, that stuffed layers are not active and that cations that maintain layer separation point to the fact that the reaction is interlamellar.

The shape and valence of the organocation had a remarkable effect on the α-pinene conversion. The order of activity was Al^{3+}/TMA^{+} > $Al^{3+}/DABCOH_2^{2+}$ > $Al^{3+}/DAPH_2^{2+}$. $DAPH_2^{2+}$ cations showed more resistance to being displaced by Al^{3+} or H^{+}, resulting in a strong blocking effect for the reactant molecule, whilst TMA^{+} and $DABCOH_2^{2+}$ left empty channels of a greater width, large enough to accommodate α-pinene. The increment in the Al^{3+} content did not cause a significant effect upon the activity because the acidity of $Al^{3+}/DABCOH_2^{2+}$ and $Al^{3+}/DAPH_2^{2+}$ were governed by the presence of protons from different competition equilibria.

The exchanging procedure had a significant influence upon the total conversion of α-pinene. It was found that fully-exchanged samples produced more effective catalysts for the process than those prepared from either natural clays or Na^{+}-exchanged forms. The order of activity for ion-exchanged samples was Al^{3+} > Ni^{2+} > Mg^{2+} > Ca^{2+} > Na^{+}, with Sap-Ca being more active than SWy-2 and SAz-1 clays. This trend in activity did not correlate well with the surface acidity of the IECs, determined by the desorption of cyclohexylamine.

The TG-FTIR-MS analysis demonstrated that cyclohexylamine breaks down to give ammonia, cyclohexene, 1,3-cyclohexadiene, benzene, cyclopentene, 1,3-cyclopentadiene, carbon monoxide and carbon dioxide. The evolution of CO and CO_2 was due to the combination of carbonaceous deposits with water. The desorption of cyclohexylamine, for Ni^{2+}-SCa sample, exhibited an earlier decomposition temperature.

CHAPTER 6

Adsorption of Alcohols and Olefins on Aluminium-Activated Clays and Aluminium-Activated OrganoClays

6.0 Introduction

As described in Chapter 2, the literature dealing with the interaction of olefins with clays stated that most of the research in this field has been carried out in the liquid phase and in some cases at high temperatures and/or high pressures. Under high temperature and/or high pressure conditions the reactant olefins (in liquid phase) are transformed to the corresponding di-alkylethers.[177-179] However, if low chain length olefins react with synthetic mica montmorillonite or zeolites in the gas phase at high pressure, oligomerisation and hydrogenation products are found in the final reaction mixture.[182,233-235] Indeed, all of these reactions have been described in numerous papers on clays exchanged with metal cations, or organometallic complexes, or pillared clays during the last 30-40 years. Yet, not many of those papers have given a detailed study of the adsorption/desorption reaction of clay-olefin samples prepared at room temperature, so that the composition of the adsorbed species formed on the surface is still unclear.

This study represents an extension of the work performed by Choren, *et al.*,[183,184] in which the author was directly involved. We reported the adsorption-condensation of light olefins on clays, alumina and porous and non-porous silica at room temperature in a vapour-solid system. These oligomeric residues were formed on the clay surface after the reaction terminated. Unfortunately, we could not identify the nature of the products formed.

In this chapter, a more detailed analysis has been carried out using Synergic Chemical Analysis of the desorption products formed during the adsorption of hept-1-ene on aluminium-activated clays (AlACs) and aluminium-activated organoclays (AlAOCs) derived from STx-1. The same sample nomenclature as given in section 3.2.2 is utilised herein, for

example ST-Al50 indicates that the raw clay was treated with 50% CEC of Al^{3+} and ST-Al10/TMA90 means that the same clay was prepared with 10% CEC of Al^{3+} and 90% CEC of TMA^{+}. These series of samples were selected because they showed a high catalytic activity towards the isomerisation of α-pinene, whilst hept-1-ene was chosen because it is a liquid and thus easier to handle than a gas (see section 3.11).

Synergic Chemical Analysis is a powerful technique that simultaneously combines different analytical instruments. The thermobalance is the heart of the technique, which can be connected through a heated transfer line to a Fourier Transform Infrared Spectrometer (Real-Time TG-FTIR). Alternatively, the TG can also be connected through another transfer line to an adsorbent trap contained in an organic trap module coupled to a Gas Chromatograph-Mass Spectrometer (TG-OTM-GC-MS). These instrumental techniques might allow a complete characterisation of the hydrocarbon products that are desorbed at certain temperatures.

Clays are known as efficient catalysts for alcohol dehydration to the corresponding olefins and/or the corresponding ethers as well as for the olefin hydration to the corresponding alcohols.[19,186,188] This alcohol-olefin equilibrium reaction is closely related to the olefin isomerisation, because it can occur through the same intermediates (*e.g.*, carbenium ions) and with the same products.[187] In particular, the dehydration of heptan-1-ol and heptan-2-ol can give rise to heptene. For this reason, the interaction of heptan-1-ol and heptan-2-ol over AlACs is also studied by TG.

6.1 VT-XRD

The diagrams in Figure 63 show the changes in 2θ and the intensity of the diffraction maxima with increasing temperature for the adsorption of hept-1-ene on ST-Al20 and ST-Al100 whilst those of ST-Al10/TMA90 and ST-Al90/TMA10 are given in Figure 64. The d-spacings for these samples are listed in Table 17.

	d_{001} RT	d_{001} 100 °C	d_{001} 150 °C	d_{001} 200 °C	d_{001} 300 °C
ST-Al20	14.3	13.8	13.5	11.6	10.2
ST-Al100	14.5	14.0	13.5	12.8	12.6
ST-Al10/TMA90	14.2	14.1	14.0	14.0	13.8
ST-Al90/TMA10	14.1	13.6	13.6	13.5	12.8

Table 17. Showing the basal spacings (in Å) for the adsorption of hept-1-ene on selected AlACs and AlAOCs.

The VT-XRD traces for STx-1 exchanged with different aluminium contents (20% and 100% CEC) show that heating at 200-300 °C causes a sudden reduction of the expanded layers to 10.2 Å, especially for ST-Al20, in which the intensity is also reduced. Certainly, the high calcium content (80% CEC) has a considerable influence on this particular sample. In the ST-Al100 sample there was a slight reduction in the intensity, but in general the d-spacings of 12.6±0.2 Å dominated, which indicates that the layers are still expanded even at 300 °C in the presence of hept-1-ene (Figure 63b). This result further supports the previous findings (Chapter 5) for AlACs, in which the catalytic activity was attributed to the expanded layers of AlACs that allowed the penetration of α-pinene to the interlamellar space, increasing the total conversion.

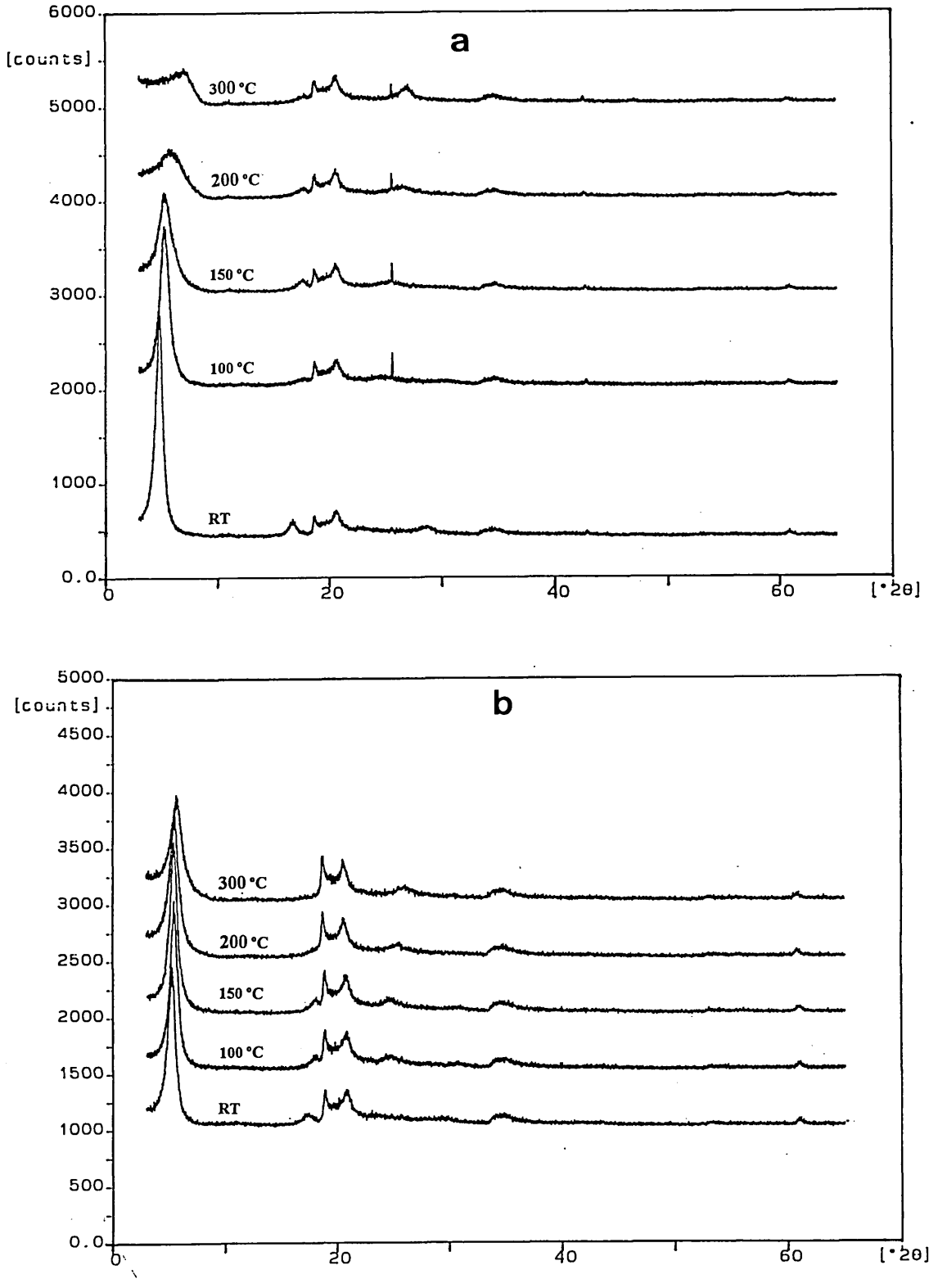

Figure 63. VT-XRD traces for the adsorption of hept-1-ene over (a) ST-Al20 and (b) ST-Al100.

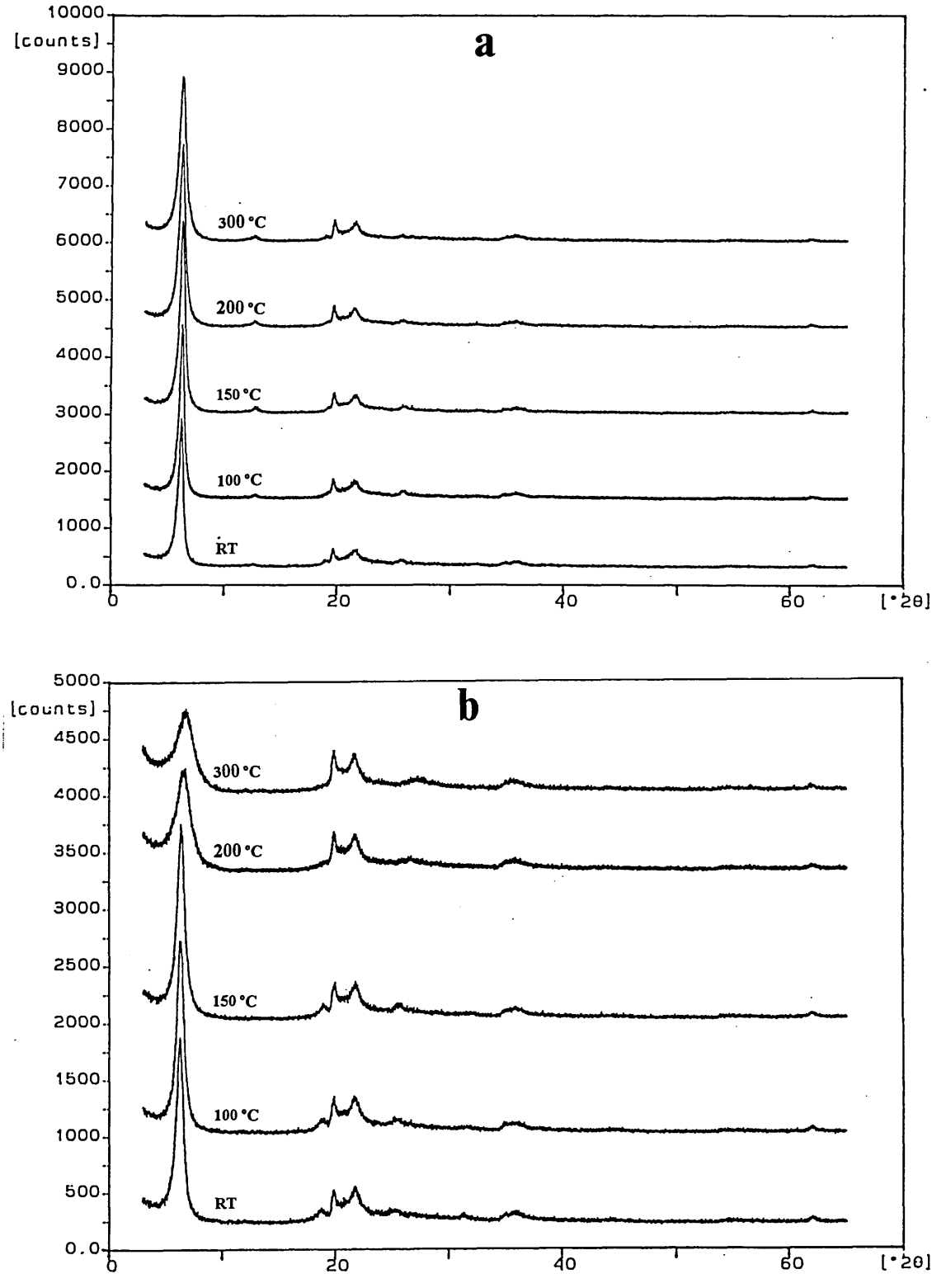

Figure 64. VT-XRD traces for the adsorption of hept-1-ene over (a) ST-Al10/TMA90 and (b) ST-Al90/TMA10.

The adsorption of hept-1-ene was carried out at room temperature on samples dried at 120 °C overnight, where a d-spacing of 14.0 Å is observed for AlACs. In fact, the reactant molecules find favourable conditions to access the interlamellar space and reach the acid centres. Therefore, a significant adsorption of hept-1-ene is anticipated in STx-1 samples prepared with high aluminium content. Samples with low Al^{3+} presented a reduced acid site population combined with the non-exchanged calcium, which, as mentioned before, is inactive for catalytic purposes.

The effect of the heating process upon AlAOCs is different to that of AlACs. At high TMA^+ content, the d-spacing is totally governed by the presence of the organocation and neither significant changes in basal spacing nor in the intensity are noticed. TMA^+ cations are resistant to thermal decomposition and hold the layers permanently apart even when the sample is dehydrated.[117] At low TMA^+ loading (10% CEC), the basal spacing at room temperature is similar to that obtained at high loadings. Nevertheless, heat treatment causes a slight diminution in the d_{001} spacing that remains essentially unchanged at further temperature increments (100-200 °C), but the peak intensity is decreased at 200 °C. Again the high aluminium content controls the expansion process, still noticed at 300 °C, although the peak is broader like that in Figure 64a.

Comparing ST-Al90/TMA10 with the ST-Al100 counterpart, it is clearly observed that the d-spacings of the former are slightly higher that the latter in the temperature range 150-300 °C. This observation indicates that even small TMA^+ loadings have a significant influence on maintaining the layers expanded.

In Chapter 5, it was demonstrated that the isomerisation of α-pinene in AlAOCs was dramatically reduced in samples prepared with high TMA^+ loadings (>50%). However, the activity of AlAOCs was similar to that for AlACs when the TMA^+ was in the range 20-30% CEC. This observation can be use to predict that in the adsorption of hept-1-ene into the interlayer region of AlAOCs (with high TMA^+ content) the alkene will have limited access to reach protonic centres due to displacement of protons by TMA^+ cations. In these particular samples it is expected that the olefin does not undergo catalytic transformation because of the lack of acid sites either on the external surface or on the interlamellar region. These inferences will be corroborated later on as the discussion progresses.

6.2 Thermogravimetric Analysis

6.2.1 Desorption of Hept-1-ene

Figure 65a shows the desorption profiles for AlACs. The derivative thermograms exhibit four desorption peaks with maxima at 90°, 140°, 235° and 620 °C. The peaks at 90° and 620 °C, as previously described, correspond to the desorption of physisorbed water combined with desorption of the physisorbed alkene and lattice dehydroxylation together with CO_2 evolution. The peak at 140 °C is attributed to the desorption of hept-1-ene on calcium cations that were not displaced by aluminium ions. This peak is very intense in ST-Al20, which still contained about 80% CEC Ca^{2+}. However, as the aluminium content offered increased, it decreased in intensity and is very weak at Al^{3+} >60%. Additionally, the region between 80-120 °C is significantly changed as the exchange calcium is displaced by aluminium, the shape of the peak in this region is controlled by the desorption of the physisorbed water and hept-1-ene (90 °C) that becomes sharper and was shifted to lower temperatures as the amount of Al^{3+}

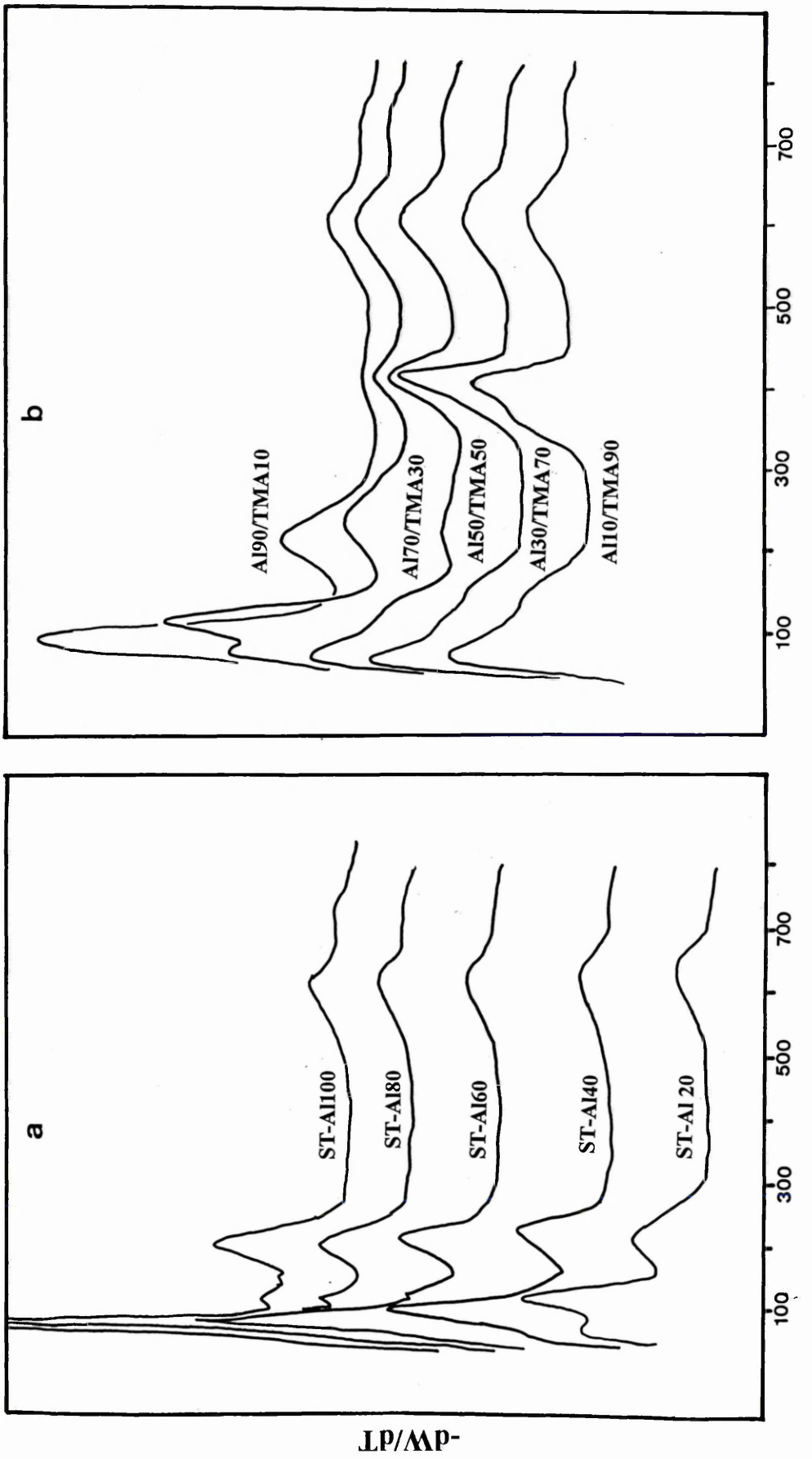

Figure 65. Desorption thermograms of hept-1-ene from (a) AlACs and (b) AlAOCs.

increased. The maximum at 235 °C corresponds to the desorption/decomposition of hept-1-ene and it is increased with aluminium content.

These data corroborate (as showed in Chapter 5) that sites with sufficient acid strength to interact with hept-1-ene are present in the AlACs. Nonetheless, the assignments already given, for the species being desorbed from the clay are, at this stage, only realistic assumptions that will be correlated against the TG-FTIR and TG-OTM-GC-MS data.

The derivative thermograms for the desorption of hept-1-ene from AlAOCs (Figure 65b) show the maxima described above together with that arising from the desorption of TMA^+ at 410 °C. This peak is reduced in intensity as the Al:TMA ratio increased. The desorption peak attributed to the desorption of hept-1-ene from Brønsted acid sites at 235 °C is not visible in samples prepared with high TMA^+ content. This peak starts to occur at Al^{3+} >70%. It is worth noticing that a broad and prolonged peak, extending from 100-200 °C, is observed in samples with low Al:TMA ratio, which changed as the ratio increased. The most plausible explanation is perhaps that, in samples with low Al:TMA ratio, hept-1-ene is desorbed unaltered from the interlamellar space where the reactant molecules do not find sufficient acid sites, due to displacement by TMA^+ cations, able to cause protonation and further transformation of hept-1-ene.

However, as the Al:TMA ratio increased, a significant fraction of molecules effectively interact with protons arising from the polarisation of water molecules in the interlamellar region. These protonic centres are sufficient acids to cause protonation of the double bond. Therefore, the maximum at 235 °C significantly increased in intensity.

These results are in complete agreement with those found for the desorption of cyclohexylamine in the same series of samples, where the TMA^+ cations (at low Al:TMA ratios) reduced the population of acid sites with the corresponding reduction in catalytic activity for the α-pinene isomerisation.

6.3 Real-Time TG-FTIR for the Desorption of Hept-1-ene

Figure 66 shows the 3D-IR spectra for the desorption of hept-1-ene from ST-Al100 as a function of time. During the first 10 min (isothermal at 22 °C), only the bands associated with the olefin can be reliably identified in this spectrum. Intense bands at 2937 and 2879 cm^{-1} belong to the asymmetric C-H and symmetric C-H stretch in the $-CH_2-$ groups. Another vibration band at 2953 cm^{-1} is seen as a left shoulder to the band 2937 cm^{-1} arising from asymmetric C-H stretch of the CH_3 group of the olefin. Additionally the =CH stretching band, which occurs at 3090 cm^{-1} is clearly noticed. Two bands at 1469 and 1649 cm^{-1} belong to the deformation vibration of the $-CH_2-$ and the olefin double bond vibrations. Two other bands at 999 cm^{-1} and 912 cm^{1} are clear in the spectrum and correspond to the olefinic C-H out-of-plane deformation.

As the temperature is increased, the spectra change considerably. At 20 min (93 °C) the =CH stretching band at 3090 cm^{-1} decreased in intensity as well as that at 1649 cm^{-1}. This proves that the sharp maximum at 90 °C in Figure 64a contains a good deal of hept-1-ene as well as water.

The two bands at 3090 and 1649 cm^{-1} disappear completely with a further temperature increment (28 min, at 225 °C where the maximum desorption/decomposition of hept-1-ene

occurs) and the spectrum is dominated by the presence of bands at 2960, 2937 and 2879 cm^{-1} from asymmetric and symmetric vibration of CH_2 and CH_3 groups. This evidence indicates the paraffinic nature of oligomeric species being desorbed or perhaps dehydration products. The C-O stretching band in the IR spectrum occurs in the frequency range 1050-1300 cm^{-1} whilst the O-H appears between 3590-3650, but the assignment of these bands to an alcohol is uncertain because the intensity of these bands is, in general, very weak. Additionally, this behaviour is further evidenced by the disappearance of the bands at 999 and 912 cm^{-1} and the appearance of two bands at 1458 and 1383 cm^{-1} that are assigned to the deformation vibration of the $-CH_2-$ and CH_3- groups in oligomeric products.

Carbon dioxide bands at 2362 and 2316 cm^{-1} appear in the whole spectra of ST-Al100 at very low intensity.

Figure 67 shows the contribution of the gases evolved to the total IR chromatogram. Four peaks are clearly seen in the reconstructed chromatogram at 3, 22, 26 and 28 min (21, 93, 140 and 230 °C). The evolution temperatures of all these peaks are exactly the same as those observed before (Figure 65a). At 21 °C there is only contribution of the hept-1-ene as described in paragraph above. At 93 °C there are contributions of unsaturated hydrocarbons along with water, alcohol, aliphatic hydrocarbons, and a small amount of CO_2. The peaks at 140 and 230 °C only represent contribution of aliphatic hydrocarbons and small amounts of unsaturated hydrocarbons.

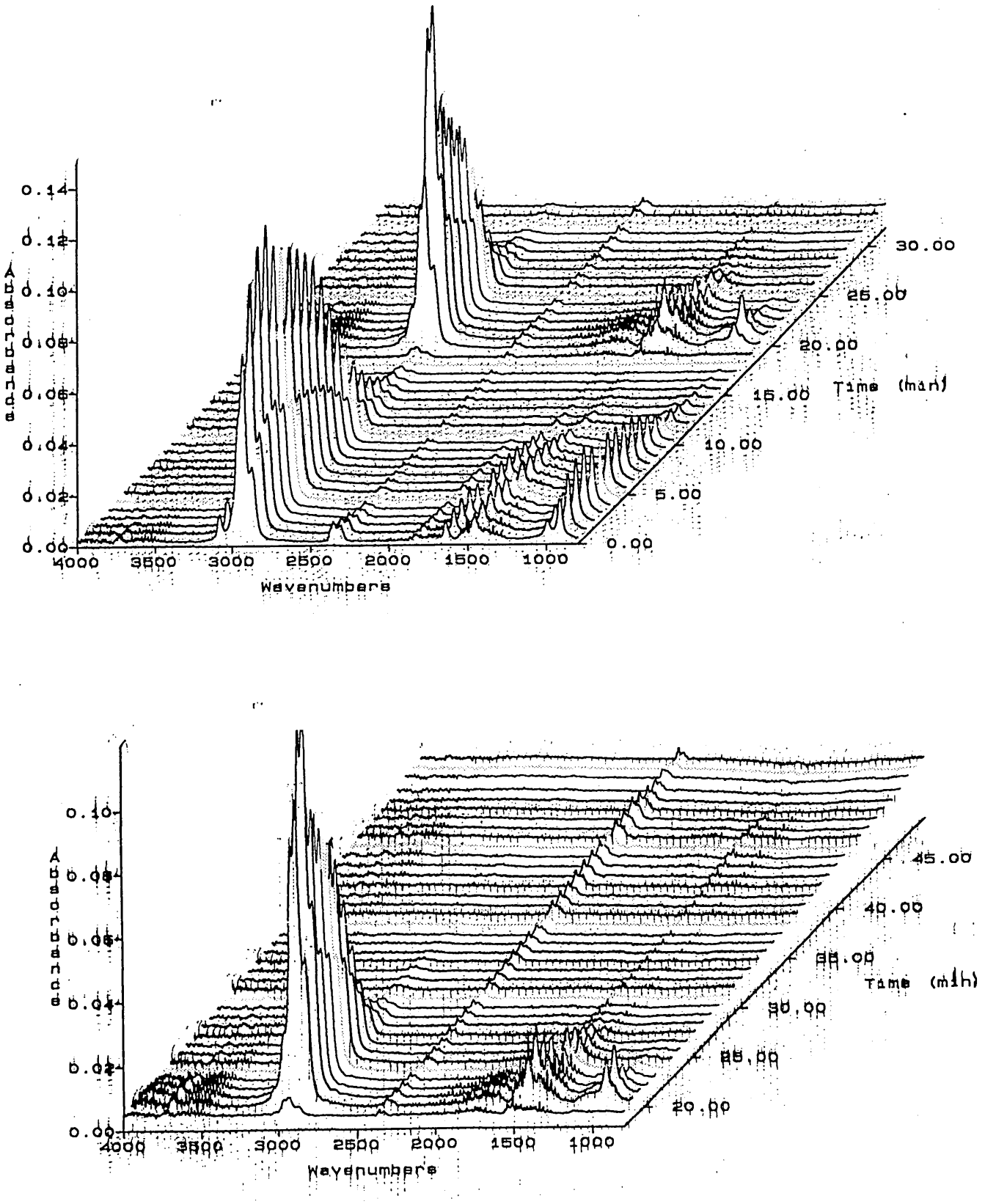

Figure 66. 3D-FTIR spectra for the desorption of hept-1-ene from ST-Al100 (a) from 0 to 30 min and (b) from 13 to 45 min.

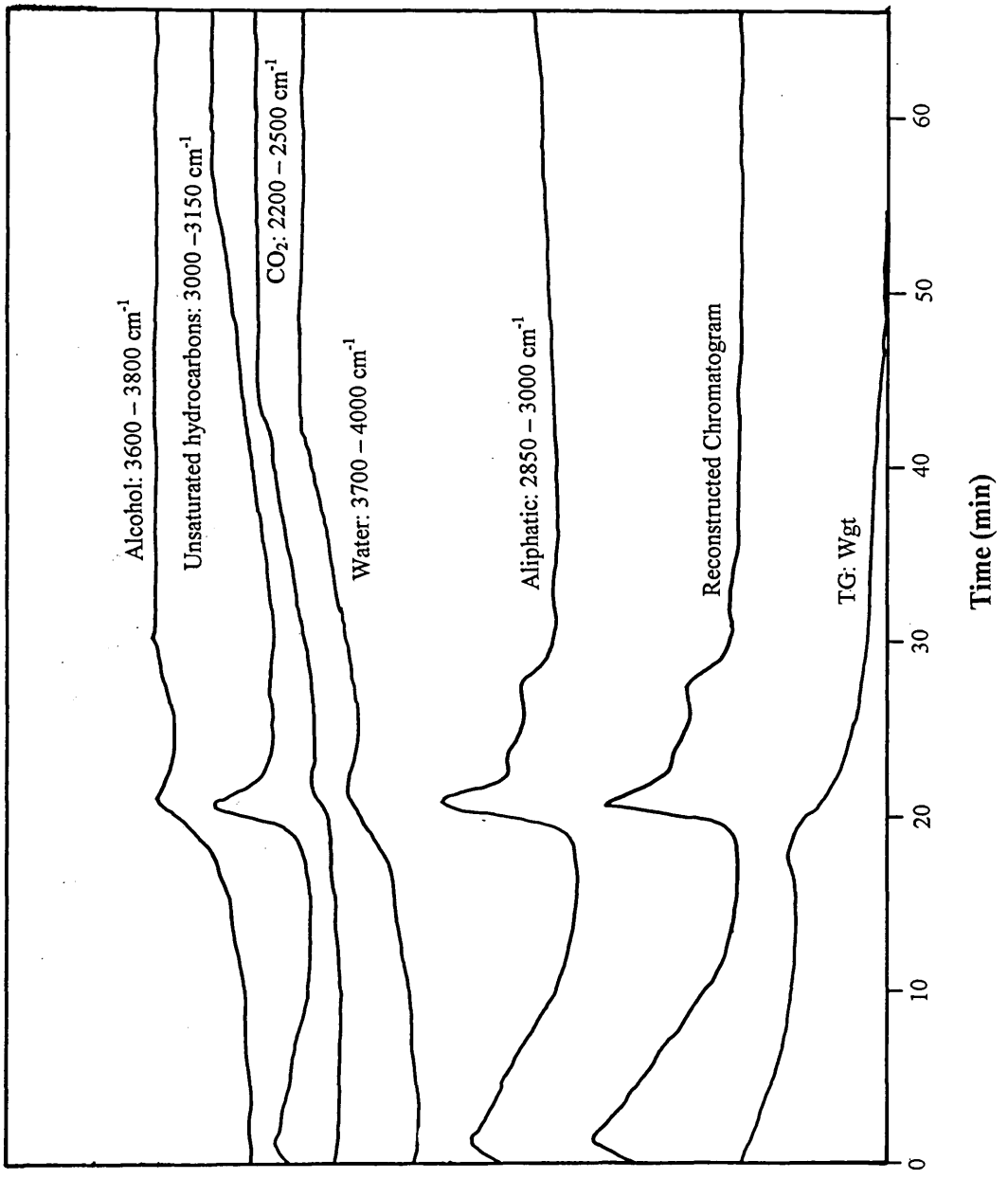

Figure 67. FTIR chromatogram for the desorption of hept-1-ene from ST-Al100.

The data presented herein demonstrates that the AlACs possess acid centres of sufficient strength to cause the protonation of the olefin. Certainly, Choren, *et al.*,[184] reported that the free Si-O-H groups only participate in the reversible adsorption of olefins but do not participate either in the isomerisation or in the oligomerisation.[184] The stretching of free silanol groups appeared as a very sharp band at 3740 cm^{-1} and it was affected by the adsorption of olefin. Additionally, they observed the absence of the double-bond band. Similarly, Trombetta, *et al.*,[236] found only reversible adsorption (at room temperature) of the n-butene on/from the surface hydroxyl of alumina, as on silica and or the HZSM5 zeolite. They attributed this behaviour to a very weak interaction allowing the breaking of the C=C double bond and the formation of the carbenium ion due to the weakness of the OHs as Brønsted acids. On the other hand they stated that the isomerisation of olefins at room temperature was favoured by the formation of allyl species, whereas at high temperature H-bonded olefins were assumed to be the precursor for carbenium ions that produce the skeletal isomerisation.

Taking into consideration Trombetta's group's[236] conclusions it is possible to predict both isomerisation and oligomeric products during the reaction process. This is due to the presence of acid sites, determined by the adsorption of cyclohexylamine (see Table 13, Chapter 5).

6.4 TG-OTM-GC-MS

Figure 68a illustrates the total ion chromatogram (TIC) *vs.* time curve obtained after ST-Al100 saturated with hept-1-ene was heated up to 500 °C and a similar product distribution was observed for ST-Al50 (Figure 68b). As can be seen, the GC-MS chromatograms of the

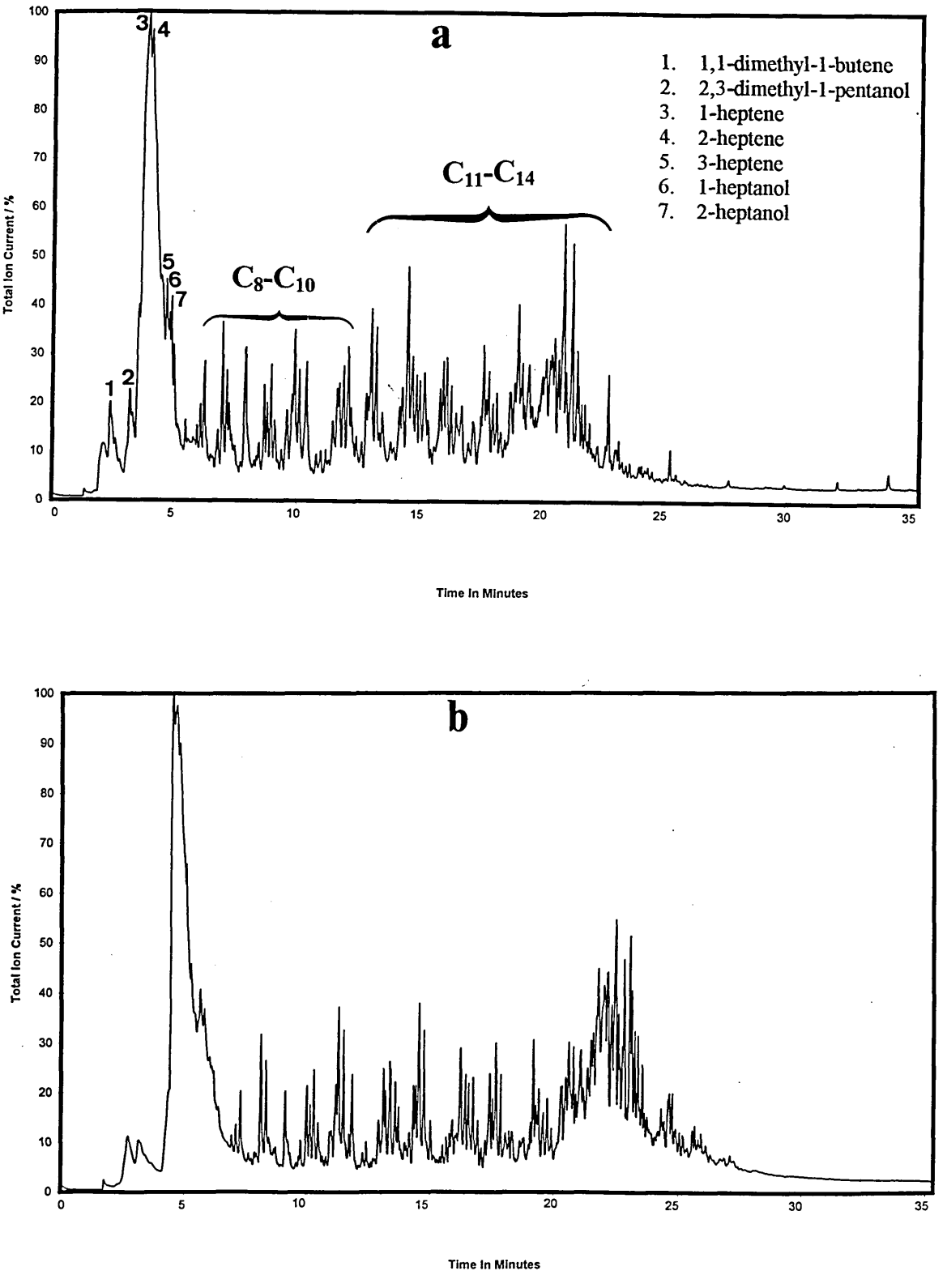

Figure 68. GC-MS chromatograms of the products evolved during the thermal desorption of hept-1-ene from (a) ST-Al100 and (b) ST-Al50 samples.

desorbed compounds consist of a complex mixture of more than 60 peaks. The data obtained herein is in line with the results reported by Stepanov, *et al.*,[185] who extracted the products formed during the adsorption of ethylene on acidic zeolite HZSM5 at room temperature and found a similar product distribution (more than 50 hydrocarbons, Figure 69).

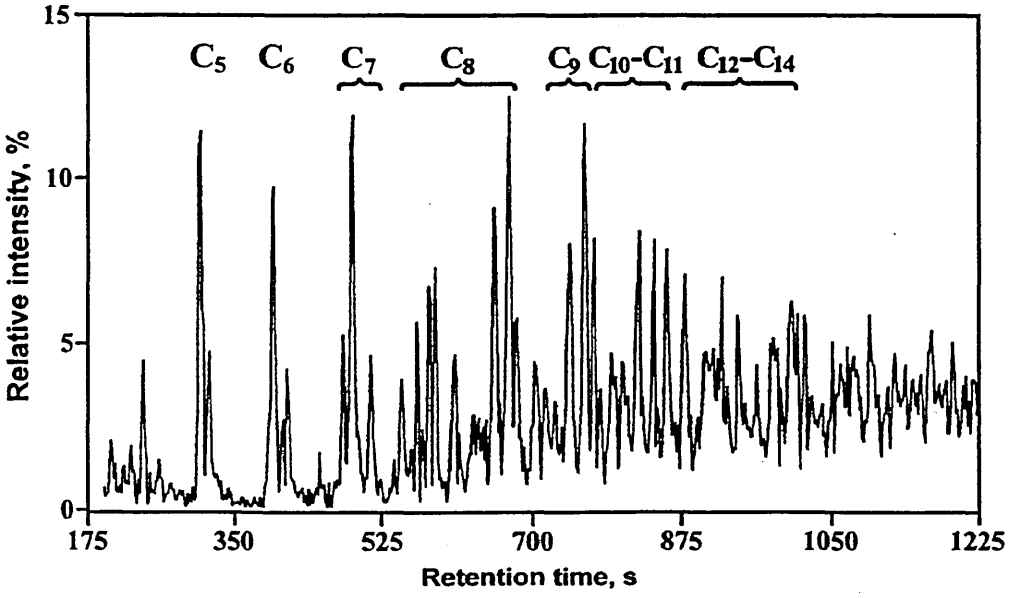

Figure 69. GC-MS spectrogram of hydrocarbon products extracted from H-ZSM-5 – ethylene system, after dissolving the zeolite sample in NaOH solution.[185]

The individual compounds resulting from the desorption of hept-1-ene were identified, using a computer matching search, from their fragmentation patterns and parent ions. It was found that the product gases were a mixture of 1,1-dimethyl-1-butene, hept-2-ene, 2,3-dimethyl-1-pentanol hept-3-ene, heptan-1-ol and heptan-2-ol that appeared next to the hept-1-ene peaks (Figure 68), all at short retention times, but not well separated. At retention times (>7 min) linear and branched n-alkanes, ranging from C_8 to C_{14}, were found. Some aromatic compounds were also found in the reaction mixture and they might have resulted from a

dehydrocyclisation reaction. Unfortunately, it was not possible to compute hydrocarbons $<C_5$, because the trap used (Vocarb 4000) does not work efficiently in that range.

The presence of TMA^+ in AlAOCs exerted a remarkable influence on the total ion chromatogram. Figures 70a-b show the distribution products during the desorption of hept-1-ene from ST-Al50/TMA50 (temperature ramp = 1 °C min^{-1}) and ST-Al70/TMA30 (temperature ramp = 5 °C min^{-1}). At short retention times (<7 min) the shape and position of the peaks for ST-Al50/TMA50 is similar to that for ST-Al100 and ST-Al50. In this region the peaks correspond mainly to the desorption of the isomerised alkenes and hydration products. However, the series of peaks attributed to the evolution of n-alkanes and the aromatic compounds, which appear at higher retention times (8-25 min), are not visible. A reasonable explanation for these experimental facts in accord with the results found in Chapter 5, may be that hept-1-ene finds insufficient acid sites to interact in the interlamellae due to the high population of TMA^+ cation, which effectively displace protons during the exchange treatment. Whatever the reason, hept-1-ene may selectively take the protons available in AlAOCs (prepared with intermediate TMA^+ loadings) to produce only isomerisation and hydration products and desorption of unaltered hept-1-ene.

In ST-Al70/TMA30 the series of peaks in the retention time region 8-25 min start to occur, but in a small amount, which indicates that both protons and an interlayer access are opened up to reaction as the TMA^+ loading decreases.

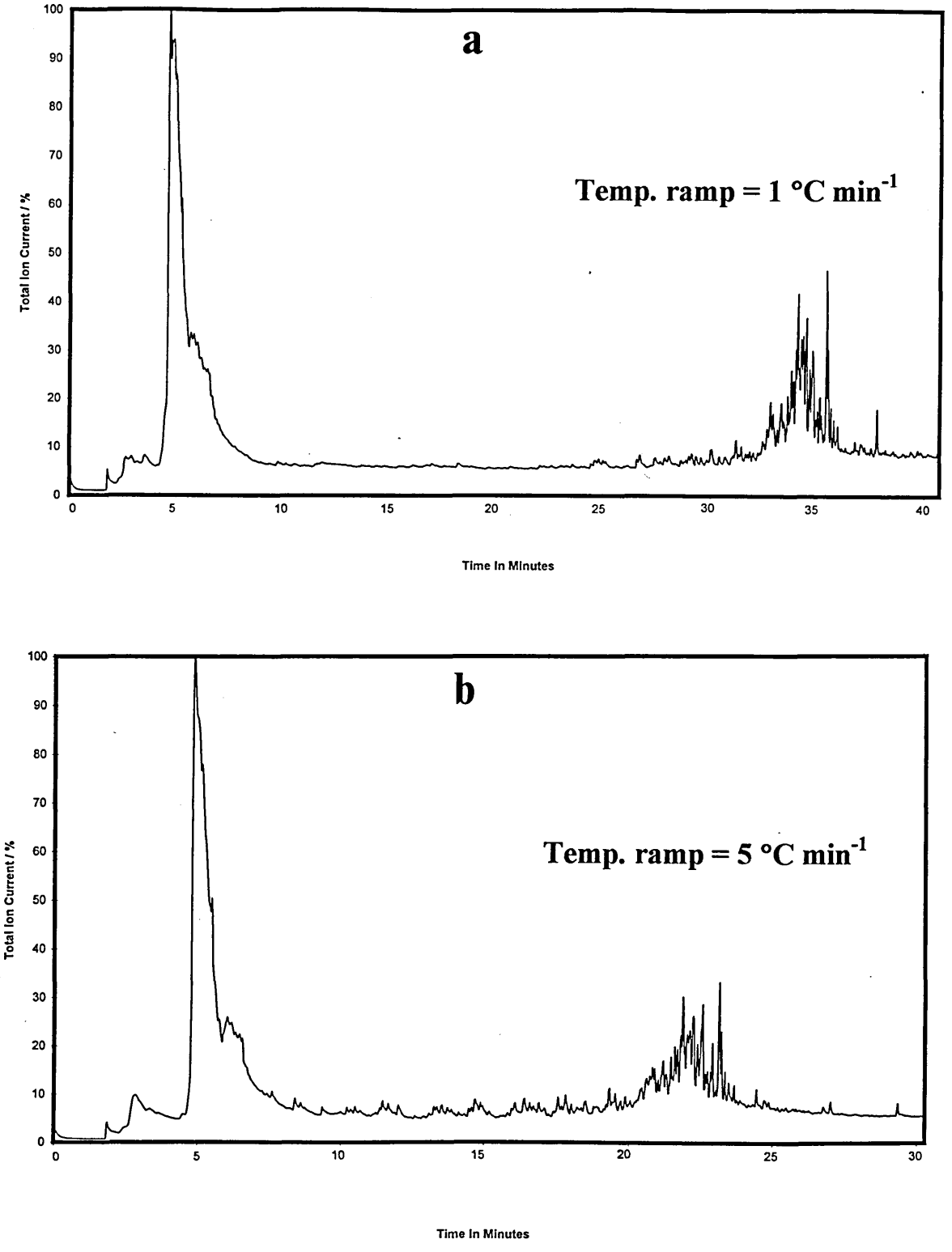

Figure 70. GC-MS chromatograms of the products evolved during the thermal desorption of hept-1-ene from (a) ST-Al50/TMA50 and (b) ST-Al70/TMA30.

It is possible to propose that the mechanisms involved in the formation of the reaction mixture could be:

1. Isomerisation of hept-1-ene arising from the formation of more stable species, in this case a secondary carbenium ion is produced upon protonation of the double bond.

2. Formation of alcohols catalysed by protons and the participation of water molecules (see Figure 18, Chapter 2). However, the formation of the dialkyl ether was not observed in the reaction products.

3. Interaction of acid sites in the galleries with hept-1-ene results in the formation of carbenium ions that can react in the interlayer region with hydrocarbons to give the corresponding formation of oligomeric species of long chain length (n-alkanes), strongly retained inside the clay framework.

In summary, the different adsorbed species that may exist in AlACs are in the form of three interconverting species, alkoxides, carbenium ion and olefin. Stephanov, *et al.*,[185] stated that the alkoxy species were the main adsorption state in zeolites saturated with ethylene at room temperature. In this system, it is believed that carbenium ion might be the major adsorption state due to the considerable number of acid sites arising from the high polarisation power of aluminium ions (especially in those samples where the Al^{3+} was high).

6.5 Thermal Desorption of Heptan-1-ol and Heptan-2-ol

Figure 71a shows the derivative thermograms for the desorption of heptan-1-ol from AlACs whilst those for the desorption of heptan-2-ol are shown in Figure 71b. Three peaks are observed for the desorption of heptan-1-ol at 100°, 145° and 630 °C, these peaks can be attributed to the desorption of physisorbed water, desorption of the alcohol and the dehydroxylation of the clay combined with carbon dioxide. The peak at 145 °C in the clay-heptan-1-ol system increased in intensity as the aluminium content increased and became more resolved from the water desorption. ST-Al40 and ST-Al60 exhibited a weak, broad desorption near 280 °C that can be attributed to the desorption of small amounts of hept-1-ene or oligomeric species, which, as shown in the previous section, presented a broad peak from 160-300 °C. However, the assignments of these series of bands is merely speculative. As the Al^{3+} content increased ST-Al80 and ST-Al100 show a series of weak and prolonged peaks in the region 280-500 °C. Again, hept-1-ene and/or oligomeric species, perhaps, are in that region, but the associations are still unclear.

As can be seen in Figure 71a, as the amount of aluminium increased the peak at 630 °C is shifted to lower temperature and presents a higher intensity. The percentage of weight loss in the region of 500-800 °C was 3.5-5% indicating that the contribution of CO_2 was negligible and governed by the dehydroxylation of the clay. The most plausible explanation for this behaviour is that, the population of acid sites increased with the amount of aluminium incorporated, therefore a rich protonic environment might favour the formation of the corresponding alkene and/or the oligomeric species, which are present in the interlayer region and as the temperature is increased they are desorbed/decomposed at a lower temperature.

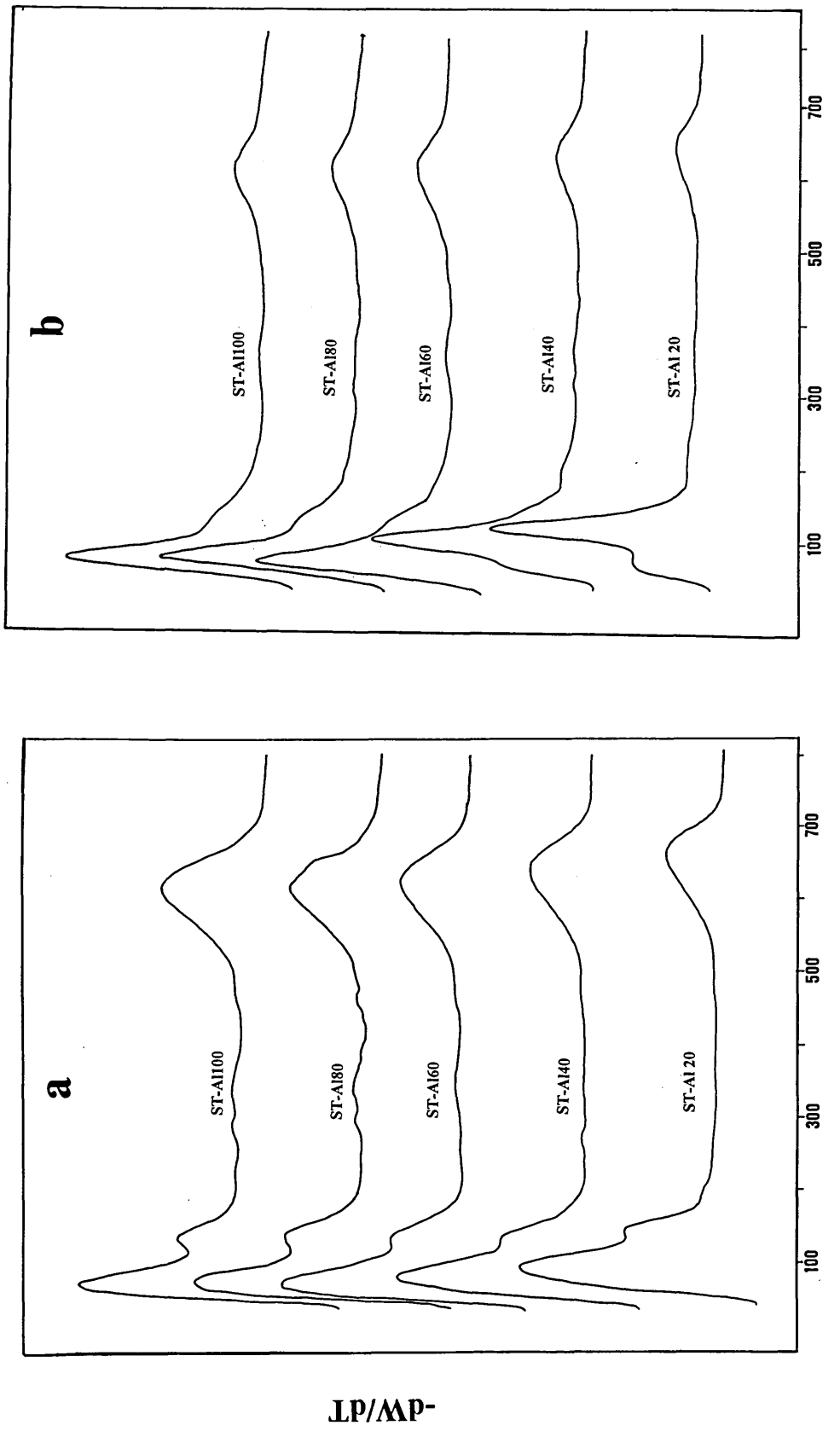

Figure 71. Derivative thermograms for the desorption of (a) heptan-1-ol and (b) heptan-2-ol from AlACs.

The desorption of heptan-2-ol from AlACs shows similar peaks to that for heptan-1-ol. However, the shape for the desorption of heptan-2-ol is different. It appears as a less intense and poorly resolved peak from the water desorption. In fact, the desorption of the secondary alcohol is completely overlapped by the desorption of water in samples with low Al^{3+} content (ST-Al20 and ST-Al40) and it becomes visible as the amount of the Al^{3+} exchange treatment increased. These series of samples show two weak peaks in the range 280-400 °C. Once again it might evidence the formation of the corresponding alkene together with other hydrocarbons.

It is believed that the peak at 135 °C is unaltered heptan-2-ol. As the aluminium content increases the alcohol is converted to heptene at a temperature lower than 120 °C and, therefore the peak at 135 °C is no longer present.

These findings are in line with those reported by Breen, *et al.*,[187] who studied the desorption of methanol, propan-1-ol, propan-2-ol and 2-methylpropan-2-ol from Na^{+}-, Ca^{2+}-, Al^{3+}-, Cr^{3+}- and Fe^{3+}-exchanged montmorillonite. They reported, using mass spectrometric analysis, evidence of the formation of the corresponding alkene as well as small quantities of oligomeric species, but no ether formation was observed. The absence of ether was attributed to the low concentration of alcohol in the interlayer region to promote the intermolecular reaction, given that the formation of the dialkyl ether only occurs when the clay is in direct contact with the liquid alcohol.[103] Using Breen's group's observations[187] to support the results found herein, the weak peaks in the region 280-500 °C might be assigned then to the presence of the heptene and small amounts of oligomeric species.

6.6 Summary of the Results Obtained

Combined application of *in situ* TG-FTIR and TG-OTM-GC-MS to the analysis of the evolved gases during the adsorption of hept-1-ene at room temperature allows drawing the following conclusion:

Hept-1-ene interacts at room temperature, with surface acid sites of AlACs via proton transfer. Under these conditions the adsorption/desorption of hept-1-ene on/from clays was very complex, and resulted in a variety of reaction mechanisms: isomerisation, hydration, oligomerisation and dehydrocyclisation. The desorption products resulted in a mixture of more than 60 hydrocarbons.

These results outlined in this chapter have further corroborated and proved the conclusions given in Chapter 5, in which the remarkable activity showed by AlACs towards the isomerisation of α-pinene was attributed to the ability of aluminium to keep the layers permanently apart allowing ingress to the incoming molecules. Additionally, it has confirmed the supposition that TMA^+, at high loadings, reduces the population of acid sites creating unfavourable conditions for the catalytic transformation of α-pinene as well as hept-1-ene.

More experimental work is required to fully characterise the evolved products during the thermal desorption of heptan-1-ol and heptan-2-ol, and also to prove that the presence of TMA^+ cations affects the reaction selectivity towards the formation of hydration and isomerisation products. All these observations will be again considered in Chapter 8, where the strategy to follow is described in more detail.

CHAPTER 7

Thermal Stability of OrganoClays

7.0 Introduction

The exchangeable cations on natural clays can be replaced with different organocations by simple ion exchange. A variety of alkylammonium ions may be used in this regard to form organoclays that are effective adsorbents for removing organic contaminants from water.[13,15,136-141]

Depending on the size of the organic cations and the layer charge of the mineral, the alkyl chain of the organocations may form flat lying monolayer, bilayer, pseudotrimolecular layer, or paraffin complexes (see Figure 11, Chapter 2).[138,143,144] The alkylammonium ions are preferentially adsorbed onto the cation-exchange sites of montmorillonites.

Cowan and White[145] studied the adsorption of straight-chain monoalkylammonium salts by Na-Bentonites. A linear relationship between the change in the free energy and the number of carbon atoms in the aliphatic chain was found. The increment in the free energy was ascribed to van der Waals interactions between the chains. Consequently, a mechanism of the exchange process was proposed, in which the length of the hydrocarbon chain was considered to play the most important role. Similarly, Theng, *et al.*,[146] found that the affinity of the mineral for the organic molecules was linearly correlated to molecular weight of the alkylammonium ion. Therefore, the greater the length of the alkylammonium chain, the greater is the contribution of physical forces to adsorption.

The intercalation of alkylammonium ions of different chain length has been used to determine the layer charge distribution of clay minerals[143,237,238] and also to study the changes in the octahedral and tetrahedral charge of smectites after Li^+ fixation.[239,240]

More recently, Janek, *et al.*,[241] have applied the alkylammonium method to the study of the layer charge changes following autotransformation of H-smectites [H-smectite is converted spontaneously to (H,Al,Fe,Mg)-form upon ageing].[28,209] This group stated that the autotransformation of the H-smectites decreased the layer charge and concluded that protons preferentially attack the $Mg(O,OH)_6$ octahedra during the process.

The stability of the alkylammonium ion-montmorillonite complexes has been attributed partly to the van der Waals attraction of the hydrocarbon chain with its neighbouring chains and with the clay surface (this effect increases rapidly with increasing chain length).[242] The other contribution is due to a partly thermodynamic stabilisation of the alkylammonium ion at the clay surface compared with the same ion hydrated in aqueous solution.[243] As a result the organoclay complexes are relatively heat stable up to 250 °C.[150] However, as it has been shown in Chapters 4 and 5 of this thesis, the organoclay complexes possessed a temperature onset at approximately 410 °C. To date, the thermal stability of organoclays prepared from autotransformed clays using the alkylammonium method is unknown.

Therefore, in this chapter the focus is to study the exchange of quaternary ammonium (n-alkylammonium chlorides), with a variable carbon chain length, into Na-form clays and autotransformed H-clays with different crystallinity and homogeneity of charge distribution. In fact, special emphasis has been placed on the determination of whether autotransformation produces an improved stability and to evaluate the thermal desorption/decomposition process of the organoclays using real time TG-FTIR. The four clays chosen permitted the investigation of how layer charge and elemental composition of the octahedral sheet influence the decomposition of the alkylammonium ions. In particular the use of ST and

SWa-1 provided the possibility of determining if structural iron exerted any influence on the alkylammonium decomposition.

7.1 Materials and Methods

7.1.1 Clays Used

The <2 μm fractions of four bentonites were utilised in this study. The general descriptions are given in Table 18 and the elemental compositions are listed in Table 19. Co-workers in Bratislava prepared all the clays used in this investigation.

Sample	Mineralogy	Source
Jelšový Potok (JP)	Al-montmorillonite	Slovakia
Cheto (SAz-1)	Mg-montmorillonite	Arizona, USA
Stebno (ST)	Fe-beidellite	Czech Republic
Nontronite (SWa-1)	Ferruginous smectite	Washington, USA

Table 18. General descriptions of the clays utilised.

Sample	Si (Th)	Al (Th)	Al (Oh)	Fe^{3+} (Oh)	Mg (Oh)	Interlayer Me^{+}
JP	3.95	0.05	1.51	0.13	0.36	0.43
SAz-1	4.00	-	1.34	0.07	0.60	0.56
ST	3.61	0.39	0.98	0.80	0.29	0.47
SWa-1	3.64	0.36	0.42	1.46	0.14	0.44

Table 19. Structural formulae (per $O_{10}(OH)_2$) of smectites.[241]

7.1.2 Alkylammonium Exchange

JP, SAz-1, ST and SWa-1 were first saturated with Na^+ using 1 M NaCl solution, washed free of excess ions using de-ionised water and ethanol, air dried at 60 °C, and ground to pass through a 0.2 mm sieve. Approximately 100 mg of the Na-form samples were exchanged with 2 ml of 0.1 M aqueous solutions of primary alkylammonium salts of increasing chain length from C_6 to C_{16}.[238]

Batches of the H-samples were prepared from the Na-form clays. 100 mg of the Na-form clays were treated first with a solution of 1 M NaCl + 0.1 M $Na_2C_2O_4$ + 0.1 M HCl for 5 min in an ultrasonic bath and for 25 min in a shaker. The solid phase was separated by centrifugation and dispersed in 1 M NaCl + 0.1 M $Na_2C_2O_4$ solution and shaken for 30 min. The centrifugation treatment was repeated five times. The freshly prepared H-smectite dispersion was left to age in a tightly sealed polyethylene flask at 90 °C for four days during which autotransformation occurred. Then the solids were washed with water and ethanol to remove the excess ion and finally dispersed in re-distilled water to prepare a 1% dispersion. A 2 ml quantity of the dispersion, after the centrifugation and re-dispersion treatments, was exchanged with alkylammonium cations as mentioned above. More details of the experimental procedure are given elsewhere.[241]

Samples arising from these two procedures are hereinafter designated as ST-Na-$C_6NH_3^+$ and JP-An-$C_{16}NH_3^+$, which denotes that the Na-form of ST was first prepared and then exchanged with $C_6NH_3^+$ alkylammonium ion and that JP was autotransformed and then exchanged with $C_{16}NH_3^+$ alkylammonium ion.

7.1.3 Thermogravimetric Analysis

Thermogravimetic (TG) analysis was utilised to measure the thermal stability of the Na- and autotransformed organoclays, using a Mettler TG 50 thermobalance. The same experimental procedure and operational conditions as described in section 3.5 (Chapter 3) were used to obtain the thermograms.

7.1.4 Real Time TG-FTIR

The infrared spectrum of the gases evolved during the heating process was recorded using the same thermobalance (Cahn TG131) - FTIR assembly and experimental conditions given in section 3.8 (Chapter 3).

7.2 Results and Discussion

7.2.1 Thermogravimetric Studies

In this section the derivative thermograms for the desorption/decomposition of alkylammonium ions of pair chain length (C_6, C_8, C_{10}, C_{12}, C_{14} and C_{16}) are described for both the Na-form and the autotransformed clays. The general trends are discussed below:

SAz-1

The thermogravimetric traces for the series prepared using Na-SAz-1 (Figure 72a) show five maxima at 80°, 290°, near 400°, 500-680° (very weak) and 710 °C. These peaks are assigned to: (80 °C) desorption of physisorbed water, (290 and 400 °C) decomposition of the organocations that breakdown to produce (as will be shown in the next section) ammonia, water, aliphatic species and small amounts of CO_2, (500-680 °C) and (710 °C) formation of CO_2 combined with the dehydroxylation of the clay. Figures 73 and 74 show the 3D-FTIR of

the evolution of all the species mentioned above, which will be discussed in more detail later on.

In the series prepared using An-SAz-1 (Figure 72b), the decomposition of the organocations occurs at a lower temperature (maximum near 300 °C, Figure 75). The peak at 290 °C in Na-SAz-1 is shifted to 210 °C and masked by that at 300 °C. In the dehydroxylation region the evolution of CO_2 appears in two broad and prolonged peaks (500-760 °C). These two maxima are observed at 600 and 700 °C. The intensities of the latter two peaks are higher than that for Na-SAz-1.

Figure 76 shows the changes in the weight loss curves for both series of samples. A weight loss of 5% in the region of 500-800 °C is clearly noticed in Na-SAz-1, which indicates that the contribution of CO_2 is not significant and it is mainly due to the dehydroxylation of the clay. The weight loss in the region of 140-500 °C increased linearly with the number of carbon atoms, as expected. This trend is not reflected in An-SAz-1 samples, which show a weigh loss >10% between 500-800 °C. In this case CO_2 presents a considerable influence. The weight loss in the region of 140-500 °C increased with the carbon chain length, but the decomposition takes place over a wider range than Na-SAz-1. The maxima temperatures are relatively stable (Figure 75) for both Na- and An-SAz-1. However, in the former the maximum at 380-430 °C is higher than in the latter at 290-330 °C.

The percentages of expected weight loss from each organocation in each clay are given in Table 20 where the weight loss determined by TGA in the region of 140-500 °C is also reported to provide a comparison.

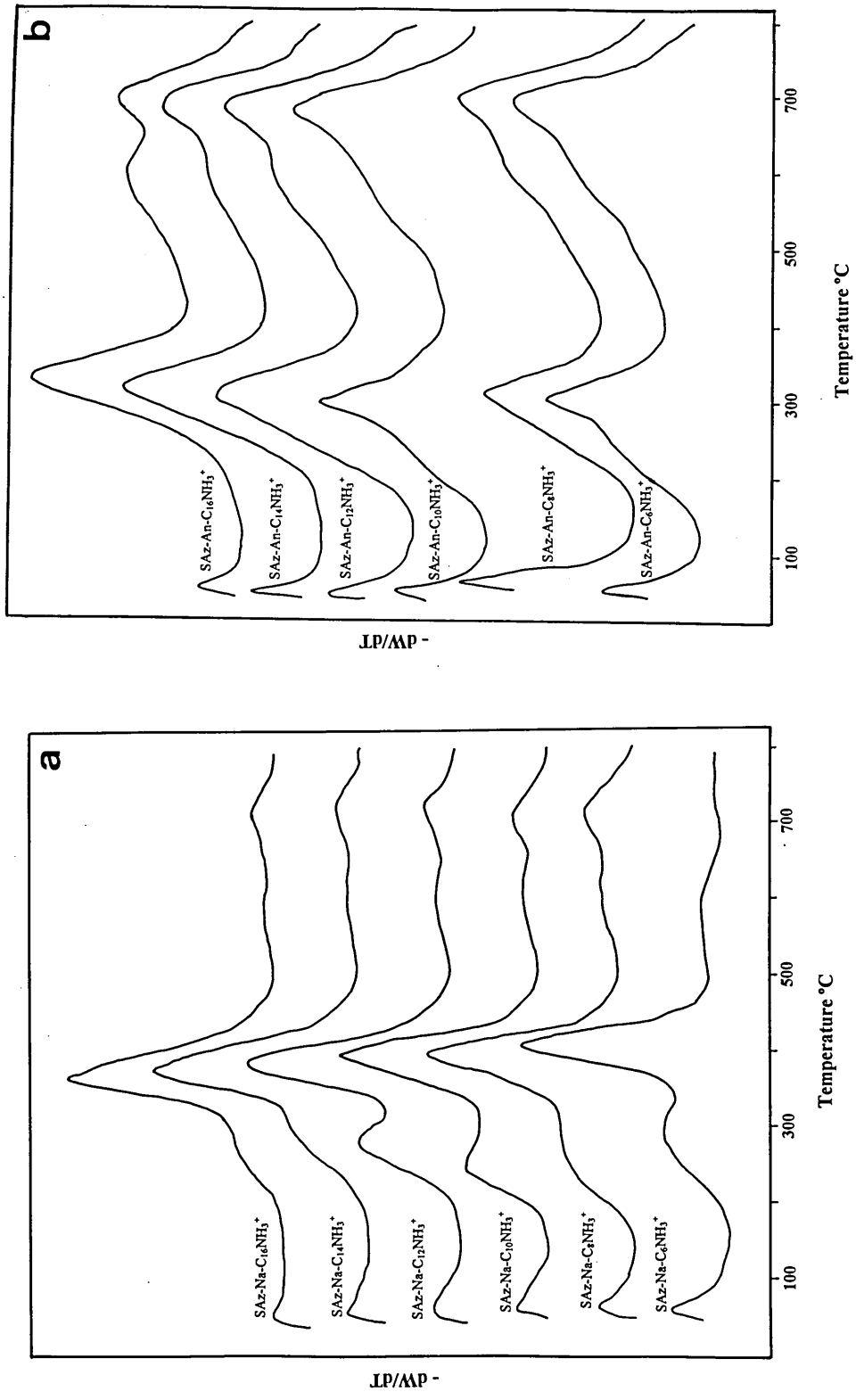

Figure 72. Derivative thermograms for the decomposition of alkylammonium ions from (a) Na-SAz-1 and (b) An-SAz-1 samples.

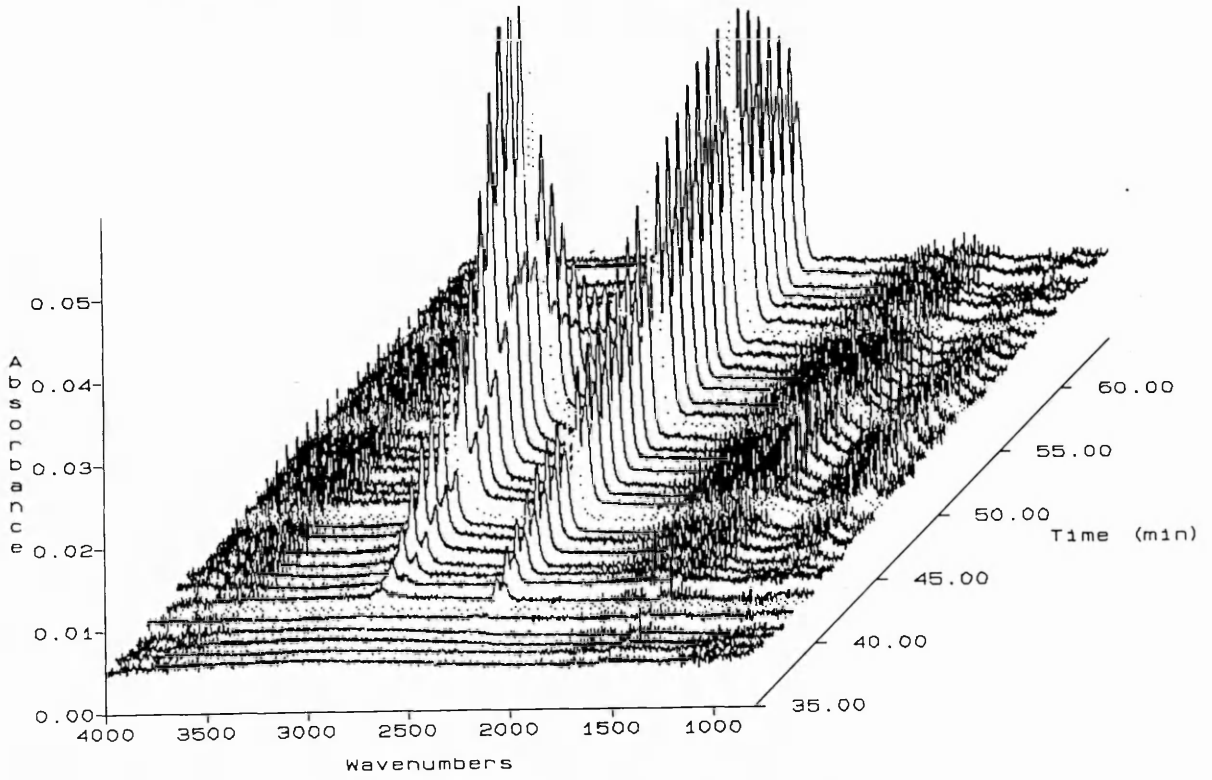

Figure 73. Showing the 3D-FTIR spectra for the decomposition of SAz-Na-$C_6NH_3^+$.

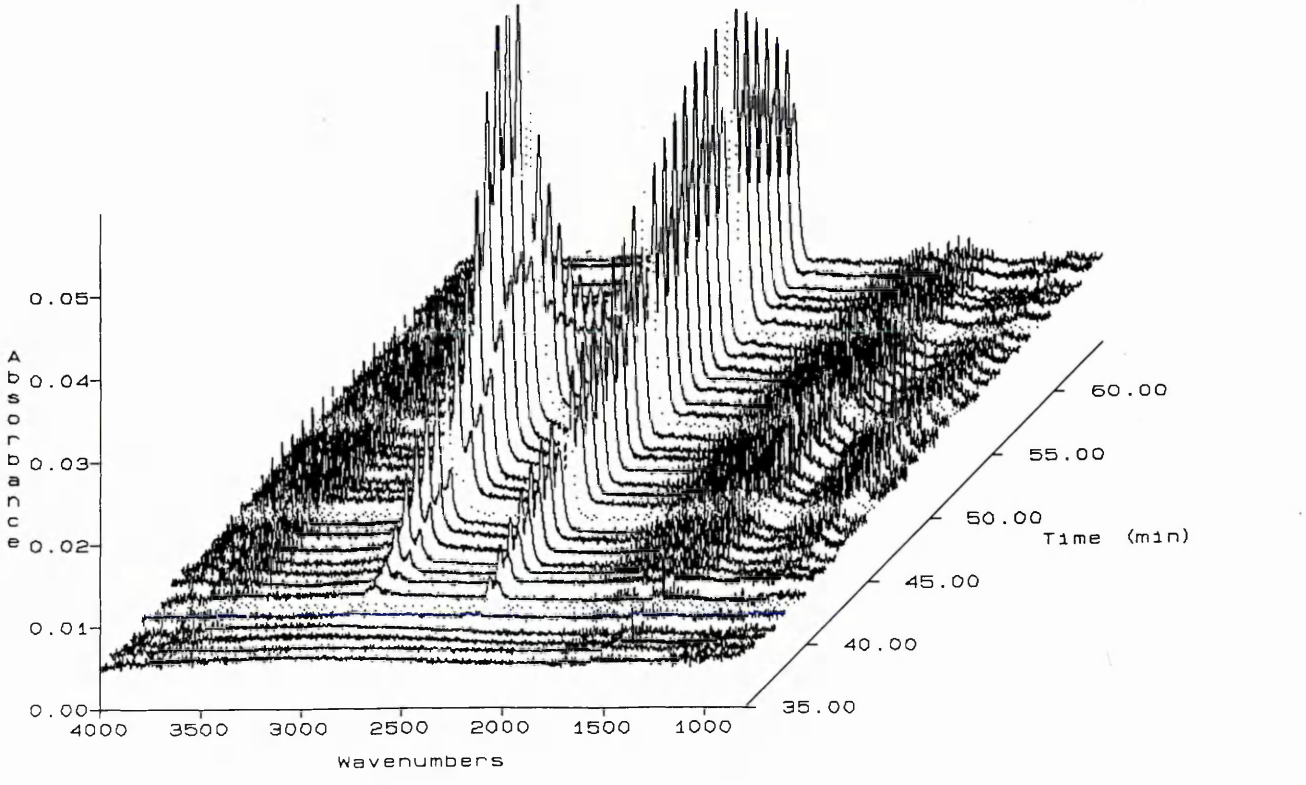

Figure 74. Showing the 3D-FTIR spectra for the decomposition of SA-An-$C_{12}NH_3^+$.

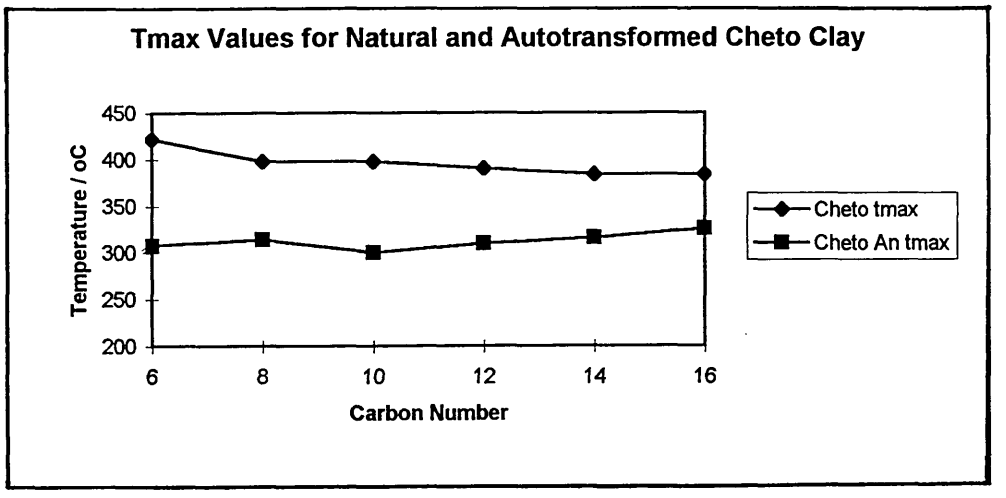

Figure 75. Showing the maxima decomposition temperatures for Na- and An-SAz-1.

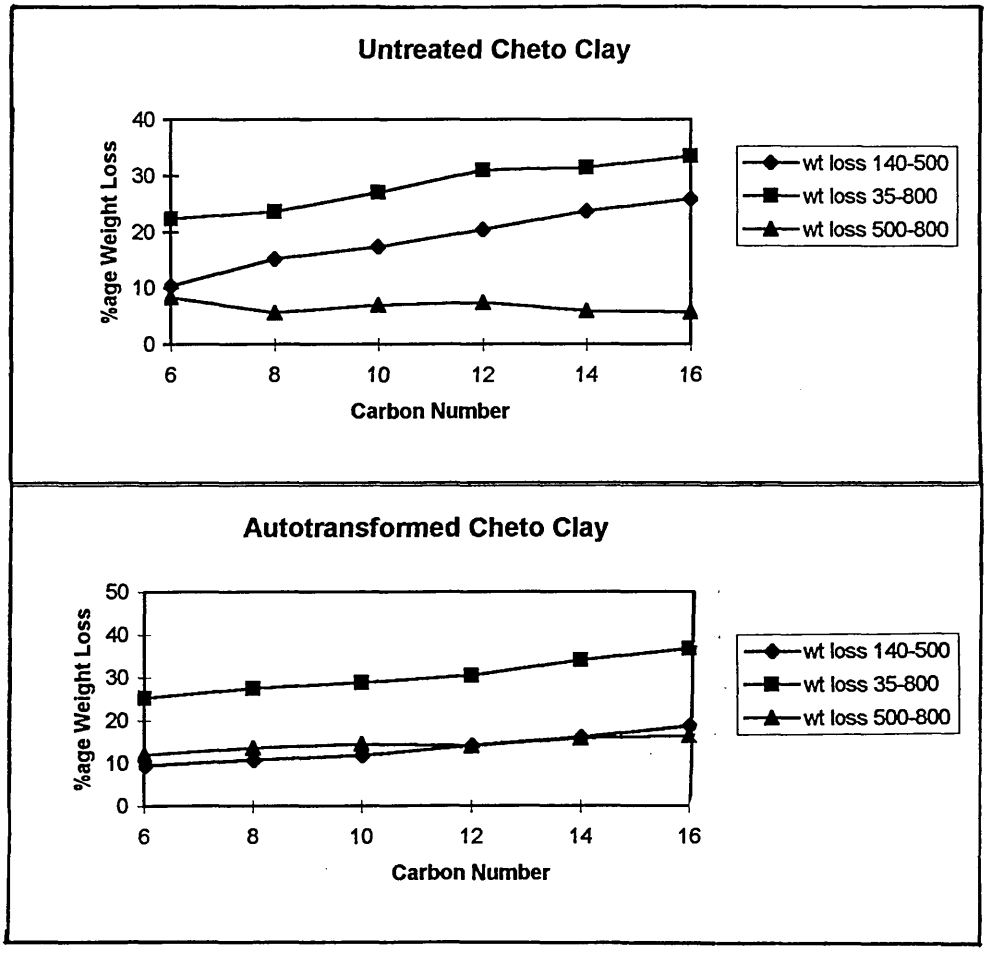

Figure 76. Weight loss curves at different temperatures for Na-SAz-1 and An-SAz-1.

	SAz-1	SWa-1	JP	ST
$C_6NH_3^+$	10.8 (14.0)	11.5 (11.9)	9.3 (14.1)	8.6 (13.9)
$C_8NH_3^+$	13.5 (18.0)	14.1 (12.6)	11.5 (13.6)	10.7 (14.2)
$C_{10}NH_3^+$	15.9 (20.1)	16.7 (17.8)	13.6 (15.5)	12.7 (16.1)
$C_{12}NH_3^+$	18.2 (23.6)	19.1 (18.5)	15.7 (18.0)	14.6 (18.0)
$C_{14}NH_3^+$	20.4 (25.5)	21.4 (20.6)	17.6 (23.7)	16.4 (18.8)
$C_{16}NH_3^+$	22.5 (27.8)	23.5 (24.5)	19.5 (23.8)	18.2 (21.6)

Table 20. Percentages of expected weight loss from each organocation in each clay. Figures in parenthesis represent the percentage of weight loss detected by TGA for Na-alkylammonium clays in the region of 140-500 °C.

As can be seen from Table 20, the weight losses increase as the carbon chain length increases. There is a correlation between the calculated weight losses (from the CEC of each clay) and the experimental values observed by TGA in the region of 140-500 °C. In this region contribution of physisorbed water and evolution of CO_2 to the thermograms are insignificant. The differences in weight losses among the clays are explained in terms of their CECs.

JP

The behaviour of Na-JP and An-JP samples is similar to that of SAz-1 counterparts. The TG traces are shown in Figures 77a and 77b. The desorption/decomposition for Na-JP samples results in a sharp and intense peak near 420 °C. This maximum shifted to lower temperatures as the carbon chain length increased. Another broad and weak peak is observed near 300 °C, which is more obvious in samples with short carbon chain lengths. In the dehydroxylation region two peaks of weak intensity developed at 630 and 750 °C.

In An-JP samples the decomposition of the alkylammonium ions occurs at lower temperatures than for Na-JP (near 300 °C). This maximum is slightly shifted to higher temperatures with the increment of carbon chain length. A small peak at 230 °C starts to occur in samples with the highest carbon chain lengths. In the dehydroxylation region, two intense peaks are also noticed, with maxima at 600 and 720 °C. An approximate weight loss of 5% was observed in Na-JP and 10% in An-JP in the region of 500-800 °C. This observation further supports the findings previously discussed for SAz-1. The weight loss increased as the chain length increased (Table 20), and the Na-JP (380-430 °C) samples are thermally more stable than An-JP (290-300 °C).

ST

In Na-ST samples, the maximum associated with the decomposition of the alkylammonium ions appears near 360 °C (Figure 78a). However, it shifted to higher temperatures as the chain length increased (C_{14} and C_{16}). The peak at 280 °C is also noticed and is less pronounced as the chain length increased, in which it is overlapped by that at 360 °C. The dehydroxylation results in a very sharp and intense peak near 600 °C. In the ST-Na-$C_{16}NH_3^+$ sample this peak appears at 660 °C.

In the autotransformed samples (Figure 78b) the breakdown of the organocations is found near 270 °C and the formation of CO_2 combined with the dehydroxylation appears as a broad and prolonged band extending from 340 to 620 °C.

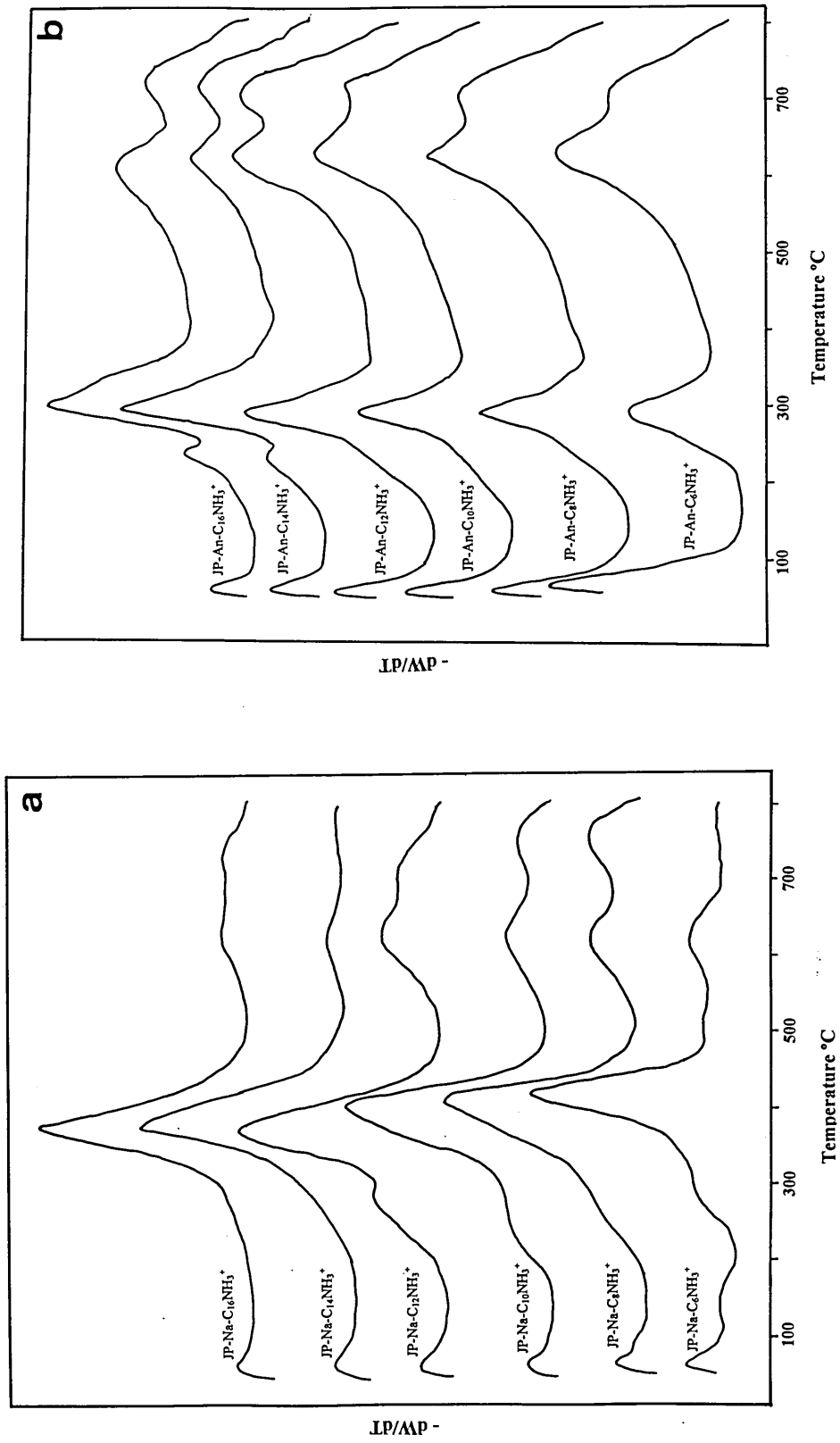

Figure 77. Derivative thermograms for the decomposition of alkylammonium ions from (a) Na-JP and (b) An-JP samples.

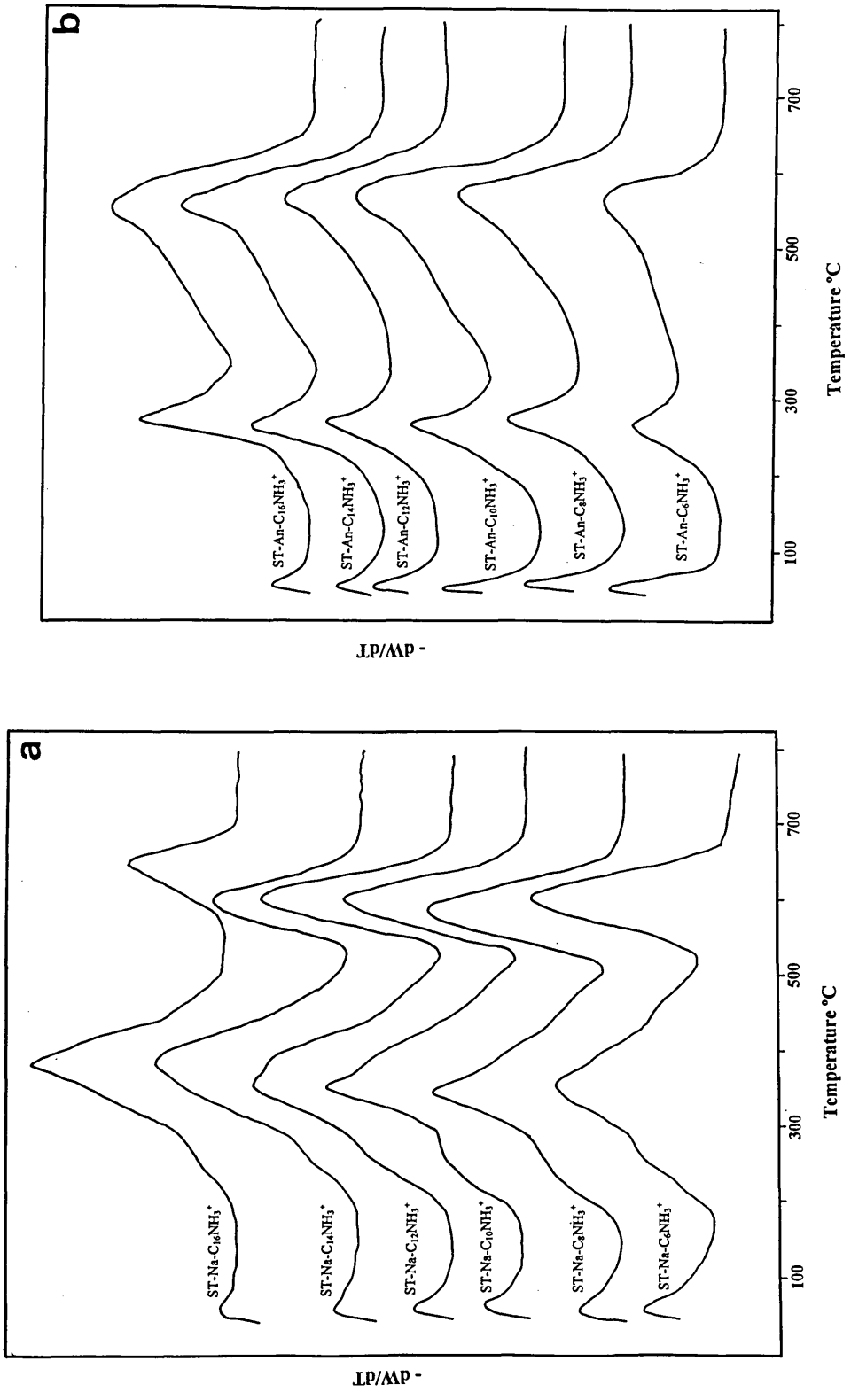

Figure 78. Derivative thermograms for the decomposition of alkylammonium ions from (a) Na-ST and (b) An-ST samples.

ST samples show a similar trend to those derived from SAz-1 and JP. Certainly, in Na-ST only a weight loss of 6% was observed between 500-800 °C, which indicates that, as described before, only the dehydroxylation significantly contributes to this loss, the evolution of CO_2 being negligible. In An-ST this loss was >10% demonstrating that in autotransformed samples the formation of CO_2 from carbonaceous deposits has a significant influence. Again, in the region of 140-500 °C the weight loss increased sharply in Na-ST, but not in An-ST. The decomposition temperature maxima are essentially constant in both series of samples and once more Na-ST samples are more stable than those of An-ST.

SWa-1

Na-SWa-1 samples present two maxima at 250 and 330 °C (Figure 79a). These peaks appear at slightly higher temperatures in the other clays studied. As the alkylammonium chain length increased from $C_{10}NH_3^+$ to $C_{16}NH_3^+$ another peak next to the 330 °C is developed (at 400 °C). The intensity of the latter is lower than the former in $C_{10}NH_3^+$ and $C_{12}NH_3^+$ samples, but the peak at 400 °C is more intense when $C_{12}NH_3^+$ or $C_{14}NH_3^+$ was intercalated. The dehydroxylation is manifested in a maximum near 660 °C.

An-SWa-1 samples displayed a similar behaviour to their Na-counterparts (Figure 79b), except that the second peak at 400 °C starts to occur from $C_{12}NH_3^+$ and it possesses the same intensity as that at 330 °C in $C_{12}NH_3^+$ and $C_{14}NH_3^+$. Nonetheless, in $C_{16}NH_3^+$ the intensity of the 330 °C is much higher than for 400 °C. In these series of samples the intensity of the dehydroxylation peak is lower than that of Na-SWa-1 samples and occurs at a higher temperature (680 °C). However, in SWa-An-$C_{16}NH_3^+$ sample it appears at 620 °C.

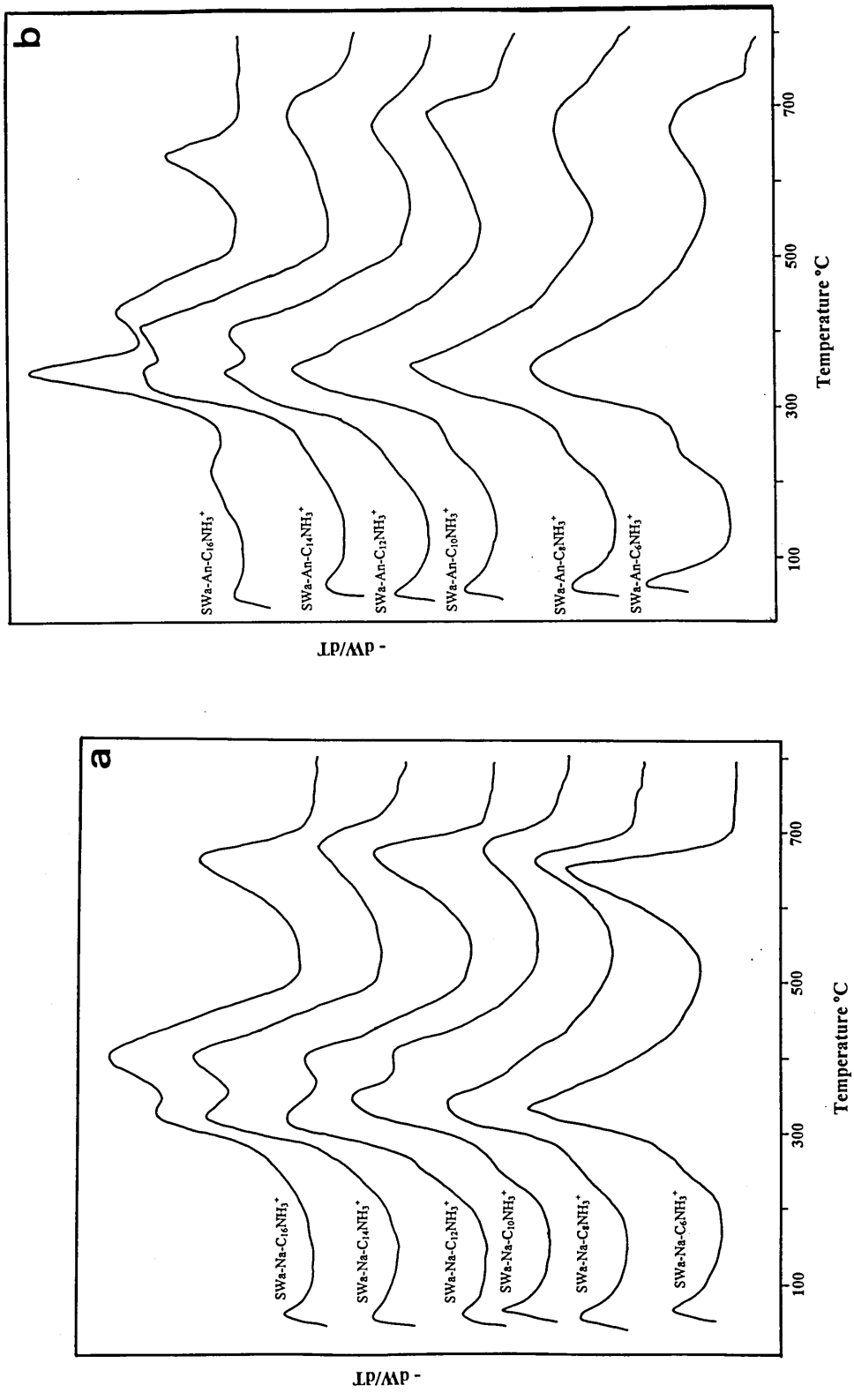

Figure 79. Derivative thermograms for the decomposition of alkylammonium ions from (a) SWa-Na and (b) SWa-An samples.

In this particular clay, the dehydroxylation region (500-800 °C) for both Na-SWa-1 and for An-SWa-1 presents the same weight loss (approximately 7%), indicating that the formation of CO_2 is insignificant (Figure 80). In both series of samples, the weight loss in the range 140-500 increased as the number of carbon atoms increased. Additionally, no differences in temperature maxima were observed between Na-SWa-1 and An-SWa-1 (Figure 81). Perhaps there was no air leak in the SWa-1 samples.

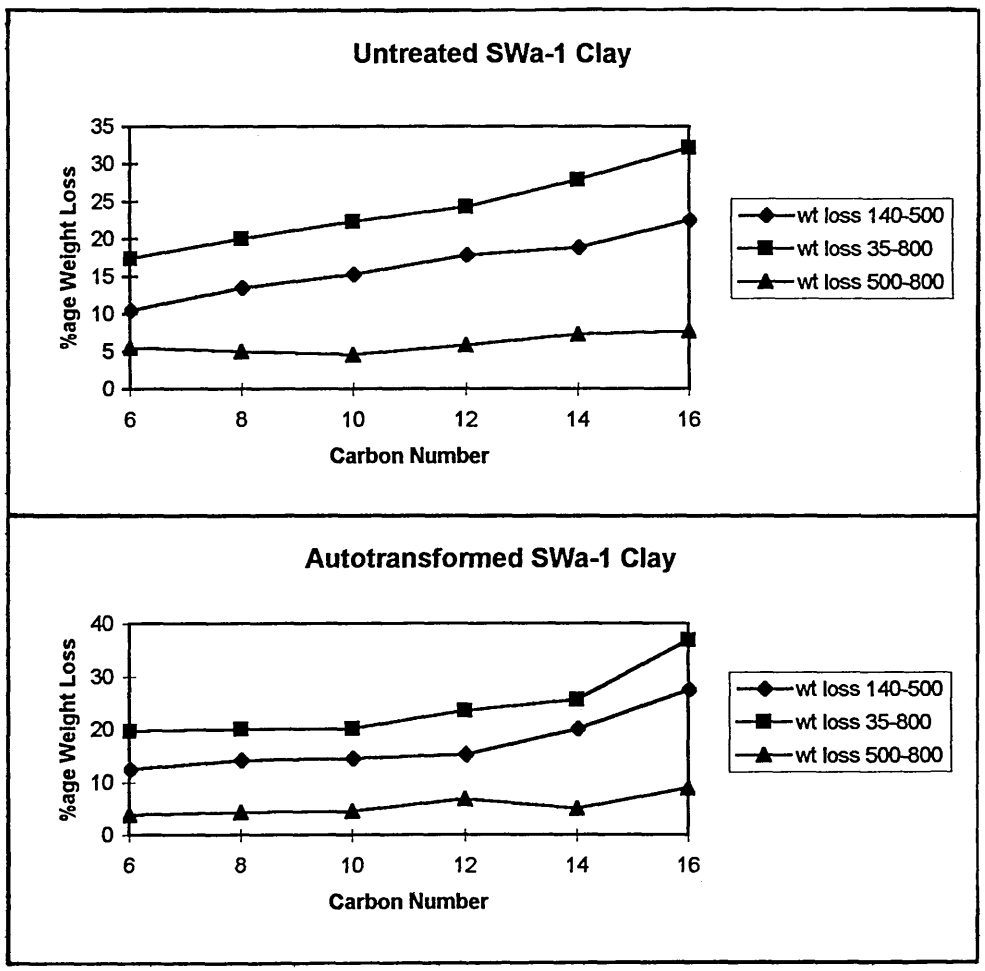

Figure 80. Weight loss curves at different temperatures for Na-SWa-1 and An-SWa-1.

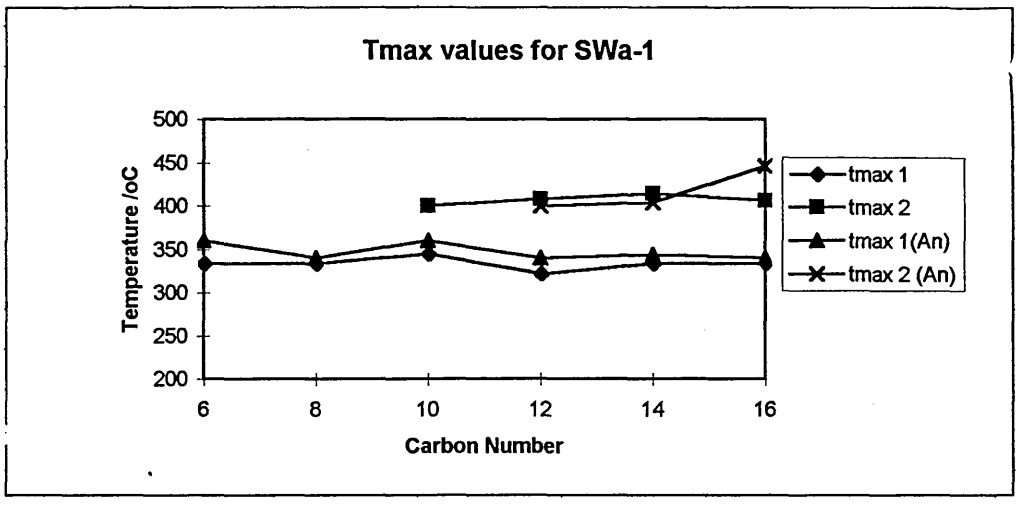

Figure 81. Showing the maxima decomposition temperatures for Na- and An-SWa-1.

General trends:

- The organoclays prepared from the Na-forms were more resistant to thermal decomposition than those resulting from the autotransformation procedure, which indicates that both series of samples underwent different decomposition routes. This was true for samples derived from SAz-1, JP and ST. Nevertheless, this trend was not reflected in samples derived form SWa-1, in which the thermal stability of the organoclays obtained from the Na-form was similar to the autotransformed organoclays.
- The weight losses registered for autotransformed organoclays were higher than for Na-form organoclays, despite the fact XRD revealed more reduced interlayer spacing after autotransformation.[241]
- The untreated clays do not have a significant H_2O/CO_2 maximum at temperatures >500 °C whereas there is considerable amount of CO_2 combined with water in the autotransformed samples (except for SWa-1).

- The weight loss in the region of 150-500 °C increased linearly with the increment of the molecular weight of the alkylammonium ions for Na-form, but not for autotransformed organoclays, where the increment was not linear. This observation is in complete agreement with the results reported by Cowan and White,[145] Theng, *et al.*,[146] Vansant and Uytterhoeven[197] and Watson[194] who reported that the affinity of the clay for the organocation was linearly related to molecular weight of the alkylammonium ion. The greater the chain length the greater is the contribution of physical forces.

The considerably higher thermal stability of organoclays prepared from the Na-forms can be explained as follows: Na^+ cations are very weak and can be easily displaced by alkylammonium ions resulting in a strong coordination of the organocation in exchange sites, which are more resistant to decomposition by heating. In the autotransformed samples, there are protons or octahedral cations occupying exchange sites, these inorganic species are strongly bound to the clay surface and the displacement by organocations is not very straightforward. Under these circumstances, the alkylammonium ions are weakly associated in the interlamellar space. Therefore, the heating process causes a more rapid decomposition of the organocations present in the edge sites and in the interlamellar region. Another more likely possibility is that the autotransformed clays possess a reduced charge density and therefore the alkylammonium ions are desorbed/decomposed earlier in temperature. The formation of CO_2 in autotransformed samples may possibly be attributed to the Al^{3+}/H^+ catalysing the breakdown of the alkylammonium ions via Hoffmann degradation (see section 5.3.3.1, Chapter 5).

The greater weight loss registered in autotransformed samples in comparison with Na-counterparts may be ascribed to (i) the generation of a more hydrophobic surface during the autotransformation process or (ii) that more of the organocations are lost during autotransformation. Perhaps there is still carbon on the surface of the Na-form clays.

There is no clear explanation for the unexpected behaviour observed in SWa-1. A possible reason can be that this clay presents the lowest incorporation of organocation in the interlamellar space (53%) compared with the other clays (Table 21).[241]

	SAz-1	JP	ST	SWa-1
C_t	1.20	1.0	0.92	1.27
$C_{t,An}$	0.88	0.97	0.82	1.04
ΔC_t	0.32	0.03	0.10	0.23
$C_{i,An}$	0.84	0.76	0.82	0.68
$C_{i,An}/C_t$	70	76	89	53

Table 21. Changes in the total CEC (C_t) derived from potentiometric titration and interlamellar CEC of autotransformed clays ($C_{i,An}$).[241]

Certainly, the values presented in Table 21 indicate that SWa-1 has a considerable concentration of exchange sites located on the external surface. In other words, a significant fraction of the alkylammonium ions reside on those sites and therefore, the heat treatment may easily induce the desorption/decomposition of the organocations at the same temperature in both Na-SWa-1 and An-SWa-1. In the other clays, the organocations reside on interlamellar exchange sites (>70% CEC), in which, as explained before, the interactions are

stronger in Na-forms than in An-forms. As a result, the former present a higher thermal stability. From Table 21, it is clear that autotransformation reduces the charge density, especially in SAz-1 and SWa-1.

7.2.2 Real-Time TG-FTIR

As it has been shown, the desorption/decomposition mechanism of the alkylammonium ions (using the Mettler thermobalance) from the Na-forms was different than with the An-forms. For this reason, the gases evolved during the heating process of all $C_6NH_3^+$ and $C_{12}NH_3^+$ alkylammonium ions for both the Na-form and the autotransformed clays were followed by Fourier Transform Infrared Spectroscopy in order to investigate these systems in more detail.

Figure 82 shows the total infrared chromatogram evolution of aliphatic species, carbon dioxide, ammonia and water as a function of time for (a) ST-Na-$C_6NH_3^+$ and (b) ST-Na-$C_{12}NH_3^+$, the total weight loss curve and the reconstructed chromatogram are also included. The same series of samples derived from autotransformation are represented in Figure 83.

In Figure 82a (ST-Na-$C_6NH_3^+$) there is a broad band in the reconstructed chromatogram from 25 to 45 min. In this time range, it is clearly seen that this band contains contributions from the breakdown of the alkylammonium ions to give mainly aliphatic hydrocarbons, ammonia, water and a small amount of carbon dioxide. The aliphatic species present two maxima at 31 and 39 min (310 and 472 °C), the desorption of ammonia also has two maxima, but not well resolved, the highest maximum is centred at 36 min (428 °C). The maximum of water occurs at 35 min (384 °C). After 45 min, only the evolution of CO_2 is observed in the chromatogram, which reaches the maximum absorbance at 63 min (950 °C).

Figure 82b (ST-Na-$C_{12}NH_3^+$) shows a similar behaviour. However, the maximum for the evolution of aliphatic hydrocarbons appears at a slightly earlier time 37 min (430 °C). Water, ammonia and CO_2 appeared at the same time as those for ST-Na-$C_6NH_3^+$. No evolution of hydrocarbon desorption was observed at high temperature. In ST-Na-$C_{12}NH_3^+$ the decomposition seems cleaner than ST-Na-$C_6NH_3^+$ over a narrower temperature range.

According to the results obtained from the Mettler thermobalance, Figure 82 should have a sharp peak near 600 °C (see Figure 78). However, such a peak is absent in both Figures 82a-b, even at the same temperature (600 °C, 46 min). The differences in evolved temperatures and times between the Cahn and Mettler thermobalances can be explained as follows: in the Cahn the crucible is much bigger than the Mettler and the nitrogen flow rate was 70 cm^3min^{-1} in the former and 30 cm^3 min^{-1} in the latter. Certainly, the heat transfer in the crucible of the Cahn thermobalance is more effective than that of the Mettler, this effect combined with the higher N_2 flow rate allows the quick entrainment of the species evolved and then shifts the peaks to a lower temperature.

The decomposition of alkylammonium ions in autotransformed samples occurs at a lower temperature than in those derived from the Na-form, as was shown in the previous section. Indeed, the maxima for the evolution of CH species in ST-An-$C_6NH_3^+$ (Figure 83a) appeared at 27 and 33 min (250 and 353 °C). Ammonia is found in a very broad band centred at 32 min (330 °C), as well as water, the maximum for CO_2 occurs at 64 min (977 °C).

In ST-An-$C_{12}NH_3^+$ (Figure 83b) the two maxima for the evolution of CH are more obvious at 29 and 34 min (280 and 380 °C), the maximum for water is reached at 31 min (310 °C). The

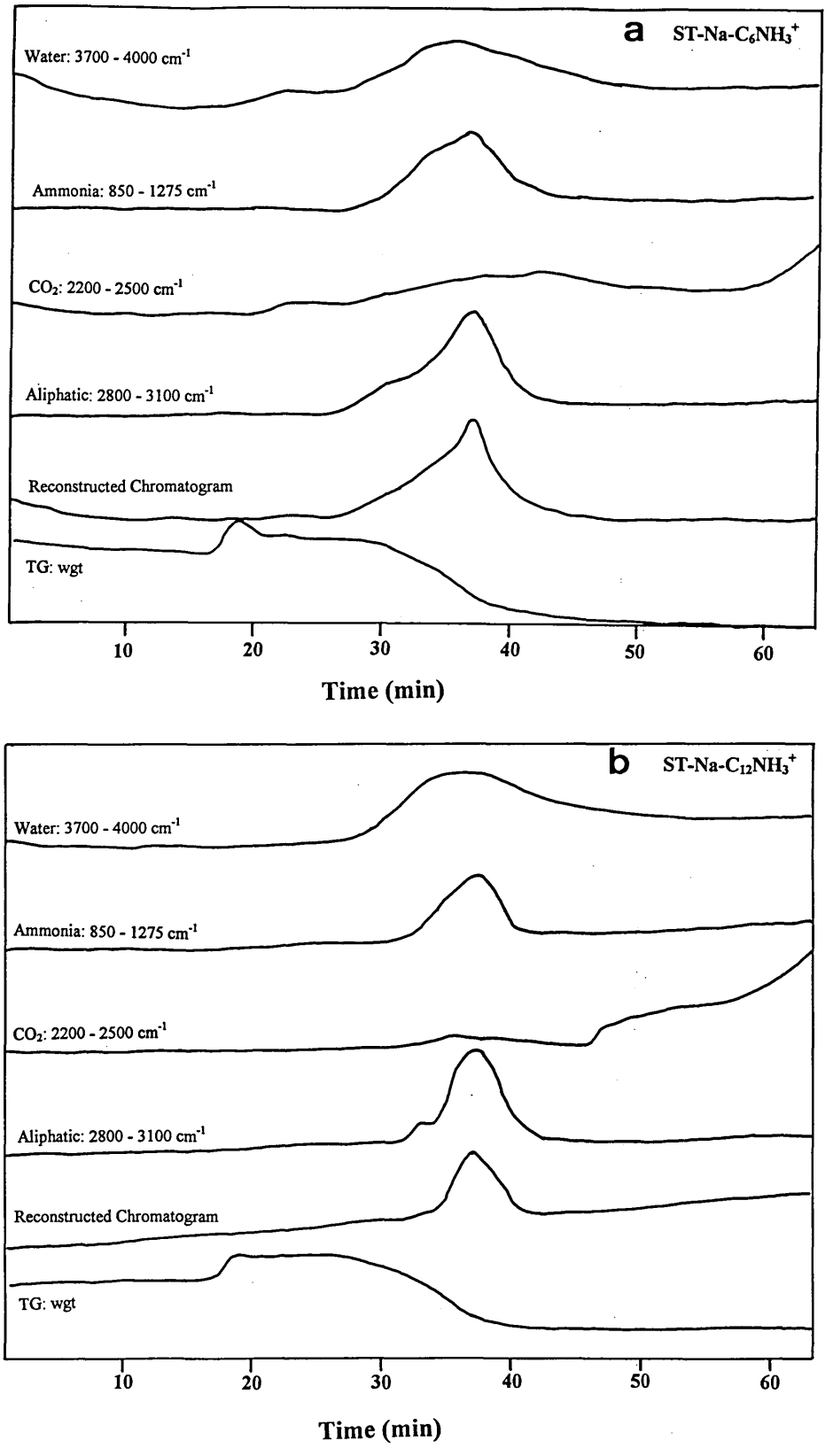

Figure 82. FTIR chromatogram for the decomposition of alkylammonium ions from (a) ST-Na-$C_6NH_3^+$ and (b) ST-Na-$C_{12}NH_3^+$.

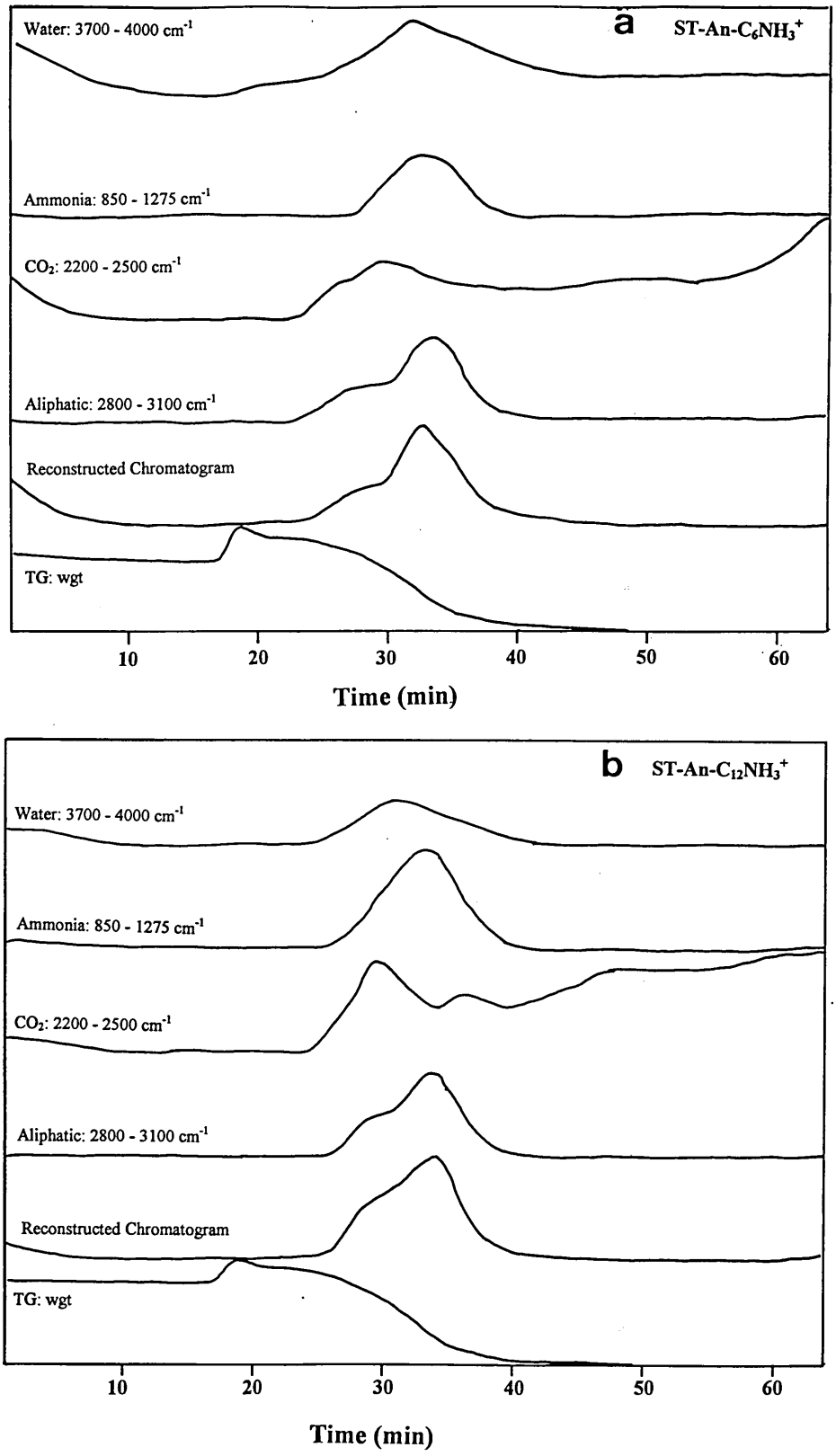

Figure 83. FTIR chromatogram for the decomposition of alkylammonium ions from (a) ST-An-$C_6NH_3^+$ and (b) ST-An-$C_{12}NH_3^+$.

maximum for ammonia again is observed at 32 min (330 °C) and finally the maximum for CO_2 appears at 63 min (959 °C). The evolution of CO_2 contributes to rising baseline in Figure 78b and also the maximum at 30 min (280 °C) coincides with that at the same temperature in Figure 78a-b.

The evolved time and temperature of the species involved in the decomposition process for all samples are gathered in Table 22, where only the highest maxima are listed. In general, the decomposition of the organocations occur between 31 – 39 min (310-470 °C), in this range, the species present are water (for SWa-1 and ST), ammonia, aliphatic hydrocarbons and a small amount of CO_2. The evolution of CO_2 at this stage, as mentioned before, indicates that the alkylammonium ions undergo thermal degradation. As the temperature increases the absorbance of the bands associated with CH (2868, 2937 and 2972 cm^{-1}), NH_3 (931 and 960 cm^{-1}) and H_2O (3500-4000 cm^{-1}) gradually decrease and the bands of CO_2 (2328 and 2368 cm^{-1}) and CO (2183 and 2108 cm^{-1}) start to increase (Figures 73 and 74).

As can be seen from Table 22, some samples did not present maxima for the evolution of water (SAz-1 and JP). Indeed, in the FTIR chromatogram, the desorption of water resulted in a flat line throughout the heat treatment of all these samples. Figure 84 shows the contribution of water, ammonia, aliphatic species and carbon dioxide for SAz-Na-$C_6NH_3^+$ and SAz-An-$C_6NH_3^+$. In SAz-Na-$C_6NH_3^+$ two maxima for the evolution of aliphatic hydrocarbons are observed at 33 and 38 min (350 and 451 °C), ammonia presents two maxima at 35 and 38 min (380 and 451 °C) whilst CO_2 shows three small peaks at 24, 33 and 39 min (160, 350 and 470 °C).

Sample	Water min / °C	Aliphatic min / °C	Ammonia min / °C	CO_2 min / °C
SW-Na-$C_6NH_3^+$	32 / 330	36 / 411	34 / 363	61 / 924
SW-Na-$C_{12}NH_3^+$	33 / 350	38 / 451	33 / 354	49 / 688
SW-An-$C_6NH_3^+$	31 / 308	34 / 385	35 / 400	47 / 635
SW-An-$C_{12}NH_3^+$	31 / 308	34 / 385	31 / 308	57 / 830
SAz-Na-$C_6NH_3^+$	--	38 / 451	38 / 451	52 / 751
SAz-Na-$C_{12}NH_3^+$	--	34 / 380	33 / 356	63 / 953
SAz-An-$C_6NH_3^+$	--	36 / 415	33 / 353	48 / 650
SAz-An-$C_{12}NH_3^+$	--	37 / 421	32 / 331	52 / 750
ST-Na-$C_6NH_3^+$	35 / 384	39 / 472	36 / 428	63 / 958
ST-Na-$C_{12}NH_3^+$	35 / 384	37 / 430	36 / 428	63 / 958
ST-An-$C_6NH_3^+$	32 / 330	33 / 353	32 / 330	64 / 977
ST-An-$C_{12}NH_3^+$	31 / 310	34 / 380	32 / 330	63 / 959
JP-Na-$C_6NH_3^+$	--	38 / 450	38 / 450	63 / 960
JP-Na-$C_{12}NH_3^+$	--	37 / 420	35 / 390	63 / 960
JP-An-$C_6NH_3^+$	--	38 / 451	38 / 451	45 / 588
JP-An-$C_{12}NH_3^+$	--	37 / 420	37 / 420	47 / 630

Table 22. Maxima decomposition time and temperature for alkylammonium clays.

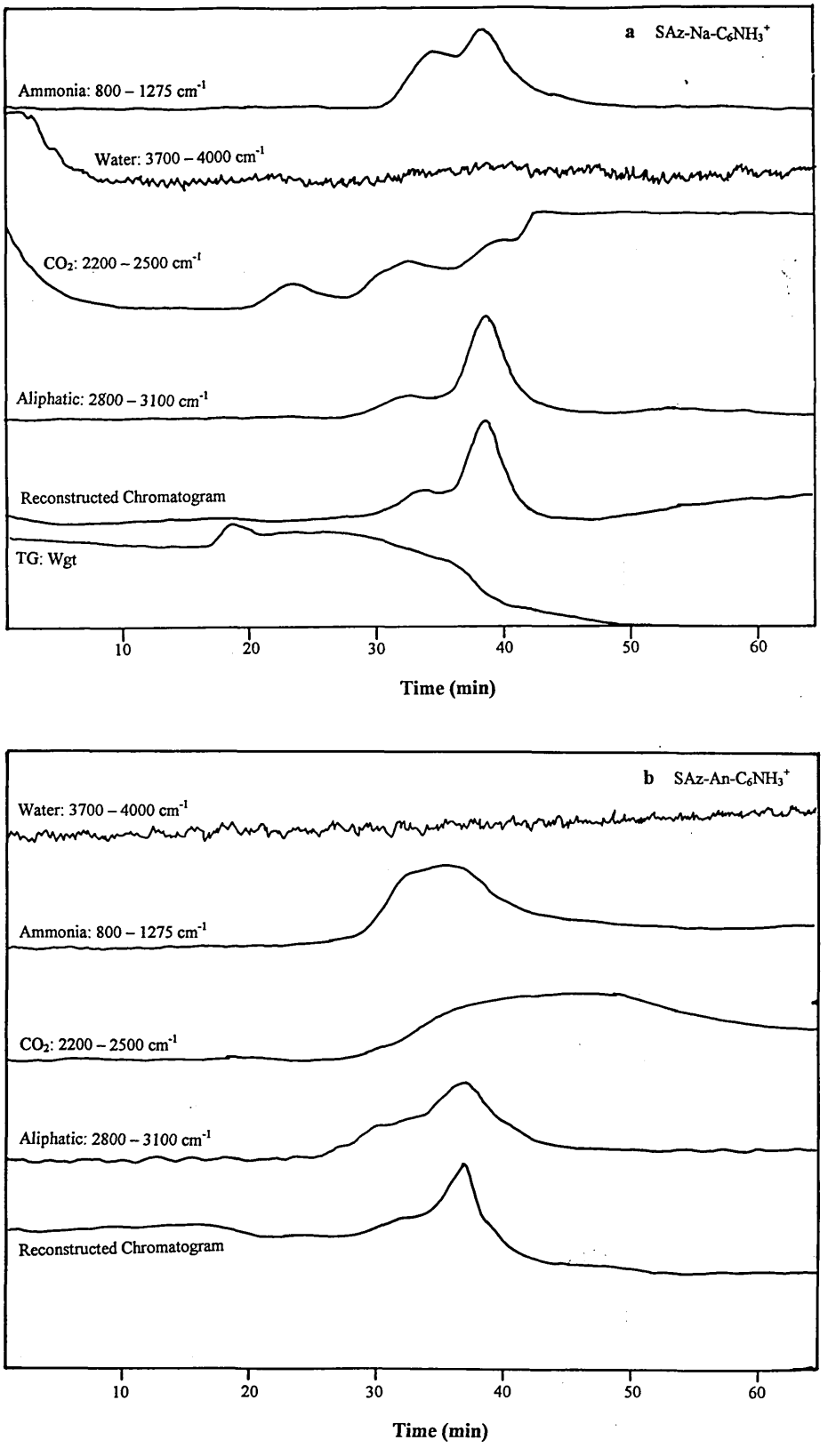

Figure 84. FTIR chromatogram for the decomposition of alkylammonium ions from (a) SAz-Na-$C_6NH_3^+$ and (b) SAz-An-$C_6NH_3^+$.

In SAz-An-$C_6NH_3^+$ the contribution of aliphatic hydrocarbons to the total chromatogram has two maxima at 31 and 37 min (310 and 420 °C), ammonia appears as a broad band centred at 33 min (350 °C) and finally CO_2 is developed as a prolonged band from 28 min to 60 min with maximum at approximately 48 min (650 °C). In both samples water is not shown. It could be possible, perhaps, to infer that water in these particular samples is used to form carbon dioxide due to the earlier appearance of CO_2, especially in SAz-An-$C_6NH_3^+$. Additionally, SAz-1 and JP present a low water content.

The percentages of total weight loss, of selected samples, determined from both Cahn and Mettler thermobalances are listed in Table 23. For both thermobalances the weight loss detected in An-samples was higher than for Na-clays. In the Mettler this difference is more obvious than for the Cahn. The percentages of weight loss observed are different in both thermobalances, being in the Mettler much higher. The explanation for this dichotomy may be due to that in the Mettler there might have been incorporation of air giving rise to the production of CO_2. In the Cahn, this effect is avoided because the system is more sealed and only the formation of coke takes place.

	SAz-1		**SWa-1**		**JP**		**ST**	
	Cahn	Mettler	Cahn	Mettler	Cahn	Mettler	Cahn	Mettler
Na-C_6	16.2	22.3	15.3	17.4	13.4	19.0	15.3	20.0
An-C_6	18.3	25.2	16.3	19.6	13.5	20.3	16.5	27.3
Na-C_{12}	25.1	31.0	18.3	24.3	15.2	23.5	18.8	24.6
An-C_{12}	26.1	30.8	19.2	23.5	16.1	26.0	22.9	31.3

Table 23. Percentages of total weight loss determined by Cahn and Mettler thermobalances.

7.3 Summary of Thermal Stability Investigation

In this study, it has been demonstrated that the thermal stability of alkylammonium samples derived from the Na-clays was higher than those resulting from autotransformation. The results were explained in terms of the high coordination strength of the organocation in exchange sites in Na-clays. A clay with high octahedral iron (SWa-1) showed no differences in thermal stability, this particular clay presented the lowest CEC value in the interlamellar space.

The weight loss in autotransformed samples was higher than for Na- counterparts. This trend was ascribed to the generation of more hydrophobic surface during the autotransformation process. In general the weight loss increased as the carbon chain length increased.

The weight loss in the region of 500-800 °C was almost 5% in all Na-clays and was mainly due to the dehydroxylation of the clay, the contribution of CO_2 being insignificant. In An-clays the weight loss was >10% and CO_2 presented a significant influence. It is thought that Al^{3+}/H^{+} may have catalysed the breakdown of the alkylammonium ions via Hoffmann degradation. There were discrepancies between the weight loss values obtained from Cahn and Mettler thermobalances.

TG-FTIR results revealed that all samples underwent similar decomposition behaviour and that during the heat treatment of alkylammonium clays, the organocation is decomposed to produce ammonia, aliphatic hydrocarbons, water and small amounts of CO_2. Further work is required to identify the nature of the aliphatic hydrocarbons by TG-OTM-GC-MS.

CHAPTER 8

Conclusions and Future Work

8.0 Introduction

The catalytic activity towards the isomerisation of α-pinene of four acid-activated organoclays [AAOCs (SWy-2, STx-1, SAz-1 and Sap-Ca)] prepared using tetramethylammonium (TMA^+) cations with variable acid concentrations was investigated. The catalytic ability of the AAOCs was compared with samples prepared in the absence of TMA^+, acid-activated clays (AACs). Aluminium-activated organoclays (AlAOCs), using TMA^+ cations, and aluminium-activated clays (AlACs) were also studied. AlAOCs derived from SWy-2 using divalent organocations of different shapes (1,4-diazabicyclo[2.2.2]octane, DABCO and 1,5-diaminopentane, DAP) were evaluated. The test reaction was applied to montmorillonites saturated with various inorganic cations (Al, Ca, Mg, Na and Ni) to study the effect of the interlayer cation on the catalytic activity.

The adsorption of hept-1-ene, heptan-1-ol and heptan-2-ol (at room temperature) on one of the most active clays (STx-1) in the form of AlACs and AlAOCs was carried out in order to identify the products that are desorbed at certain temperatures. Finally, the last part of the thesis was addressed to evaluate the thermal stability of four clays (SWa-1, ST, SAz-1 and JP) exchanged with quaternary ammonium (n-alkylammonium) of variable carbon chain length (C_6 – C_{16}) into Na-exchanged and autotransformed clays. The general findings will now be summarised to give appropriate additional information.

8.1 Catalysis by AACs and AAOCs

8.1.1 Nature of the Clay

It was shown (section 4.2.1, Figure 35), that the nature of the raw clay played an important role in the catalytic properties of the AACs. In the absence of TMA^+ both Sap-Ca and STx-1

were more effective catalysts for the process than SWy-2 and SAz-1. Clays from different deposits were attacked to different levels by the same acid treatment. For example, the high activity of Sap-Ca was attributed to the extensive leaching of the clay as acid treatment progressed because it possesses a magnesium rich octahedral sheet. The total conversion for AAOCs derived from SWy-2 exhibited the largest increase in yield (from 50% for SWy-2-H) to 88%, which incidentally represented an eightfold increase over SWy-2-TMA/H. The conversion over STx-1-TMA/H samples increased slightly from 62% to 73% whereas the yields for Sap-Ca-TMA/H and SAz-1-TMA/H samples decreased from 60% to 50% and from 35% to 20%, respectively.

8.1.2 Extension of the Acid Treatment

The reduction in activity of Sap-Ca-TMA/H was attributed to the occupancy of TMA^+ cations into the available surface created by the protonic attack of the octahedral sheet, rendering these active sites inaccessible to α-pinene molecules (section 4.2.1, Figure 37). Under those circumstances, α-pinene molecules only accessed the acid sites in the interlamellar space. SAz-1-TMA/H presented a very low H^+ content and a high TMA^+ content (section 4.1.4, Table 9) which represents a reduction in available acid centres for the isomerisation of α-pinene.

A direct comparison of the catalytic activity of all four clays was not possible due to the depletion of the octahedral sheet of Sap-Ca. Aluminium-activated clays and organoclays were prepared to compare the clays directly. However, another route to achieve this aim could be the acid treatment of SWy-2, STx-1 and SAz-1 at high temperature (95 °C) for different times (30, 90 and 180 min). This acid treatment would cause a considerable

depletion of the octahedral sheet of SWy-2, STx-1 and SAz-1, making them similar to mild acid treated Sap-Ca.

8.1.3 Effect of the Organocation

The catalytic activity and the thermal stability of AAOCs derived from SWy-2 and prepared with TMA^+ were compared with those of SWy-2 exchanged with trimethylphenylammonium ions ($TMPA^+$). It was found that the total α-pinene conversions for SWy-2-TMPA/H samples (section 4.2.2, Figure 39) were relatively lower than those of SWy-2-TMA/H, with 40-50% less at a lower acid-activation treatment (12-48 mmol H^+). As the severity of the acid activation increased, the activity for SWy-2-TMPA rose, but the conversions were still 10-20% lower in comparison with SWy-2-TMA/H samples. This reduction in activity, in samples treated at low acid concentration, was attributed to the significantly higher $TMPA^+$ content, which proved more resistant to displacement by protons than did TMA^+. The thermal stability of $TMPA^+$ was higher than that for TMA^+. Additionally, TG analysis of SWy-2-TMPA/H samples showed two maxima at 580 and 700 °C, and they were attributed to the production of CO_2 in two stages, the first from the phenyl-ring and the second from the methyl groups. However, the assignments for these maxima are not yet clear, and further work is required to study the gases evolved during the heat treatment of SWy-2-TMPA/H and SWy-2-TMA/H by real-time TG-FTIR to precisely assign those maxima.

8.1.4 Resistance of TMA^+ Cations

In this part of this study, it was found that TMA^+ cations, at a fixed amount (1 CEC), was able to compete effectively for exchange sites when in simultaneous competition (in aqueous solution) with higher amounts of acid (120 CEC). Breen's group[24,25] prepared samples with a

fixed amount of organocations or polycation and then displaced (partially or completely) it from the clay surface using acid treatment. More work is needed to evaluate the displacement of protons by organocations when samples are initially acid activated and to compare the catalytic activity of the resulting samples.

8.2 Catalysis by AlACs, AlAOCs and IECs

8.2.1 Effect of the Aluminium and TMA^+ Content

It was shown that the total α-pinene conversion varied with the aluminium content in AlACs and in AlAOCs (section 5.1.3, Figure 44). The maximum conversions obtained were very similar to those observed using H^+- and H^+/TMA^+-exchanged clays (section 4.2.1) and were directly comparable with the values of 80% and 90% for zeolite, pillared clays and Pt/Al_2O_3 catalysts as reported in the literature. The type of clay used had a significant influence on the total conversion obtained using the isomerisation of α-pinene. In either the absence or presence of TMA^+ both Sap-Ca (90%) and STx-1 (84%) were more efficient catalysts for the process than SWy-2 (69%) and SAz-1 (27%). In all cases the presence of Al^{3+} resulted in an improved catalytic activity. The AlAOCs gave lower conversions than their AlACs counterparts with low Al^{3+} content (10-40% CEC). However, the values were similar at Al^{3+} contents > 50% CEC when the amount of TMA^+ present was gradually decreased. The reduced conversion of α-pinene to its isomers in AlAOCs suggested a significant reduction in the number of acid centres available because of displacement of protons by TMA^+ cations with the concomitant drop of the acidity and the catalytic activity.

8.2.2 Aluminium Ions Kept the Layers Expanded in Presence of Pinene

VT-XRD data demonstrated that AlACs saturated with α-pinene (section 5.1.7, Table 14) hold the layers apart in a wide range of temperatures. This result indicated that the AlACs presented expanded layers allowing the reactant molecules to access the interlamellar region and to reach the acid centres, as well as in samples with low TMA^+ loadings (20-30% CEC). This conclusion explained the similarity in catalytic activity showed by AlAOCs and AlACs at higher aluminium contents (*e.g.*, >70%).

8.2.3 The Charge Reduction Improved the Activity

The poorest catalysts for the isomerisation of α-pinene were, in all cases, those derived from the SAz-1 source clay. This behaviour was attributed to the highest layer charge and suspected inability to expand the layers in AACs. Preliminary results demonstrated that Li-charge reduction of Na-SAz-1 samples caused a significant improvement in the catalytic activity (section 5.1.8, Figures 50 and 51). The highest conversion (67%) was observed when SAz-1 was charge reduced by 50% of the original CEC. However, in these series of samples, only the effect of aluminium was studied, therefore, further work is necessary to evaluate the combined effect of TMA^+ and Al^{3+} cations on reduced charge samples, as well as the extension of temperature and time of activation.

8.2.4 The Shape and Valence of the Organocation Influenced the Activity

The shape and valence of the organocation affected the conversion of α-pinene. The order of activity was Al^{3+}/TMA^+ (60%) > $Al^{3+}/DABCOH_2^{2+}$ (38%) > $Al^{3+}/DAPH_2^{2+}$ (13%). $DAPH_2^{2+}$ cations showed the highest resistance to displacement by Al^{3+} or H^+ and resulted in a strong blocking effect for the α-pinene. TMA^+ and $DABCOH_2^{2+}$ cations presented higher d-

spacings than $DAPH_2^{2+}$, which favoured the ingress of the reactant molecule. The increase in Al^{3+} content did not enhance the activity. The acidity of $Al^{3+}/DABCOH_2^{2+}$ and $Al^{3+}/DAPH_2^{2+}$ samples was governed by the presence of protons arising from different competition equilibria (section 5.2.4, Figure 57). Further experimental work is required to fully understand $Al^{3+}/DAPH_2^{2+}$ and $Al^{3+}/DABCOH_2^{2+}$ systems and to elucidate which source of protons contributes to the catalytic activity, especially for $Al^{3+}/DABCOH_2^{2+}$ catalysts, which displayed a better activity than those of $Al^{3+}/DAPH_2^{2+}$. One way could be the use of commercial available DABCO·2HCl and DAP·2HCl. This could avoid the participation of free protons from solution when both organocations are protonated with HCl. Molecular modelling calculations would help establish the dimensions of DAP and DABCO to correlate them with the d-spacings and the molecular dimension of α-pinene. This would give an idea of whether or not pinene can access the interlamellar region, especially in SWy-2-H/DAP samples.

A direct correlation between the activity and the acidity was not possible in SWy-2-Al/DAP and SWy-2-Al/DABCO samples (using the desorption of cyclohexylamine) because both the desorption/breakdown of cyclohexylamine and DAP or DABCO appeared at the same temperature. Determinations of the acidity using pyridine may give a better correlation.

8.2.5 The Exchange Treatment and the Interlayer Cation Affected the Activity

The exchange treatment displayed a remarkable effect on the total conversion of α-pinene. It was found that fully-exchanged samples were more effective catalysts for the process than those prepared when the natural clays or the Na^+-exchanged forms were exchanged with the right amount of cations to satisfy the CEC. The order of activity for ion-exchanged samples

was $Al^{3+} > Ni^{2+} > Mg^{2+} > Ca^{2+} > Na^{+}$. Sap-Ca samples were more active than SWy-2 and SAz-1 clays. The activity did not correlate well with the surface acidity of the ion exchanged clays (section 5.3.2, Table 16), determined by the desorption of cyclohexylamine. Again, pyridine adsorption (followed by IR) could provide a better correlation of the acidity with the activity.

8.2.6 Cyclohexylamine Decomposed as the Temperature Increased

FTIR-MS analysis of the gases evolved during the thermal desorption/decomposition of cyclohexylamine from ion-exchanged clays demonstrated that the base breaks down to produce ammonia, cyclohexene, 1,3-cyclohexadiene, benzene, cyclopentene, 1,3-cyclopentadiene, carbon monoxide and carbon dioxide. The results were explained using Hofmann degradation. The evolution of CO and CO_2 was due to the combination of carbonaceous deposits with water. The desorption of cyclohexylamine exhibited a different mechanism, especially in Ni^{2+}-SCa. It was observed that all these products evolved at the same time.

8.3 Adsorption of Hept-1-ene and Alcohols

8.3.1 Protons from Polarised Water Improved the Reaction Process

The thermal desorption of hept-1-ene from AlACs gave products of isomerisation, hydration, oligomerisation and dehydrocyclisation (section 6.4, Figure 68). It is thought that the carbenium ion was the major adsorption state due to the considerable number of acid sites arising from the high polarisation power of aluminium.

The presence of TMA^+ cations reduced the formation of oligomeric products (section 6.6, Figure 70). The acid centres available might have been used to selectively generate isomers and hydration products. The interaction of hept-1-ene with AlAOCs at high temperature (100 °C) in a closed vessel reactor will be an important test to further support this assumption.

It was not possible to detect hydrocarbons $<C_5$, because the trap used (Vocarb 4000) did not work efficiently in that range. The use of a trap that retains these fractions would permit a more detailed characterisation of all desorbed compounds. Additionally, the utilisation of a more effective capillary column to better separate all the isomeric products would be very useful, and also to determine whether or not the current column is bleeding.

8.3.2 Formation of Hept-1-ene from Heptan-1- and -2-ol

Due to a lack of time, the desorption of heptan-1-ol and heptan-2-ol was studied only by TG analysis. It was found that samples with a high amount of Al^{3+} (80%-100%) developed a series of weak and prolonged peaks in the region of 280-500 °C (section 6.5, Figure 71). They were deliberately attributed to the desorption of hept-1-ene and/or oligomeric species. Further experimental work is required to fully characterise the gases evolved during the thermal desorption of these alcohols by TG-FTIR and TG-OTM-GC-MS and to corroborate these assumptions.

8.4 Organoclays of Increased Carbon Chain Length.

8.4.1 Evaluation of the Thermal Stability

It was observed that organoclays prepared from alkylammonium ions of different carbon chain lengths from the Na-forms were more resistant to thermal decomposition than those

resulting from autotransformation (section 7.1.2, Figures 72, 77 and 78) for SAz-1, JP and ST. However, this trend was not reflected in SWa-1 (section 7.1.2, Figure 79), in which Na- and autotransformed samples showed the same thermal stability. The findings for SAz-1, JP and ST were explained in terms of the better effectiveness of the alkylammonium ions to displace Na^+ (in Na-clays) than Al^{3+}, Fe^{3+}, Mg^{2+} or H^+ (in autotransformed clays), resulting in a stronger interaction in the former than in the latter. SWa-1 presented the lowest CEC in the interlamellar region, which means that a significant amount of alkylammonium ions reside on the external surface, therefore no significant differences were expected between Na- and autotransformed samples.

In general, the weight loss of alkylammonium in autotransformed samples was higher than for Na-form clays. The weight loss in the region of 500-800 °C was almost 5% in all Na-clays and was mainly due to the dehydroxylation of the clay, the contribution of CO_2 being insignificant. In autotransformed clays the weight loss was >10% and CO_2 presented a significant influence. It is thought that Al^{3+}/H^+ may have catalysed the decomposition of the alkylammonium ions via Hoffmann degradation.

The percentages of weight loss determined from Cahn and Mettler balances were different, being in the latter much higher (section 7.2.2, Table 23). The results were explained in terms of the incorporation of air in the Mettler that gave rise to the production of CO_2. Cahn's system is more sealed and only the formation of coke took place. Further work is required to prove these inferences, especially the carefully checking of all the possible sources of air incorporation in the Mettler balance and then the re-running of selected samples.

8.4.2 Decomposition Mechanism

The heat treatment of the organoclays resulted in the evolution of ammonia, water, aliphatic species and small amounts of carbon dioxide in the temperature range 310-470 °C. However, the identification of the aliphatic species has not yet been established. The thermal decomposition of these organocations may result in the formation of alkenes in a similar mechanism to that given for the desorption of cyclohexylamine (section 5.3.3.1). TG-OTM-GC-MS is needed to further investigate the nature of these hydrocarbons.

CHAPTER 9

Postgraduate Study, Presentations, Publications and References

9.1 Postgraduate Study

The courses attended during the period of the research studies are listed below:

Date	Location	Course	Duration
1996-1997	Sheffield Hallam University	Crystallography	8 hours
1996-1997	Sheffield Hallam University	Infrared Spectroscopy for Materials Analysis	8 hours
1997	Sheffield Hallam University	Liquid Crystals and Polymers	8 hours
1997	Sheffield Hallam University	Microscopy and X-ray Diffraction	8 hours
1998	Sheffield Hallam University	Computational Chemistry	8 hours
1999	University of Sheffield	English for Scientists	15 hours

9.2 Presentations

Part of the results of this thesis have been presented at the following conferences:

1. Presentation entitled "Organoarcillas Activadas con Tratamiento Acido: Actividad Catalítica para la Reacción de Isomerización de α-Pineno" by A. Moronta and C. Breen. **XVI Simposio Iberoamericano de Catálisis**. Cartagena de Indias - COLOMBIA, 23-28 August 1998.

2. Poster entitled "Preparation, Characterisation and Catalytic Activity of Mildly Acid-Activated Tetraalkylammonium-Exchanged Clays" by A. Moronta and C. Breen. **Physical and Chemical Characterisation of Mineral Suspensions**, Mineralogical Society, Clay Minerals and Applied Mineralogy Groups. University of Bath - ENGLAND, 7-8 September 1998.

3. Presentation (to be given) entitled "Organoarcillas Activadas con Aluminio: Actividad Catalítica para la Isomerización de α-Pineno" by A. Moronta and C. Breen. **XVII Simposio Iberoamericano de Catálisis**. Porto - PORTUGAL, 16-21 July 2000.

9.3 Articles Published and in Preparation

The following articles have been accepted for publication:

Influence of Layer Charge on the Catalytic Activity of Mildly Acid-Activated Tetramethylammonium-Exchanged Bentonites.
C. Breen and A. Moronta.
The Journal of Physical Chemistry, 103 (27), 5675-5680, 1999.

Characterization and Catalytic Activity of Aluminum- and Aluminum/Tetramethylammonium Bentonites.
C. Breen and A. Moronta.
Submitted to *The Journal of Physical Chemistry.*

The following articles are in preparation:

Effect of the Cation Shape on the Catalytic Activity of Aluminium-Activated Organoclays.
C. Breen and A. Moronta
For submission to Clay Minerals

Preparation, Characterisation and Catalytic Activity of Ion-Exchanged Clays.
C. Breen and A. Moronta.
For submission to Catalysis Letters.

Adsorption of Olefins and Alcohols on Aluminium-Exchanged Bentonites. Identification of the Products Formed at Room Temperature by Synergic Chemical Analysis.
A. Moronta, S. Taylor and C. Breen.
For submission to Clays and Clay Minerals.

9.4 References

1. Laszlo, P. Catalysis of Organic Reactions by Inorganic Solids. *Acc. Chem. Res.*, **19**, 121-127, 1986.

2. Cornelis, A., Laszlo, P. in: Chemical Reactions in Organic and Inorganic Constrained Systems. (Setton, R., ed.), Reidel, New York, 213, 1986.

3. Ballantine, J.A., Purnell, J.H., Thomas, J.M. Organic Reactions in Clay Microenvironment. *Clay Miner.*, **18**, 347-356, 1983.

4. Kaplan, H. One Step Process of Acid Activating Mineral Clays and Alkylating Phenolic Compounds with an Alkene Hydrocarbon. *U.S. Patent*, **3,287,422**, 4, 1966.

5. Hojabri, F. Gas-Phase Catalytic Alkylation of Aromatic Hydrocarbons. *J. Appl. Chem. Biotechnol.*, **21**, 87-89, 1971.

6. Njopwouo, D., Roques, G., Wandji, R. A Contribution to the Study of the Catalytic Action of Clays on the Polymerization of Styrene: I. Characterization of Polystyrenes. *Clay Miner.*, **22**, 145-156, 1987.

7. Morgan, D.A., Shaw, D.B., Sidebottom, M.J., Soon, T.C., Taylor, R.S. The Function of Bleaching Earths on the Processing of Palm Kernel, and Coconut Oils. *J. Am. Oil Soc.*, **62**, 292-299, 1985.

8. Fahn R., Fenderl, K. Reaction Products of Organic Dye Molecules with Acid-Treated Montmorillonite. *Clay Miner.*, **18**, 447-458, 1983.

9. Lagaly, G. Characterization of Clays by Organic Compounds. *Clay Miner.*, **16**, 1-21, 1981.

10. Lagaly, G., Fernandez-Gonzalez, M., Weiss A. Problems in Layer-Charge Determination of Montmorillonites. *Clay Miner.*, **11**, 173-187, 1976.

11. Lee, J.F., Mortland, M.M., Chiou, C.T., Kile, D.E., Boyd, S.A. Adsorption of Benzene, Toluene and Xylene by Two Tetramethylammonium-Smectites Having Different Charge Density. *Clays Clay Miner.*, **38**, 113-120, 1990.

12. Nzengung, V.A., Voudrias, E.A., Nkedi-Kizza, P., Wampler, J.M., Weaver, C.E. Organic Cosolvent Effects on Sorption Equilibrium of Hydrophobic Organic Chemicals by Organoclays. *Environ. Sci. Technol.*, **30**, 89-96, 1996.

13. Wolfe, T.A., Demirel, T., Baumann, E.R. Adsorption of Organic Pollutans on Montmorillonites Treated with Amines. *J. Water Pollut. Control Fed.*, **58**, 68-76, 1986.

14. Boyd, S.A., Lee, J.F., Mortland, M.M. Attenuating Organic Contaminant Mobility by Soil Modification. *Nature*, **333**, 345-347, 1988.

15. McBride, M.B., Pinnavaia, T.J., Mortland, M.M. Adsorption of Aromatic Molecules by Clays in Aqueous Suspension. *Adv. Envoron. Sci. Technol.*, **8**, 145-154, 1977.

16. Kukkadapu, R.K., Boyd, S.A. Tetramethylphosphonium- and Tetramethylammonium-Smectites as Adsorbents of Aromatic and Chlorinated Hydrocarbons: Effect of Water on Adsorption Efficiency. *Clays Clay Miner.*, **43**, 318-323, 1995.

17. Lee, J.F., Mortland, M.M., Boyd, S.A. Shape-Selective Adsorption of Aromatic Molecules from Water by Tetramethylammonium-Smectite. *J. Chem. Soc. Faraday Trans.*, **85**, 2953-2962, 1989.

18. Barrer, R.M., Perry, G.S. Sorption Mixtures, and Selectivity in Alkylammonium Montmorillonites. Part II. Tetramethylammonium Montmorillonite. *J. Chem. Soc.*, I, 850-858, 1961.

19. Ballantine, J.A., Davies, M., Purnell, H., Rayanakorn, M., Thomas, J.M. Chemical Conversions Using Sheet Silicates: Novel Intermolecular Dehydration of Alcohols to Ether and Polymers. *J. Chem. Soc. Chem. Commun.*, 427-428, 1981.

20. Atkins, M.P., Smith, D.J.H., Westlake, D.J. Montmorillonite Catalysts for Ethylene Hydration. *Clay Miner.*, **18**, 423-429, 1983.

21. Vaccary, A. Preparation and Catalytic Properties of Cationic and Anionic Clays. *Catal. Today*, **41**, 53-71, 1998.

22. Mokaya, R., Jones, W. Pillared Clays and Pillared Acid-Activated Clays: A Comparative Study of Physical, Acidity, and Catalytic Properties. *J. Catal.*, **153**, 76-85, 1995.

23. Pinnavaia, T.J., Tzou, M.S., Landau, S.D., Raythatha, R.H. On the Pillaring and Delamination of Smectite Clay Catalysts by Polyoxo Cations of Aluminum. *J. Mol. Catal.*, **27**, 195-212, 1984.

24. Breen, C., Watson, R. Acid-Activated Organoclays: Preparation, Characterisation and Catalytic Activity of Polycation-Treated Bentonites. *Appl. Clay Sci.*, **12**, 479-494, 1998.

25. Breen, C., Watson, R., Madejová, J., Komadel, P., Klapyta, Z. Acid-Activated Organoclays: Preparation, Characterisation and Catalytic Activity of Acid-Treated Tetramethylammonium-Exchanged Smectites. *Langmuir*, **13**, 6473-6479, 1997.

26. Osthaus, B.B. Kinetic Studies on Montmorillonites and Nontronite by Acid Dissolution Technique. *Clays Clay Miner.*, **4**, 301-321, 1956.

27. Norvak, I., Cicel, B. Dissolution of Smectites in Hydrochloric Acid: II. Dissolution Rate as a Function of Crystallochemical Decomposition. *Clays Clay Miner.*, **26**, 341-344, 1978.

28. Janek, M., Komadel, P. Autotransformation of H-Smectites in Aqueous Solution. The Effect of Octahedral Iron Content. *Geol. Carpath. Ser. Clays*, **44**, 59-64, 1993.

29. Breen, C., Zahoor, F.D., Madejová, J., Komadel, P. Characterization and Catalytic Activity of Acid-Treated, Size-Fractioned Smectites. *J. Phys. Chem.*, **101**, 5324-5331, 1997.

30. Grim, R.E. Applied Clay Mineralogy. McGraw Hill, New York, 1962.

31. Guggenheim, S., Martin, R.T. Definition of Clay and Clay Mineral: Joint Report of the AIPEA Nomenclature and CMS Nomenclature Committees. *Clays Clay Miner.*, **43**, 255-256, 1995.

32. Bondt, N., Deiman, J.R., van Troostwyk, P., Lowrenberg, A. *Ann. Chim. Phys.*, **21**, 48-71 1797.

33. Murray, H.H. Applied Clay Mineralogy Today and Tomorrow. *Clay Miner.*, **34**, 39-49, 1999.

34. Hoffmann, U., Endell, K., Wilm, D., Kristalstruktur und Quellung von Montmorrillonit. *Z. Krist.*, **86**, 340-348, 1933.

35. Marshall, C.E. Layer Lattice and Base-Exchange Clays. *Z. Krist.*, **91**, 433-449, 1935.

36. Maegdefrau, E., Hoffman, U. Die Kristalstruktur des Montmorillonit. *Z Krist.*, **98**, 299-323, 1937.

37. Johnston, C.T. Sorption of Organic Compounds on Clay Minerals: A surface Functional Group Approach, 1-44 in: Organic Pollutants in the Environment. (Shawhney B.L., ed.) Clay Mineral Society Workshop, Lectures 8, Boulder, CO, USA, 1996.

38. Grimshaw, R.W. Chemistry and Physics of Clays. Benn, London, 1971.

39. Brindley, G.W., Brown, G. Crystal Structure of Clay Minerals and their X-ray Identification. Mineralogical Society, London, 1980.

40. Quirk, J.P. Negative and Positive Adsorption of Chloride by Kaolinite. *Nature*, **188**, 253-254, 1960.

41. Grim, R.E., Kulbicki, G. Montmorillonite: High Temperature Reactions and Classification. *Am. Miner.*, **46**, 1329-1369, 1961.

42. Grim, R.E., Bray, R.H. The Mineral Constitution of Various Ceramic Clays. *J. Am. Ceram. Soc.*, **19**, 307-315, 1936.

43. Bar, A.L., Tenderloo, H.J. *Kolloid-Beihefter*, **44**, 97, 1936.

44. McCabe, R.W. Clay Chemistry, 314-363 in: Inorganic Materials. (Bruce, D.W., O'Hare, D., eds.) John Wiley & Sons, England, 1996.

45. Robertson, R.H.S., Ward, R.M. Assay of Pharmaceutical Clays. *J. Pharm. Pharmcol.*, **3**, 27-35, 1951.

46. Brindley, G.W., Thompson, T.D. Methylene Blue Absorption by Montmorillonites. Determination of Surface Area and Exchange Capacities with Different Initial Cation Saturations (Clay-Organic Studies XIX). *Israel J. Chem.*, **8**, 409-415, 1970.

47. Jaynes, W.F., Bigham, J.M. Multiple Cation-Exchange Capacity Measurements on Standard Clays Using a Commercial Mechanical Extractor. *Clays Clay Miner.*, **34**, 93-98, 1986.

48. Rhodes, C.N., Brown, D.R. Rapid Determination of the Cation Exchange Capacity of Clays Using Co(II). *Clay Miner.*, **29**, 799-801, 1994.

49. Bergaya, F., Vayer, M. CEC of Clays: Measurement by Adsorption of a Copper Ethylenediamine Complex. *Appl. Clay Sci.*, **12**, 275-280, 1997.

50. Hoffman, U., Klemen, R. Verlust der Austauschfahigkeit von Lithiumionen an Bentonit durch Erhitzung. *Z. Anorg. Chem.*, **262**, 95-99, 1950.

51. Greene-Keller, R. Dehydration of the Montmorillonite Minerals. *Miner. Mag.*, **30**, 604-515, 1955.

52. Greene-Keller, R. Irreversible Dehydration in Montmorillonite Part II. *Clay Miner. Bull.*, **2**, 52-56, 1953.

53. Sposito, G., Prost, R., Gaultier, J.-P. Infrared Spectroscopy Study of Adsorbed Water on Reduced-Charge Na/Li-Montmorillonites. *Clays Clay Miner.*, **31**, 9-16, 1983.

54. Srasra, E., Bergaya, F., Fripiat, J.J. Infrared Spectroscopy Study of Tetrahedral and Octahedral Substitutions in an Interstratified Illite-Smectite Clay. *Clays Clay Miner.*, **42**, 237-241, 1994.

55. Tettenhorts, R. Cation Migration in Montmorillonites. *Am. Miner.*, **47**, 769-773, 1962.

56. Luca, V., Cardile, C.M. Thermal Induced Cation Migration in Na and Li Montmorillonite. *Phys. Chem. Miner.*, **16**, 98-103, 1988.

57. Alvero, R., Alba, M.D., Castro, M.A., Trillo, J.M. Reversible Migration of Lithium in Montmorillonites. *J. Phys. Chem.*, **98**, 7848-7853, 1994.

58. Russell, J.D., Farmer, V.C. Infrared Spectroscopy Study of the Dehydration of Montmorillonite and Saponite. *Clay Miner. Bull.*, **5**, 443-464, 1964.

59. Calvet, R., Prost, R. Cation Migration into Empty Octahedral Sites and Surface Properties of Clays. *Clays Clay Miner.*, **19**, 175-186, 1971.

60. Madejová, J., Bujdák, J., Gates, W.P., Komadel, P. Preparation and Infrared Spectroscopic Characterization of Reduced-Charge Montmorillonite with Various Li Contents. *Clay Miner.*, **31**, 233-241, 1996.

61. Komadel, P., Bujdák, J., Madejová, J., Šucha, V., Elsass, F. Effect of Non-Swelling Layers on the Dissolution of Reduced-Charge Montmorillonite in Hydrochloric Acid. *Clay Miner.*, **31**, 333-345, 1996.

62. Purnell, J.H., Thomas, J.M., Diddams, P., Ballantine, J.A., Jones, W. The Influence of Exchangeable Aluminium Ion Concentration and of Layer Charge on the Catalytic Activity of Montmorillonite Clays. *Catal. Lett.*, **2**, 125-128, 1989.

63. Low, P.F., Ravina, I., White, J.L.Change in b Dimension of Na-Montmorillonite with Interlayer Swelling. *Nature*, **226**, 445-446, 1970.

64. Velde, B. Composition and Mineralogy of Clays in: Origin and Mineralogy of Clays, Clays and the Environment. Springer, Berlin, 1995.

65. Bradley, W.F., Grim, R.E. High Temperature Effects of Clay and Related Materials. *Am. Miner.*, **36**, 182-201, 1951.

66. Serratosa, J.M. Dehydration Studies by Infrared Spectroscopy. *Am. Miner.*, **45**, 1101-1104, 1960.

67. Mortland, M.M., Raman, K.V. Surface Acidity of Smectites in Relation to Hydration, Exchangeable Cation and Structure. *Clays Clay Miner.*, **16**, 393-398, 1968.

68. Theng, B.K.G. The Chemistry of Clay-Organic Reactions. (Hilger, A., ed.) London, 1974.

69. McAtee, J.L., Concilio, C.B. Effect of Heat on an Organo-Montmorillonite Complex. *Am. Miner.*, **44**, 1219-1229, 1959.

70. Frenkel, M. Surface Acidity of Montmorillonites. *Clays Clay Miner.*, **22**, 435-441, 1974.

71. Benesi, H.A., Winquist, H.C. Surface Acidity of Solid Catalysts. *Adv. Catal.*, **27**, 98-176, 1978.

72. Walling, C. The Acid Strength of Surfaces. *J. Am. Chem. Soc.*, 72, 1164-1168, 1950.

73. Benesi, H.A. Acidity of Catalyst Surfaces. I. Acid Strength from Colors of Adsorbed Indicators. *J. Am. Chem. Soc.*, **78**, 5990-5494,1956.

74. Barth, R.T., Ballou, E.V. Determination of Acid Sites on Solid Catalysts by Ammonia Gas Adsorption. *Anal. Chem.*, **33**, 1080-1084, 1961.

75. Kubokawa, Y. Determination of Acidity of Solid Catalyst by Ammonia Chemisorption. *J. Phys. Chem.*, **67**, 769-771, 1963.

76. Pliskin, W.A., Eischens, R.P. The Effect of Using the Pressed-Salt Technique to Obtain the Spectrum of Chemisorbed Ammonia. *J. Phys. Chem.*, **59**, 1156-1159, 1955.

77. Mortland, M.M., Fripiat, J.J., Chaussidon, J., Uytterhoeven, J. Interaction between Ammonia and the Expanding Lattice of Montmorillonite and Vermiculite. *J. Phys. Chem.*, **67**, 248-258, 1963.

78. Helsen, J.J. Determination of the Type of Acidity and Spectrometric Measurement of the Dissociation of Water from Montmorillonites through Adsorption of Triphenylcarbinol. *Bull. Groupe Fr. Argiles*, **22**, 139-155, 1970.

79. Parry, E.P. An Infrared Study of Pyridine Adsorbed on Acidic Solids. Characterization of Surface Acidity. *J. Catal.*, **2**, 371-379, 1963.

80. Connerton, J., Joyner, T.W., Padley, M.B. Characterisation of the Acidity of well Defined Cu-ZSM-5 Catalysts using Pyridine as a Probe Molecule. *J. Chem. Soc. Faraday Trans,*. **91**, 1841-1844, 1995.

81. Swoboda, A.R., Kunze, G.W. Infrared Study of Pyridine Adsorbed on Montmorillonites Surface. *Clays Clay Miner.*, **13**, 277-288, 1964.

82. Emeis, C.A. Determination of Integrated Molar Extinction Coefficient for Infrared Absorption Bands of Pyridine Adsorbed on Solid Acid Catalysts. *J. Catal.*, **141**, 347-354, 1993.

83. Ballantine, J.A., Graham, P., Patel, I., Purnell, J.H., Williams, K.J., Thomas, J.M. New Differential Thermogravimetric Analysis Method Using Cyclohexylamine for Measuring the Concentration of Interlamellar Protons in Clay Catalysts. *Proc. Int. Clay Conf. Denver,* 1985. (Schultz, L.G., van Olphen, H., Mumpton, F.A. eds.) The Clay Mineral Society, Bloomington, Indiana, 311-318, 1987.

84. Breen, C., Deane, A.T., Flynn, J.J. The Acidity of Trivalent Cation-Exchanged Montmorillonite. Temperature-Programmed Desorption and Infrared Studies of Pyridine and n-Butylamine. *Clay Miner.*, **22**, 169-178, 1987.

85. Breen, C. Thermogravimetric Study of the Desorption of Cyclohexylamine and Pyridine from Acid-Treated Wyoming Bentonite. *Clay Miner.*, **26**, 473-484, 1991.

86. Ryland, L.B., Tamele, M.W., Wilson, J.N. in Catalysis. (Emmett, P.H., ed.) New York, **7**, chap 1, 1960.

87. Norvak, I., Gregor, M. Surface Area and Decolourising Ability of some Acid-Treated Montmorillonites. *Proc. Int. Clay Conf. Tokio,* 851-857, 1969.

88. Hirokawa, A. Characteristics and Applications of the Acid-Treated "Acid Clay". *Nendo Kagaku,* **20**, 99-106, 1980.

89. Brunauer, S., Emmett, P.H., Teller, E. Adsorption of Gases in Multimolecular Layers. *J. Am. Chem. Soc.*, **60**, 309-318, 1938.

90. Vicente, M.A., Suárez, M., López-González, J.D., Bañares-Muñoz, M.A. Characterization, Surface Area, and Porosity Analyses of the Solids Obtained by Acid Leaching of a Saponite. *Langmuir*, **12**, 566-572, 1996.

91. Mendioroz, S., Pajares, J.A. Texture Evolution of Montmorillonite under Progressive Acid Treatment: Change form H3 to H2 Type of Hysteresis. *Langmuir*, **3**, 676-681, 1987.

92. Taylor, D.R., Jenkins, D.B. Acid-Activated Clays. *Soc. Min. Eng. AIME Trans.*, **282**, 1901-1910, 1986.

93. Kheok, S.C., Lim, E.E. Mechanism of Palm Oil Bleaching by Montmorillonite Clay Activated at Various Acid Concentrations. *J. Am. Oil. Chem. Soc.*, **59**, 129-131, 1982.

94. Kaviratna, H., Pinnavaia, T.J. Acid Hydrolysis of Octahedral Mg^{2+} Sites in 2:1 Layered Silicates: An Assessment of Edge Attack and Gallery Access Mechanisms. *Clays Clay Miner.*, **42**, 717-723, 1994.

95. Mills, G.A., Holmes, J., Cornelius, E.B. Acid Activation of some Bentonites Clays. *J. Phys. Colloid Chem.*, **54**, 1170-1185, 1950.

96. Heyding, R.D., Ironside, R., Norris, A.R., Prysiazniuk, R.Y. Acid Activation of Montmorillonite. *Can. J. Chem.*, **38**, 1003-1016, 1960.

97. Thomas, C.L., Hickey, J., Stecker, G. Chemistry of Clay Cracking Catalysts. *Ind. Eng. Chem.*, **42**, 866-871, 1950.

98. Tkác, I., Komadel, P., Müller, D. Acid-Treated Montmorillonites- A Study by ^{29}Si and ^{27}Al MAS NMR. *Clay Miner.*, **29**, 11-19, 1994.

99. Breen, C., Madejová, J., Komadel, P. Correlation of Catalytic Activity with Infrared ^{29}Si MAS NMR and Acidity Data for HCl-treated Fine Fractions of Montmorillonite. *Appl. Clay Sci.*, **10**, 219-230, 1995.

100. Breen, C., Madejová, J., Komadel, P. Characterisation of Moderately Acid-Treated, Size-Fractionated Montmorillonite Using IR and MAS NMR Spectroscopy and Thermal Analysis. *J. Mater. Chem.*, **5**, 469-474, 1995.

101. Komadel, P., Madejová, J., Janek, M., Gates, W.P., Kirkpatrick, R.J., Stucki, J.W. Dissolution of Hectorite in Inorganic Acids. *Clays Clay Miner.*, **44**, 228-236, 1996.

102. Granquist, W.T., Gardner Sumner, G. Acid Dissolution of a Texas Bentonite. *Clays Clay Miner.*, **6**, 292-308, 1959.

103. Tennakoon, D.T.B., Schlögl, R., Rayment, T., Klinowski, J., Jones, W., Thomas, J.M. The Characterization of Clay-Organic Systems. *Clay Miner.*, **18**, 357-371, 1983.

104. Gregory, R., Smith, D.J.H., Westlake, D.J. The Production of Ethyl Acetate from Ethylene and Acetic Acid using Clay Catalysts. *Clay Miner.*, **18**, 431-435, 1983.

105. Purnell, J.H., Williams, J., Yun, L. Charge Reduction and Regeneration in K^+, Na^+, Mg^{2+}, Ni^{2+} and Co^{2+}-Exchange Wyoming Bentonite. *Catal. Lett.*, **10**, 63-70, 1991.

106. Mitre, R.P., Sindhu, P.S. Acid Character of Sauconite: Increase in Cation Exchange Capacity on Aging in Water and the Role of Zn^{2+} and Al^{3+} Ions. *Clays Clay Miner.*, **19**, 391-397, 1971.

107. Breen, C. Thermogravimetric and Infrared Study of the Desorption of Butylamine, Cyclohexylamine and Pyridine from Ni and Co Exchanged Montmorillonite. *Clay Miner.*, **26**, 487-496, 1991.

108. Brown, D.R., Rhodes, C.N. Bønsted and Lewis Acid Catalysis with Ion-Exchanged Clays. *Catal. Lett.*, **45**, 35-40, 1997.

109. Adams, J.M., Bylina, A., Graham, S.H. Conversion of 1-Hexene to di-hexylether Using a Cu^{2+}-Smectite Catalyst. *J. Catal.*, **75**, 190-195, 1982.

110. Adams, J.M., Bylina, A., Graham, S.H. Shape Selectivity in Low-Temperature Reaction of C_6-Alkenes Catalysed by a Cu^{2+}-Exchanged Montmorillonite. *Clay Miner.*, **16**, 325-332, 1981.

111. Ballantine, J.A., Davies, M., Purnell, H., Rayanakorn, M., Thomas, J.M., Williams, K.J. Chemical Conversions Using Sheet Silicates: Facile Ester Synthesis by Direct Addition of Acids to Alkenes. *J. Chem. Soc. Chem. Commun.*, 8-9, 1981.

112. Adams, J.M., Dyer, S., Martin, K., Matear, W.A., McCabe, R.W. Diels-Alder Reactions Catalysed by Cation-Exchanged Clay Minerals. *J. Chem. Soc. Perkin Trans.*, I, 761-765, 1994.

113. Adams, J.M., Clapp, T.V., Clemet. D.E. Catalysis by Montmorillonites. *Clay Miner.*, **18**, 411-421, 1983.

114. Suib, S.L., Tanguay, J.F., Occelli, M.F. Comparison of the Photochemical and Photophysical Properties of Clays, Pillared Clays, and Zeolites. *J. Am. Chem. Soc.* **108**, 6972-6977, 1986.

115. Urabe, K., Sakurai, H., Izumi, Y. Pillared Synthetic Saponite as an Efficient Alkylation Catalyst. *J. Chem. Soc. Chem. Commun.*, 1074-1076, 1986.

116. Yamanaka, S., Brindley, G.W. Hydroxy-Nickel Interlayering in Montmorillonite by Titration Method. *Clays Clay Miner.*, **26**, 21-24, 1978.

117. Barrer, R.M., Macleod, D.M. Activation of Montmorillonite by Ion Exchange and Sorption Complexes of Tetra-alkylammonium Montmorillonite. *Trans. Faraday Soc.*, **51**, 1290-1300, 1955.

118. Shabtai., J., Frydman, N., Lazar, R. Synthesis and Catalytic Properties of a 1,4-Diazabicyclo[2.2.2]octane-Montmorillonite System-a Novel Type of Molecular Sieve. *Proc. 6Th Int. Congr. Catal.*, Chemical Society, London, **B5**, 1-7, 1976.

119. Pinnavaia, T.J. Intercalated Clay Catalysts. *Science*, **220**, 365-371, 1983.

120. Brindley, G.W., Semples, R.E. Preparation and Properties of some Hydroxy-Aluminum Beidelites. *Clay Miner.*, **12**, 229-236, 1977.

121. Yamanaka, S., Brindley, G.W. High Surface Area Solids Obtained by Reaction in Montmorillonite with Zirconyl Chloride. *Clays Clay Miner.*, **27**, 119-124, 1979.

122. Yamanaka, S., Nishihara, T., Hattori, M. Preparation and Properties of Titania Pillared Clays. *Mater. Chem. Phys.* **17**, 87-101, 1987.

123. Pinnavaia, T.J., Tzou, M., Landau, S.D. New Chromia Pillared Clay Catalysts. *J. Am. Chem. Soc.*, **107**, 4783-4685, 1985.

124. Bellaoui, A., Plee, D., Meriaudeau, P. Gallium Containing Pillared Interlayer Clays. Preparation, Characterization and Catalytic Properties. *Appl. Catal.*, **63**, L7-L10, 1990.

125. Gonzalez, F., Pesquera, C., Blanco, C., Benito, I., Mendioroz, S. Synthesis and Characterization of Al-Ga Pillared Clays with High thermal and Hydrothermal Stability. *Inor. Chem.* **31**, 727-731, 1992.

126. Occelli, M.L. Surface and Catalytic Properties of some Pillared Clays. *Proc. Int. Clay Conf., Denver*, 319-323, 1985.

127. Sterte, J., Shabtai, J. Cross-Linked Smectites. V. Synthesis and Properties of Hydroxy-Silicoaluminum Montmorillonite and Fluorohectorites. *Clays Clay Miner.*, **35**, 429-439, 1987.

128. Kikuchi, E., Matsuda, T. Shape Selective Acid Catalysis by Pillared Clays. *Catal. Today*, **2**, 297-307, 1988.

129. Malla, P.B., Komarneni, S. Properties and Characterization of Al_2O_3 and SiO_2-TiO_2 Pillared Saponite. *Clays Clay Miner.*, **41**, 472-483, 1993.

130. Takahana, K., Yokoyama, M., Hirao, S., Yamanaka, S., Hattori., M. Supercritical Drying of SiO_2-TiO_2 Sol-Pillared Clays. *J. Mat. Sci.*, **27**, 1297-1301, 1992.

131. Ohtsuka, K., Hayashi., Y., Suda., M. Microporous ZrO_2-Pillared Clays Derived from three kinds of Zr Polynuclear Ionic Species. *Chem. Mater.*, **5**, 1823-1829, 1993.

132. Kooli, F., Jones, W. Al and Zr Pillared Acid-Activated Saponite Clays: Characterization and Properties. *J. Mater. Chem.*, **8**, 2119-2124, 1998.

133. Bovey, J., Jones, W. Characterisation of Al-Pillared Acid Activated Clay Catalysts. *J. Mater. Chem.*, **5**, 2027-2035, 1995.

134. Mokaya, R., Jones, W. Pillared Acid-Activated Clay Catalysts. *J. Chem. Soc. Chem. Commun.*, **8**, 929-930, 1994.

135. Mokaya, R., Jones, W., Davies, M.E., Whittle, M.E. Preparation of Alumina-Pillared Acid-Activated Clays and their Use as Chlorophyll Adsorbents. *J. Mater. Chem.*, **3**, 381-387, 1993.

136. Sheng, G., Xu, S., Boyd, S.A. Surface Heterogeneity of Trimethylphenylammonium-Smectite as Revealed by Adsorption of Aromatic Hydrocarbons from Water. *Clays Clay Miner.*, **45**, 659-669, 1997.

137. Sheng, G., Xu, S., Boyd, S.A. Cosorption of Organic Contaminants from Water by Hexadecyltrimethylammonium-Exchanged Clays. *Wat. Res.*, **30**, 1483-1489, 1996.

138. Jaynes, W,F., Boyd, S.A. Clay Mineral Type and Organic Compound Sorption by Hexadecyltrimethylammonium Exchanged Clays. *Soil Sci. Soc. Am. J.*, **55**, 43-48, 1991.

139. Jaynes, W.F., Boyd, S.A. Hydrophobicity of Siloxanes Surfaces in Smectites as Revealed by Aromatic Hydrocarbon Adsorption from Water. *Clays Clay Miner.*, **39**, 428-436, 1991.

140. Socías-Viciana, M.M., Hermosin, M.C., Cornejo, J. Removing Prometrone from Water by Clays and Organo Clays. *Chemosphere*, **37**, 289-300, 1998.

141. Stul, M.S., Uytterhoeven, J.B., Bock, J.D. The Adsorption of n-Aliphatic Alcohols from Dilute Aqueous Solutions on RNH_3-Montmorillonites. II. Interlamellar Association of the Adsorbate. *Clays Clay Miner.*, **27**, 377-386, 1979.

142. Boyd, S.A., Jaynes, W.F. Role of the Layer Charge in Organic Contaminant Sorption by Organo-Clays, 48-77 in: Layer Charge Characteristics of 2:2 Silicate Clay Minerals, (Mermut, A.R. ed.) Clay Mineral Society Workshop, Lecture 6, Boulder, CO, USA, 1994.

143. Lagaly, G., Weiss, A. Determination of the Layer Charge in Mica-Type Later Silicates, 61-80 in: *Proc. Int. Clay Conf., Tokyo*. (Heller, L., ed.) Israel Univ. Press, **1**, 1969.

144. Lagaly, G. Layer Charge Heterogeneity in Vermiculites. *Clays Clay Miner.*, **30**, 215-222, 1982.

145. Cowan, C.T., White, D. The Mechanism of Exchange Reactions Occurring between Sodium Montmorillonite and Various n-Primary Aliphatic Amines Salts. *Trans. Faraday Soc.*, **54**, 691-697, 1958.

146. Theng, B.K.G. Greenland, D.J., Quirk, J.P. Adsorption of Alkylammonium Cations by Montmorillonite. *Clay Miner.*, **7**, 1-17, 1967.

147. Vansant, E.F., Peeters, G. The Exchange of Alkylammonium Ions on Na-Laponite. *Clays Clay Miner.*, **26**, 279-284, 1978.

148. Serratosa, J.M. *Clays Clay Miner.*, **14**, 385-391, 1966.

149. Mortland, M.M. Clay-Organic Complexes and Interactions. *Adv. Agron.*, **22**, 75-117, 1970.

150. Jones, T.R. The Properties and Uses of Clays which Swell in Organic Solvents. *Clay Miner.*, **18**, 399-410, 1983.

151. Mortland, M.M., Barake, N. Interaction of ethylamine and Metal Ions on Montmorillonites. *Trans. 8Th Int. Congr. Soil Sci.*, Bucharest, Publising House, Acad. Soc. Rep. Romania, **3**, 433-443, 1964.

152. McNeal, B.L. Effect of Exchangeable Cations on Glycol Retention by Clay Minerals. *Soil Sci.*, **97**, 96-102, 1964.

153. Bissada, K.K, Johns, W.D., Cheng, F.S. Cation-Dipole Interactions in Clay Organic Complexes. *Clay Miner.*, 7, 155-166, 1967.

154. Dowdy, R.H., Mortland, M.M. Alcohol-Water Interactions on Montmorillonite Surfaces: II. Ethylene Glycol. *Soil Sci.*, **105**, 36-43, 1968.

155. Keay, J., Wild, A. Hydration Properties of Vermiculite. *Clay Miner. Bull.*, **4**, 221-228, 1961.

156. Kijne, J.W. Interaction of Water Molecules and Montmorillonite Surfaces. *Soil Sci. Soc. Am. Proc.*, **33**, 539-543, 1969.

157. Parfitt, R.L., Mortland, M.M. Ketone Adsorption on Montmorillonite. *Soil Sci. Soc. Am. Proc.*, **32**, 355-363, 1968.

158. Mortland, M.M. *J. Agr. Food Chem.*, **16**, 706-707, 1968.

159. Pashley, R.M., McGuiggan, P.M., Ninham, B.W. Attractive Forces between Uncharged Hydrophobic Surfaces: Direct Measurements in Aqueous Solution. *Science*, **229**, 1088-1089, 1985.

160. McBride, M.B., Pinnavaia, T.J., Mortland, M.M. Adsorption of Aromatic Molecules by Clays in Aqueous Suspensions: in Fate of Pollutants in the Air and Water Environments. Part I. (Suffet, I.H. ed.) Wiley, New York, 145-154, 1977.

161. Cowan, C.T., White, D. Adsorption by Organo-Clay Complexes. *Clays Clay Miner.*, **9**, 459-467, 1962.

162. Slabaugh, W.H., Carter, L.S. The Hydrophilic-Hydrophobic Character of Organomontmorillonites. *J. Coll. Inter. Sci.*, **27**, 235-238, 1968.

163. Mortland, M.M., Shaobai, S., Boyd, S.A. Clay-Organic Complexes as Adsorbents for Phenol and Chlorophenols. *Clays Clay Miner.*, **34**, 581-585, 1986.

164. Jaynes, W.F., Boyd, S.A. Trimethylphenylammonium-Smectite as an Efficient Adsorbent of Water Soluble Aromatic Hydrocarbons. *J. Air Waste Mgnt. Assoc.*, **40**, 1649-1653, 1990.

165. Rhodes, C.N., Brown, D.R. Catalytic Activity of Acid-Treated Montmorillonite in Polar and Non-Polar Reaction Media. *Catal. Lett.*, **24**, 285-291, 1994.

166. Corma, A., Mifsud, A., Sanz, E. Influence of the Chemical Composition and Textural Characteristics of Palygorskite on the Acid Leaching of Octahedral Cations. *Clay Miner.*, **22**, 225-232, 1987.

167. De Stefanis, A., Perez, G., Ursini, O., Tomlinson, A.A.G. PLS versus Zeolites as Sorbents and Catalysts II. Terpene Conversions in Alumina-Pillared Clays and Phosphates and Medium Pore Zeolites. *Appl. Catal.*, **132**, 353-365, 1995.

168. Mortland, M.M., Berkheiser, V. Triethylene Diamine-Clay Complexes as Matrices for Adsorption and Catalytic Reactions. *Clays Clay Miner.*, **24**, 60-63, 1976

169. Dupont, G., Dulou, R. Study of the Catalytic Properties of Clays. *J. Am. Ceram. Soc.*, **31**, 143, 1948.

170. Banthorpe, D.V., Whittaker., D. Rearrangements of Pinane Derivatives. *Quart. Rev.*, **20**, 373-387, 1966.

171. Severino, A., Vital, J., Lobo, L.S. Isomerization of α-Pinene over TiO_2: Kinetics and Catalyst Optimization. *Heterogeneous Catalysis and Fine Chemicals* III, **78**, 685-692, 1993.

172. Rudakov, G.A. Chemistry and Technology of Camphor. Moscow, 208, 1976.

173. Albert, R.M., Traynor, S.G., Webb, R.L. Fragance and Flavor Chemicals, in Naval Store-Production, Chemistry, Utilization. (Zinkel, D.F., Russell, J., eds.) PULP Chemical Association, New York, 479, 1989.

174. Allahverdiev, A.I., Gündüz, G., Murzin, D.Y. Kinetics of α-Pinene Isomerization. *Ind. Eng. Chem. Res.*, **37**, 2373-2377, 1998.

175. Krishnasamy, V., Mathur, P., Chandrasekharan, K. Catalysed Transformation of α-Pinene over Platinum-Alumina. *J. Chem. Tech. Biotechnol.*, **32**, 454-461, 1982.

176. Williams, C.M., Whittaker, D. Rearrangements of Pinane Derivatives. Part I. Products of Acid Catalysed Hydration of α-Pinene and β-Pinene. *J. Chem. Soc.*, 668-672, 1971.

177. Adams, J.M., Ballantine, J.A., Graham, S.H., Laub, R.J., Purnell, J.H., Reid, P.I., Shaman, W.Y.M., Thomas, J.M. Selective Chemical Conversion Using Sheet Silicate Intercalates: Low-Temperature Addition of Water to 1-Alkenes. *J. Catal.*, **58**, 238-252, 1979.

178. Adams, J.M., Clapp, T.V., Clement, D.E., Reid, P.I. Reactions of Alk-1-enes over Ion-Exchanged Montmorillonites. *J. Mol. Catal.*, **27**, 179-194, 1984.

179. Thomas, J.M. Sheet Silicates Intercalates. New Agents for Unusual Chemical Conversions. 56-99 in: Intercalation Chemistry. (Whittingham, M.S., Jacobson, A.J., eds.) Academic Press, New York, 1982.

180. Bylina, A., Adams, J.M., Graham, S.H., Thomas, J.M. Chemical Conversion Using Sheet Silicates: A Simple Method for Producing Methyl t-Buthyl Ether. *J. Chem. Soc. Chem. Commun.*, 1003-1004, 1980.

181. Adams, J.M., Clement, D.E., Graham, S.H. Synthesis of Methyl-t-Buthyl Ether from Methanol and Isobutene Using Clay Catalyst. *Clays Clay Miner.*, **30**, 129-134, 1982.

182. Vogel, A.P., O'Connor, C.T., Kojima, M. Thermogravimetric Analysis of the Iso-Butene Oligomerization Activity of Various Forms of Synthetic Mica-Montmorillonite. *Clay Miner.*, **25**, 355-362, 1990.

183. Choren, E., Moronta, A., Varela, G., Arteaga, A., Sánchez, J. Condensation of Olefins on Clays. Gas-Solid Systems. Part I. Gravimetric Methods. *Clays Clay Miner.*, **45**, 213-220, 1997.

184. Choren, E., Moronta, A., Arteaga, A., Sánchez, J. Condensation of Olefins on Clays. Gas-Solid Systems. Part II. Spectroscopic Methods. *Clays Clay Miner.*, **45**, 221-225, 1997.

185. Stepanov, A., Luzgin, M.V., Romannikov, V.N., Sidelnikov, V.N., Paukshtis, E.A. The Nature, Structure, and Composition of Adsorbed Hydrocarbon Products of Ambient Temperature Oligomerization of Ethylene on Acid Zeolite H-ZSM-5. *J. Catal.*, **178**, 466-477, 1998.

186. Ballantine, J.A., Davies, M., Patel, I., Purnell, J.H., Rayanakorn, M., Williams, K.J., Thomas, J.M. Organic Reactions Catalysed by Sheet Silicates: Ether Formation by the Intermolecular Dehydration of Alcohols and by Adding Alcohols to Alkenes. *J. Mol. Catal.*, **26**, 37-56, 1987.

187. Breen, C., Flynn, J.J., Parkes, M.B. Thermogravimetric, Infrared and Mass-Spectroscopic Analysis of the Desorption of Methanol, Propan-1-ol and 2-Methylpropan-2-ol from Montmorillonite. *Clay Miner.*, **28**, 123-137, 1993.

188. Taber, R.L., Champion, W.C. Dehydration of 2-Methylcyclohexanol. *J. Chem. Edu.*, **44**, 620, 1967.

189. Jaynes, W.F., Bigham, J.M. Charge Reduction, Octahedral Charge, and Lithium Retention in Heated, Li-Saturated Smectites. *Clays Clay Miner.*, **35**, 440-448, 1987.

190. Brown, G., Edwards, B., Ormerod, E.C., Weir, A.H. A Simple Diffractometer Heating Stage. *Clay Miner.*, **9**, 407-414, 1972.

191. Dodd, J.W., Tonge, K.H. Thermal Methods. (Currell, B.R., ed.) John Wiley & Sons, London, 44, 1987.

192. Breen, C., Last, P.M. Catalytic Transformation of the Gases Evolved During the Thermal Decomposition of HDPE Using Acid-Activated and Pillared Clays. *J. Mater. Chem.*, **9**, 813-818, 1999.

193. Finar, I.L. Organic Chemistry. Vol II Stereochemistry and the Chemistry of Natural Products. Longmans, London, 288, 1964.

194. Watson, R. Organoclays: Preparation, Characterisation and Use as Sorbents and Catalysts. *PhD Thesis*. Sheffield Hallam University, 1997.

195. Little, L.R. Infrared Spectra of Adsorbed Species. Academic Press, London, 1966.

196. Maes, A., Cremers, A. Charge Density Effects in Ion Exchange. Part I. Heterovalent Exchange Equilibria. *J. Chem. Soc. Faraday Trans.*, **73**, 1807-1814, 1977.

197. Vansant, E.F., Uytterhoeven, J.B. The Adsorption of Aromatic, Heterocyclic and Cyclic Ammonium Cations by Montmorillonite. *Clay Miner.*, **10**, 61-69, 1973.

198. Kinter, E.B., Diamond, S. Characterization of Montmorillonite Saturated with Short-Chain Amine Cations: 2. Interlayer Surface Coverage by the Amine Cations. *Clays Clay Miner.*, **12**, 174-190, 1963.

199. Stevens, J.J., Anderson, S.J. An FTIR Study of Water Sorption on TMA- and TMPA-Montmorillonite. *Clays Clay Miner.*, **44**, 142-150, 1996.

200. Shuali, U., Steinberg, M., Yariv, S., Muller-Vonmoos, M., Kahr, G., Rub, A. Thermal Analysis of Sepiolite and Palygorskite Treated with Butylamine. *Clay Miner.*, **25**, 107-119, 1990.

201. Yariv, S., Heller, L. Sorption of Cyclohexylamine by Montmorillonites. *Israel J. Chem.*, **8**, 935-945, 1970.

202. Silverstein, R.M., Bassler, G.C. Spectrometric Identification of Organic Compounds. John Wiley & Son, London, 1967.

203. Dreoni, D.P., Pinelli, D., Trifiro, F., Busca, G., Lorenzelli, V. J. FT-IR and Flow Reactor Studies on Heterogeneously Catalized Gas-Phase Ammoximation of Cyclohexanone. *J. Mol. Catal.*, **71**, 111-127, 1992.

204. Keattch, C.J. Analysis of Carbonaceous Materials. Society of Chemical Industry Monograph. Society of Chemical Industry, London, **18**, 279, 1964.

205. Beltramé, P., Bunton, C.A., Dunlop, A., Whittaker, D. Solvolysis of some Trimethylnorbornyl Chlorides. *J. Chem. Soc.*, I, 658-667, 1964.

206. Mercier, L., Detellier, C. Intercalation of Tetraalkylammonium Cations into Smectites and its Application to Internal Surface Area Measurements. *Clays Clay Miner.*, **42**, 71-76, 1994.

207. Feldkamp, J.R., Stauffer, T.B. Interactions of Binary Solvents with Charge Expandable Clays. 1. Theory. *J. Phys. Chem.*, **98**, 13594-13600, 1994.

208. Feldkamp, J.R., Stauffer, T.B. Interactions of Binary Solvents with Charge Expandable Clays. 2. Experiment. *J. Phys. Chem.*, **98**, 13601-13606, 1994.

209. Komadel, P., Janek, M., Medejová, J., Weekes, A., Breen, C. Acidity and Catalytic Activity of Mildly Acid-Treated Mg-rich Montmorillonite and Hectorite. *J. Chem. Soc. Faraday Trans.*, **93**, 4207-4210, 1997.

210. Yu, J.Q., Zhou, P., Xiao, S.D. Highly Selective Hydration Reaction of α-Pinene over H-Mordenites Prepared with Quaternary Ammonium-Salts. *Chin. J. Chem.*, **13**, 280-283, 1995.

211. Cruz-Costa, M.C., Johnstone, R.A.W., Whittaker, D. Catalysis of Gas and Liquid Phase Ionic and Radical Rearrangements of α- and β-Pinene by Metal (IV) Phosphate Polymers. *J. Mol. Catal.*, **104**, 251-259, 1996.

212. Carrado, K.A. Preparation of Hectorite Clays Utilizing Organic and Organometallic Complexes during Hydrothermal Crystallization. *Ind. Eng. Chem. Res.*, **31**, 1654-1659, 1992.

213. Jones, J.R., Purnell, J.H. The Catalytic Dehydration of Pentan-1-ol by Alumina Pillared Texas Montmorillonite of Differing Pillar Density. *Catal. Lett.*, **28**, 283-289, 1994.

214. Yariv, S., Heller, L., Sofer, Z. Sorption of Aniline by Montmorillonite. *Israel J. Chem.*, **6**, 741-756, 1968.

215. Kullaj, S. Effect of the Characteristics of Activated Clays on their Ability to Lead to Isomerisation of α-Pinene into Camphene and Tricyclene. *Bull, Shkencave Nat.*, **43**, 81-85, 1989. Chem. Abstr. 1990, 112,21154z.

216. Clementz, D.M., Mortland, M.M. Properties of Reduced Charge Montmorillonite: Tetra-Alkylammonium Ion Exchange Forms. *Clays Clay Miner.*, **22**, 223-229, 1974.

217. Williams, J., Purnell, J.H., Ballantine, J.A. The Mechanism of Layer Charge Reduction and Regeneration in Li^+-Exchanged Montmorillonite. *Catal. Lett.*, **9**, 115-120, 1991.

218. Barrer, R.M., Brummer, K. Relations between Partial Ion Exchange and Interlamellar Sorption in Alkylammonium Montmorillonites. *Trans. Faraday Soc.*, **59**, 959-968, 1963.

219. Vahedi-Faridi, A., Guggenheim, S. Crystal Structure of Tetramethylammonium-Exchanged Vermiculite. *Clays Clay Miner.*, **45**, 859-866, 1997.

220. Barrer, R.M., Millington, A.D. Sorption and Intracrystalline Porosity in Organo-Clays. *J. Coll. Interf. Sci.*, **25**, 359-372, 1967.

221. Weiss, A. Mica-Type Layer Silicates with Alkylammonium Ions. *Clays Clay Miner.*, **10**, 191-224, 1963.

222. Slade, P.G., Schultz, P.K., Tiekink, E.R. Structure of a 1,4-Diazabicyclo[2,2,2]octane-Vermiculite Intercalate. *Clays Clay Miner.*, **37**, 81-88, 1989.

223. Breen, C., Watson, R. Polycation-Exchanged Clays as Sorbents for Organic Pollutants: Influence of Layer Charge on Pollutant Sorption Capacity. *J. Colloid Interf. Sci.*, **208**, 422-429, 1998.

224. Farmer, V.C., Mortland M.M. An Infrarde Study of the Co-ordination of Pyridine and Water to Exchangeable Cations in Montmorillonite and Saponite. *J. Chem. Soc.*, A, 344-351, 1966.

225. Farmer, V.C., Mortland, M.M. An Infrared Study of Complexes of Ethylamine with Ethylammonium and Copper Ions in Montmorillonites. *J. Phys. Chem.*, **69**, 683-686, 1965.

226. Purnell, J.H., Lu, Y. Ionic Migration and Charge Reduction in Ni^{2+}-Exchanged, Co^{2+}-Exchanged and Zn^{2+}-Exchanged Texas Montmorillonite. *Catal. Lett.*, **18**, 235-241, 1993.

227. Cseri, T., Békássy, S., Figueras, F., Rizner, S. Benzylation of Aromatics on Ion-Exchanged Clays. *J. Mol. Catal.*, **98**, 101-107, 1995.

228. Ghosh, A.K., Keats, N.G., Curthoys, G. Temperature Programmed Desorption of Ammonia and n-Buthylamine on Mordenites. *J. Catal.*, **96**, 288-291, 1985.

229. Ghosh, A.K., Curthoys, G. Characterization of Zeolite Activity. A Thermal Study of n-Butylamine and Ammonia Adsorbed on Mordenites. *J. Phys. Chem.*, **88**, 1130-1132, 1984.

230. Jacobs, P.A., Uytterhoeven, J.B. Quantitative Infrared Spectroscopy of Amines in Synthetic Zeolites X and Y. I. Alkylammonium Y Zeolites as Precursor of Acid Hydroxyls in Deaminated Zeolites Y. *J. Catal.*, **26**, 175-190, 1972.

231. Guil, J.M., Herrero, J.E., Pamege Ruiz, A. Thermal Desorption of n-Buthylamine from Silica-Alumina Surface. *J. Coll. Interf. Sci.*, **102**, 111-120, 1984.

232. Takahashi, M., Iwasawa, Y., Ogasawara, S. The Nature of Adsorbed Sites on Catalysts II. Behavior of Basic Compounds on Silica-Alumina Catalyst at Elevated Temperatures. *J. Catal.*, **45**, 15-24, 1976.

233. O'Connor, C.T., Jacobs, L.L., Kojima, M. Propene Oligomerization over Synthetic Mica-Montmorillonite (SMM) and SMM Incorporating Nickel, Zinc and Cobalt. *Appl. Catal.*, **40**, 277-290, 1988.

234. Fletcher, J.C.Q., Kojima, M., O'Connor, C.T. Acidity and Catalytic Activity of Synthetic Mica-Montmorillonite Part II. Propene Oligomerization. *Appl. Catal.*, **28**, 181-191, 1986.

235. Schwarz, S., Kojima, M., O'Connor, C.T. Effect of Silicon-to-Aluminium Ratio and Synthesis Time on High-Pressure Olefin Oligomerization over ZSM-5. *Appl. Catal.*, **56**, 263-280, 1989.

236. Trombetta, M., Busca, G., Rossini, S.A, Piccoli, V., Cornaro, U. FTIR Studies on Light Olefin Skeletal Isomerisation Catalysis I. The Interaction of C_4 Olefins and Alcohols with Pure γ-Alumina. *J. Catal.*, **168**, 334-348, 1997.

237. Laird, D.A., Scott, A.D., Fenton, T.E. Evaluation of the Alkylammonium Method of Determining Layer Charge. *Clays Clay Miner.*, **37**, 41-46, 1989.

238. Lagaly, G. Layer Charge Determination by Alkylammonium Ions. 1-46 in: Layer Charge Characteristics of 2:1 Silicate Clay Minerals. (Mermut, A.R., ed.) Clay Minerals Society Workshop Lectures 6, Boulder, CO, USA, 1994.

239. Malla, P.B., Lowell, A.D. Layer Charge Properties of Smectites and Vermiculites: Tetrahedral vs. Octahedral. *Soil Sci. Soc. Am. J.*, **51**, 1362-1366, 1987.

240. Maes, A., Stul, M.S., Cremers, A. Layer Charge – Cation-Exchange Capacity Relationship in Montmorillonite. *Clays Clay Miner.*, **27**, 387-392, 1979.

241. Janek, M., Komadel, P., Lagaly, G. Effect of Autotransformation on the Layer Charge of Smectites Determined by the Alkylammonium Method. *Clay Miner.*, **32**, 623-632, 1997.

242. Theng, B.K.G., Greenland, D.J., Quirk, J.P. The Effect of Exchangeable Alkylammonium Ions on the Swelling of Montmorillonite in Water. *Clay Miner.*, **7**, 271-393, 1968.

243. Maes, A., Marynen, P., Cremers, A. The Ion-Exchange Adsorption of Alkylammonium Ion: An Alternative View. *Clays Clay Miner.*, **25**, 309-310, 1977.

Influence of Layer Charge on the Catalytic Activity of Mildly Acid-Activated Tetramethylammonium-Exchanged Bentonites

C. Breen and A. Moronta

Materials Research Institute, Sheffield Hallam University, Sheffield S1 1WB, U.K.

The Journal of
Physical Chemistry B®

Reprinted from
Volume 103, Number 27, Pages 5675–5680

Influence of Layer Charge on the Catalytic Activity of Mildly Acid-Activated Tetramethylammonium-Exchanged Bentonites

C. Breen* and A. Moronta†

Materials Research Institute, Sheffield Hallam University, Sheffield S1 1WB, U.K.

Received: January 12, 1999

SWy-2 (Wyoming), STx-1 (Texas), and SAz-1 (Cheto, Arizona) montmorillonite and Sap-Ca saponite (California) were treated with different amounts of 12 M HCl and 1 M tetramethylammonium (TMA^+) chloride solution at room temperature. The catalytic activity of these hybrid acid-activated organoclays (AAOCs) was directly measured using the isomerization of α-pinene at 120 °C for 1 h to yield camphene, limonene, and other minor products and compared to clays acid-treated in the absence of TMA^+ cations. The total conversion for the isomerization of α-pinene was excellent for AAOCs formed from SWy-2 (88%) and STx-1 (73%), moderate for Sap-Ca (50%), and low for SAz-1 (20%). Samples treated with TMA^+ alone did not exhibit any marked catalytic activity. Acid-treated Sap-Ca and STx-1, which contained no TMA^+ cations were also effective catalysts for the isomerization process. TMA^+ cations were unexpectedly resistant to exchange by protons.

Introduction

Acid-activated clays have been used as solid catalysts for many years and their activity has been demonstrated in a wide variety of reactions. These minerals are highly versatile, affording both industrial (petroleum, etc.) and laboratory catalysts with excellent activity.[1,2] Acid-treated clays are used commercially for decolorizing oils and the effect of acid attack on properties such as surface area and decolorizing ability have been widely studied.[3,4] Another commercial usage of acid-treated clays is in color formation with leuco dyes in pressure sensitive recording paper.[5,6]

Treatment of clays with cold, dilute acid has little effect on the elemental composition of the host layer and results in an essentially proton-exchanged clay, whereas activation with hot concentrated acid results in the removal of ions associated with the octahedral sheet and may not produce an exclusively proton-exchanged clay.[7] Recent results obtained after acid-leaching five clays of differing elemental composition have shown that the type of clay used had little influence on the catalytic activity, which was determined mainly by the extent of octahedral sheet depletion and proton content.[8] However, it is imperative that the activation conditions are optimized for a given clay.

It is now accepted that the acid attack on the clay structure progresses inward from both the edge and the basal surface of the clay platelets, leaching cations, particularly Mg if present, from the octahedral sheet. Acid activation causes little damage to the silicate layer, and consequently, the structure in the center of the platelet, at the limit of acid attack, remains intact.[4,6,8] The rate of dissolution of the octahedral sheet is a first-order process[9,10] that increases not only with increasing concentration of acid, temperature, and contact time but also with increasing Mg content in the octahedral sheet.[3,4,8]

It is long established that the hydrophilic nature of swelling clays can be rendered hydrophobic by exchanging the naturally occurring inorganic cations (Ca^{2+}, Na^+, K^+) with organocations such as monoalkylammonium,[11] tetramethylammonium,[12] octadecyltrimethylammonium,[13] and phenyltrimethylammonium[14] to select a few from an extensive list. The interactions between alkylammonium-exchanged montmorillonites and organic compounds have shown that modified montmorillonites are effective adsorbents for the improvement of water quality. When a clay mineral has metal cations occupying cation-exchange sites, its surface is hydrophilic because of the water molecules solvating the cations and is thus not suited to the removal of poorly soluble organic molecules from water.[15] However, clays with organic cations (possessing long-chain alkyl groups) on the surface impart a hydrophobic quality to the mineral surface[16] and are able to sorb hydrophobic molecules.[17,18]

In a recent study it was established that mild acid activation of an organoclay could increase the activity of simple acid-treated clays for reactions involving nonpolar reactants.[19] In particular, tetramethylammonium (TMA^+)-exchanged clays treated at room temperature with only 0.1 M HCl proved to be effective catalysts for the conversion of α-pinene to camphene and limonene. Total conversions of 60−80% were obtained, making them effective competitors for zeolites and pillared clays for this isomerization.[20] Moderate success was also achieved using polycation exchanged bentonites but similar conversions required activation in hot 6 M HCl.[21] Both these preliminary studies indicated that (i) acid-activated organoclays (AAOCs) were more effective when the galleries were not congested with large organocations (hence AAOCs derived from TMA^+-exchanged clays were found to be the most effective), (ii) the activity was influenced by the nature of the starting clay, and (iii) preadsorbed TMA^+ cations appeared unexpectedly resistant to subsequent displacement by protons.

The current investigation was designed to further elucidate the factors that influence the activity of AAOCs toward the isomerization of α-pinene. Four source clays of differing elemental composition, charge density, and locus of isomorphous substitution were selected: SWy-2 (dioctahedral, aluminum rich bentonite), STx-1 (dioctahedral, bentonite of low iron content), SAz-1 (dioctahedral, magnesium rich bentonite), and

* Corresponding author. Phone: +44-114-225-3008. Fax: +44-114-225-3501. E-mail: CBREEN@SHU.AC.UK.

† On leave from Centro de Superficies y Catálisis, Facultad de Ingeniería, Universidad del Zulia, Maracaibo 4003A, Venezuela.

10.1021/jp9901646 CCC: $18.00
Published on Web 06/19/1999

Sap-Ca (trioctahedral, magnesium rich saponite). SAz-1 has a higher charge density than SWy-2 and STx-1 even though isomorphous substitution occurs mainly in the octahedral sheet of all three. In contrast, isomorphous substitution in Sap-Ca occurs in the tetrahedral sheet. Moroever, because of its high octahedral magnesium content, Sap-Ca will be extensively leached under the mild acid-activation conditions used herein and will thus provide an interesting comparison with the activity of mildly acid-activated clays, which will lose little of their octahedral population. In addition, the ability of TMA^+ cations to compete with protons for exchange sites has been assessed by consistently offering a fixed quantity of organocation in the presence of increasing quantities of acid. The properties and activities of the H^+/TMA^+ clays were compared with catalysts prepared without TMA^+.

Experimental Section

Materials. Three montmorillonites and one saponite were used in this study. The dominant material in these fractions were: Na−montmorillonite (SWy-2) (Wyoming), Ca−montmorillonite (STx-1) (Texas), Ca−montmorillonite (SAz-1) (Arizona), and Ca−saponite (Sap-Ca) (California). All samples were obtained from The Clay Mineral Repository of the Clay Minerals Society and used without further purification. The cation-exchange capacities (CEC) of SWy-2, STx-1, SAz-1, and Sap-Ca are: 0.80, 0.84, 1.20, and 0.92 mequiv (g clay)$^{-1}$. Thus SAz-1 has a significantly higher charge density than the other two montmorillonites.

Equipment and Methods. A 1 g amount of SWy-2, STx-1, SAz-1, or Sap-Ca H^+/TMA^+ clays was prepared by adding the raw clay to a solution containing sufficient 1 M tetramethylammonium chloride (Aldrich, 97%) to satisfy 1 CEC and selected volumes of 12 M hydrochloric acid (Fisons, 38%) to prepare solutions with an aqueous H^+ content from 1.2 to 120 mmol (from 1.2 to 120 times the CEC). This approach was used to evaluate the effect of different acid concentrations on the organoclays formed using a fixed initial concentration of TMA^+ and to survey the competitive sorption behavior between TMA^+ and H^+. H^+ clays were made in exactly the same way except that the TMACl was excluded. Other pretreatments are indicated herein. The mixture was kept at 25 °C for 18 h and centrifuged at 17 000 rpm for 20 min and the centrifugate washed with 30 cm^3 of deionized water. Clay samples were dried at 120 °C overnight and ground <0.2 mm prior to storage. The acid or organoacid treatment is identified in the sample name. Thus, SW-12H indicates that SWy-2 was treated with 12 mmol H^+ and SCa-TMA/120H means that Sap-Ca was treated with 1 CEC TMA^+ and 120 mmol H^+.

Sample Characterization. A Spectro (Analytical Instrument) model P, direct emission spectrometer was used to determine the amount of Al^{3+}, Ca^{2+}, Fe^{3+}, Mg^{2+}, and Na^+ in the supernatants from the various preparation procedures.

X-ray powder diffraction traces of the clays were recorded using a Philips PW 1130 diffractometer operating at 30 kV and 30 mA at a scan rate of 2° 2θ min^{-1} using Cu Kα radiation (λ = 1.5418 Å).

Thermogravimetic data were obtained on a Mettler TG50 thermobalance equipped with a TC10A processor. A 7−10 mg sample was weighed into a ceramic crucible and heated from 35 to 800 °C at 20 °C min^{-1} under a flow of 30 cm^3 min^{-1} dry nitrogen carrier gas. Samples for thermogravimetry were exposed to reagent grade cyclohexylamine for periods in excess of 48 h.

Catalytic Activity. To establish the best operational conditions, the α-pinene reaction was carried out under reflux at 80, 100, 120, and 140 °C for 2 h using SW-TMA/48H. A 1 cm^3 aliquot of the reaction mixture was taken every 15 min and analyzed. It was evident that increasing the reaction temperature caused a substantial increase in reactivity. At 80 and 100 °C the conversion after the first 15 min was quite low and then gradually increased to a maximum of 52% and 72% at 2 h, respectively. At 120 °C the activity changed drastically compared with that at 80 and 100 °C. A high percentage yield was initially noticed and reached a maximum of 82% after 60 min and then remained almost constant. At 140 °C the maximum yield was achieved in less than 15 min (90% conversion) and was invariant through the total reaction time. GC analysis confirmed that no isomerization products occurred as a result of preheating the α-pinene before addition of the acid-activated organoclays. On the basis of these preliminary results, 120 °C and 1 h were taken as optimal conditions to carry out the α-pinene reaction using the prepared catalysts. Clay (100 mg) was dried at 120 °C overnight to remove water, placed in a stoppered container, and left in a desiccator to cool without rehydrating. The catalyst was then added rapidly to the preheated (120 °C) 10 cm^3 (0.06 mol) of α-pinene (Aldrich 98%, used as received) and kept at 120 °C for 1 h. The amount of camphene, limonene, and other minor products was determined using capillary GC with FID detection. A packed column 6 ft × $^1/_8$ in. SS, containing 3% OV 225 chromosorb WHP mesh size 80/100, with nitrogen carrier gas, was used for all separations. The experimental conditions employed were 1 μL of sample, isothermal for 10 min at 70 °C, injector and detector temperature 150 °C, air and hydrogen pressure 20 psi, and nitrogen flow rate 10 cm^3 min^{-1}.

TABLE 1: Percent of Available Oxide Released from the Clay at 120 mmol of H^+[a]

	SWy-2	STx-1	SAz-1	Sap-Ca
% Na_2O	66.4 (1.70)	84.2 (0.38)	66.6 (0.07)	96.5 (1.37)
% CaO	91.0 (1.76)	83.5 (1.76)	94.6 (3.16)	98.4 (1.50)
% MgO	18.0 (2.77)	10.3 (3.56)	9.6 (7.24)	54.8 (28.2)
% Al_2O_3	1.5 (20.6)	2.2 (16.8)	3.4 (19.7)	43.9 (5.29)
% Fe_2O_3	8.5 (4.63)	5.1 (0.78)	2.5 (1.59)	42.9 (1.36)

[a] Figures in parentheses represent the actual weight percentage of the oxide in the clay structure.

Results and Discussion

Catalyst Characterization. The relationship between the amount of cation released (reported as percentage of metal oxide) using 120 mmol of H^+ and the total available metal oxide content, determined by XRF[22] is listed in Table 1. For example, 54.8% of the available MgO content (28.2 wt %MgO) of saponite was released, which means that there was still 12.8 wt % MgO remaining in the leached clay. It can be clearly seen that Sap-Ca was substantially affected by the acid treatment. The relatively high percentage of Mg^{2+} and Fe^{3+} released from SWy-2 is due to Mg^{2+} cations on exchange sites and dissolution of Fe-containing impurities.

The amount of metal cation displaced during acid treatment and/or TMA^+ exchange is shown in Figure 1. It is well-known that protons displace the resident exchange cations during mild acid treatment while increasing the severity of acid treatment progressively leaches the basic clay constituents—magnesium, iron, and aluminum—at similar rates.[23] Complete displacement of the exchangeable Na^+ and Ca^{2+} ions by H^+ (or TMA^+) was observed for all the clays, provided at least 1.2 CEC was used. ICP data also confirmed that a small portion of the total Mg^{2+} content was easily removed from SWy-2, STx-1, and SAz-1

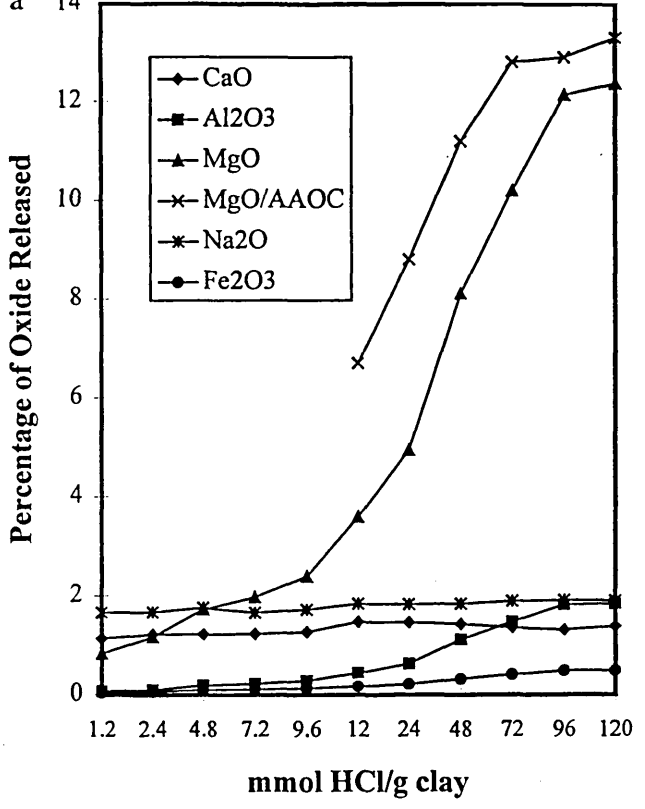

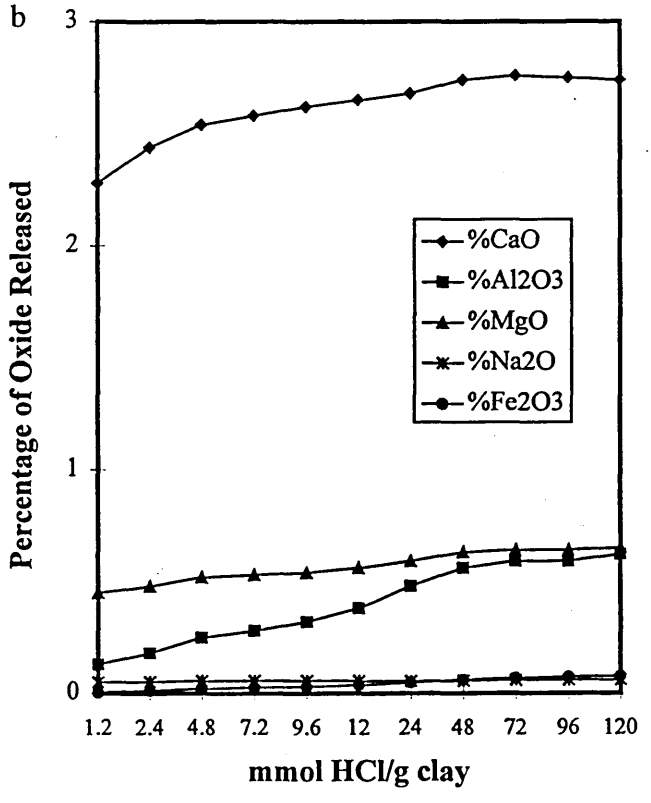

Figure 1. Percentage of oxide released during acid treatment of (a) Sap-Ca and (b) SAz-1: (*) Na_2O; (◆) CaO; (■) Al_2O_3; (●) Fe_2O_3; MgO in the absence (▲) and presence (×) of TMA^+.

samples, suggesting the presence of Mg^{2+} on exchange sites. However, for Sap-Ca, which contains much more octahedral Mg^{2+}, significant amounts of Mg^{2+} were released at $[H^+]$ > 10 mmol/g. A gradual increment in Al^{3+} was observed in the leachate from SWy-2, STx-1, and SAz-1 (not illustrated), although the total amount removed as a percentage of Al

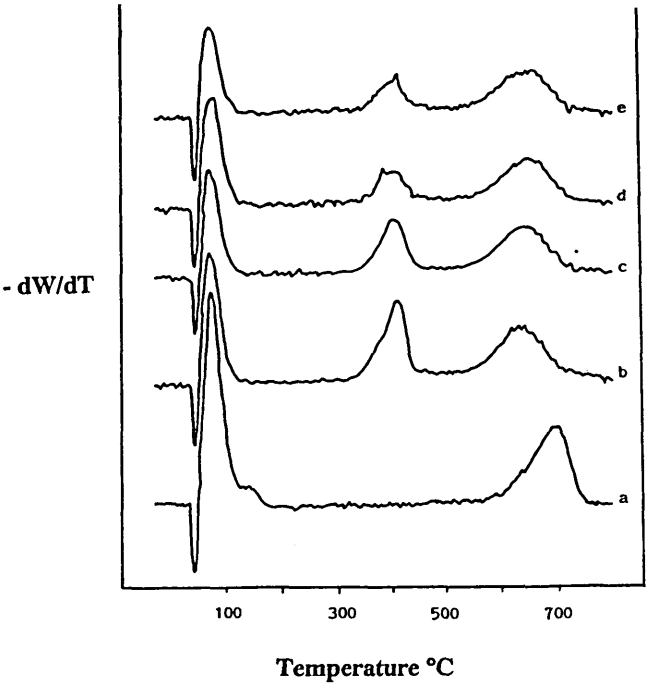

Figure 2. Derivative thermograms for (a) untreated SWy-2, (b) SW-TMA/12H, (c) SW-TMA/24H, (d) SW-TMA/96H, and (e) SW-TMA/120H.

available was small. The addition of TMA^+ to the initial mixture had no effect on the removal of cations from SWy-2, STx-1, and SAz-1 because this was simply an ion-exchange process. However, it did increase the amount of Mg^{2+} released from Sap-Ca (Figure 1a), perhaps because the TMA^+ cations propped the layers apart and facilitated the ingress of protons into the interlayer space where they could enter the layer through the ditrigonal cavity and displace Mg^{2+}. In our previous study,[19] we found that octahedral depopulation was retarded when the gallery is fully occupied by alkyltrimethyammonium cations. Thus, the nature of the organocation has an influential role to play in the preparation of AAOCs.

The diffraction traces (not shown) for H^+ clays exhibited sharp and intense 001 peaks together with several higher order reflections and contained evidence of small amounts of crystalline impurities. It was found that the 001 reflections were weaker and much broader in samples such as SW-TMA/72H and SW-TMA/120H, suggesting that the organoclay samples formed poorer films than the parent clay materials. XRD traces for Sap-Ca samples treated with more than 24 mmol of H^+ contained an amorphous hump[24] centered on 22° 2θ, which is characteristic of extensively acid-leached clays, in addition to the peaks for Sap-Ca.

The derivative thermogram for a fully TMA^+-exchanged clay (Figure 2) exhibited three maxima near 90, 420, and 620 °C. The peak at 90 °C is attributed to loss of sorbed water and that near 620 °C is associated with dehydroxylation of the stucture.[25] The maximum near 420 °C corresponds to the desorption and/or breakdown of the TMA^+ cations to produce mainly H_2O and CO_2.[26] These results confirm that TMA^+ was present in the clay structure and that the complexes were thermally stable up to 280 °C. The reduction in the 420 °C maximum with increasing $[H^+]$ confirms that H^+ was able to compete with TMA^+ when the $[H^+]$ level was high. The amount of TMA^+ present in the H^+/TMA^+ samples was determined using TGA and followed the order SAz-1 > SWy-2 = STx-1 > Sap-Ca in all cases. Moreover, the amount of TMA^+ in SAz-1, SWy-2,

the Samples after Activation

	SW-TMA	ST-TMA	SA-TMA	SCa-TMA
0 mmol of H^+	44	47	37	25
1.2 mmol of H^+	60	42	52	34
12 mmol of H^+	42	37	45	26
24 mmol of H^+	32	37	45	22
48 mmol of H^+	30	26	40	22
72 mmol of H^+	26	24	38	21
96 mmol of H^+	24	24	36	17
120 mmol of H^+	24	24	35	16

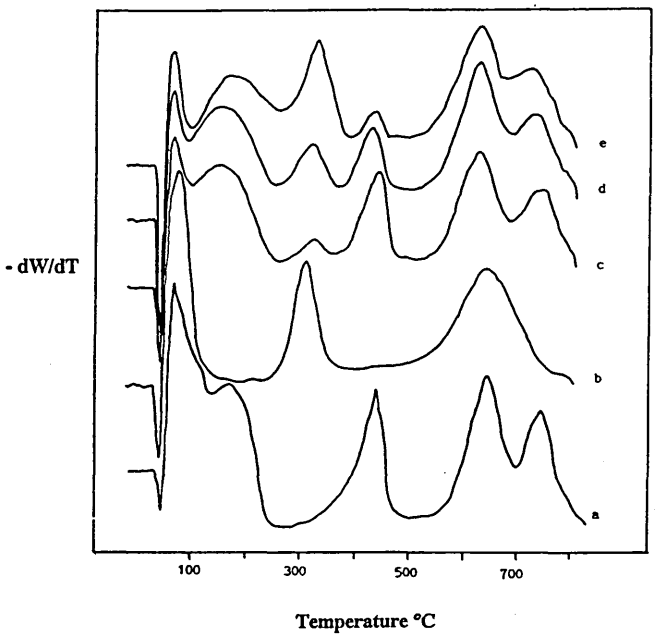

Figure 3. Desorption thermograms of cyclohexylamine on (a) SW-TMA, (b) SW-12H, (c) SW-TMA/12H, (d) SW-TMA/48H, and (e) SW-TMA/120H.

and STx-1 was high even when in competition with substantially higher amounts of acid. The TMA^+ content (as % CEC) remaining in the clays after activation (Table 2) reinforces its remarkable resistance to displacement by protons. A considerable amount of TMA^+ was present in SWy-2, STx-1, and SAz-1 even when only 1 mmol of TMA^+ was competing with 120 mmol of H^+. Indeed, the amount of TMA^+ on the exchange sites was increased by small quantities of acid. ICP-AES analysis of the supernatants confirmed that TMA^+ was effective at displacing Na^+ cations but less able to displace Ca^{2+} and Mg^{2+}. However, it appears that TMA^+ was able to displace some of the protons that had already replaced Ca^{2+} and Mg^{2+} ions. Much less TMA^+ was retained in the Sap-Ca samples because the number of cations on exchange sites decreased as the layer was leached. It is known that the CEC decreases as the isomorphous substitution sites are dissolved away, thus the number of TMA^+ cations will reduce as Sap-Ca is extensively leached.

To confirm the presence of protons in the H^+/TMA^+ samples, a selection of samples was exposed to cyclohexylamine vapor (Figure 3). Figure 3a shows that the derivative thermogram for the desorption of cyclohexylamine from SW-TMA exhibited three desorption maxima (prior to the dehydroxylation peak at 620 °C), at 60, 140, and 400 °C, which correspond to the loss of physisorbed water and the desorption of cyclohexylamine and TMA^+, respectively. Ballantine et al.[27] and Breen[28] have shown in their studies on Al^{3+}—montmorillonites and acid-activated montmorillonites that the desorption of cyclohexylamine from strong acid sites occurs near 300 °C, but there is little evidence for such a peak in this sample. In contrast, the

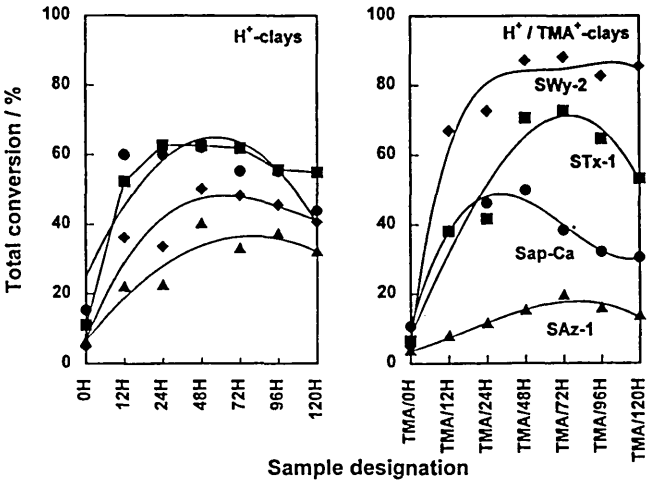

Figure 4. Total conversion for (a, left) natural and acid-treated clays and (b, right) TMA^+-exchanged and TMA/H clays: (◆) SWy-2; (■) STx-1; (▲) SAz-1; (●) Sap-Ca.

desorption thermogram of cyclohexylamine from acid-treated Wyoming bentonite (Figure 3b) did exhibit a sharp, intense peak at 300 °C corresponding to the desorption of cyclohexylamine from Brønsted sites.[27]

The derivative thermogram for the desorption of cyclohexylamine from SW-TMA/H samples (Figures 3c—e) contained evidence for both protonated cyclohexylamine and TMA^+ cations. A broad peak in the 120—220 °C region is clearly observed, which becomes less intense and shifts slightly as more acid is used. The TMA^+ desorption maximum at 415 °C for SW-TMA/12H is much more intense than that for cyclohexylamine desorption at 310 °C, which reflects the lower proton content. However, as the amount of acid used in sample preparation increased, the maximum at 310 °C grew while that at 415 °C decreased. This confirms that both protons and TMA^+ cations reside on the exchange sites and that the relative occupancy of protons increased as the acid concentration increased. This figure further reinforces the fact that TMA^+ ions can compete very effectively with protons for exchange sites on the clay. The desorption in the dehydroxylation region shows two peaks with maxima at 620 and 725 °C. The intensity of the former remained constant in all samples, but the maximum at 725 °C, which was resolved from its neighbor, decreased in intensity and is attributed to the desorption of CO_2 produced as carbonaceous deposits (derived from cyclohexylamine) combined with water evolved during dehydroxylation.[27,29]

α-Pinene is known to react readily in the presence of acid.[30] Under nonaqueous conditions, isomerization via ring expansion takes place to yield camphene. In highly polar protic solvents (e.g., H_2SO_4) monocyclic terpenes are formed via a ring-opening process to give a mixture of *p*-menthadienes including limonene. This isomerization was chosen by Rhodes and Brown[31] to support their contention that extensively acid-leached clays, which are essentially hydrophobic silica, were particularly suited for conversions involving nonpolar substrates. Their results, based upon work with a clay similar to STx-1, showed that the nature of that particular clay surface was more significant than the number of available acid sites.

Clearly, the type of clay has a profound effect upon the catalytic activity for α-pinene isomerization (Figure 4). In the absence of TMA^+ both Sap-Ca and STx-1 were more effective catalysts for the process than SWy-2 and SAz-1. The high activity of Sap-Ca could realistically be attributed to the

extensive leaching of the clay as acid treatment progressed, making it similar to the catalyst used by Rhodes and Brown,[31] but this cannot explain the comparable activity of STx-1 since this was not significantly leached under the conditions herein. Preliminary studies associated with acid-activated polycation-exchanged clays have shown that mildly acid-activated SWy-2 is a more effective catalyst for this process than SAz-1 although only three samples were investigated.[21] This difference in catalytic ability between SW-H and SA-H samples is conclusively proven herein.

The type of clay utilized also influenced the activity of the TMA/H samples. In all cases the lowest activities were recorded using the TMA^+-saturated clays, confirming, as anticipated, that exchange with TMA^+ alone did not enhance the catalytic activity. The total conversion for SW-TMA/H samples exhibited the largest increase in yield (from 50% for SW-H) to 88%, which incidentally represents an 8-fold increase over SW-TMA. The conversion over ST-TMA/H samples increased slightly from 62% to 73% whereas the yields for SCa-TMA/H and SA-TMA/H samples decreased from 60% to 50% and from 35% to 20%, respectively. In general, the activity for all TMA/H samples increased with the extent of acid treatment reaching a plateau between 48 and 72 mmol H^+ before declining after preparation in more concentrated acid. The absolute yields for camphene and limonene are similar to those obtained in the preliminary studies[19,21] which were obtained after 2 h at 80 °C and are considerably higher than those reported for extensively acid-leached Texas bentonite.[31] The yields obtained herein are comparable with the values of 80 and 90% reported for ultrastable zeolite Y (USY) and Al- and Al,Fe-pillared interlayer clays (Al-PILC and Al,Fe-PILC, respectively) obtained after 5 h in a sealed glass reactor at 100 °C.[20]

As anticipated, the product distribution of terpenes (Figure 5) followed the order camphene > limonene > others, with the exception of the SW-TMA/H clays, where the yield of other products is higher than that of limonene. The selectivity toward camphene, limonene, and the minor products was essentially the same for all the clays and can be broadly described as 65 ± 10%, 25 ± 8%, and 12 ± 8%, respectively, to encompass all the catalysts. The ratio of camphene to limonene is near 2.6:1.0 compared with a value of 2.2:1.0 obtained at 80 °C for 2 h[19] and less than the ratio 3.0:1.0 obtained over USY, Al-PILC, and Al,Fe-PILC.[20] Thus, the clay-based samples are not as selective toward camphene as the permanently porous catalysts, but the yields are competitive and the catalysts are more economic to produce.

In our preliminary studies the aim was to evaluate how the nature of the selected organocation influenced the catalytic activity of a particular series of AAOCs and this unequivocally demonstrated that clays containing TMA^+ cations were much more effective than than those containing alkyltrimethyammonium cations or polycations. This difference in catalytic activity was attributed to congestion of the galleries in clays containing significant quantities of large organocations and, in the case of polycations, an inability of the organoclay complex to expand in the presence of the organic reagent. The work of Watson[22] suggested that there was a correlation between the amount of TMA^+ on the AAOC and the resulting catalytic activity but there was no comparative data with catalysts prepared using the same amount of acid in the absence of TMA^+ cations. Figure 6 suggests that the total conversion (based on α-pinene) was optimized when 25−30% of the exchange sites of SWy-2 and STx-1 were occupied by TMA^+ cations. The yield over SAz-1 may be influenced by the higher loading of TMA^+ cations on the surface, which were much more resistant to displacement

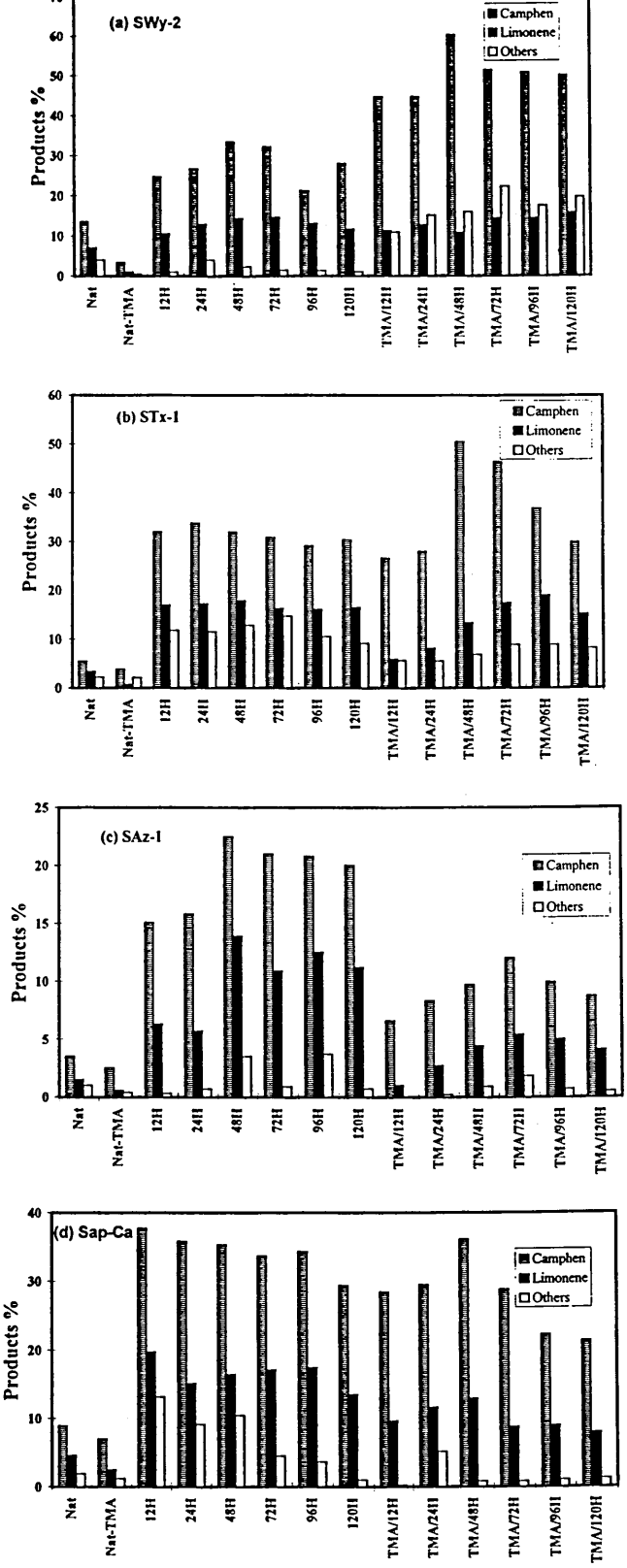

Figure 5. Product distribution for the catalysts derived from (a) SWy-2, (b) STx-1, (c) SAz-1, and (d) Sap-Ca.

by protons than TMA^+ on the other clays under investigation. Moreover, it has been suggested that the high charge density on the surface of SAz-1 means that the distance between neighboring TMA^+ cations is insufficient to accommodate benzene, toluene, and xylene molecules, thus reducing the ability of TMA^+-SAz-1 to function as an effective sorbent for the removal of these pollutant molecules from water.[32] Therefore,

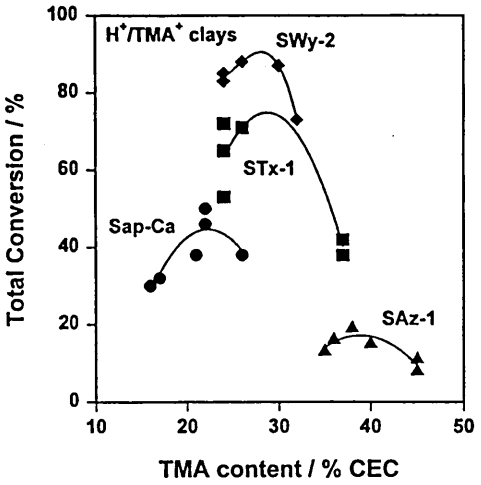

Figure 6. Correlation of the percentage of TMA^+ vs percentage of total conversion for acid-treated organoclays (◆) SWy-2, (■) STx-1, (▲) SAz-1, and (●) Sap-Ca.

the low activity of the SA-TMA/H samples may be attributed, in part, to insufficient space to accommodate the α-pinene molecules at the active site. SCa-H samples were much more catalytically active than their TMA^+-containing counterparts. Hence, the reduction in overall yield over the SCa-TMA/H samples probably reflects an extensively leached saponite surface which has TMA^+ cations occupying exchange sites that would be more effective in the isomerization process if they were occupied by protons.

Clearly, the nature of the raw clay plays an important role in the resulting properties of the AAOC. The behavior of SWy-2 closely mimics that previously observed in preliminary investigations using a Slovak montmorillonite, a Czech beidellite, and a ferruginous smectite insofar as the synergy between an organophilic surface and protons significantly enhanced the activity of the AAOC for a reaction involving a nonpolar substrate. The samples based on Sap-Ca must remain outside the present discussion because the depopulation of the octahedral sheet is more like clays rich in octahedral aluminum that have been activated in hot acid.[31] Nonetheless, it serves as an appropriate marker and emphasizes that similar activity can be imparted to SW-TMA/H samples without the production of large quantities of acidic Al^{3+}- or Mg^{2+}-containing solutions. The behavior of SAz-1 and STx-1 are more difficult to explain since these samples behave incongruously. Mildly acid-activated STx-1 is an excellent catalyst for the isomerization of α-pinene and its activity is only marginally enhanced via the incorporation of TMA^+ cations, although the dependence of total conversion on TMA^+ content closely follows that for SWy-2 (Figure 6). Currently, we have no complete explanation for the marked activity of STx-1, although a dispersion of STx-1 has a pH of 7 compared with SWy-2 which has a pH of 9. This may imply that the edge sites on STx-1 are inherently more acidic than those on SWy-2. Finally, the activity of SAz-1 is significantly reduced by the incorporation of TMA^+ cations, as it was by the incorporation of polycations.[21] One possible explanation for this behavior is that the gallery surface accessible to α-pinene in the presence of TMA^+ cations is insufficient to allow access to the catalytic sites.

Conclusions

The results herein show that the AAOCs contain a mixture of H^+ and TMA^+ ions and that they are capable of conversions zeolites. The activity depends on the nature of the parent clay utilized, and some acid-activated source clays are active in their own right whereas the activity of others is enhanced by the synergy between adsorbed H^+ and TMA^+ ions. Thus, the catalytic activity for the isomerization for α-pinene was excellent for AAOCs formed from SWy-2 and STx-1, moderate for Sap-Ca, and low for SAz-1. The major products of the isomerization of α-pinene were camphene and limonene, indicating that the reaction proceeded via expansion to derivatives of bornane and ring opening to *p*-menthene derivatives. The catalytic activity of the more active AAOCs was optimized when 25−30% of the exchange sites were occupied by TMA^+ ions.

Acknowledgment. A.M. gratefully acknowledges maintenance grants from Consejo Nacional de Investigaciones Científicas y Tecnológicas de Venezuela (CONICIT) and La Universidad del Zulia (Venezuela). We wish to thank Margaret West and Bob Burton of Sheffield Hallam University for the XRF analyses.

References and Notes

(1) Laszlo, P. *Acc. Chem. Res.* **1986**, *19*, 121.
(2) Cornelis, A.; Laszlo, P. In Chemical Reactions In *Organic and Inorganic Constrained Systems*; Setton, R., Ed.; Reidel: New York, 1986; p 213.
(3) Morgan, D. A.; Shaw, D. B.; Sidebottom, M. J.; Soon, T. C.; Taylor, R. S. *J. Am. Oil Chem. Soc.* **1985**, *62*, 292.
(4) Novak, I.; Gregor, M. *Proc. Int. Clay Conf. Tokyo* **1969**, 851.
(5) Hirokawa, A. *Nendo Kagaku* **1980**, *20*, 99.
(6) Fahn, R.; Fenderl, K. *Clay Miner* **1983**, *18*, 447.
(7) Thomas, C. L.; Hickey, J.; Stecker, G. *Ind. Eng. Chem.* **1950**, *42*, 866.
(8) Breen, C.; Zahoor, F. D.; Madejová, J.; Komadel, P. *J. Phys. Chem. B* **1997**, *101*, 5324.
(9) Osthaus, B. B. *Clays Clay Miner.* **1956**, *4*, 301.
(10) Granquist, W. T.; Gardner-Sumner, G. *Clays Clay Miner.* **1959**, *6*, 292.
(11) Bujdák, J.; Slosiariková, H.; Cícel, B. *Chem. Pap.* **1993**, *47*, 85.
(12) Lee, J. F.; Mortland, M. M.; Chiou, C. T.; Kile, D. E.; Boyd, S. A. *Clays Clay Miner.* **1990**, *38*, 113.
(13) Mortland, M. M.; Shaobai, S.; Boyd, S. A. *Clays Clay Miner.* **1986**, *34*, 581.
(14) Jaynes, W. F.; Boyd, S. A. *J. Air Waste Mgmt. Assoc.* **1990**, *40*, 1649.
(15) Boyd, S. A.; Mortland, M. M.; Chiou, C. T. *Soil Sci. Soc. Am. J.* **1988**, *52*, 652.
(16) Pashley, R. M.; McGuiggan, P. M.; Ninham, B. W.; Evans, D. F. *Science* **1985**, *229*, 1088.
(17) McBride, M. B.; Pinnavaia, T. J.; Mortland, M. M. In *Fate of Pollutants in the Air and Water Environments. Part I*; Suffet, I. H., Ed.; Wiley: New York, 1977; p 145.
(18) Wolfe, T. A.; Demirel, T.; Baumann, R. E. *J. Water Pollution Control Fed.* **1986**, *58*, 68.
(19) Breen, C.; Watson, R.; Madejová, J.; Komadel, P.; Klapyta, Z. *Langmuir* **1997**, *13*, 6473.
(20) De Stefanis, A.; Perez, G.; Ursini, O.; Tomlinson, A. A. G. *Appl. Catal. A* **1995**, *132*, 353.
(21) Breen, C.; Waston, R. *Appl. Clay Sci.* **1998**, *12*, 479.
(22) Watson, R. Ph.D. Thesis, Sheffield Hallam University, 1997.
(23) Mills, G. A.; Holmes, J.; Cornelius, E. B. *J. Phys. Colloid Chem.* **1950**, *54*, 1170.
(24) Breen, C.; Madejová, J.; Komadel, P. *Appl. Clay Sci.* **1995**, *10*, 219.
(25) Breen, C.; Deane, A. T.; Flynn, J. J. *Clay Miner.* **1987**, *22*, 169.
(26) Shuali, U.; Steinberg, M.; Yariv, S.; Muller-Vonmoos, M.; Kahr, G.; Rub, A. *Clay Miner.* **1990**, *25*, 107.
(27) Ballantine, J. A.; Graham, P.; Patel, I.; Purnell, J. H.; Williams, K.; Thomas, J. M. *Proc. Int. Clay Conf. Denver* **1987**, 311.
(28) Breen, C. *Clay Miner.* **1991**, *26*, 473.
(29) Breen, C.; Moronta, A. Unpublished results.
(30) Williams, C. M.; Whittaker, D. *J. Chem. Soc. B* **1971**, 668.
(31) Rhodes, C. N.; Brown, D. R. *Catal. Lett.* **1994**, *24*, 285.
(32) Boyd, S. A.; Jaynes, W. F. In *Layer Charge Characteristics of 2:1 Silicate Minerals*; Mermut, A. R., Ed., CMS Lecture Workshops Vol. 6; The Clay Minerals Society: Boulder, CO, **1994**; p 48.